Transitioning from MODIS to VIIRS for remote sensing of ocean, land, and atmosphere

RT in Earth Atmosphere
Multispectral Signatures
MODIS Heritage Products
VIIRS Instrument Description
Some Anticipated VIIRS Applications
(SST, Ocean Color, Vegetation, Snow, Ice, Clouds, Moisture, Fires, Dust, Low Light Imagery)

W. Paul Menzel, University of Wisconsin- Madison

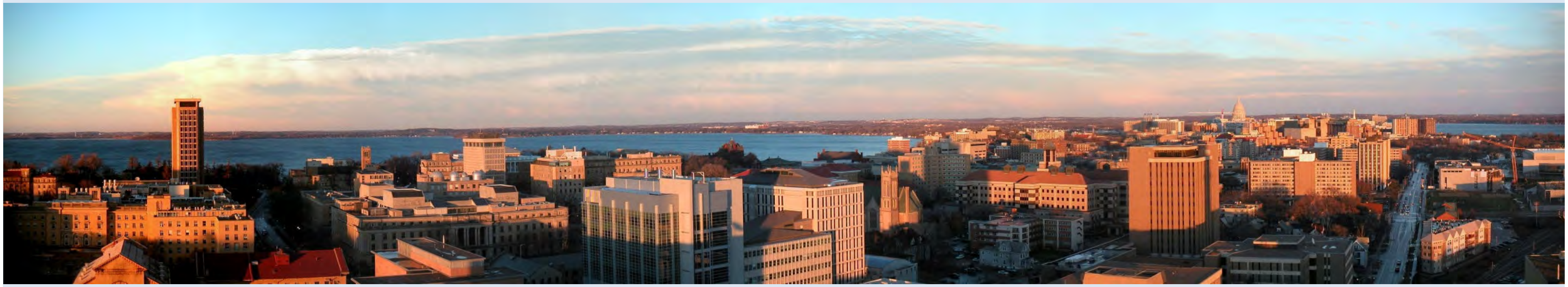

Thanks to
Jeff Puschell, Steve Miller,
Jeff Key, Liam Gumley,
Tom Rink, Geoff Cureton,
the MODIS Science Team,
and colleagues at CIMSS

Suomi National Polar-orbiting Partnership (NPP)

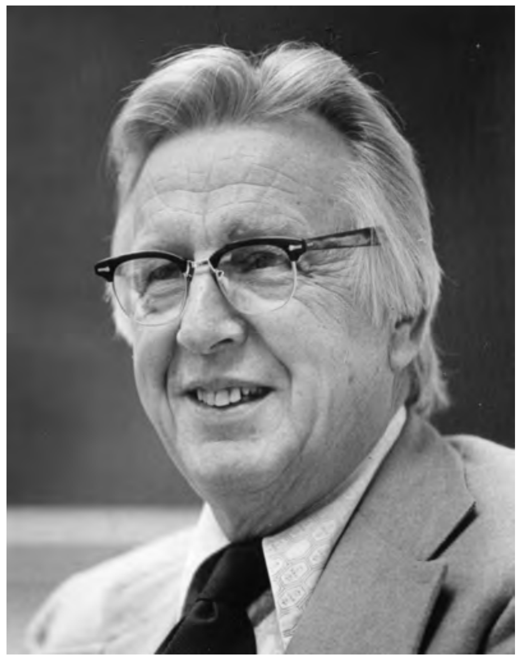

NPP was re-named Suomi NPP on 24 Jan 2012

http://npp.gsfc.nasa.gov/

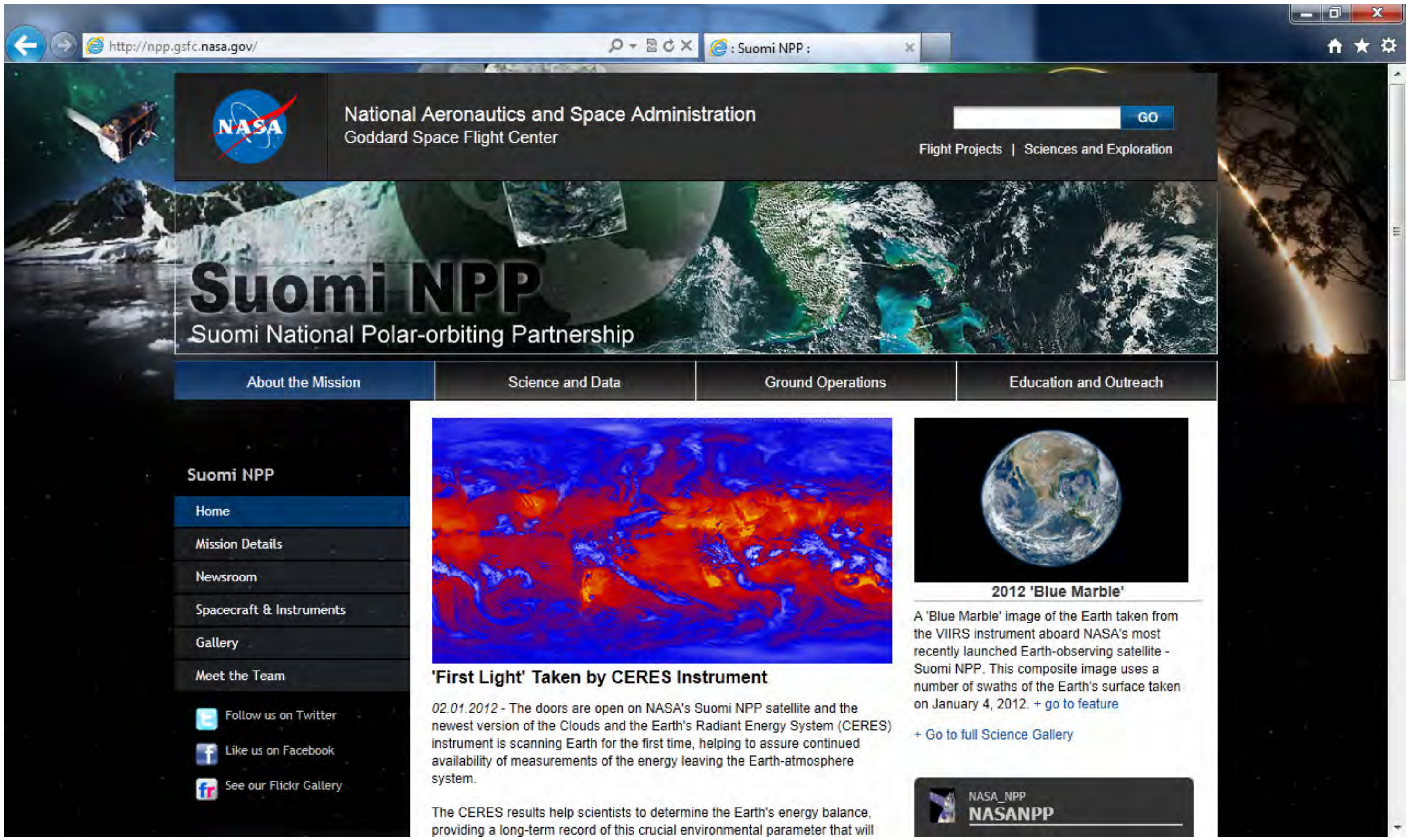

Blue Marble - VIIRS

Electromagnetic spectrum

Remote sensing uses radiant energy that is reflected and emitted from Earth at various wavelengths in the electromagnetic spectrum

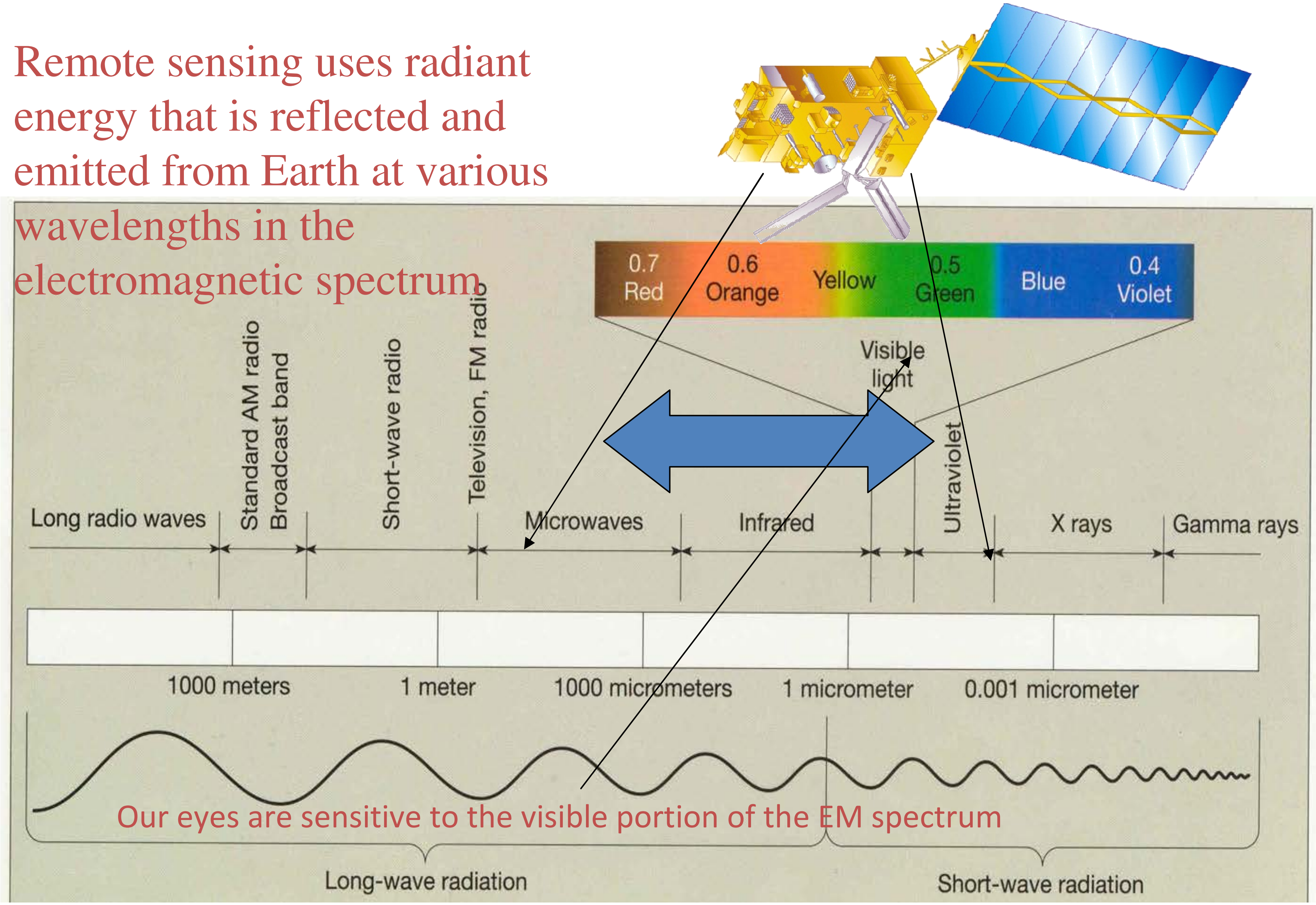

Our eyes are sensitive to the visible portion of the EM spectrum

Satellite remote sensing of the Earth-atmosphere

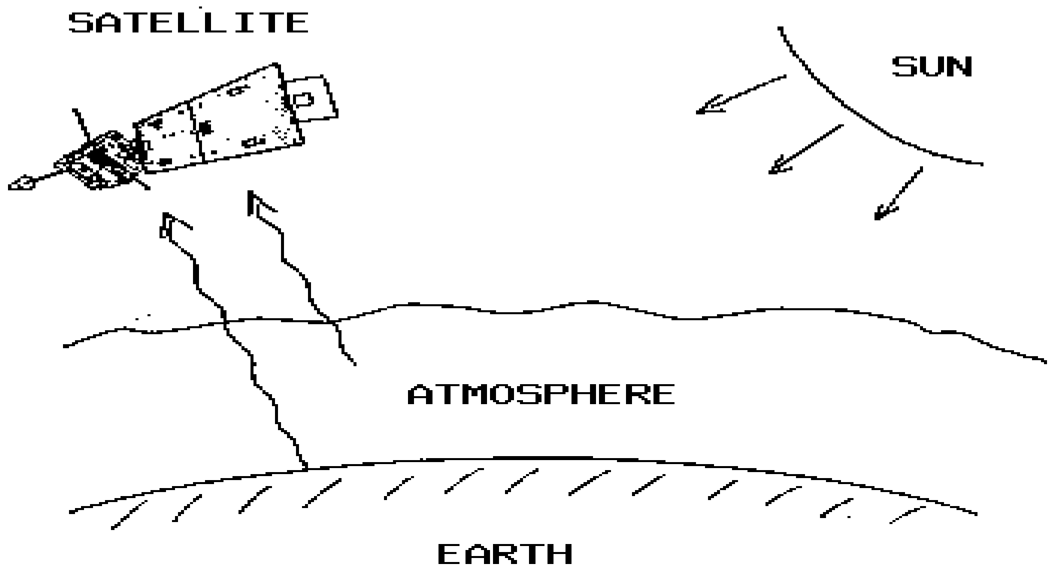

Observations depend on

telescope characteristics (resolving power, diffraction)
detector characteristics (field of view, signal to noise)
communications bandwidth (bit depth)
spectral intervals (window, absorption band)
time of day (daylight visible)
atmospheric state (T, Q, clouds)
earth surface (Ts, vegetation cover)

All Sats on NASA J-track

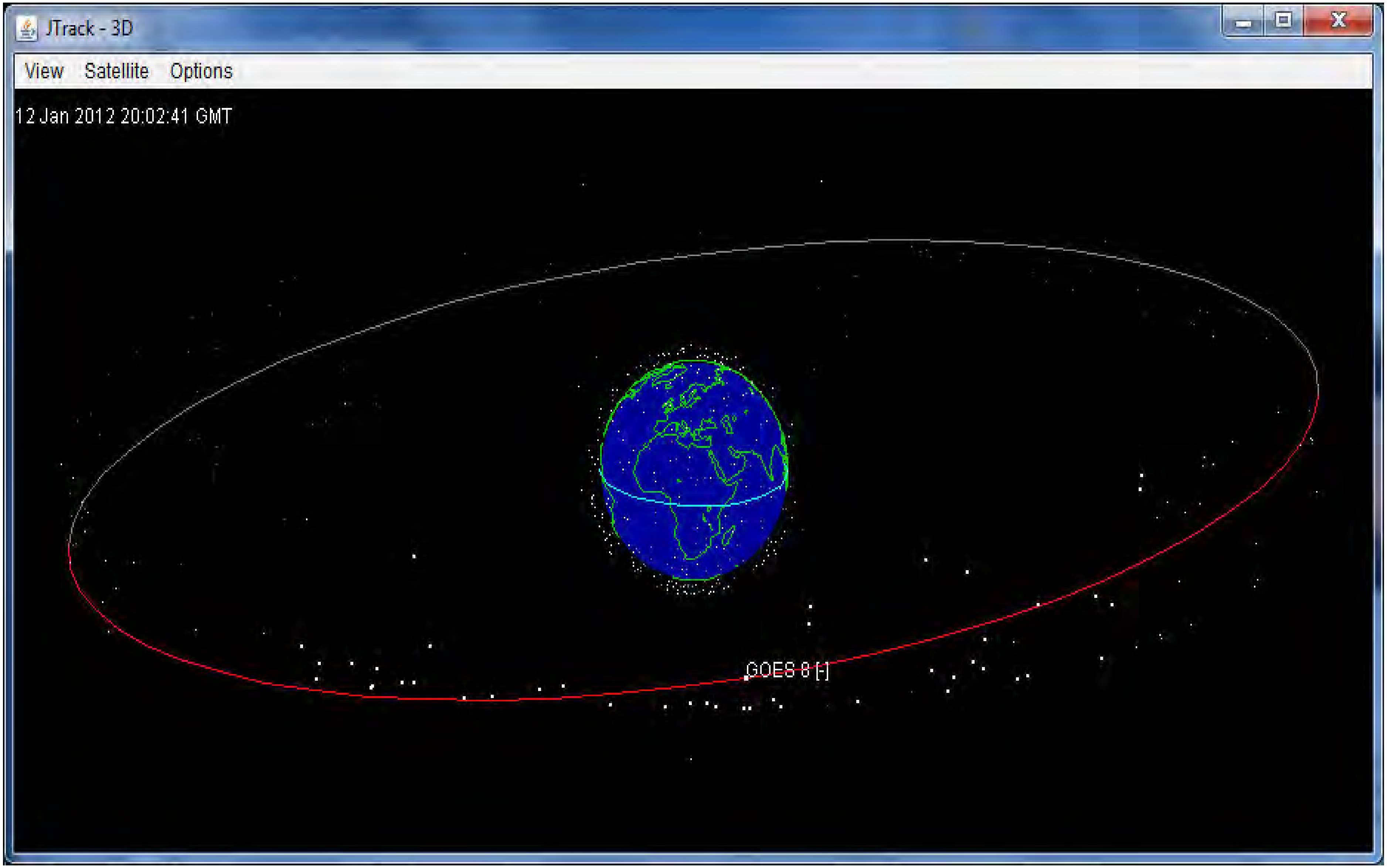

http://science.nasa.gov/realtime/jtrack/3d/JTrack3D.html/

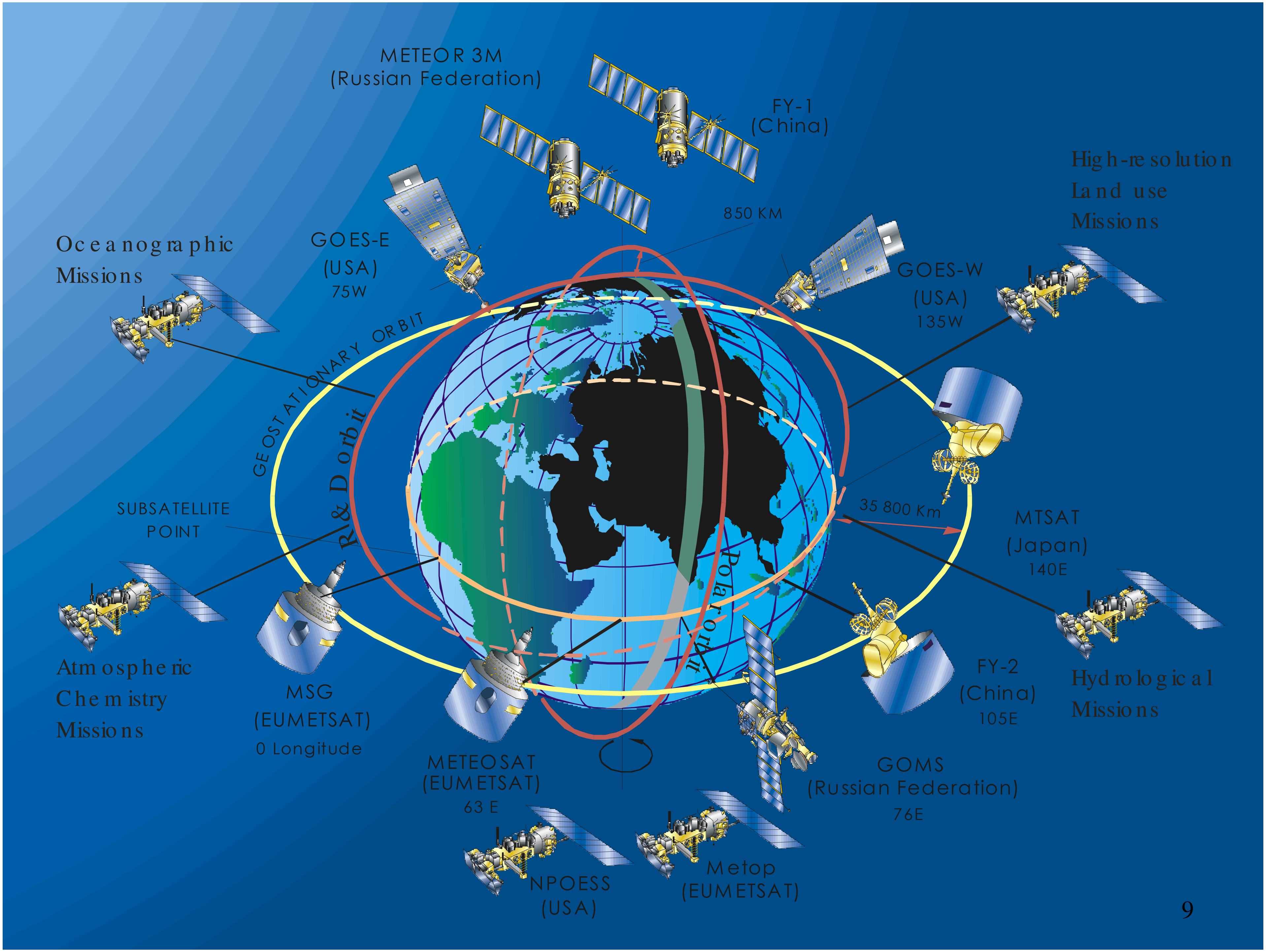
METEOR 3M
(Russian Federation)
FY-1
(China)
High-resolution
Land use
Missions
Oceanographic
Missions
GOES-E
(USA)
75W
850 KM
GOES-W
(USA)
135W
GEOSTATIONARY ORBIT
R & D orbit
SUBSATELLITE
POINT
35 800 Km
MTSAT
(Japan)
140E
Polar orbit
Atmospheric
Chemistry
Missions
MSG
(EUMETSAT)
0 Longitude
FY-2
(China)
105E
Hydrological
Missions
METEOSAT
(EUMETSAT)
63 E
GOMS
(Russian Federation)
76E
NPOESS
(USA)
Metop
(EUMETSAT)

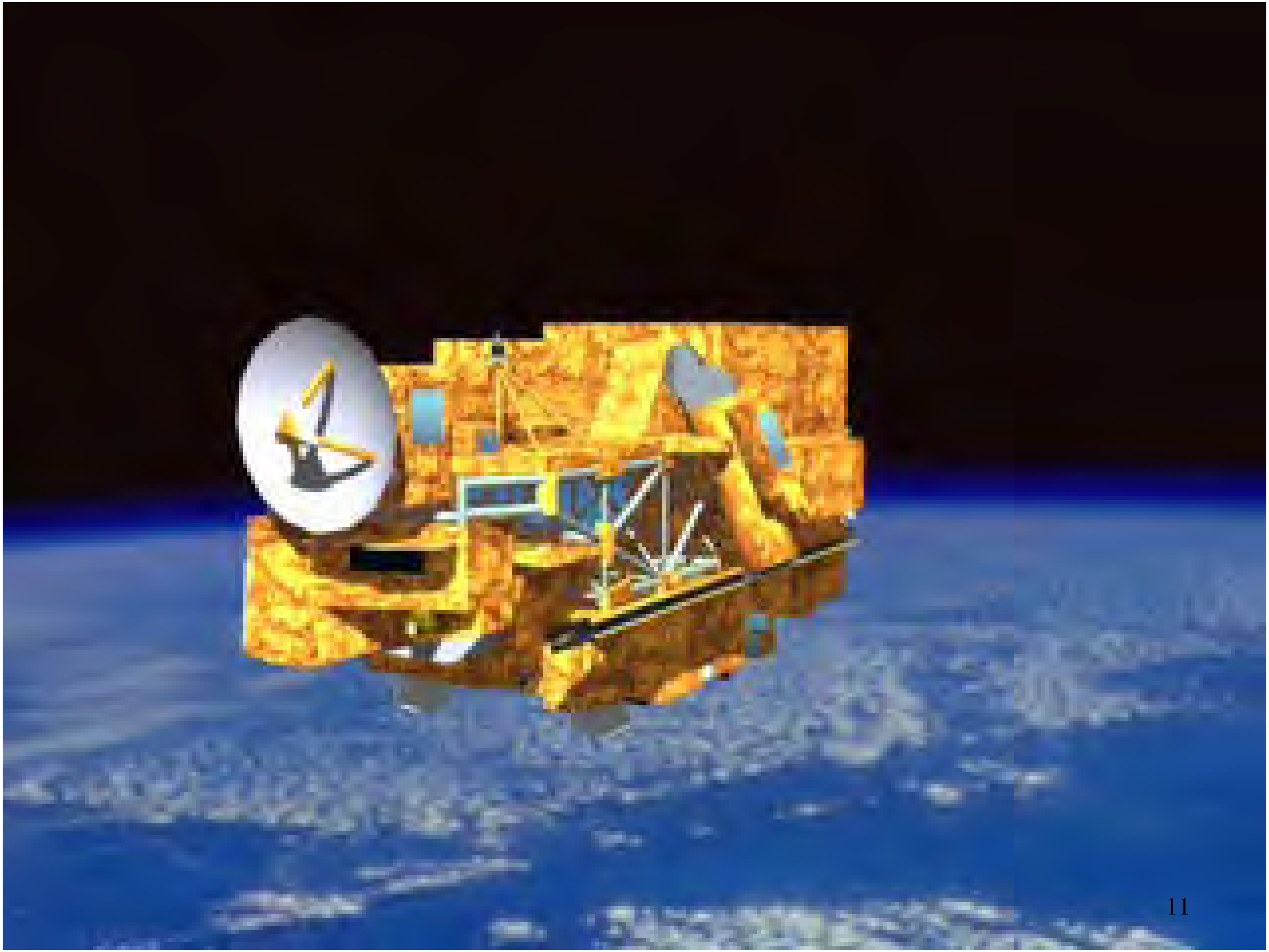

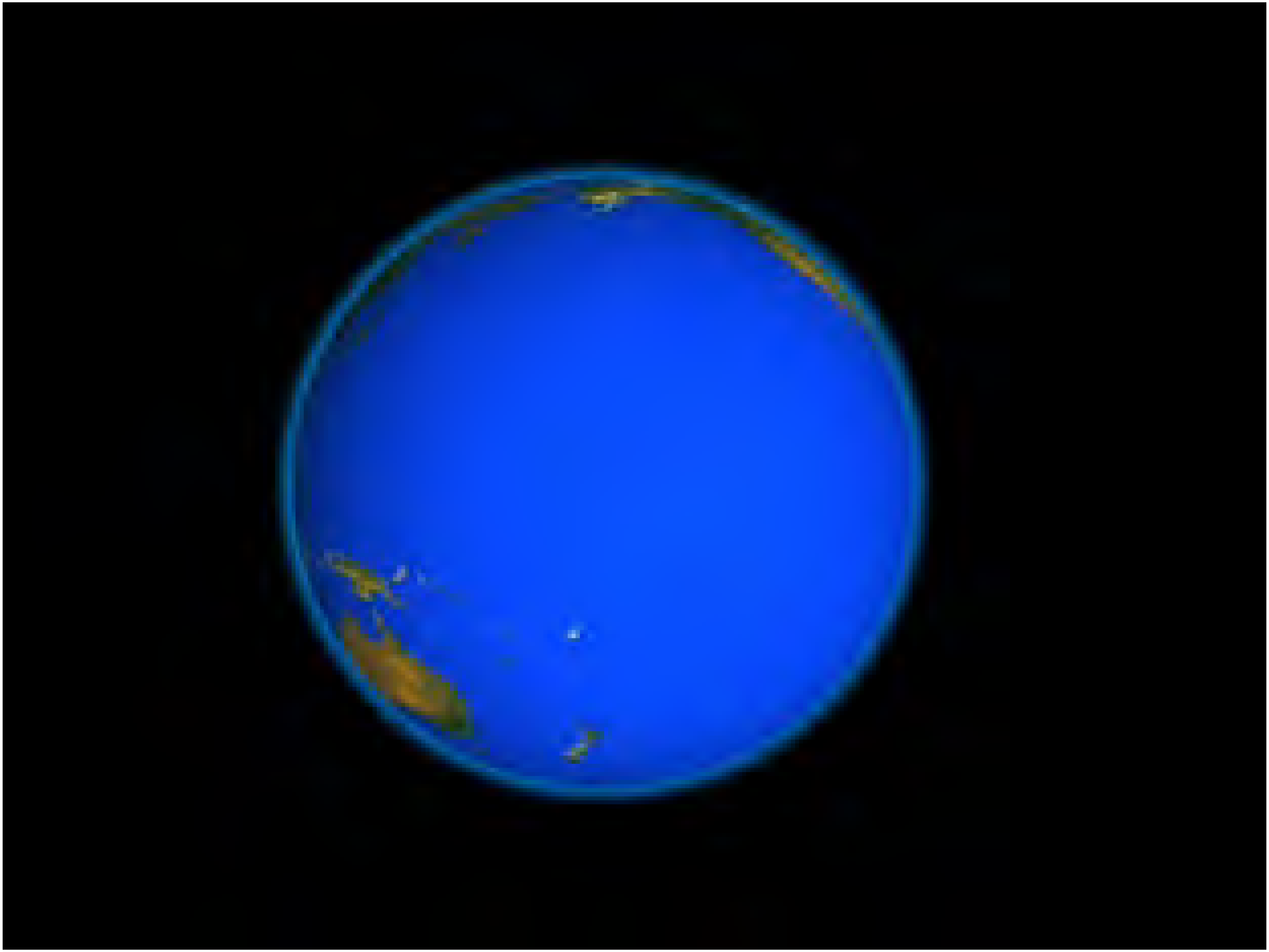

Solar reflected (visible) and Earth emitted (infrared) energy

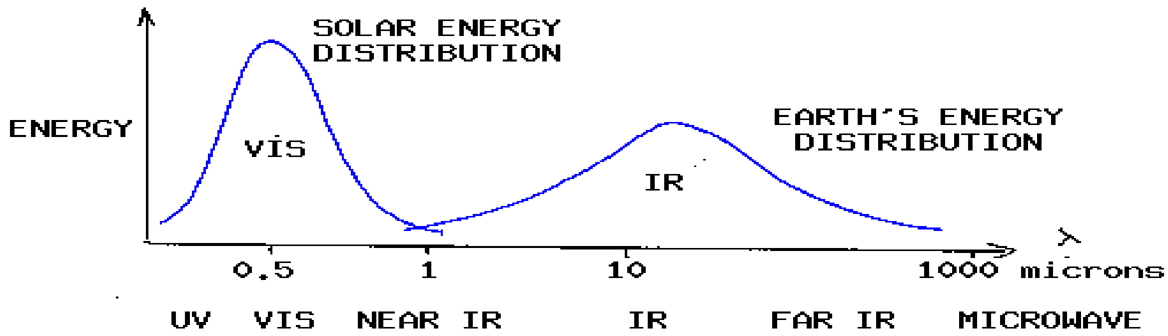

Over the annual cycle, the incoming solar energy that makes it to the earth surface (about 50 %) is balanced by the outgoing thermal infrared energy emitted through the atmosphere.

The atmosphere transmits, absorbs (by H2O, O2, O3, dust) reflects (by clouds), and scatters (by aerosols) incoming visible; the earth surface absorbs and reflects the transmitted visible. Atmospheric H2O, CO2, and O3 selectively transmit or absorb the outgoing infrared radiation. The outgoing microwave is primarily affected by H2O and O2.

Visible / Near Infrared Remote Sensing

VIIRS, MODIS, FY-1C, AVHRR Visible Near-infrared Spectral Bands

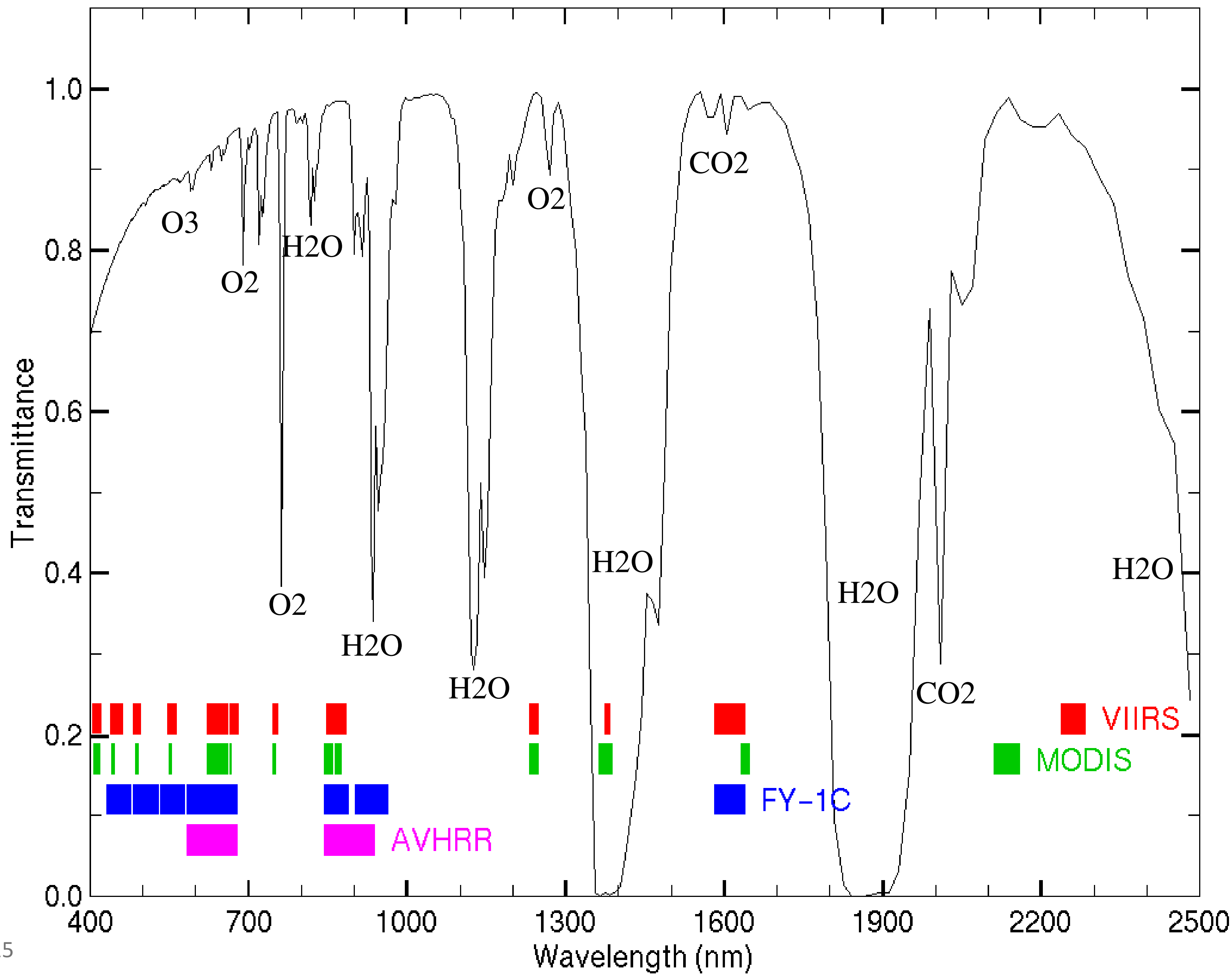

In an ideal situation with no atmosphere all of the incoming radiation would reach the surface. A portion of the photons would be absorbed at the surface. The remaining photons reflect back up into space.

NO ATMOSPHERE

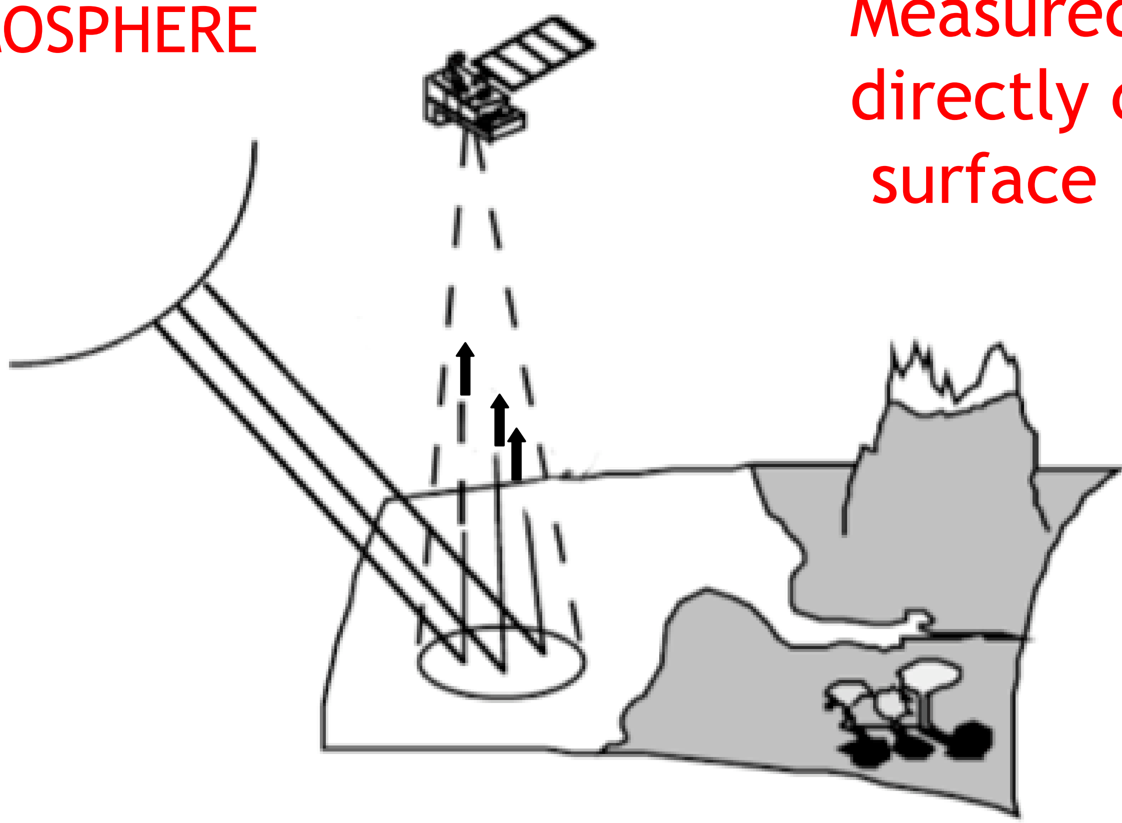

Measured radiance directly depends on surface properties

Diagrams from E. Vermote et. al, 6S manual

1) Backscattered photons which never reach the surface.

Signal or Noise?

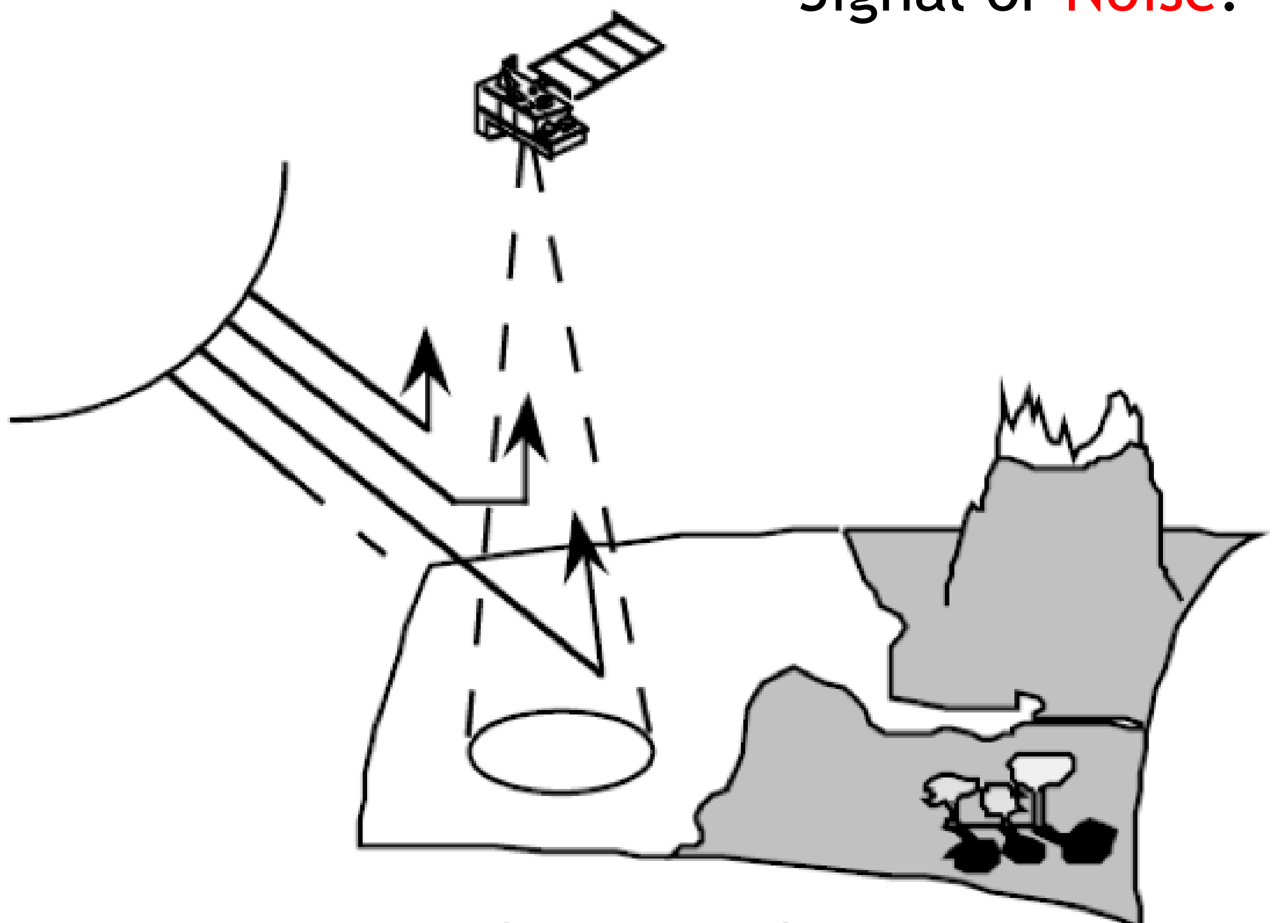

Diagram from E. Vermote et. al, 6S manual

2) Scattered photons which illuminate the ground.

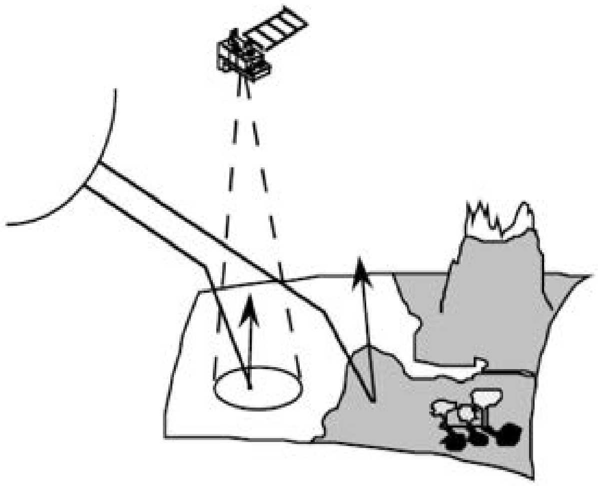

Signal or Noise?

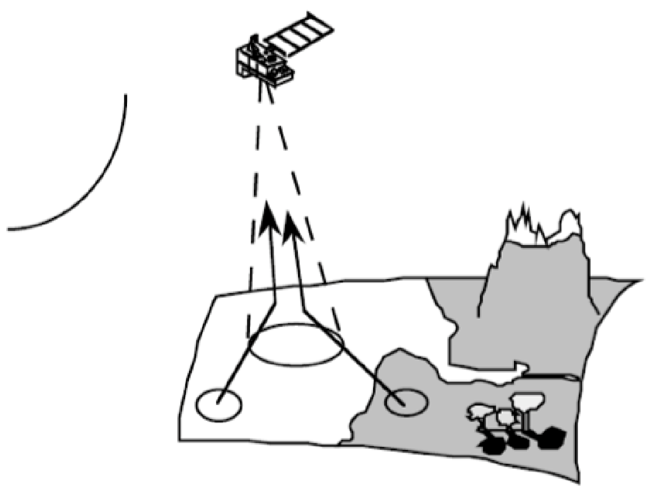

3) Photons reflected by the surface and then scattered by the atmosphere.

Diagrams from E. Vermote et. al, 6S manual

4) Multiple scattering events.

This is usually ignored after one or two interactions.

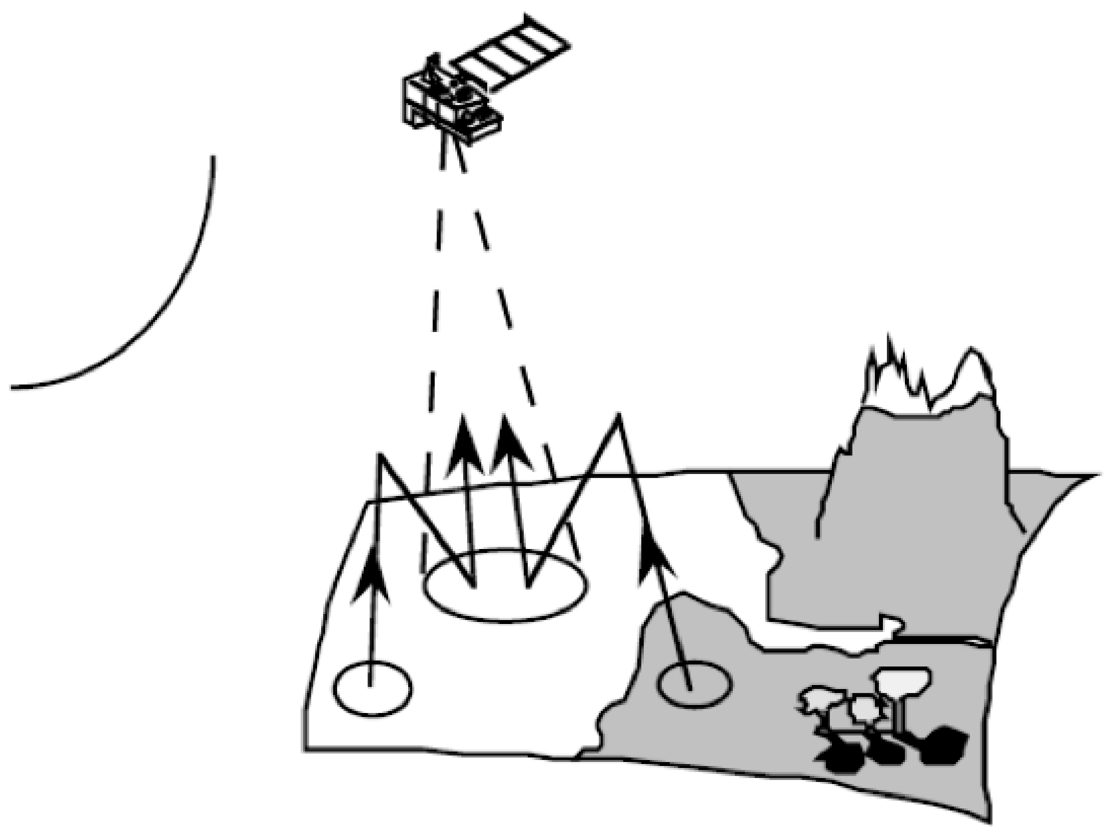

Diagram from E. Vermote et. al, 6S manual

The real atmosphere complicates the signal. Only a fraction of the photons reach the sensor so that the target seems less reflecting.

Real Atmosphere

Photons lost due to
1) Atmospheric absorption
2) Scattering

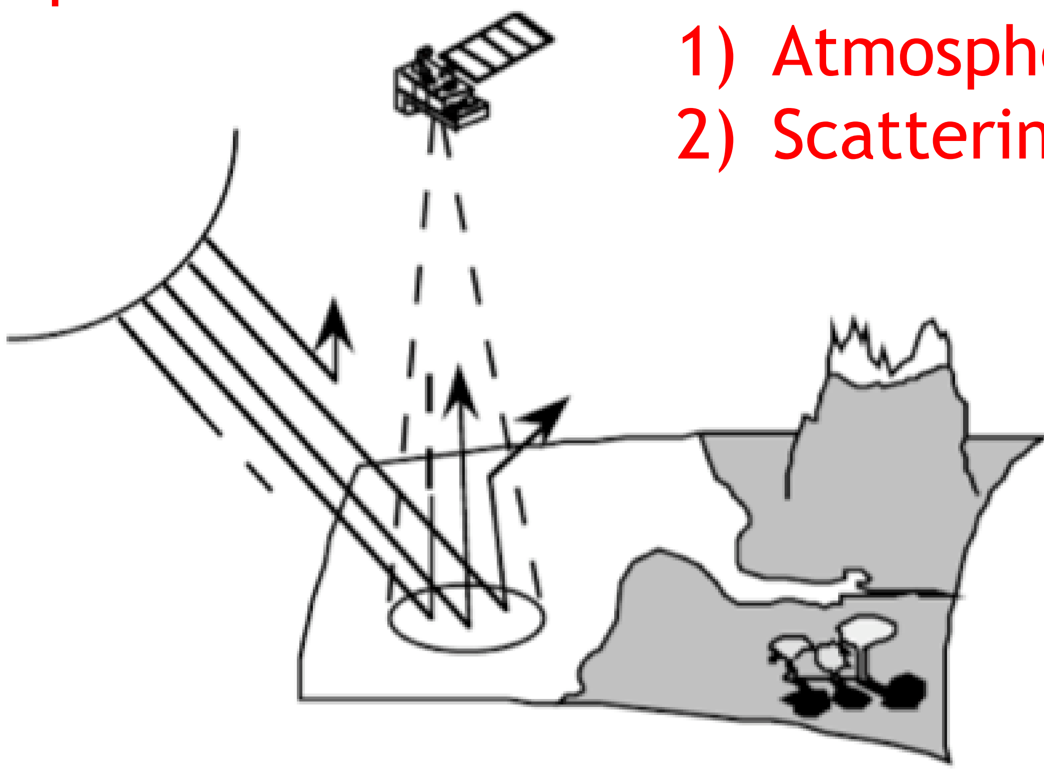

From E. Vermote et. al, 6S manual

Infrared Remote Sensing

VIIRS MODIS Infrared Spectral Bands

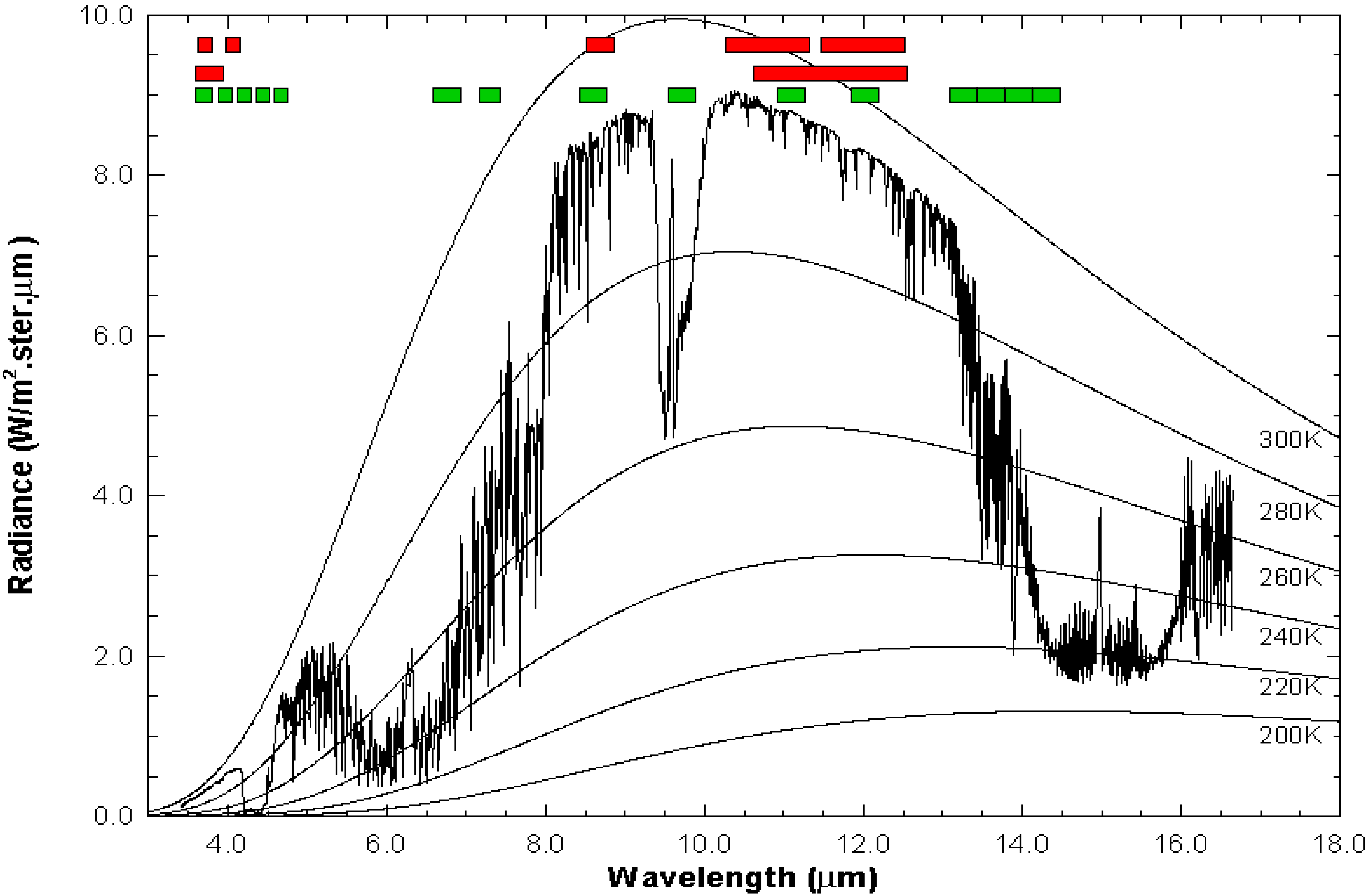

Using wavenumbers

$$B(\nu,T) = c_1\nu^3 / [e^{c_2\nu/T} - 1]$$

$(mW/m^2/ster/cm^{-1})$

ν(max in cm-1) = 1.95T

$B(\nu_{max},T) \sim T^{**}3.$

$$E = \pi \int_0^\infty B(\nu,T)\, d\nu = \sigma T^4,$$

$$T = c_2\nu/[\ln(\frac{c_1\nu^3}{B_\nu} + 1)]$$

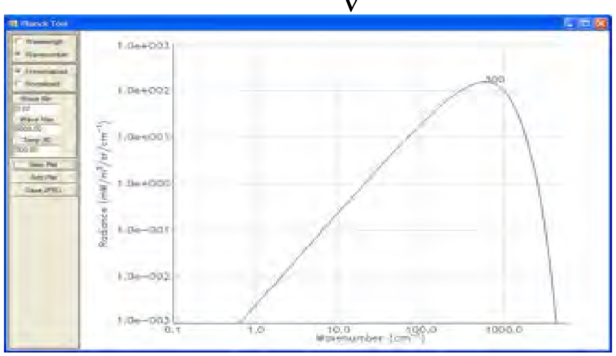

Using wavelengths

$$B(\lambda,T) = c_1 / \{ \lambda^5 [e^{c_2/\lambda T} - 1] \}$$

$(mW/m^2/ster/\mu m)$

λ(max in cm)T = 0.2897

$B(\lambda_{max},T) \sim T^{**}5.$

$$E = \pi \int_0^\infty B(\lambda,T)\, d\lambda = \sigma T^4,$$

$$T = c_2/[\lambda \ln(\frac{c_1}{\lambda^5 B_\lambda} + 1)]$$

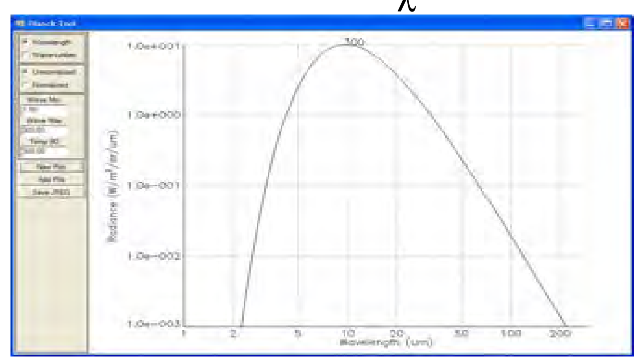

Radiative Transfer Equation

The radiance leaving the earth-atmosphere system sensed by a satellite borne radiometer is the sum of radiation emissions from the earth-surface and each atmospheric level that are transmitted to the top of the atmosphere. Considering the earth's surface to be a blackbody emitter (emissivity equal to unity), the upwelling radiance intensity, I_λ, for a cloudless atmosphere is given by the expression

$$I_\lambda = \varepsilon_\lambda^{sfc} B_\lambda(T_{sfc}) \tau_\lambda(\text{sfc - top}) + \sum_{\text{layers}} \varepsilon_\lambda^{layer} B_\lambda(T_{layer}) \tau_\lambda(\text{layer - top})$$

where the first term is the surface contribution and the second term is the atmospheric contribution to the radiance to space.

Satellite observation comes from the sfc and the layers in the atm

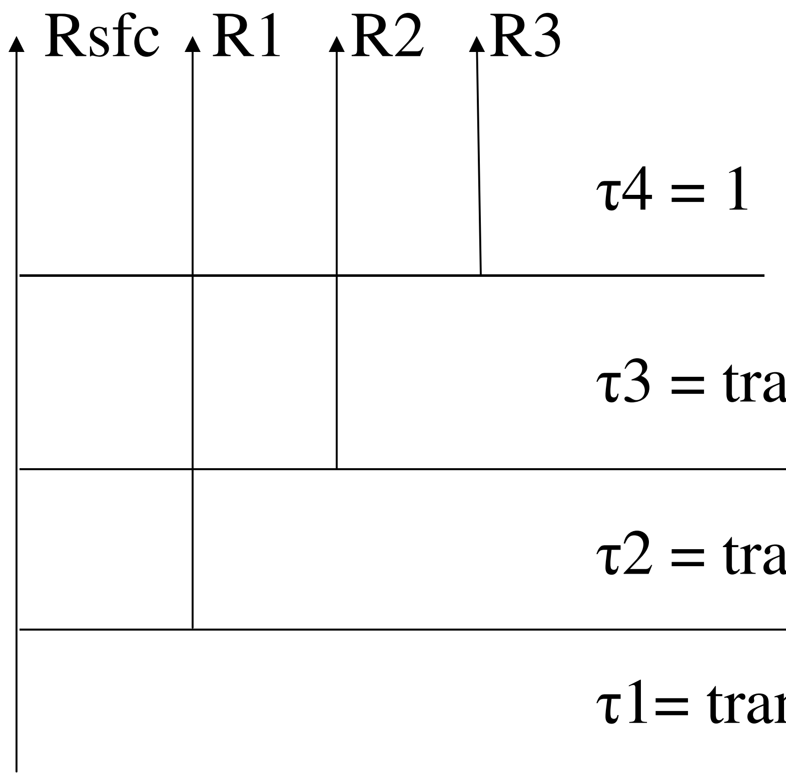

$\tau 4 = 1$

$\tau 3$ = transmittance of upper layer of atm

$\tau 2$ = transmittance of middle layer of atm

$\tau 1$= transmittance of lower layer of atm

εsfc for earth surface

recalling that $\varepsilon i = 1 - \tau i$ for each layer, then

$$Robs = \varepsilon sfc\ Bsfc\ \tau 1\ \tau 2\ \tau 3 + (1-\tau 1)\ B1\ \tau 2\ \tau 3 + (1-\tau 2)\ B2\ \tau 3 + (1-\tau 3)\ B3$$

Radiative Transfer through the Atmosphere

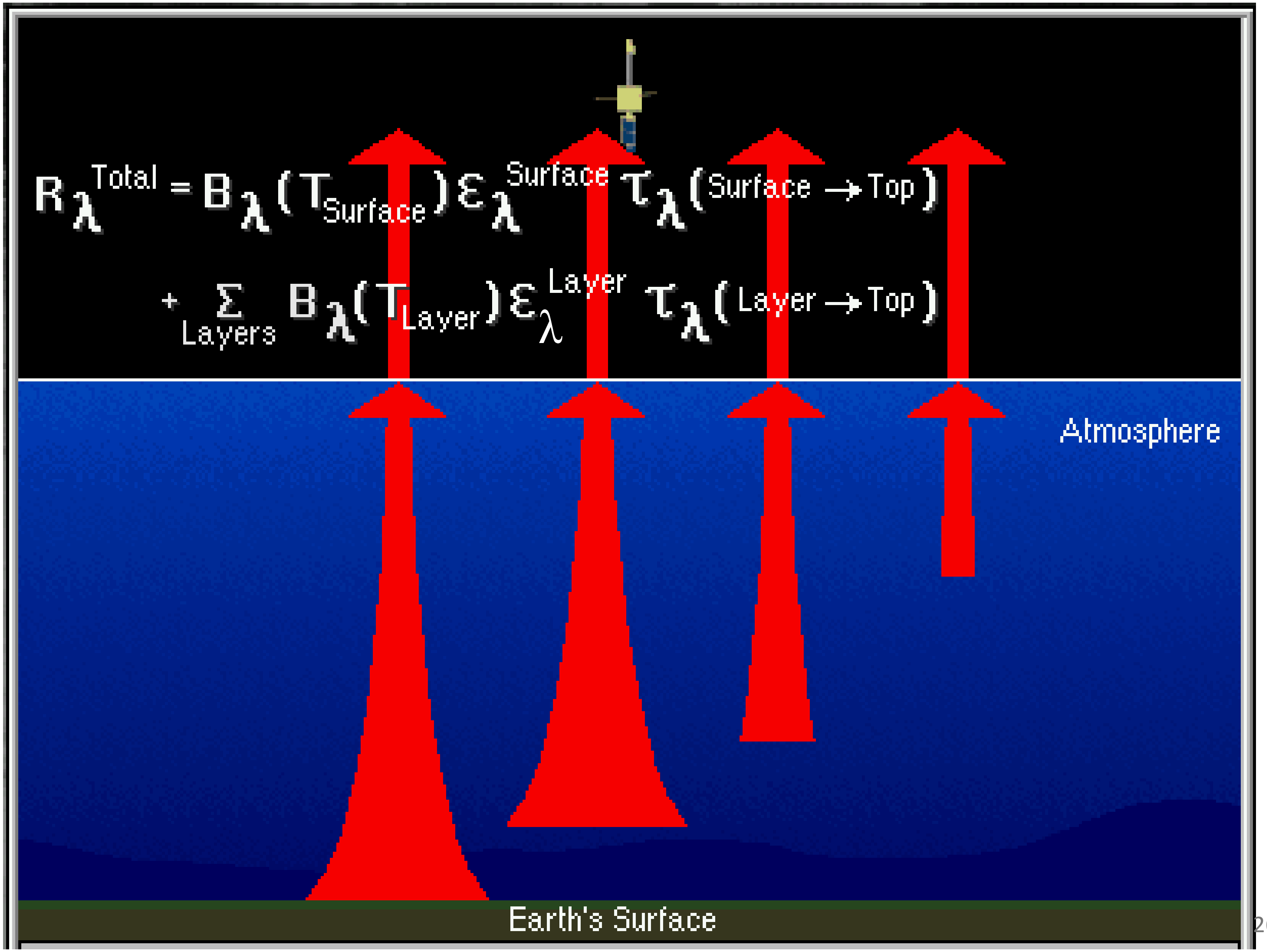

The emissivity of an infinitesimal layer of the atmosphere at pressure p is equal to the absorptance (one minus the transmittance of the layer). Consequently,

$$\varepsilon_\lambda(\text{layer})\ \tau_\lambda(\text{layer to top}) = [1 - \tau_\lambda(\text{layer})]\ \tau_\lambda(\text{layer to top})$$

Since transmittance is multiplicative

$$\tau_\lambda(\text{layer to top}) - \tau_\lambda(\text{layer})\ \tau_\lambda(\text{layer to top}) = -\Delta\tau_\lambda(\text{layer to top})$$

So we can write

$$I_\lambda = \varepsilon_\lambda^{sfc}\ B_\lambda(T(p_s))\ \tau_\lambda(p_s) - \sum_p B_\lambda(T(p))\ \Delta\tau_\lambda(p)\ .$$

which when written in integral form reads

$$I_\lambda = \varepsilon_\lambda^{sfc}\ B_\lambda(T(p_s))\ \tau_\lambda(p_s) - \int_o^{p_s} B_\lambda(T(p))\ [\ d\tau_\lambda(p) / dp\ ]\ dp\ .$$

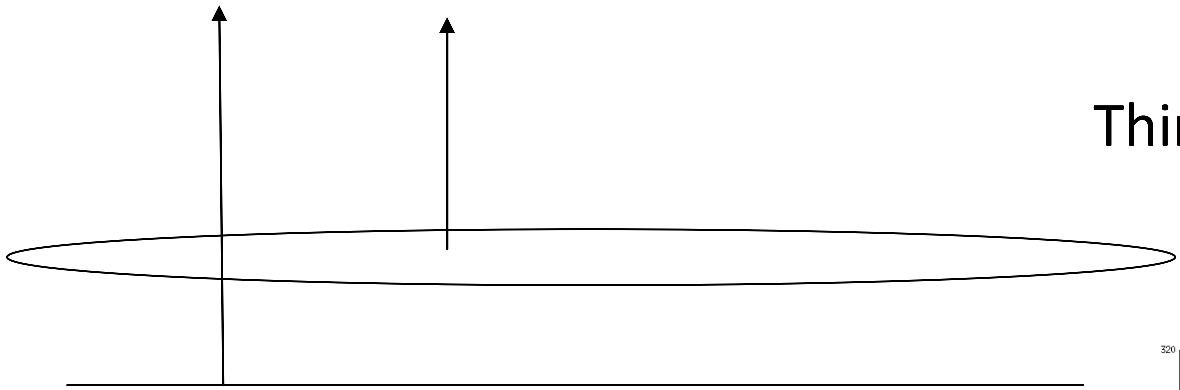

Thin ice cloud over ocean

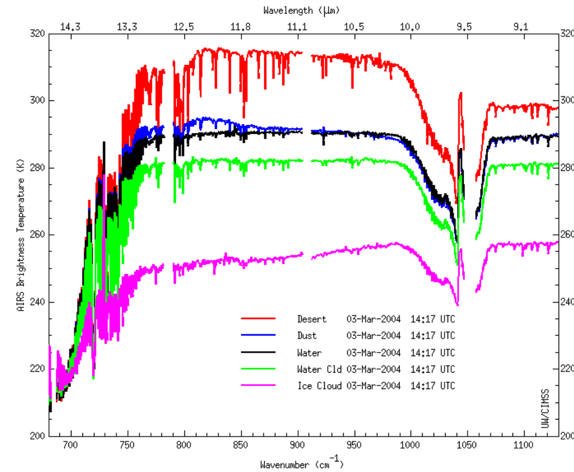

$R = \varepsilon_s B_s (1-\sigma_c) + \sigma_c B_c$

So difference of thin ice cloud over ocean from clear sky over ocean is given by

$\Delta R = - \varepsilon_s \sigma_c B_s + \sigma_c B_c$

For $B_s > B_c$

$\Delta R = - \sigma_c B_s + \sigma_c B_c = \sigma_c [B_c - B_s]$

As σ_c increases (decreases) then ΔR becomes more negative (positive)

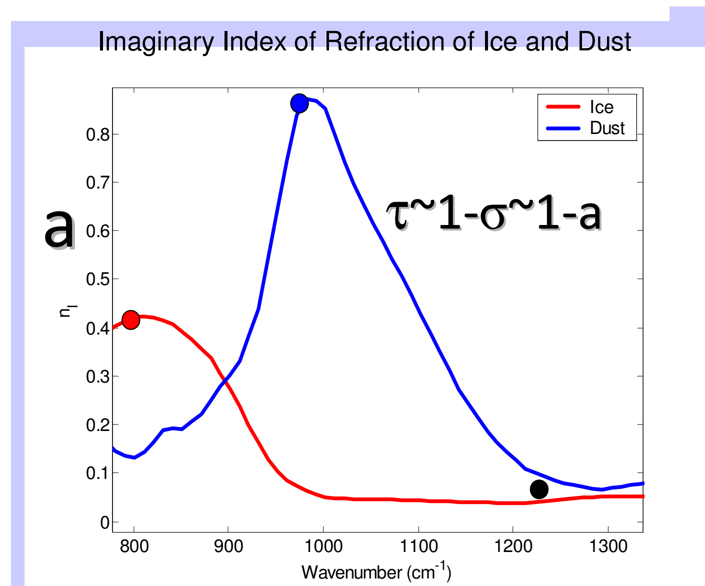

MW Remote Sensing

Microwave Spectral Features

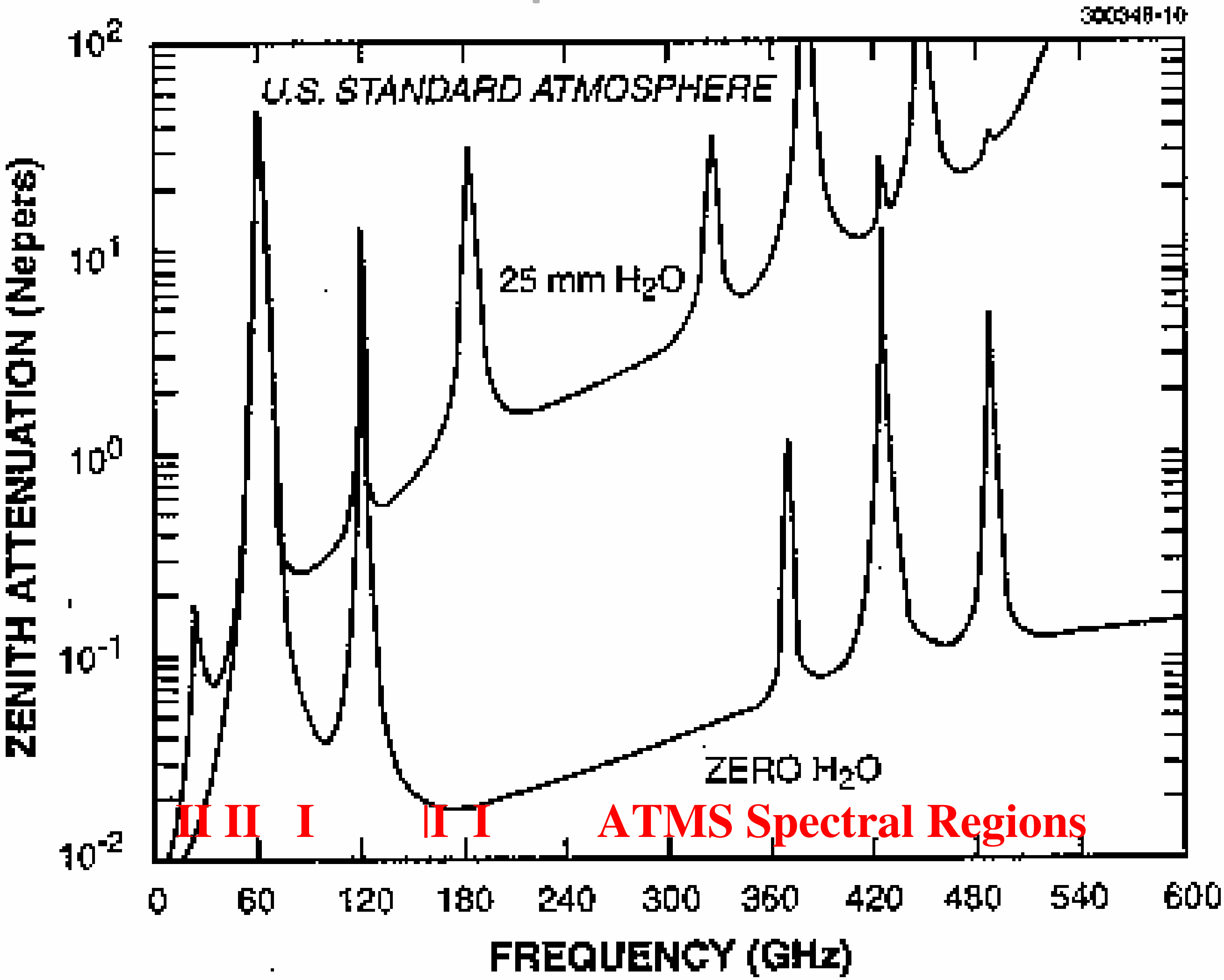

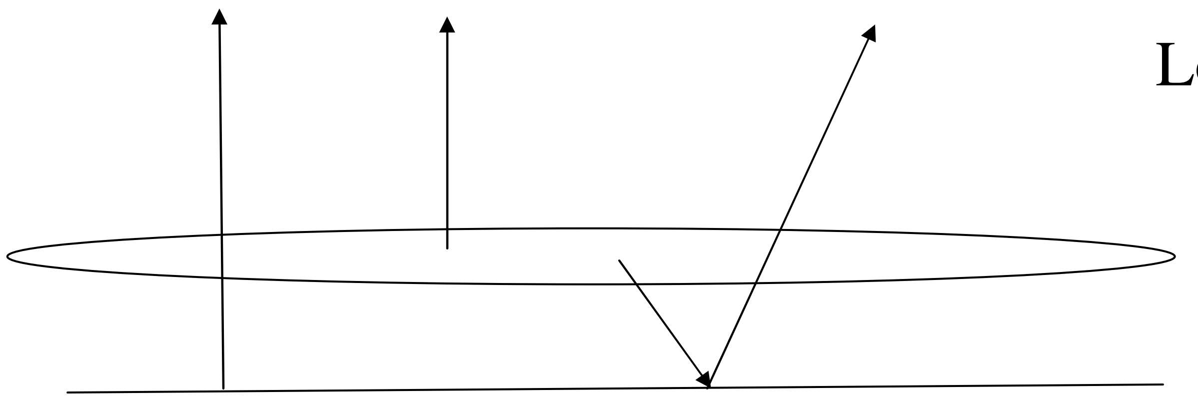

$T_b = \varepsilon_s T_s \tau_m + \varepsilon_m T_m + \varepsilon_m \mathbf{r}_s \tau_m T_m$

$T_b = \varepsilon_s T_s (1-\sigma_m) + \sigma_m T_m + \sigma_m (1-\varepsilon_s) (1-\sigma_m) T_m$

So temperature difference of low moist over ocean from clear sky over ocean is given by

$\Delta T_b = - \varepsilon_s \sigma_m T_s + \sigma_m T_m + \sigma_m (1-\varepsilon_s) (1-\sigma_m) T_m$

For $\varepsilon_s \sim 0.5$ and $T_s \sim T_m$ this is always positive for $0 < \sigma_m < 1$

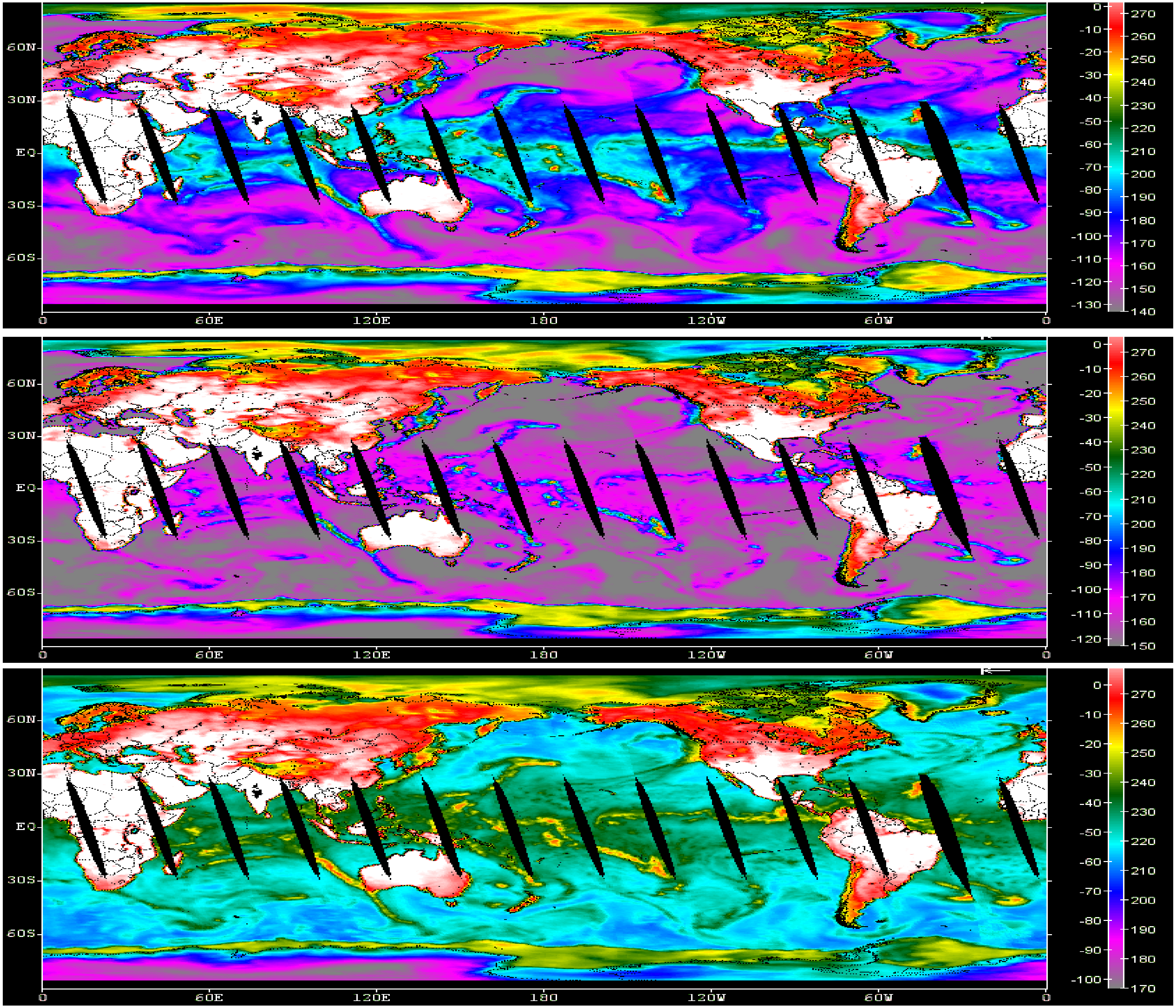

AMSU

23.8

31.4

50.3 GHz

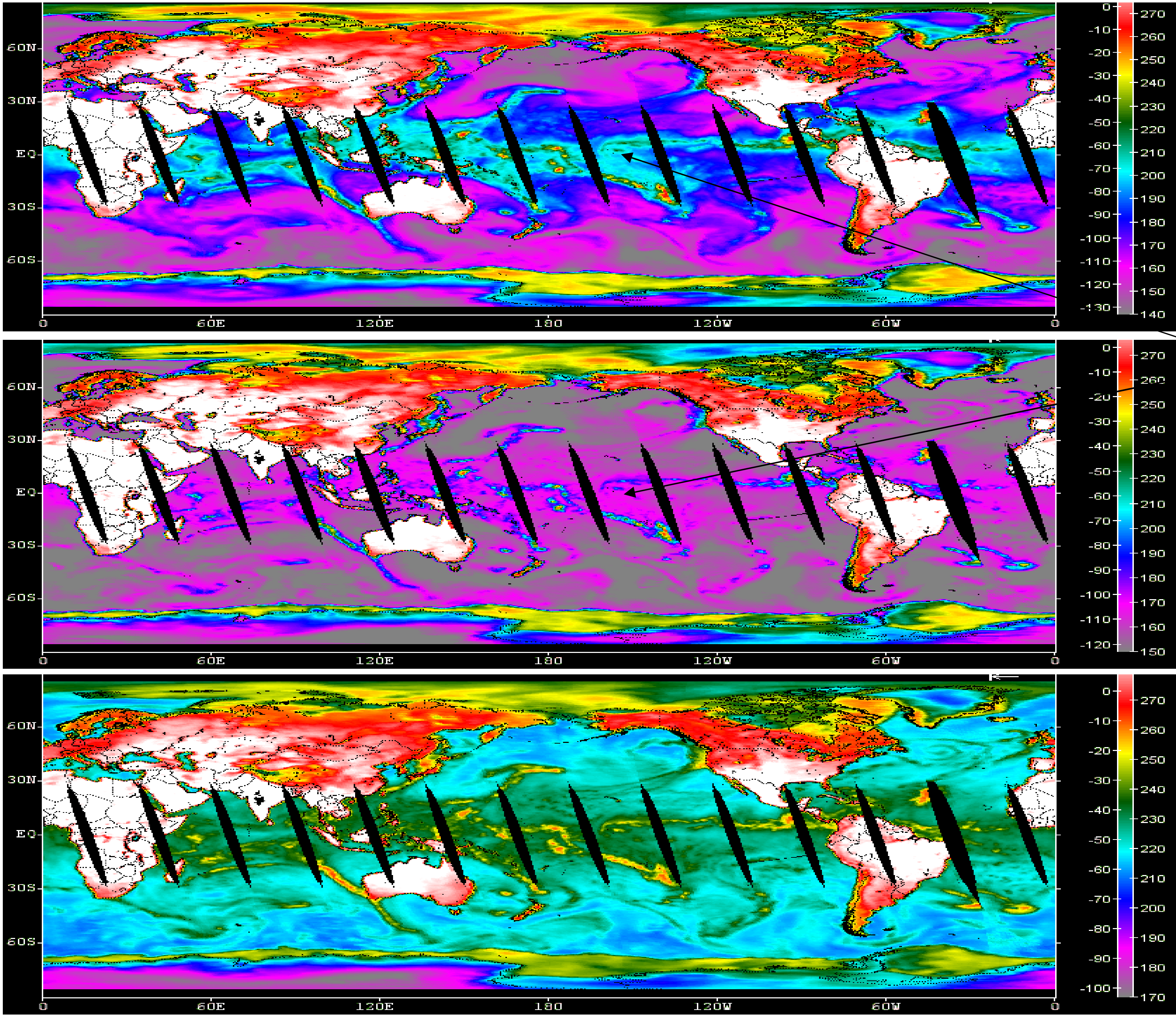

AMSU

23.8
dirty
window

atm Q
warms
BT

31.4
window

50.3
GHz

Transitioning from MODIS to VIIRS for remote sensing of ocean, land, and atmosphere

RT in Earth Atmosphere
Multispectral Signatures
MODIS Heritage Products
VIIRS Instrument Description
Some Anticipated VIIRS Applications
(SST, Ocean Color, Vegetation, Snow, Ice, Clouds, Moisture, Fires, Dust, Low Light Imagery)

W. Paul Menzel, University of Wisconsin- Madison

MODIS Studies Major Climate System Elements

ocean, land, atmosphere

Carbon Cycle

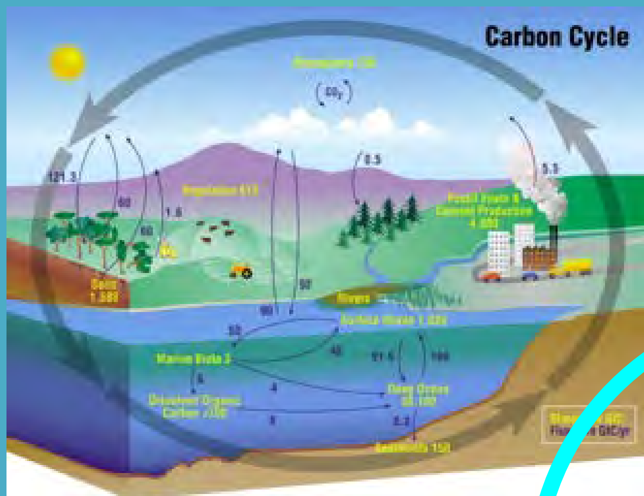

Water & Energy Cycle

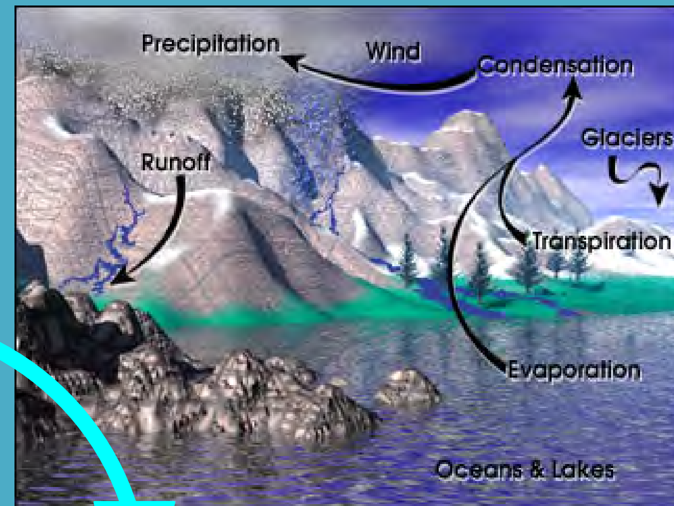

Coupled
Chaotic
Nonlinear

Atmospheric Chemistry

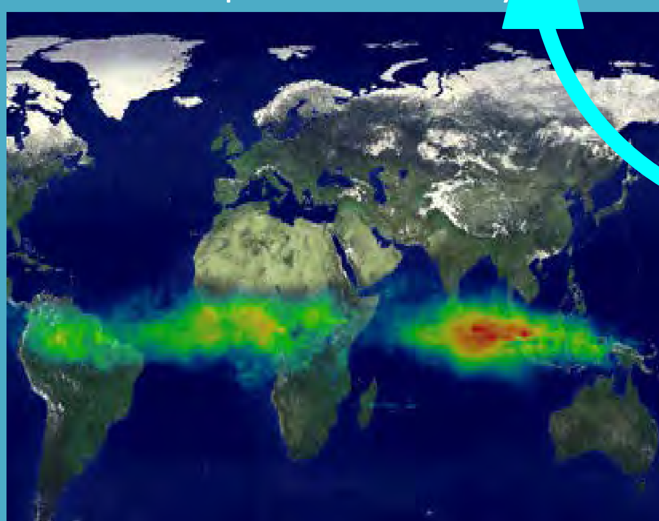

Atmosphere and Ocean Dynamics

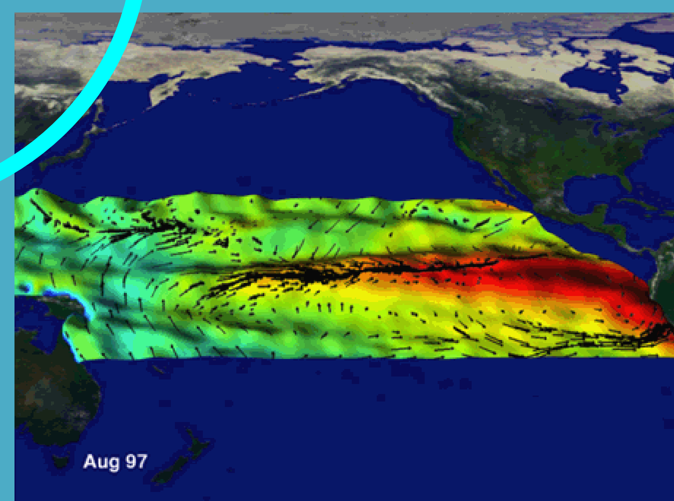

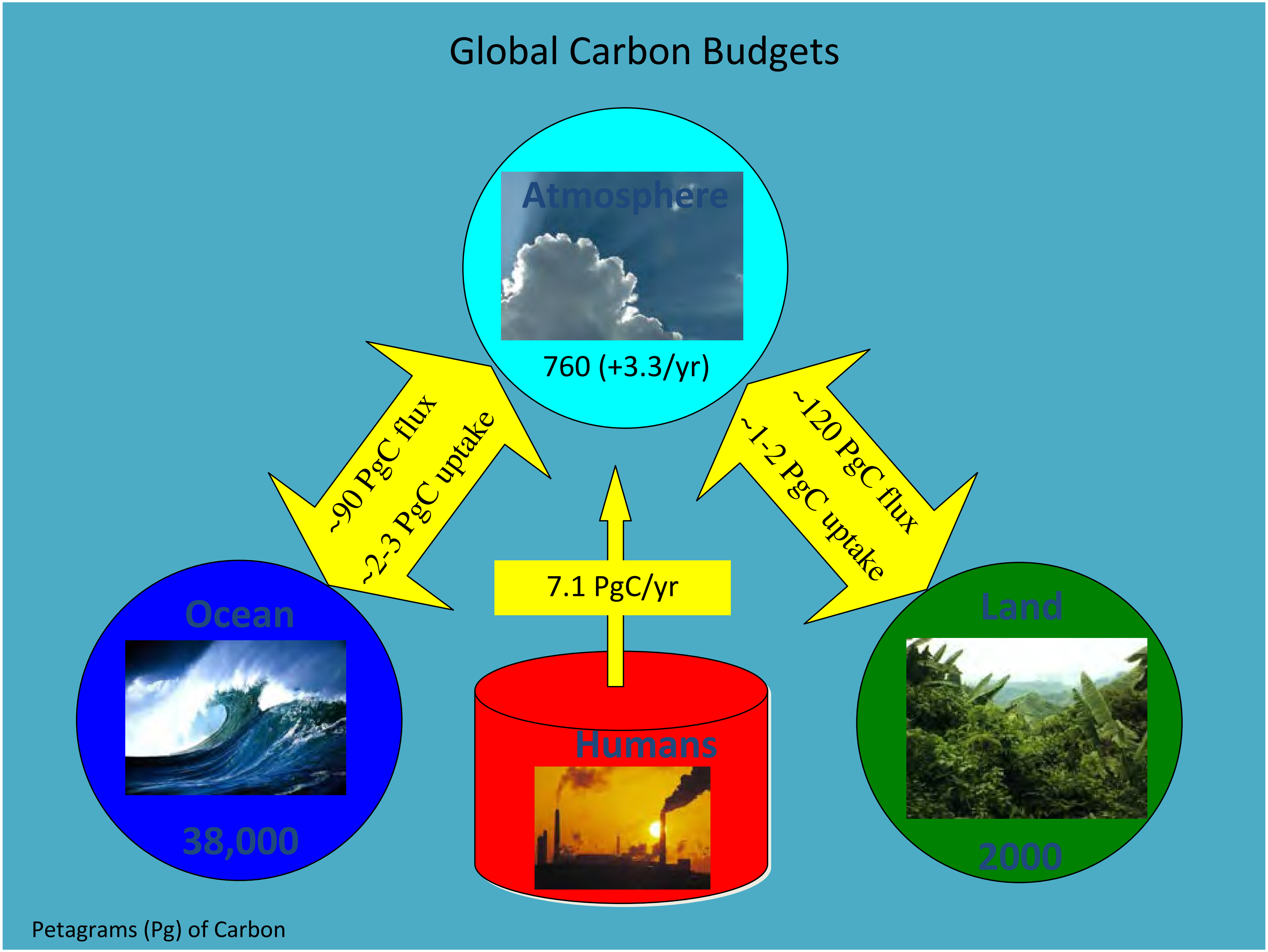
Global Carbon Budgets
Atmosphere
760 (+3.3/yr)
~90 PgC flux
~2-3 PgC uptake
~120 PgC flux
~1-2 PgC uptake
7.1 PgC/yr
Ocean
38,000
Humans
Land
2000
Petagrams (Pg) of Carbon

OCEAN-SOLAR RADIATION

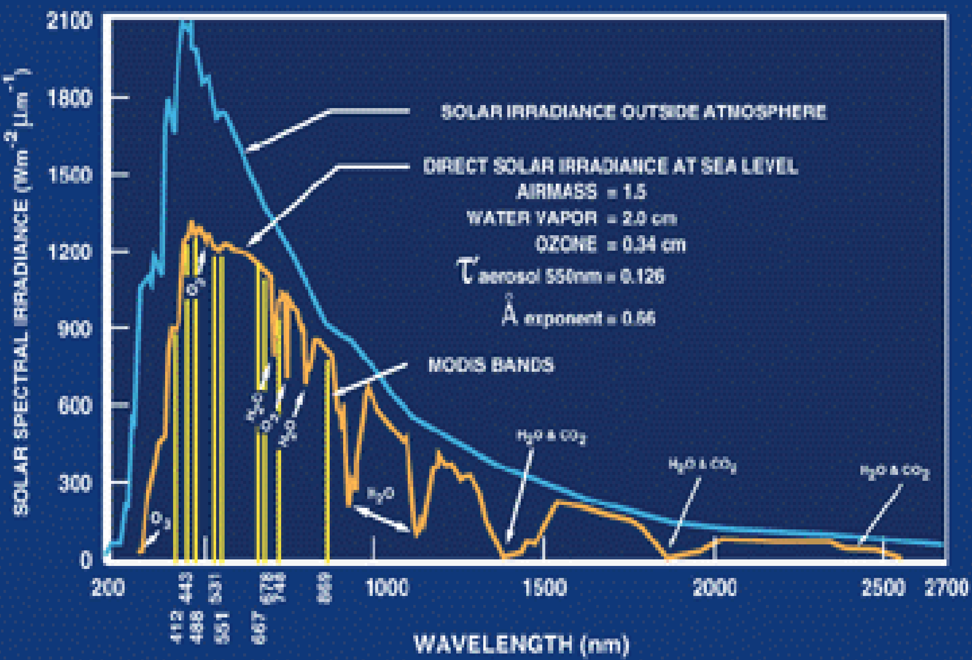

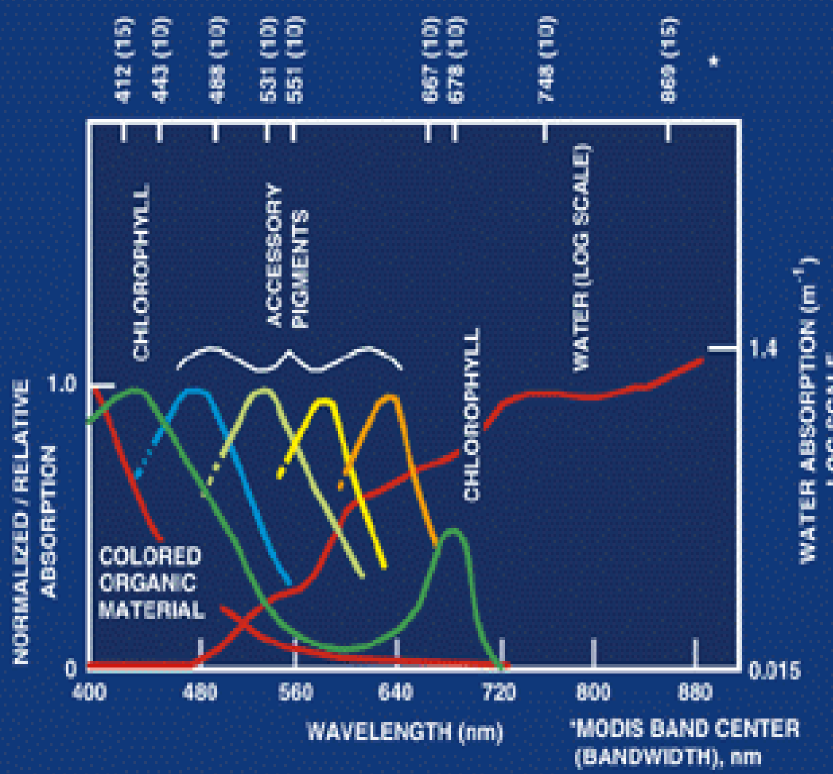

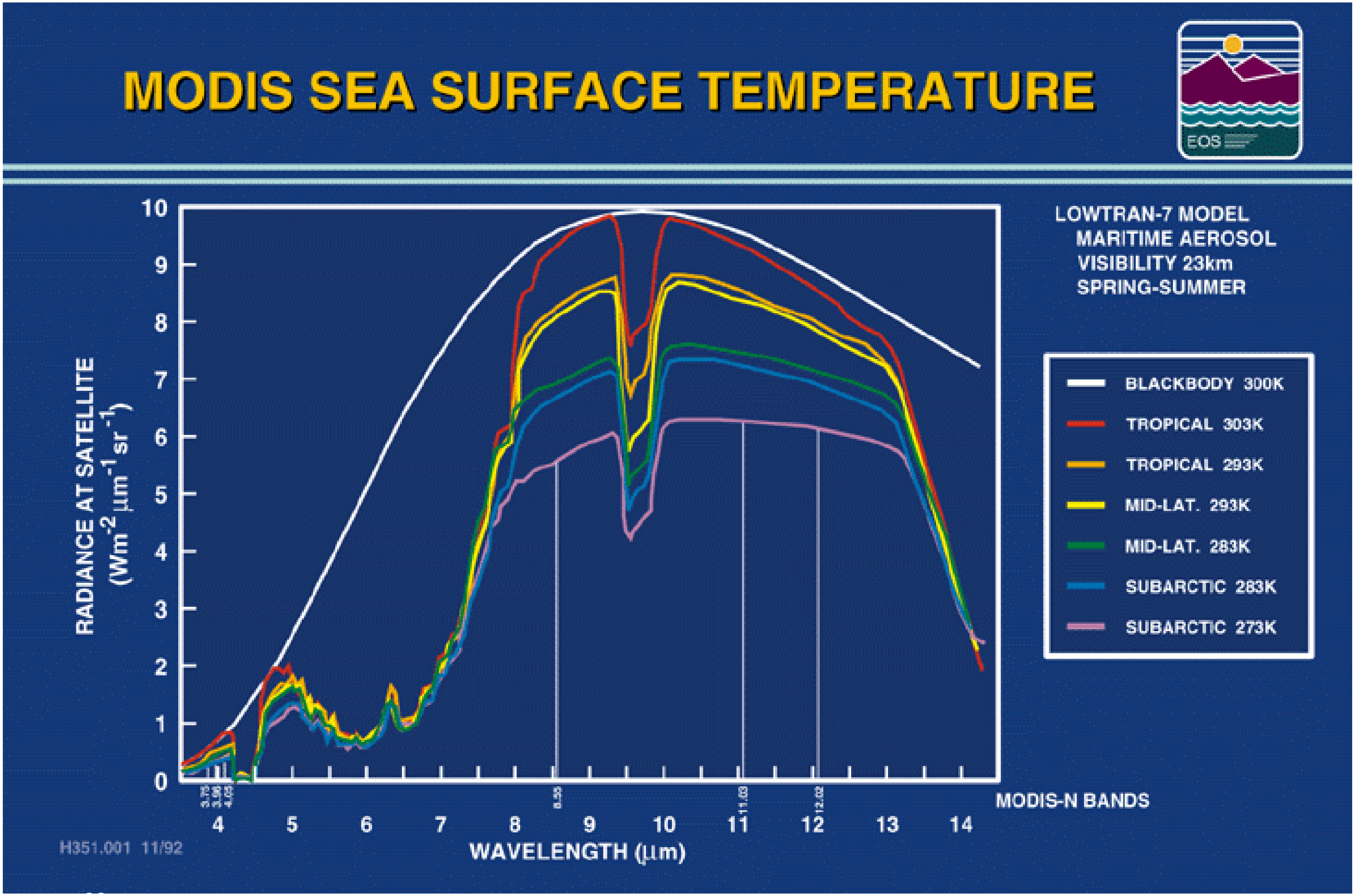
MODIS SEA SURFACE TEMPERATURE
EOS
LOWTRAN-7 MODEL
MARITIME AEROSOL
VISIBILITY 23km
SPRING-SUMMER
BLACKBODY 300K
TROPICAL 303K
TROPICAL 293K
MID-LAT. 293K
MID-LAT. 283K
SUBARCTIC 283K
SUBARCTIC 273K
RADIANCE AT SATELLITE
(Wm-2 µm-1 sr-1)
0
1
2
3
4
5
6
7
8
9
10
MODIS-N BANDS
8.55
11.03
12.02
4
5
6
7
8
9
10
11
12
13
14
WAVELENGTH (µm)
H351.001 11/92

Developing Tools to Monitor Runoff Events in the Bay

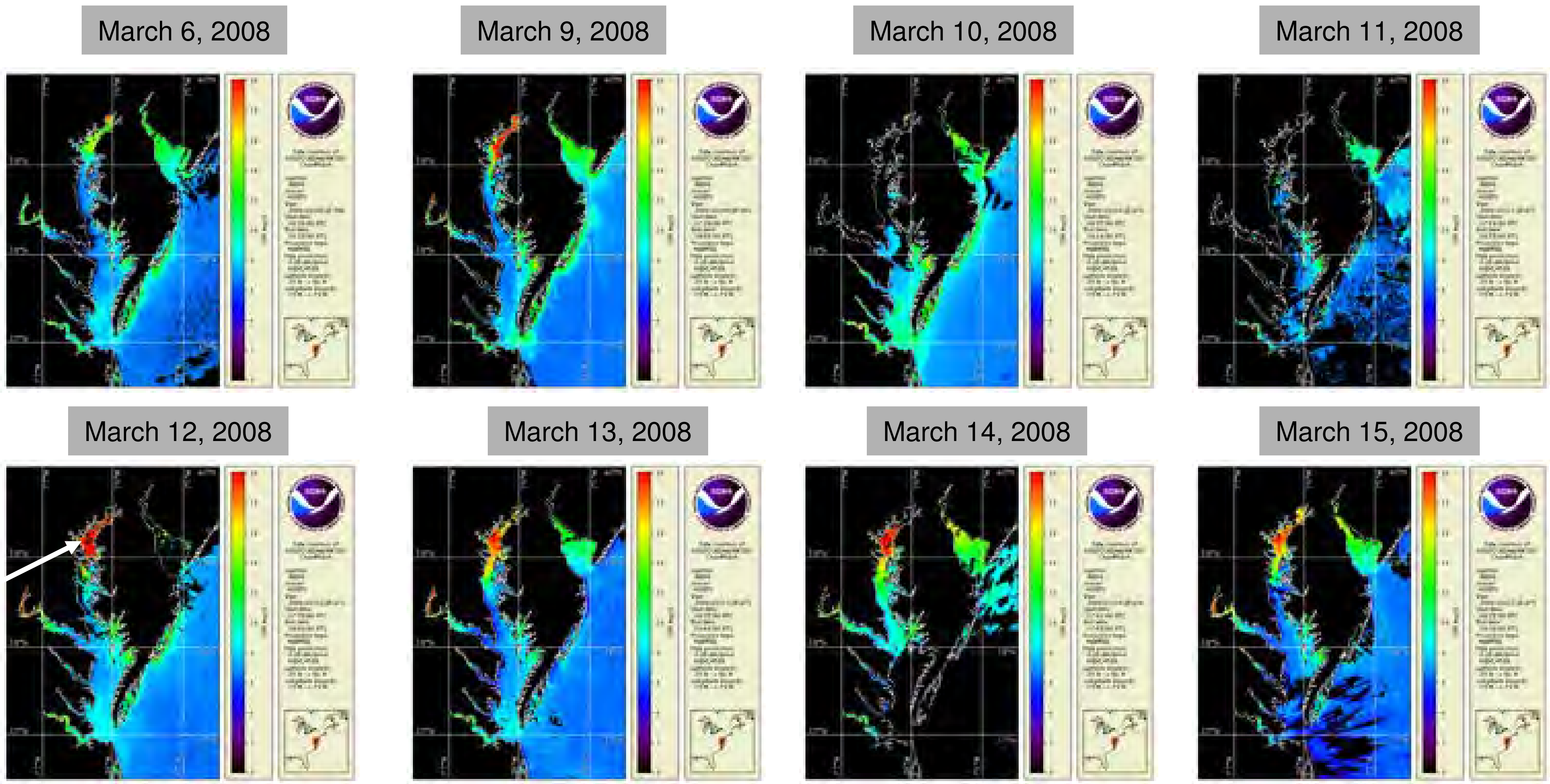

The satellite ocean color products developed by the COCE Team can be utilized to monitor sediment sources and quantify sediments loads into the Chesapeake Bay. Above: The evolution of high sediment loads in the Northern Chesapeake Bay is demonstrated during a record rain event in the Chesapeake Bay Watershed during March 2008.

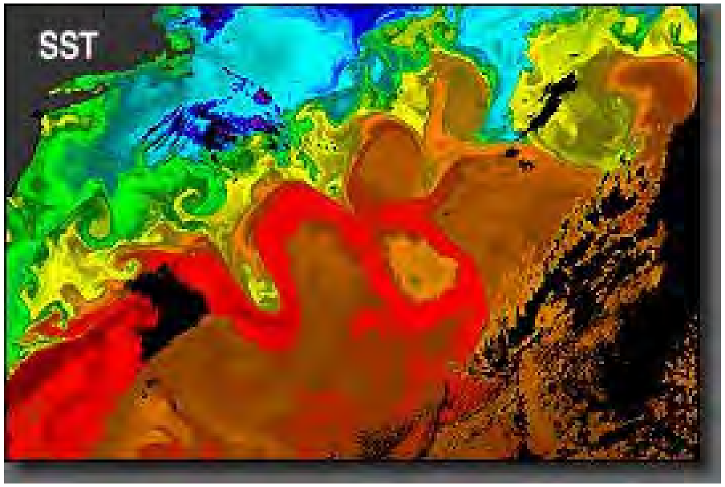

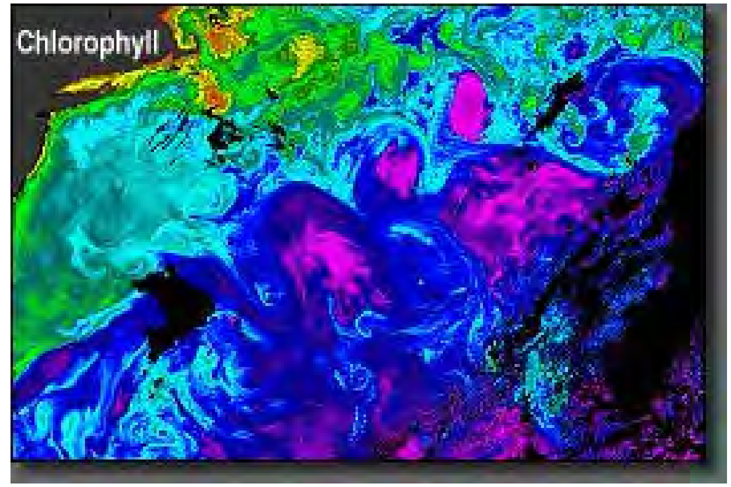

The warm heart of the Gulf Stream is readily apparent in the top SST image. As the current flows toward the northeast it begins to meander and pinch off eddies that transport warm water northward and cold water southward. The current also divides the local ocean into a low-biomass region to the south and a higher-biomass region to the north.

The data were collected by MODIS aboard Aqua on April 18, 2005.

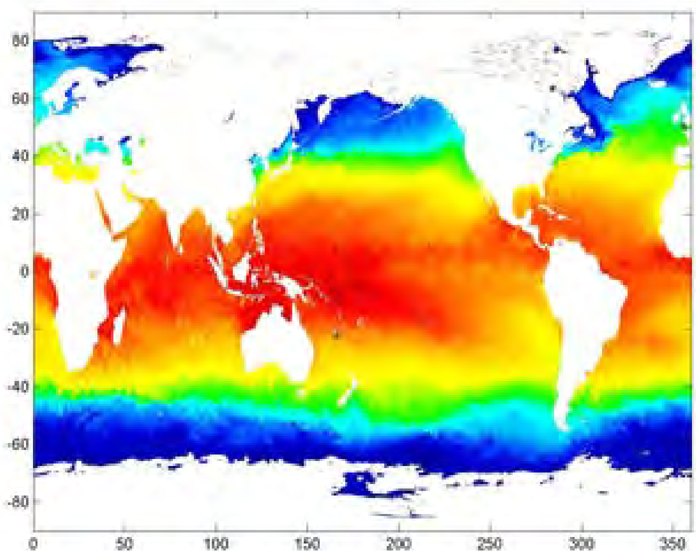
80
60
40
20
0
-20
-40
-60
-80
0
50
100
150
200
250
300
350

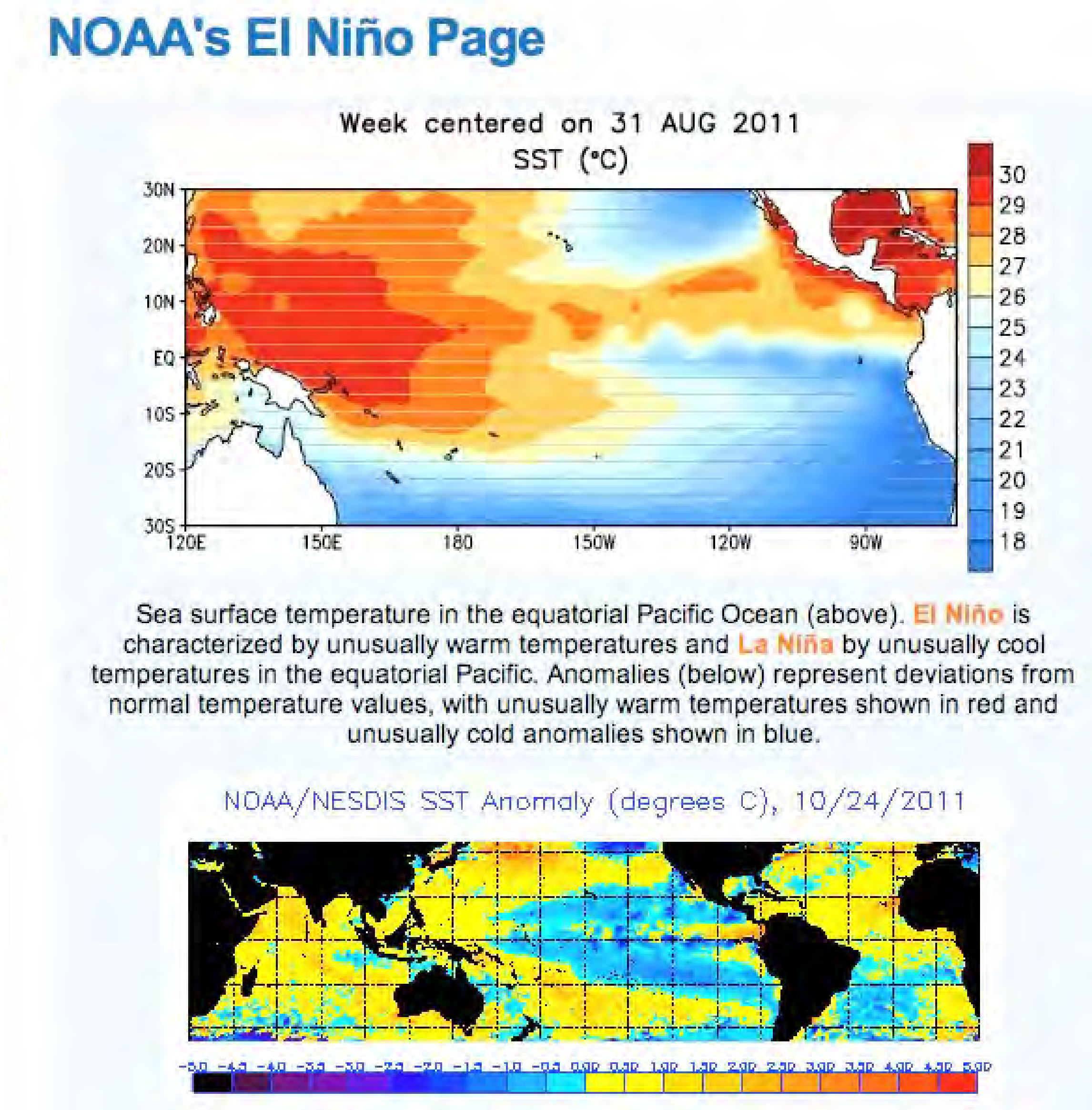
NOAA's El Niño Page
Week centered on 31 AUG 2011
SST (°C)
30N
20N
10N
EQ
10S
20S
30S
120E
150E
180
150W
120W
90W
30
29
28
27
26
25
24
23
22
21
20
19
18
Sea surface temperature in the equatorial Pacific Ocean (above). El Niño is characterized by unusually warm temperatures and La Niña by unusually cool temperatures in the equatorial Pacific. Anomalies (below) represent deviations from normal temperature values, with unusually warm temperatures shown in red and unusually cold anomalies shown in blue.
NOAA/NESDIS SST Anomaly (degrees C), 10/24/2011

MODIS SST

LAND-SOLAR RADIATION

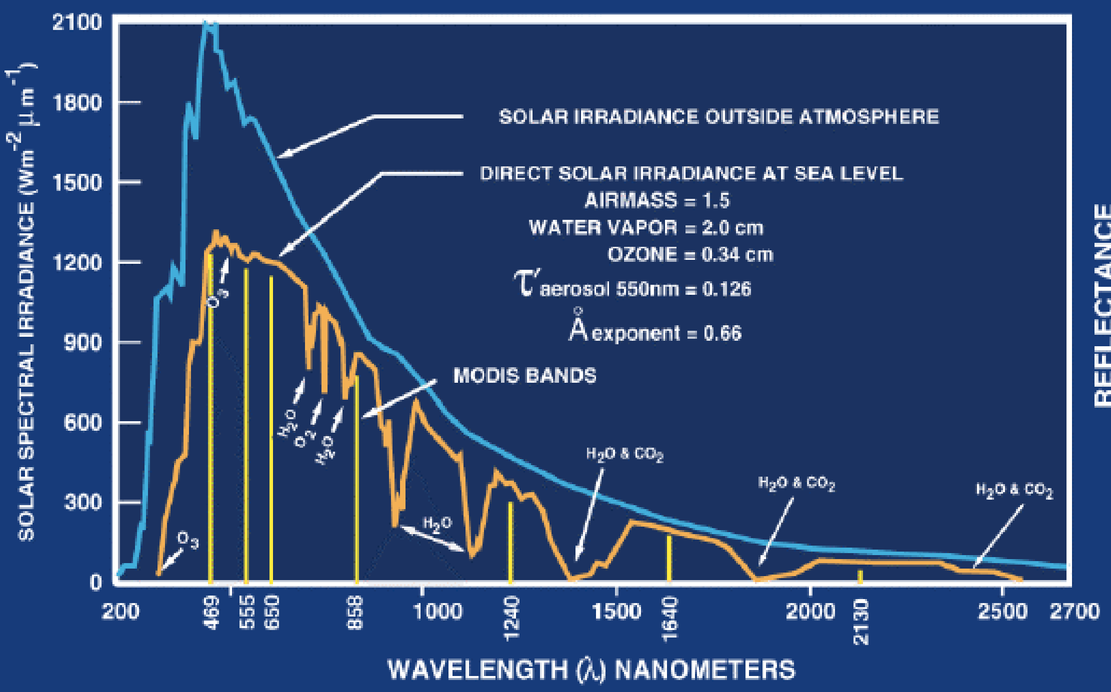

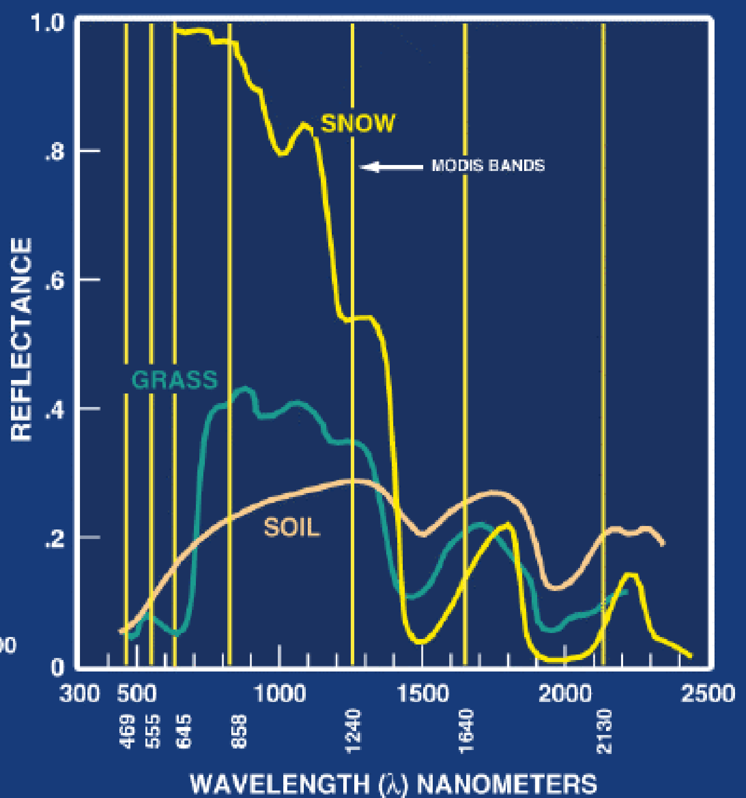

LAND - THERMAL RADIATION

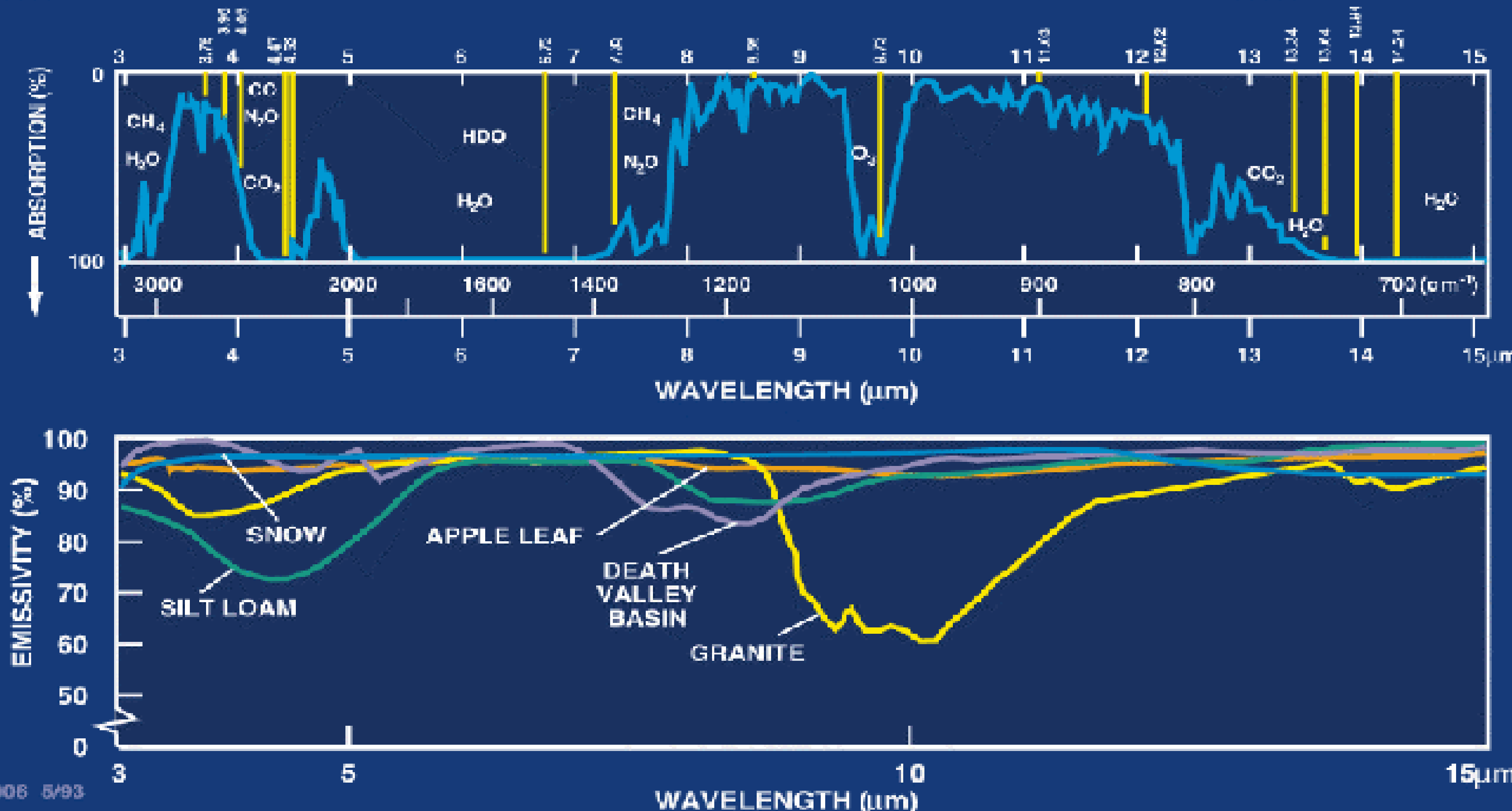

C351.006 5/93

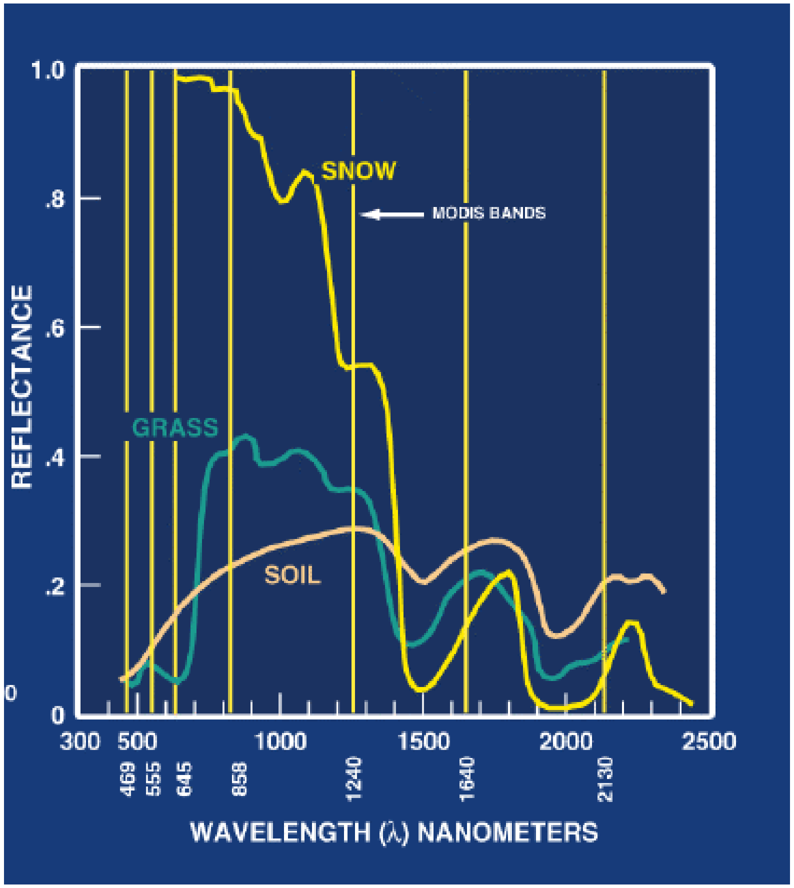

Investigating with Multi-spectral Combinations

Given the spectral response of a surface or atmospheric feature

Select a part of the spectrum where the reflectance or absorption changes with wavelength

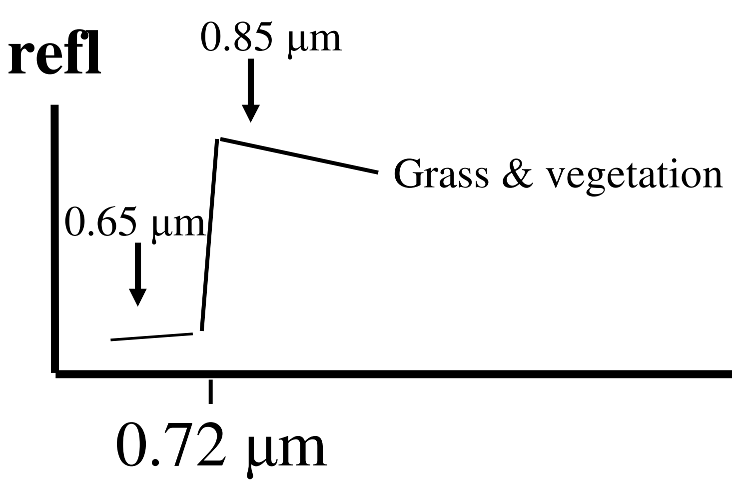

e.g. reflection from grass

If 0.65 µm and 0.85 µm channels see the same reflectance than surface viewed is not grass;
if 0.85 µm sees considerably higher reflectance than 0.65 µm then surface might be grass

Seasonal Biosphere

Ocean Chlorophyll-a & Terrestrial NDVI

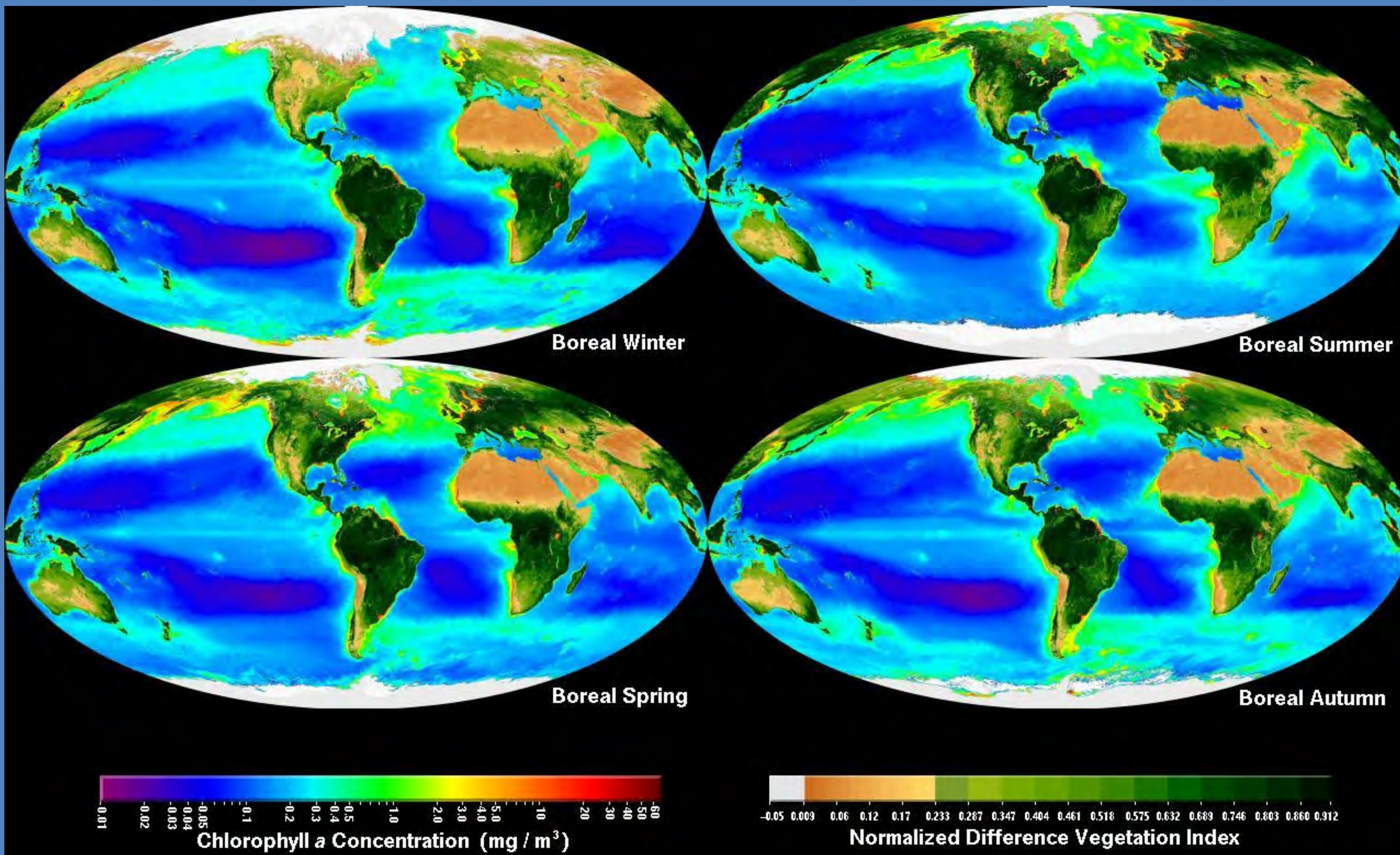

Global Fires

ATMOSPHERE-SOLAR RADIATION

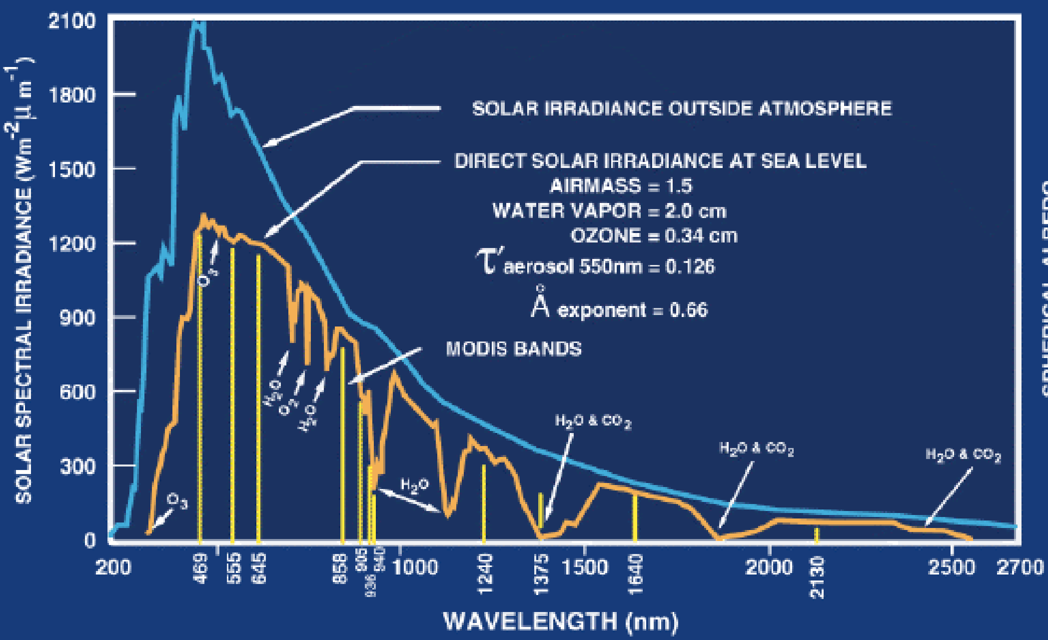

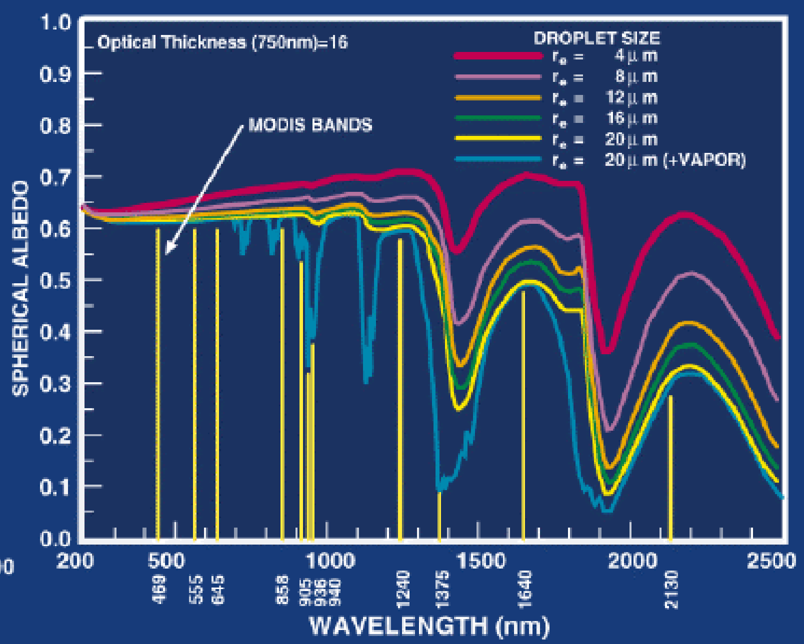

ATMOSPHERE - THERMAL RADIATION

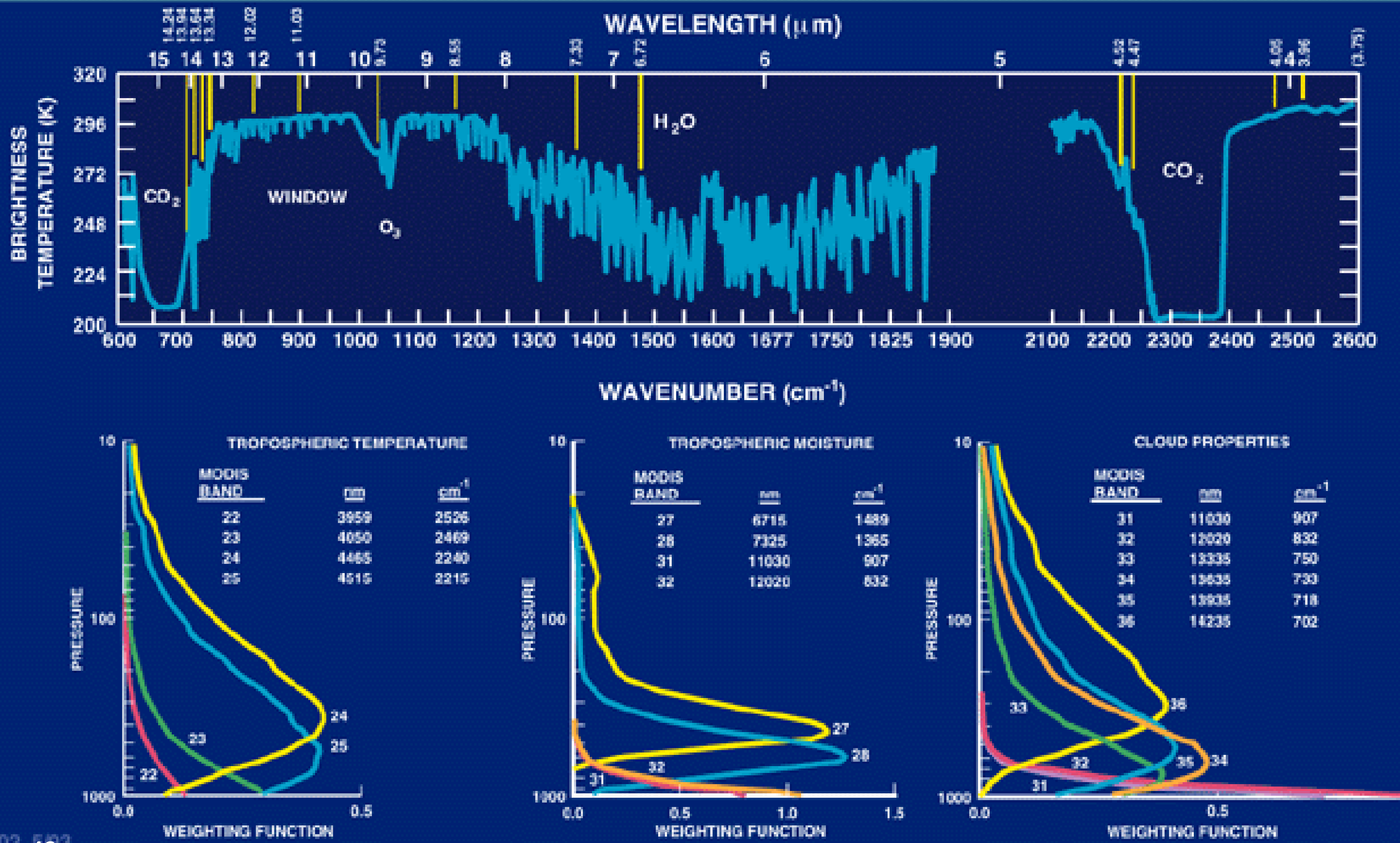

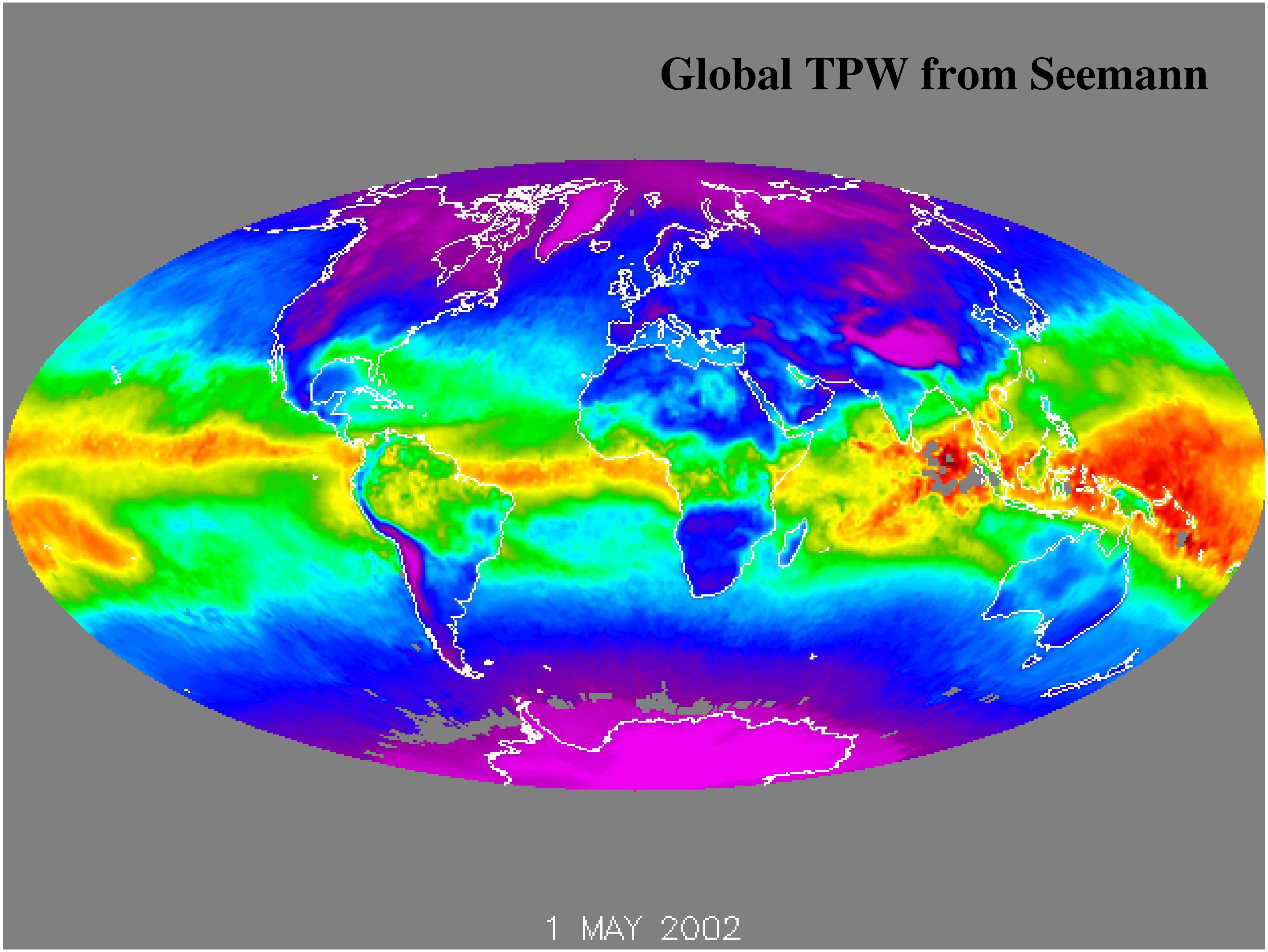
Global TPW from Seemann
1 MAY 2002

ATMOSPHERE - CLEAR SKY THERMAL EMISSION

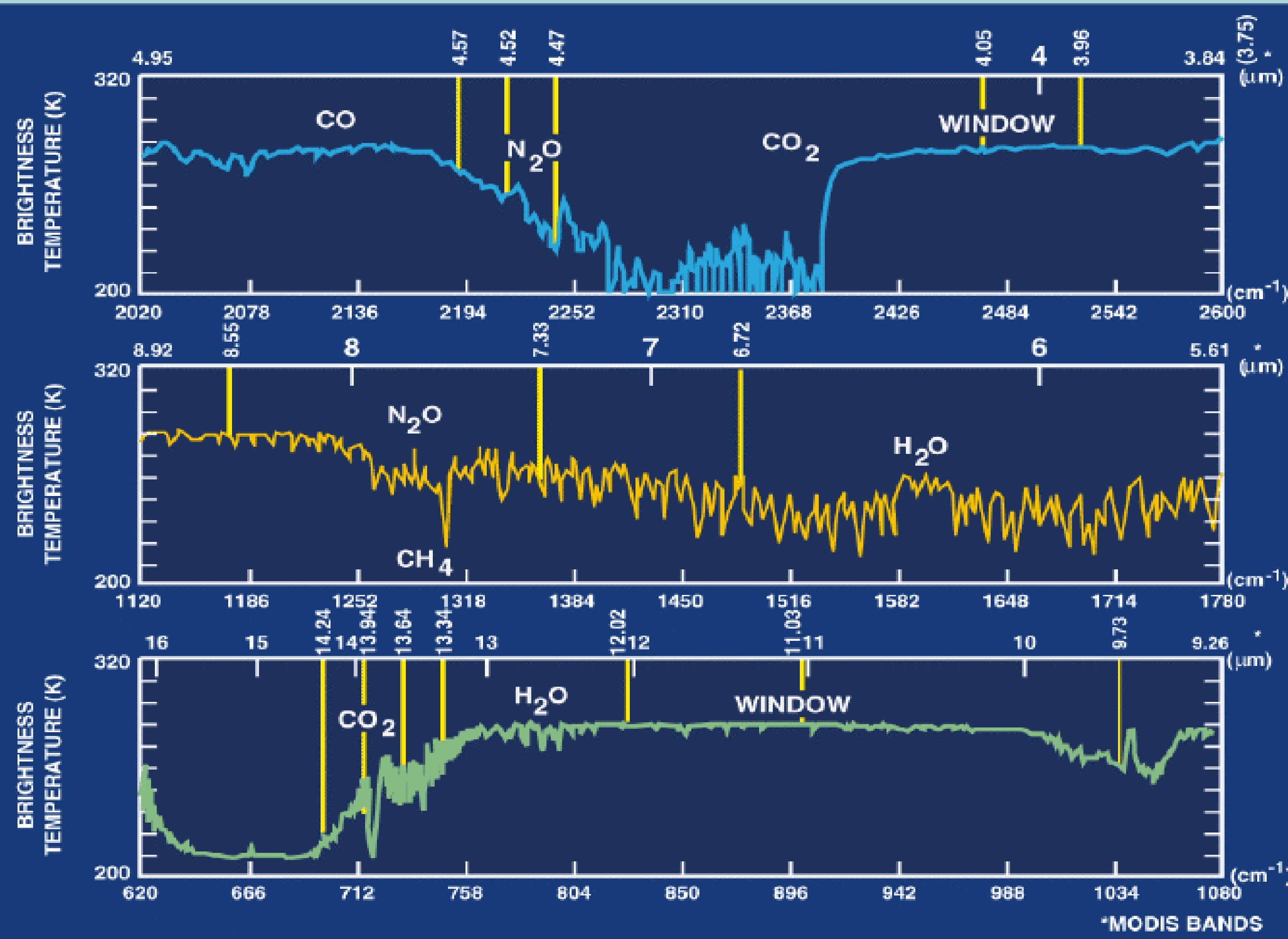

002 11/92

Snow/Cloud Discrimination

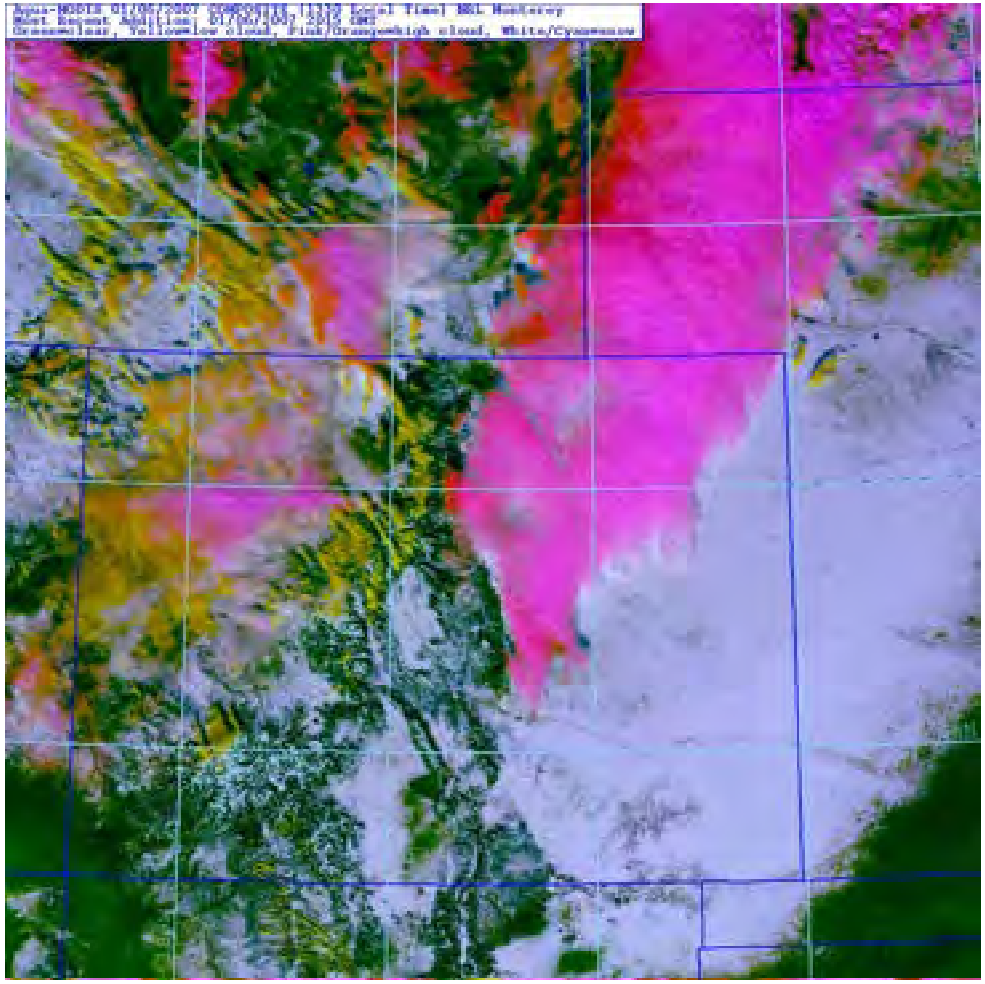

Quadri-spectral

0.6 (VIS)
1.38 (CIR)
1.6 (SIR)
11.0 (TIR)

Snow/Cloud Example with MODIS

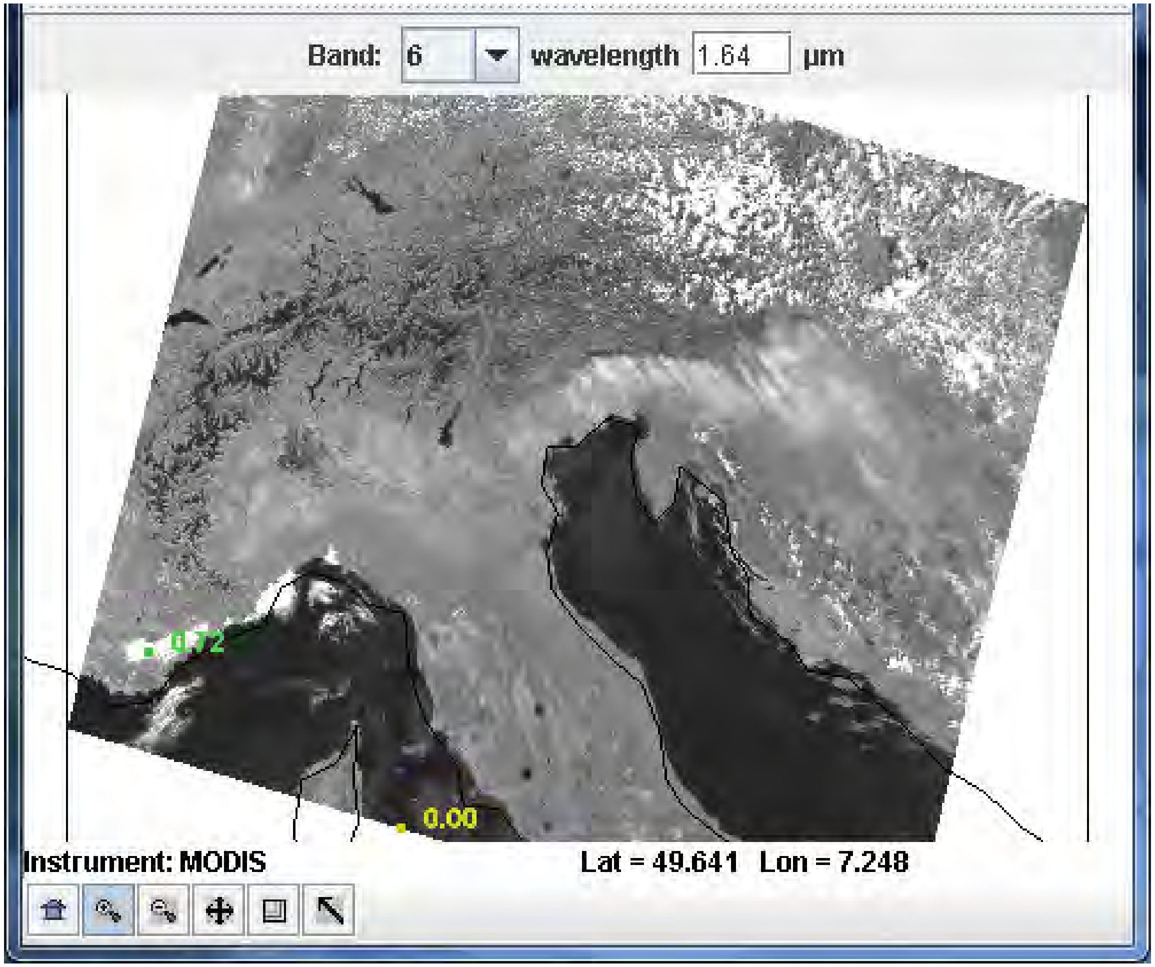

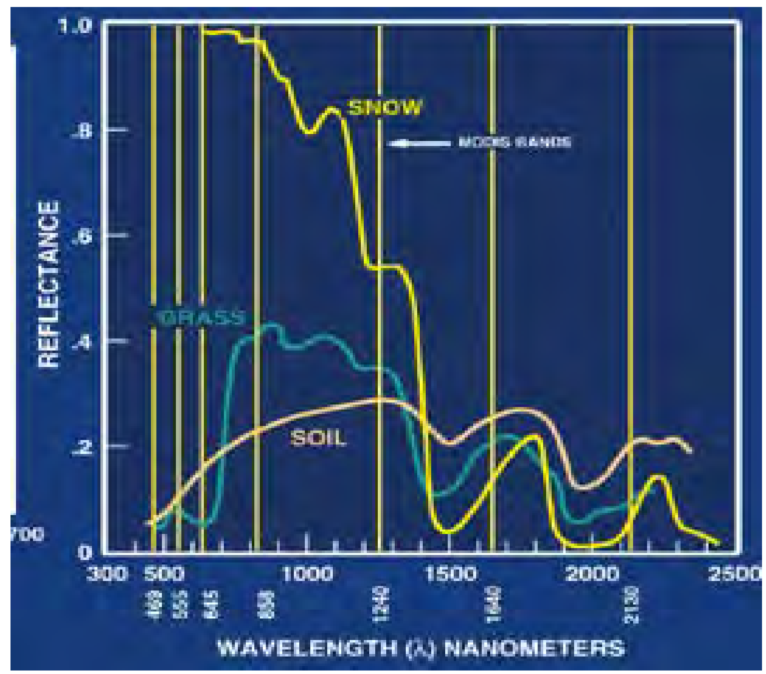

low refl at 1.6 um from snow in mountains

Snow/Cloud Example with MODIS

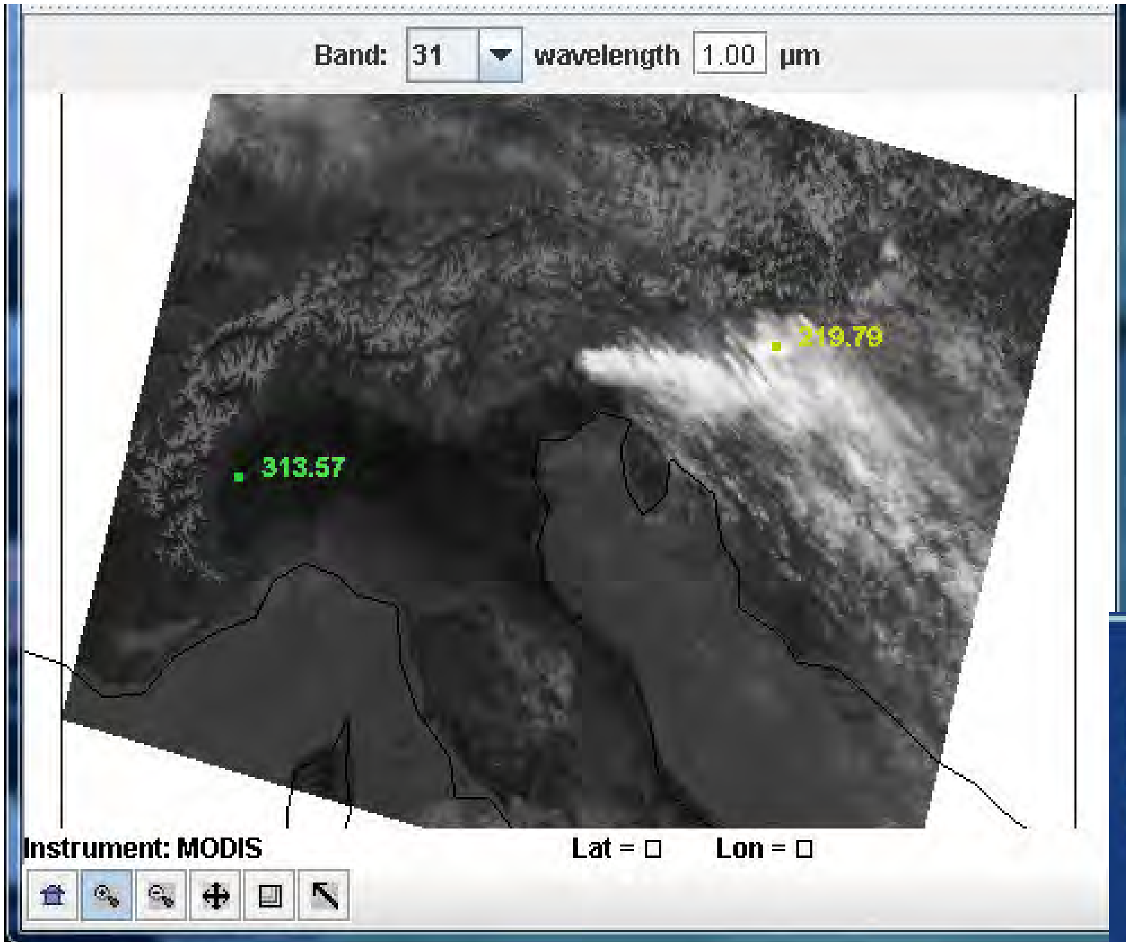

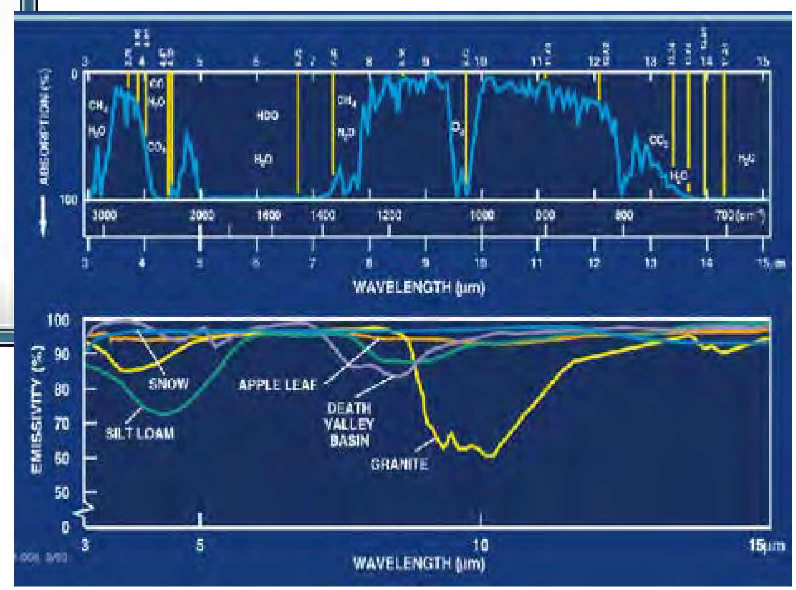

Low temp from clouds and ice at 11 um

Snow/Cloud Example with MODIS

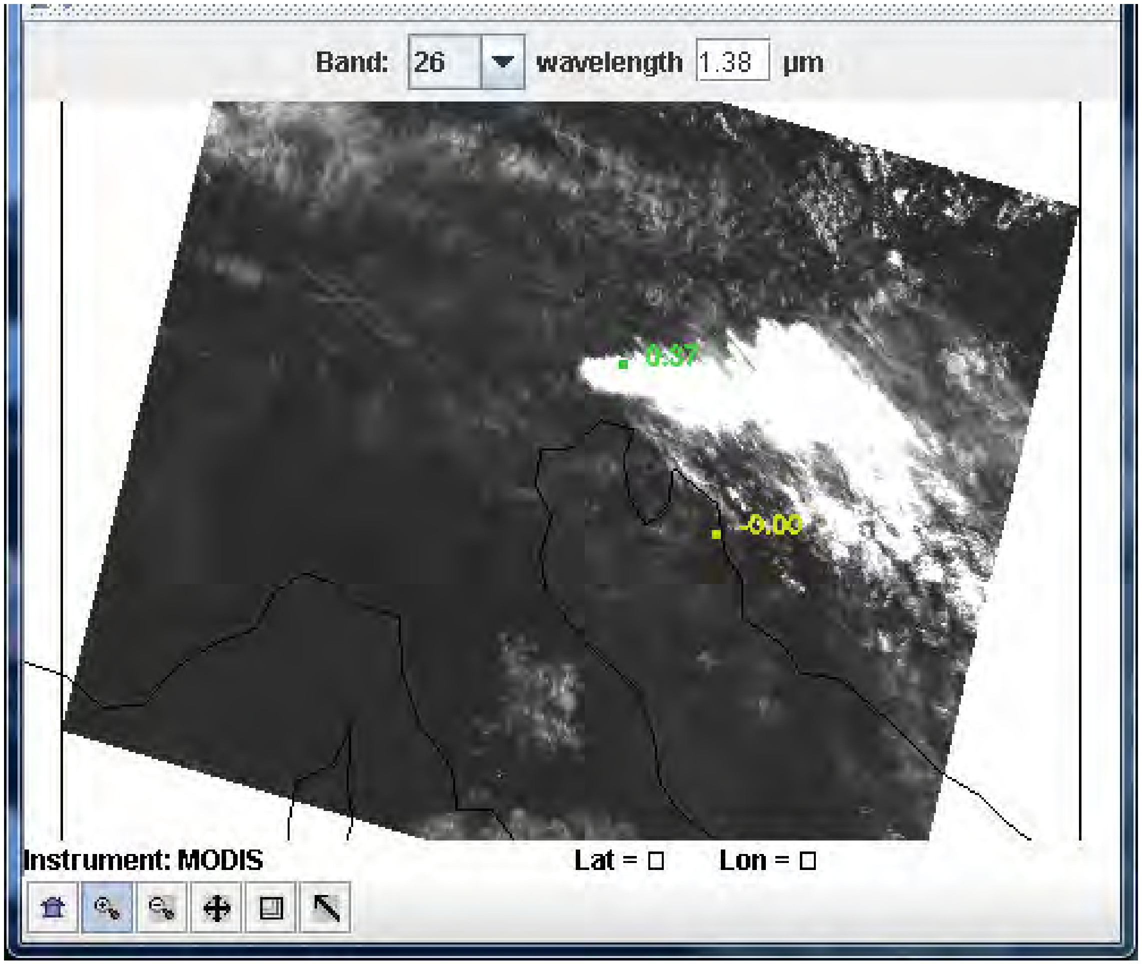

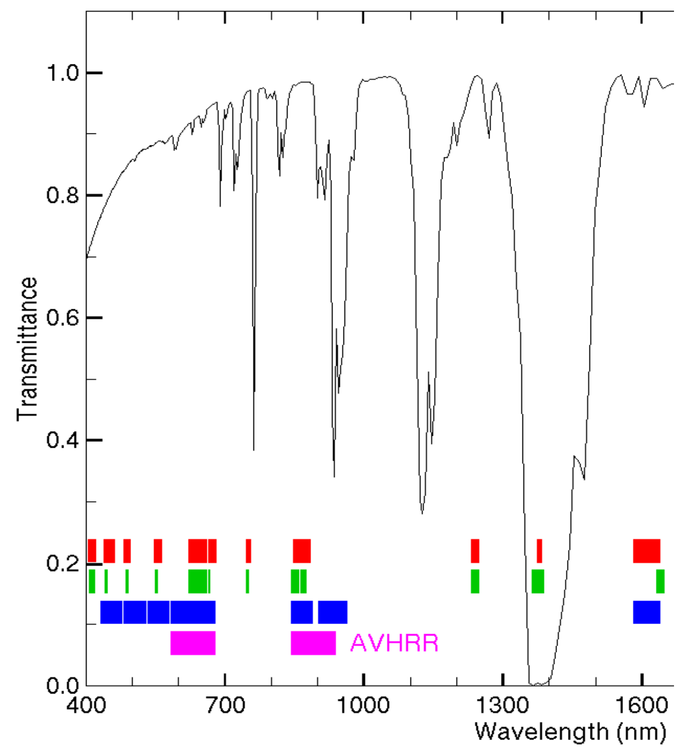

high refl at 1.38 um from high ice clouds

MODIS identifies cloud classes

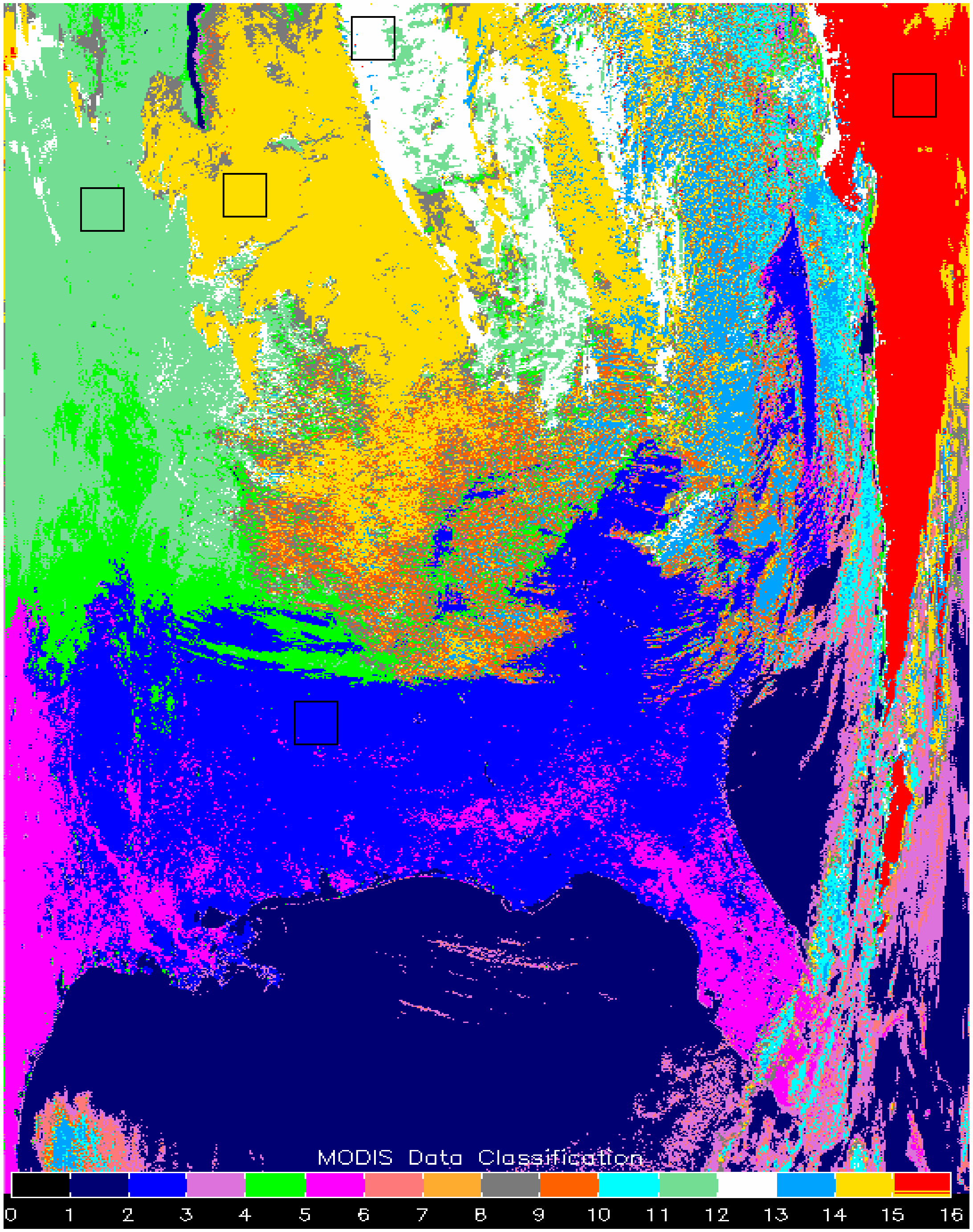

Hi cld

Mid cld

Lo cld

Snow

clr

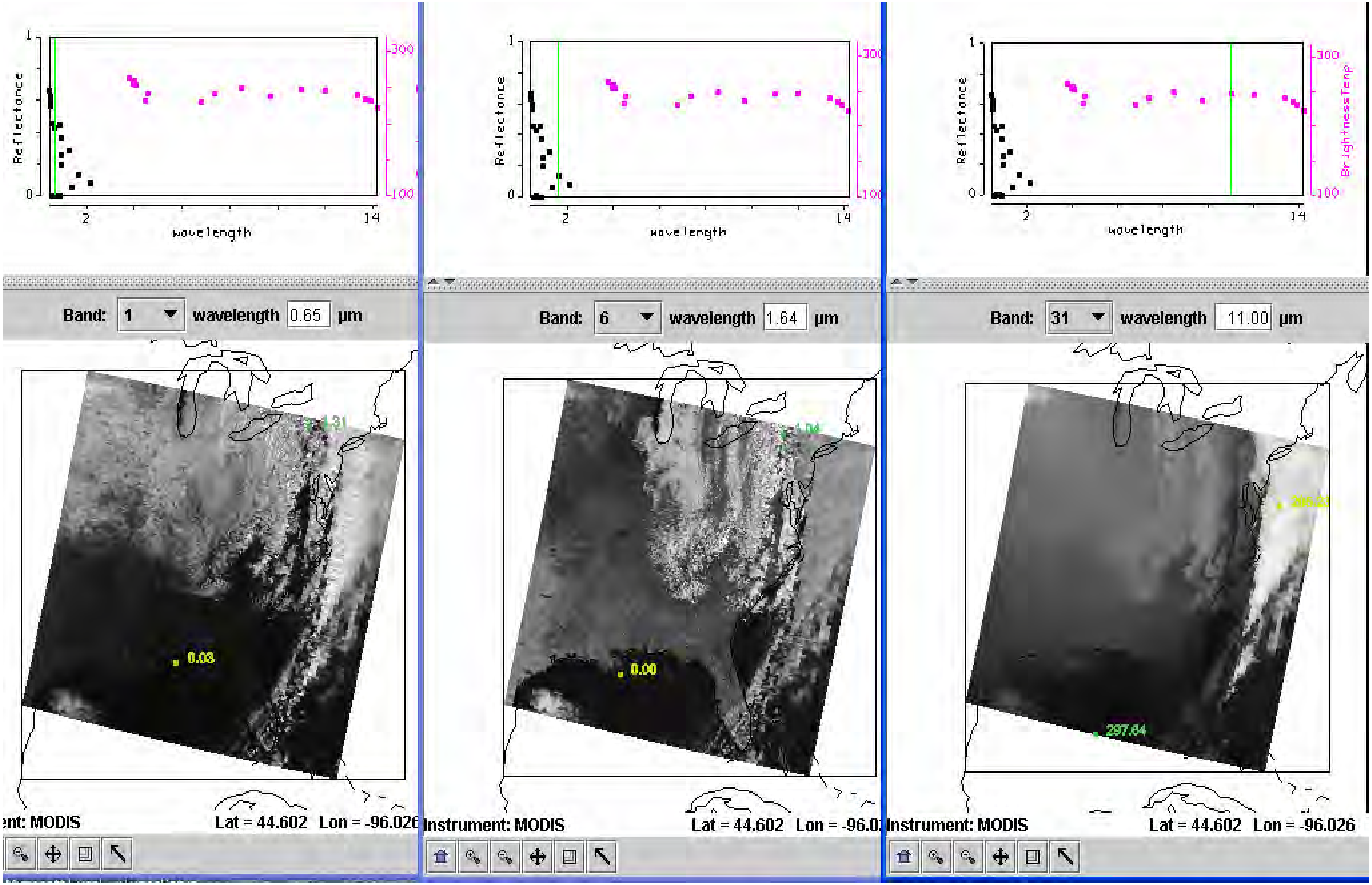

Reflectance
wavelength
BrightnessTemp
Band: 1 wavelength 0.65 µm
0.03
ent: MODIS
Lat = 44.602 Lon = -96.026
Band: 6 wavelength 1.64 µm
0.00
Instrument: MODIS
Lat = 44.602 Lon = -96.0
Band: 31 wavelength 11.00 µm
297.64
Instrument: MODIS
Lat = 44.602 Lon = -96.026

Clouds separate into classes when multispectral radiance information is viewed

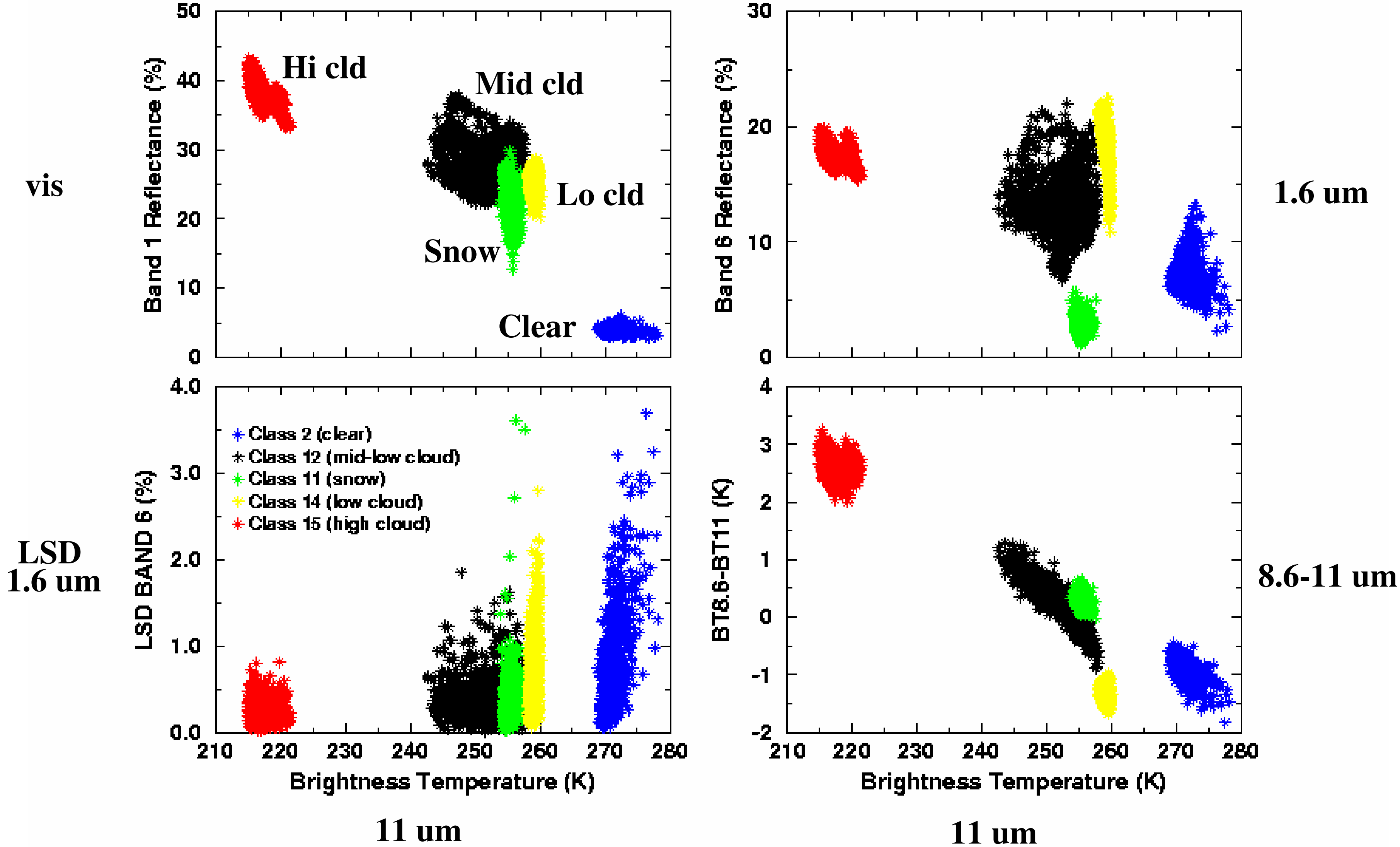

Cloud Properties

True Color Image
Cloud Mask
Land Classification
Cloud Opt Thickness
Cloud Eff Radius
Cloud Top Temp
Bispectral Phase

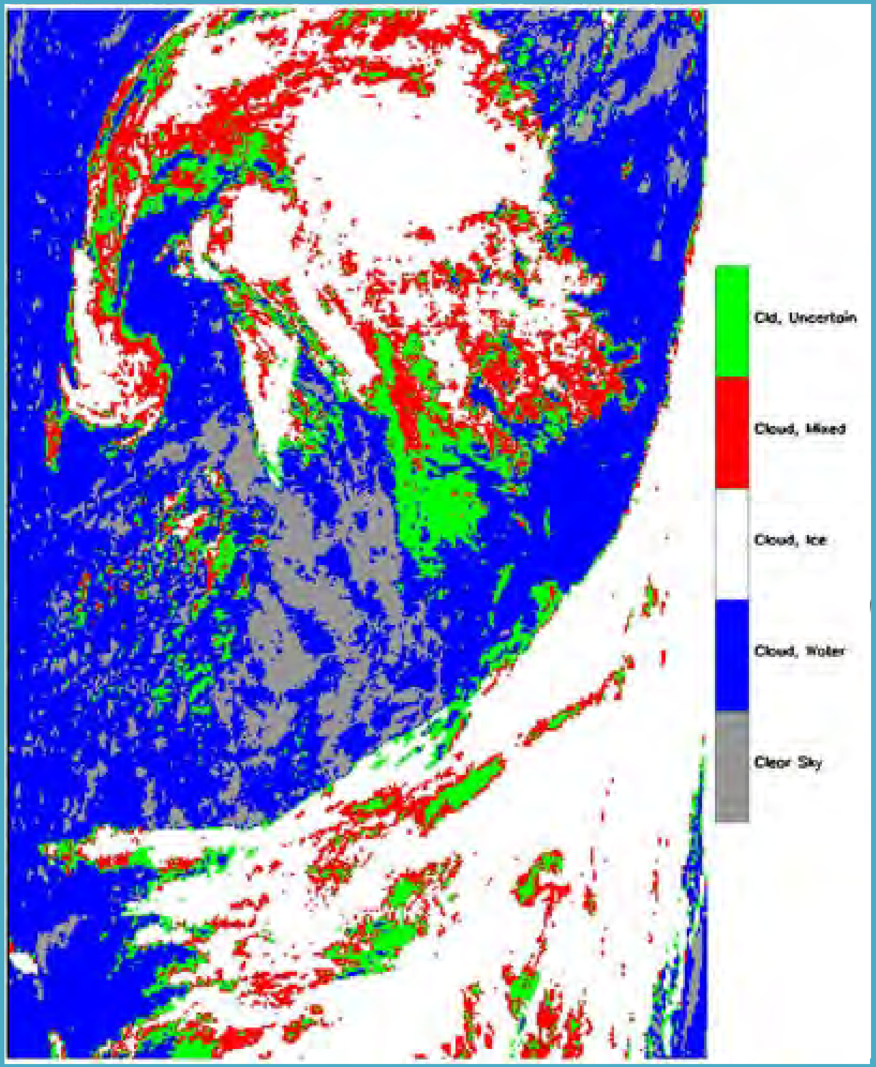

October 1, 2001

Monthly Mean Cloud Fraction (Cloud Mask)

(S. A. Ackerman, R. A. Frey et al. – Univ. Wisconsin)

April 2005
Aqua C5

Cloud_Fraction_Day
_Mean_Mean

Cloud_Fraction_Night
_Mean_Mean

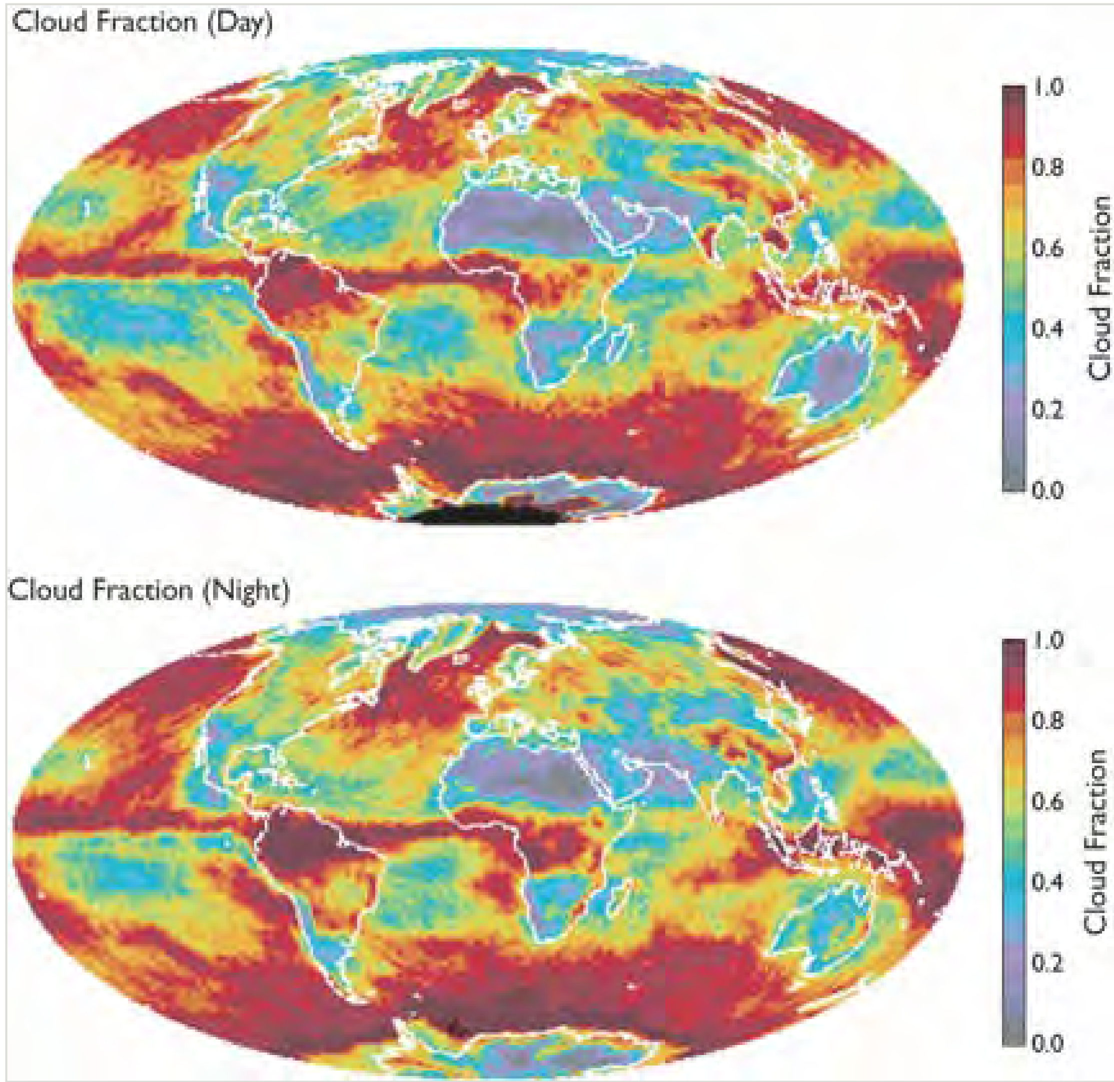

Monthly Mean Cloud Optical Thickness

(M. D. King, S. Platnick et al. – NASA GSFC)

April 2005
Aqua C5 (QA mean)

Cloud_Optical_Thickness_Liquid_QA_Mean_Mean

Cloud_Optical_Thickness_Ice_QA_Mean_Mean

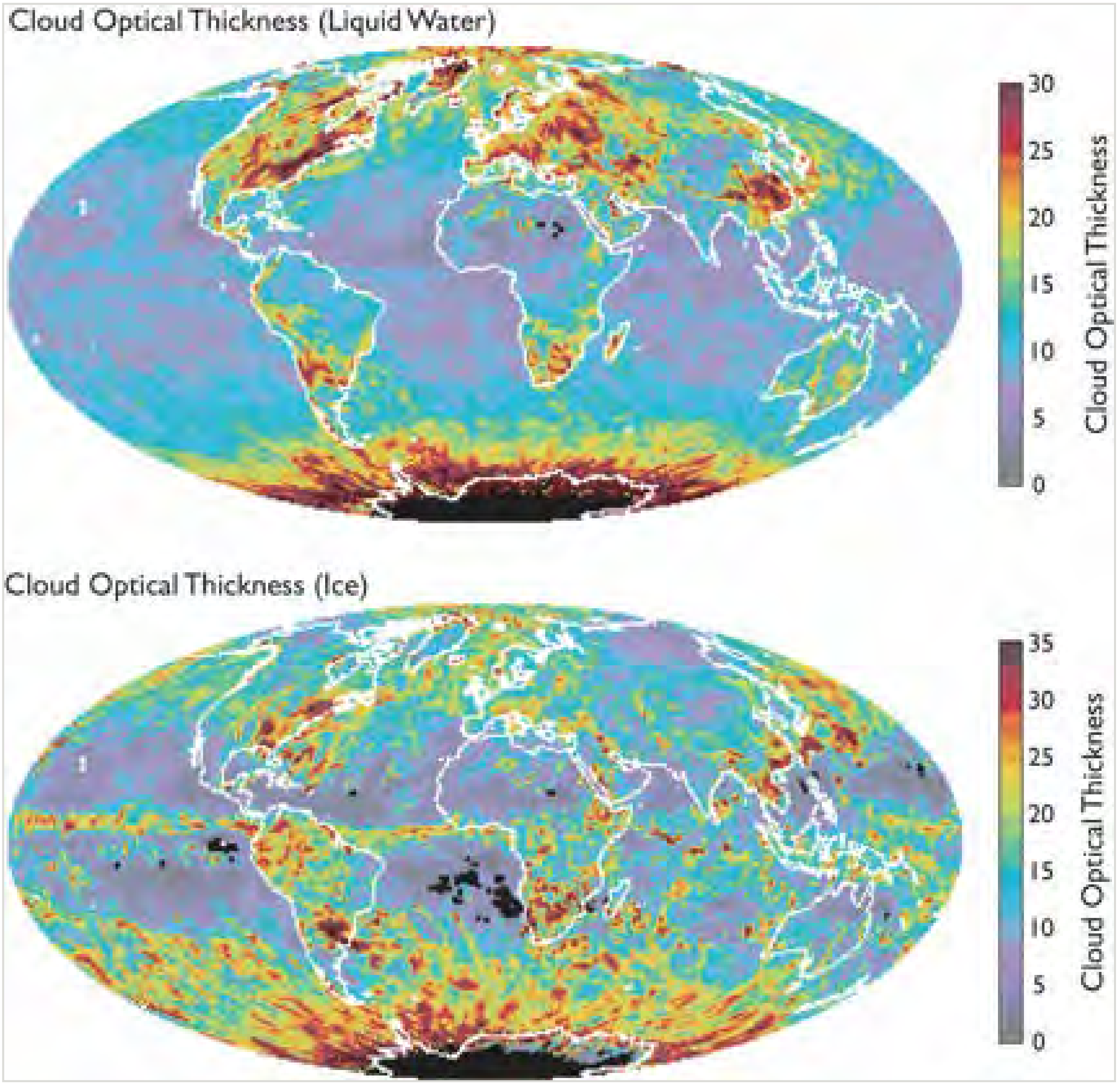

Monthly Mean Cloud Effective Radius

(M. D. King, S. Platnick et al. – NASA GSFC)

April 2005
Aqua C5 (QA mean)

Cloud_Effective_Radius _Liquid_QA_Mean_Mean

Cloud_Effective_Radius _Ice_QA_Mean_Mean

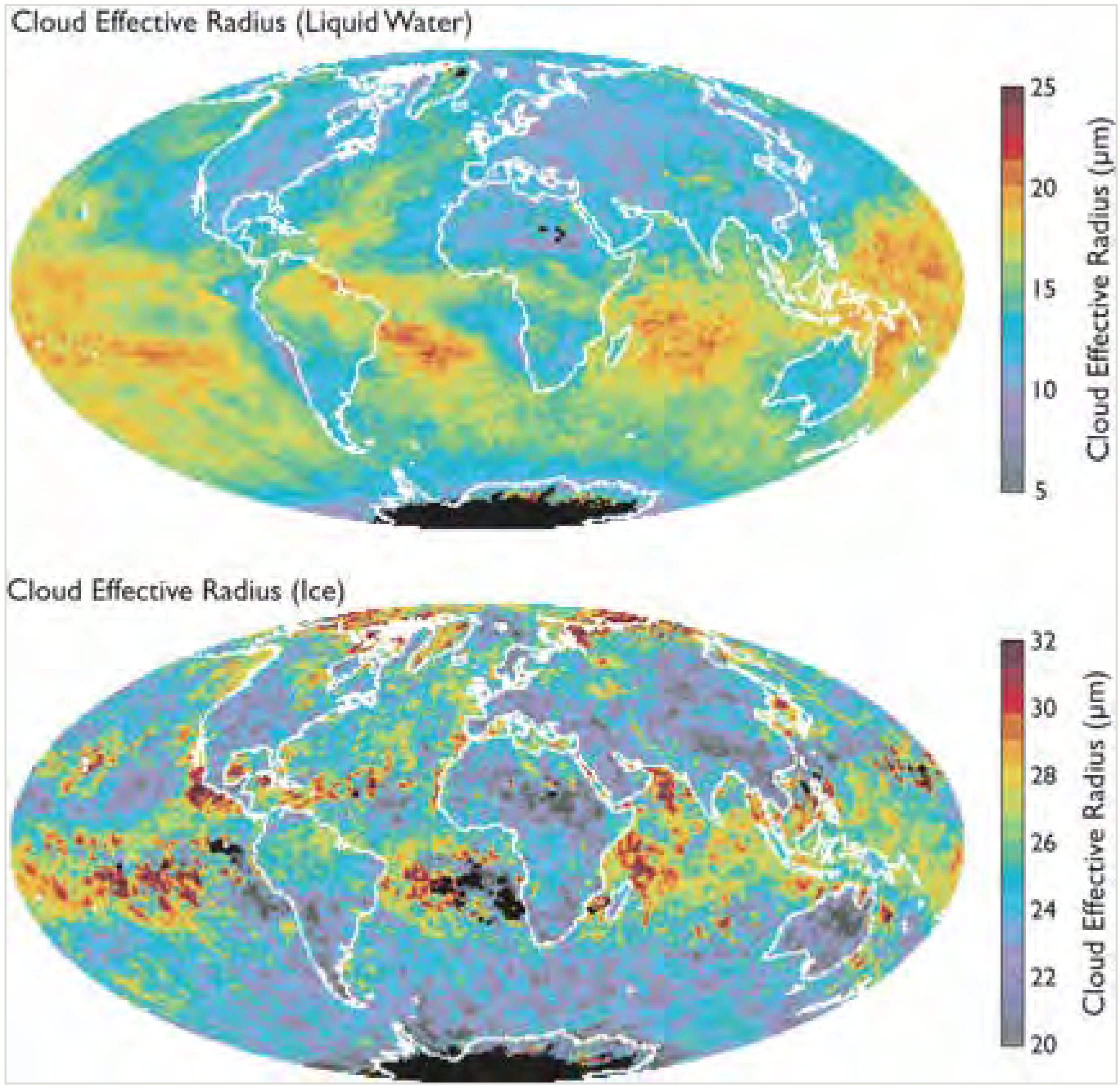

Monthly Mean Cloud-Top Properties

(W. P. Menzel, R. A. Frey et al. – Univ. Wisconsin)

April 2005
Aqua C5

Cloud_Top_Pressure
_Mean_Mean

Cloud_Top_Temperature
_Mean_Mean

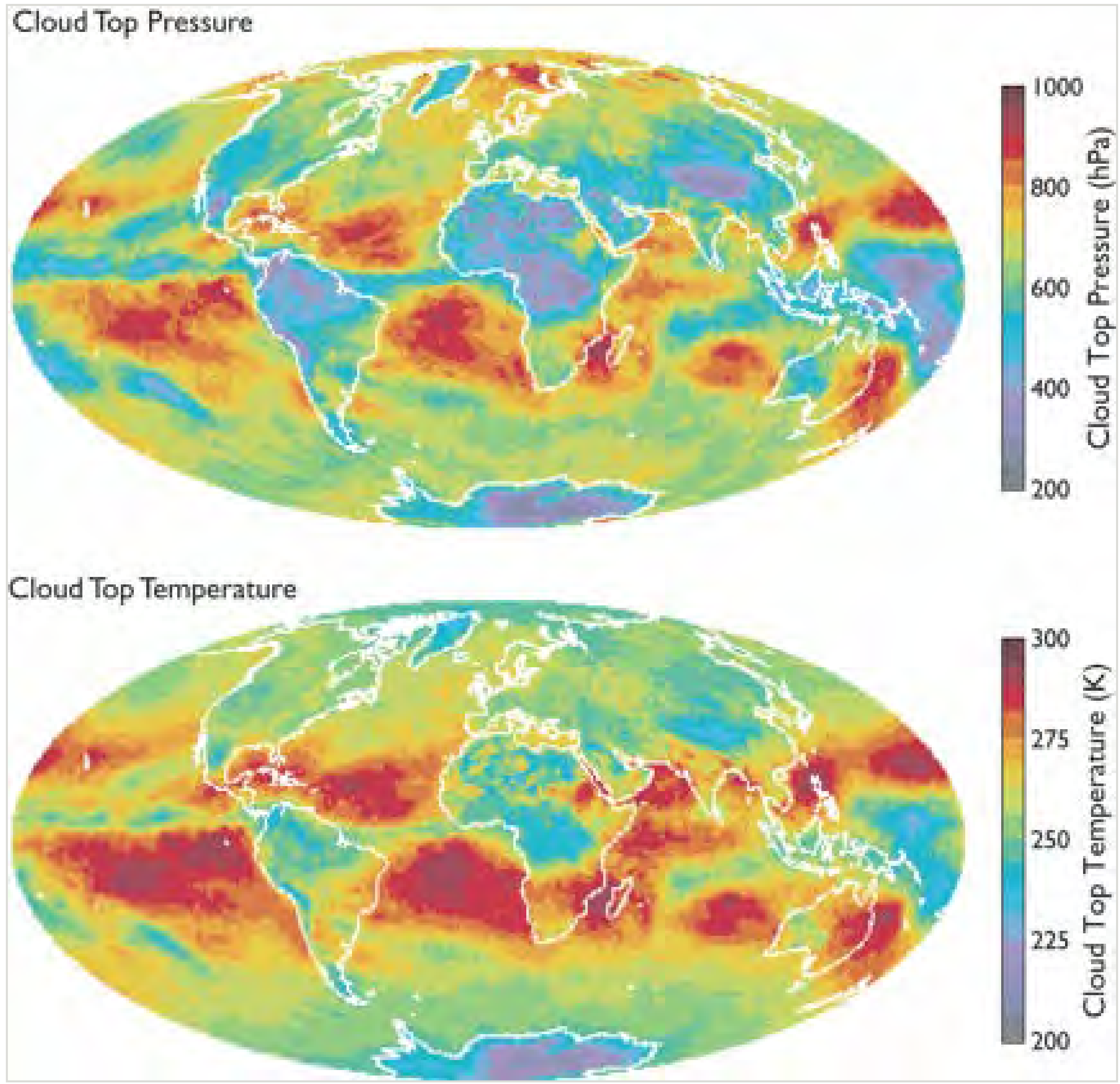

Eyjafjallajökull Eruptions

March 20 to April 12, 2010 - non-ash eruptions, lava fountains

April 14 to May 23, 2010 - mostly explosive ash cloud producing *(ash was visible in satellite imagery 32 out of 41 days)*

Marco Fulle - www.stromboli.net

Key: All flights canceled   Some flights operating   Open; only flights to or from affected areas canceled

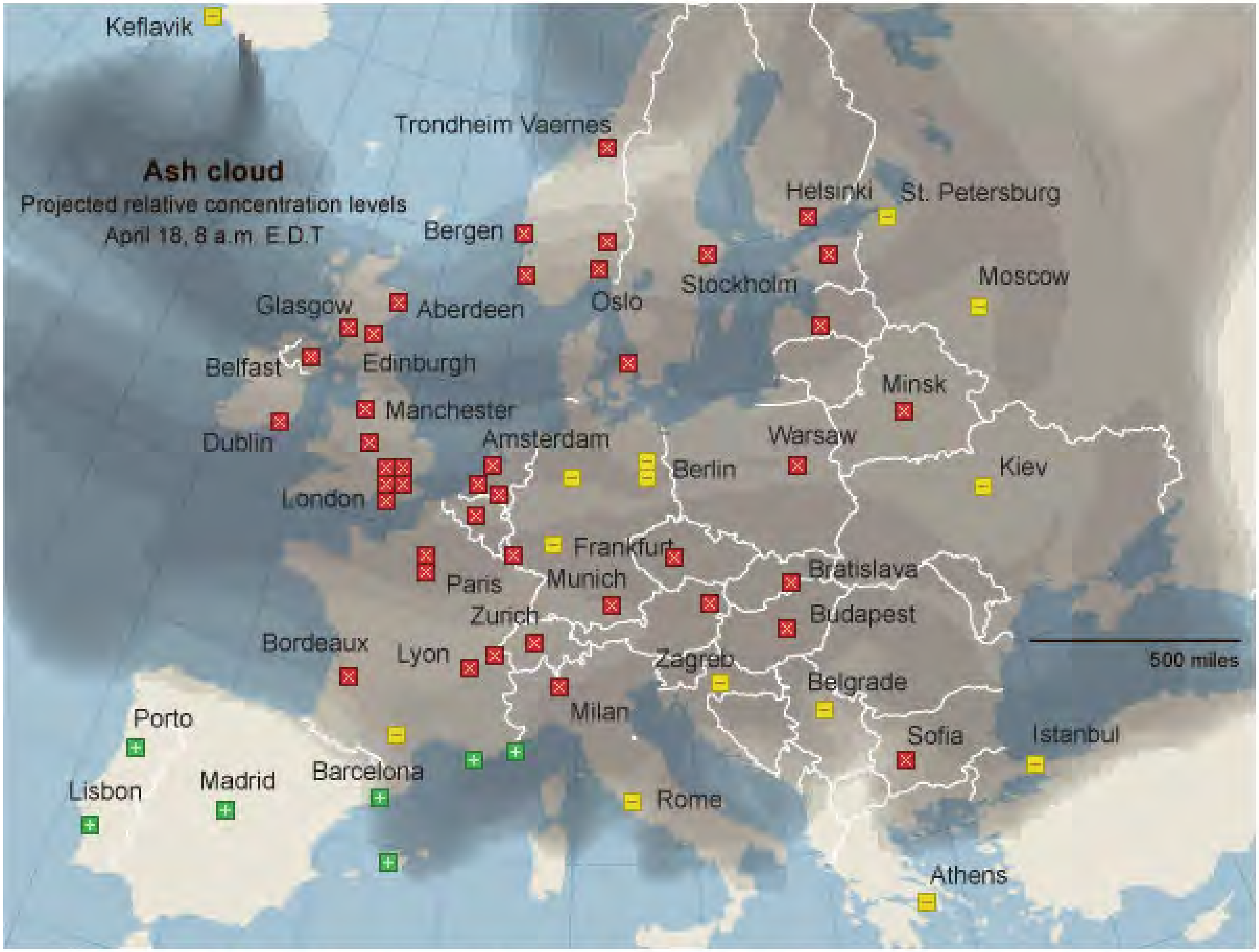

Source: Jørgen Brandt, Senior Scientist, National Environmental Research Institute at Aarhus University, Denmark

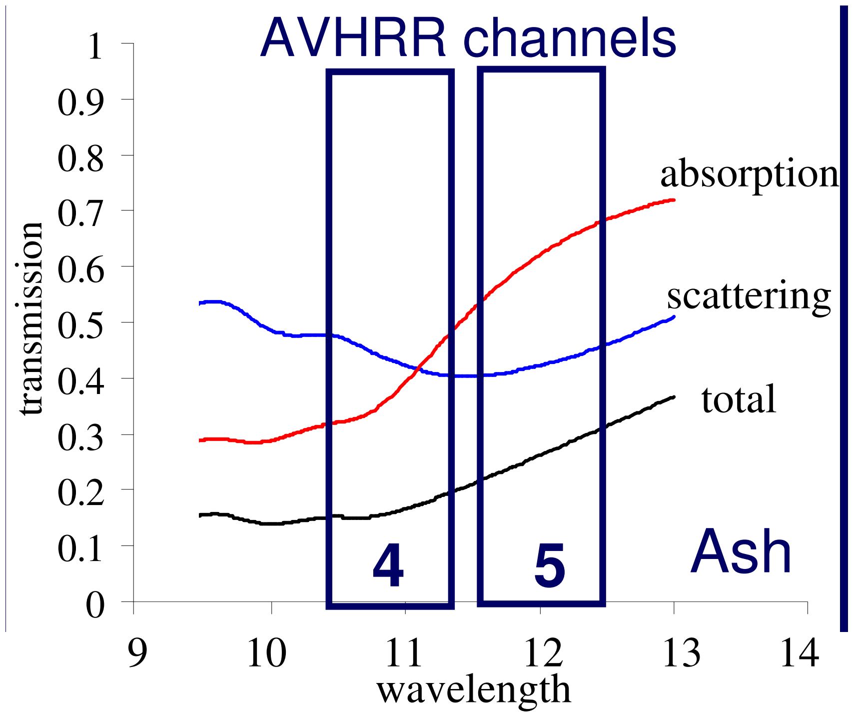

Investigating with Multi-spectral Combinations

Given the spectral response of a surface or atmospheric feature

Select a part of the spectrum where the reflectance or absorption changes with wavelength

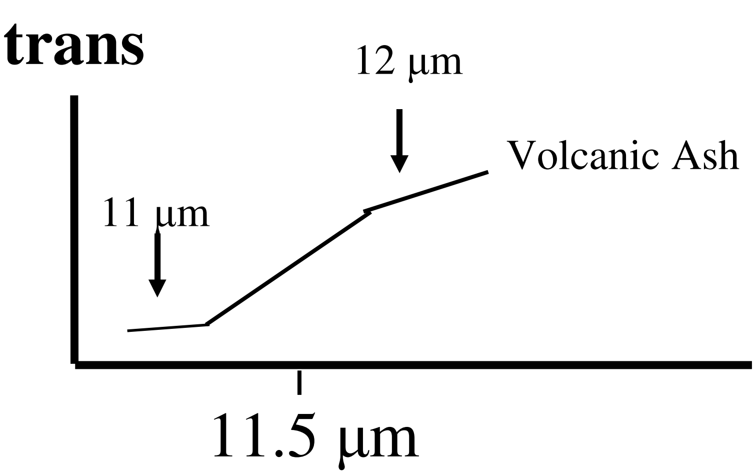

e.g. transmission through ash

If 11 µm sees the same or higher BT than 12 µm the atmosphere viewed does not contain volcanic ash;
if 12 µm sees considerably higher BT than 11 µm then the atmosphere probably contains volcanic ash

Frank Honey, CSIRO 1980s

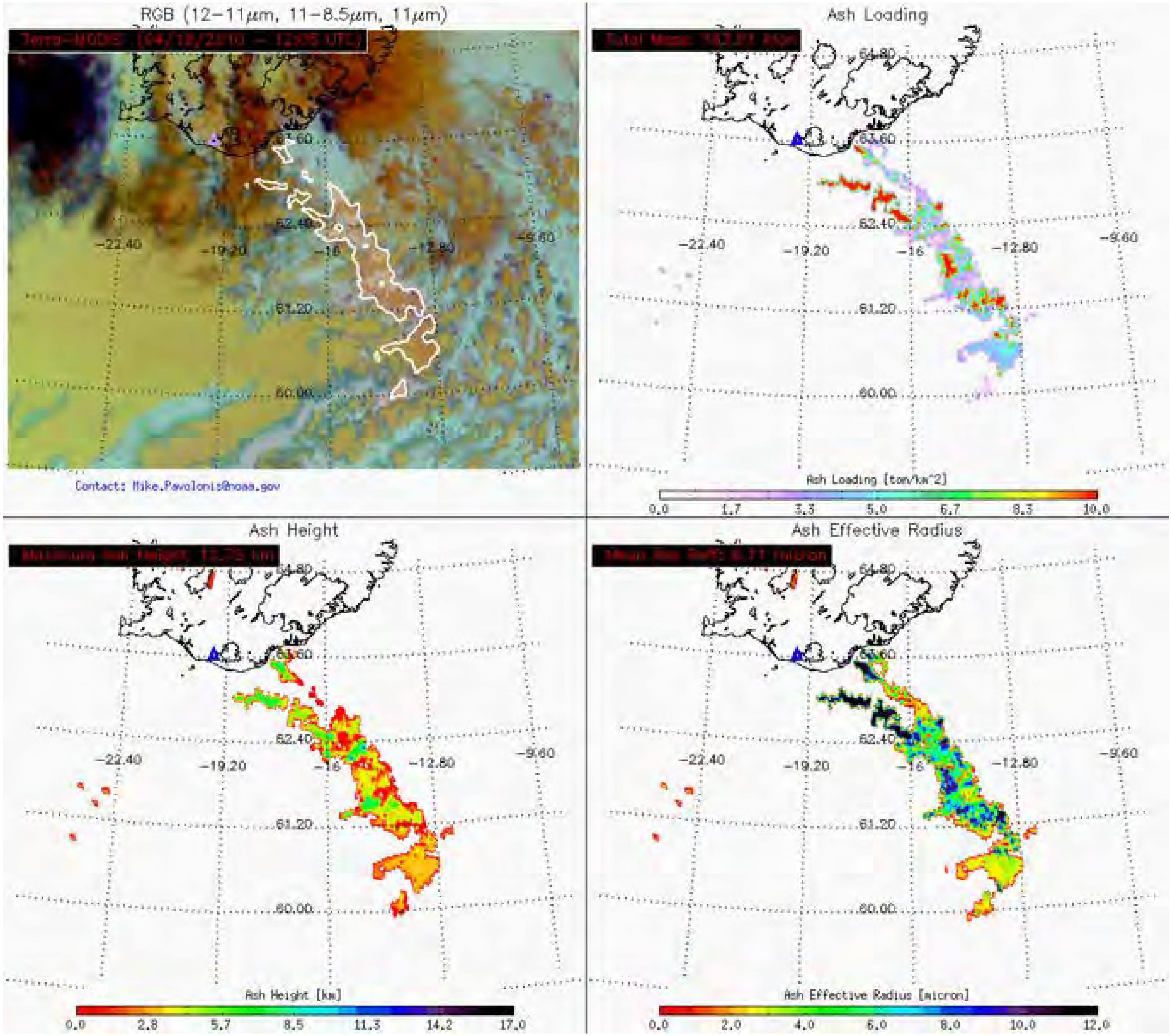

Terra-Aqua MODIS provide am & pm snapshots

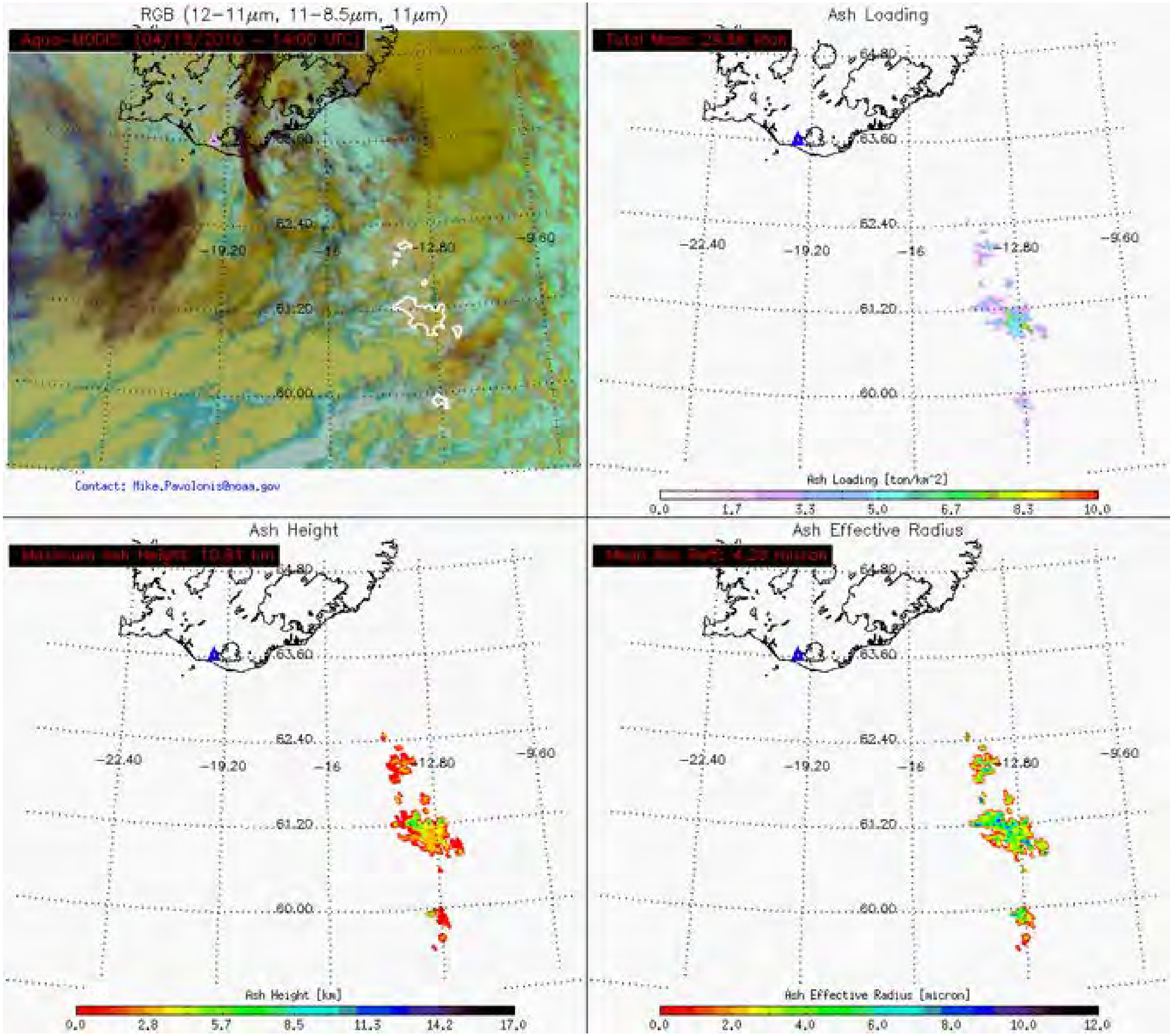

Terra-Aqua MODIS provide am & pm snapshots

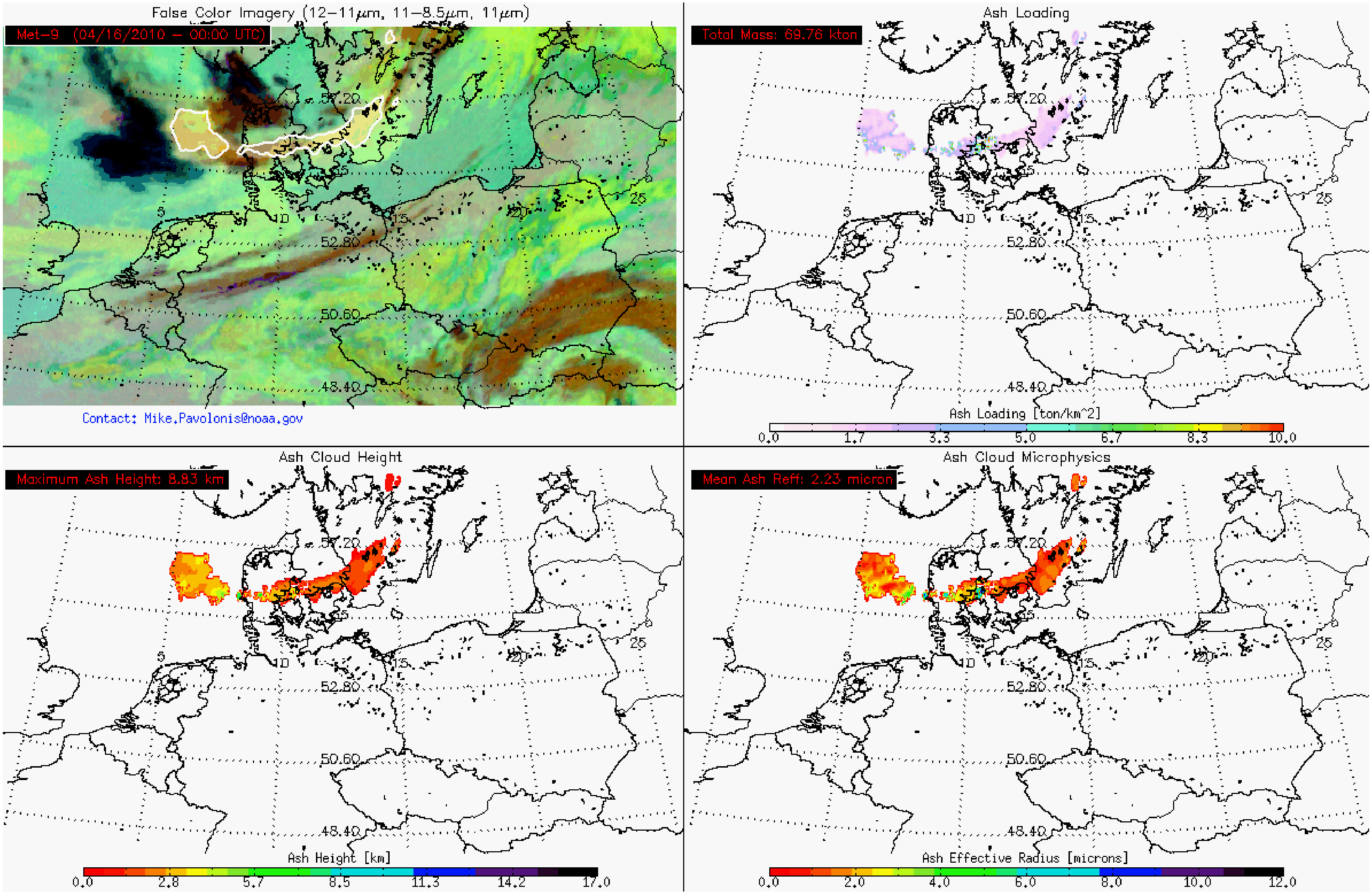

SEVIRI provides time continuous monitoring of ash location and amount

Polar winds and CTPs
Sodankylä DB Examples

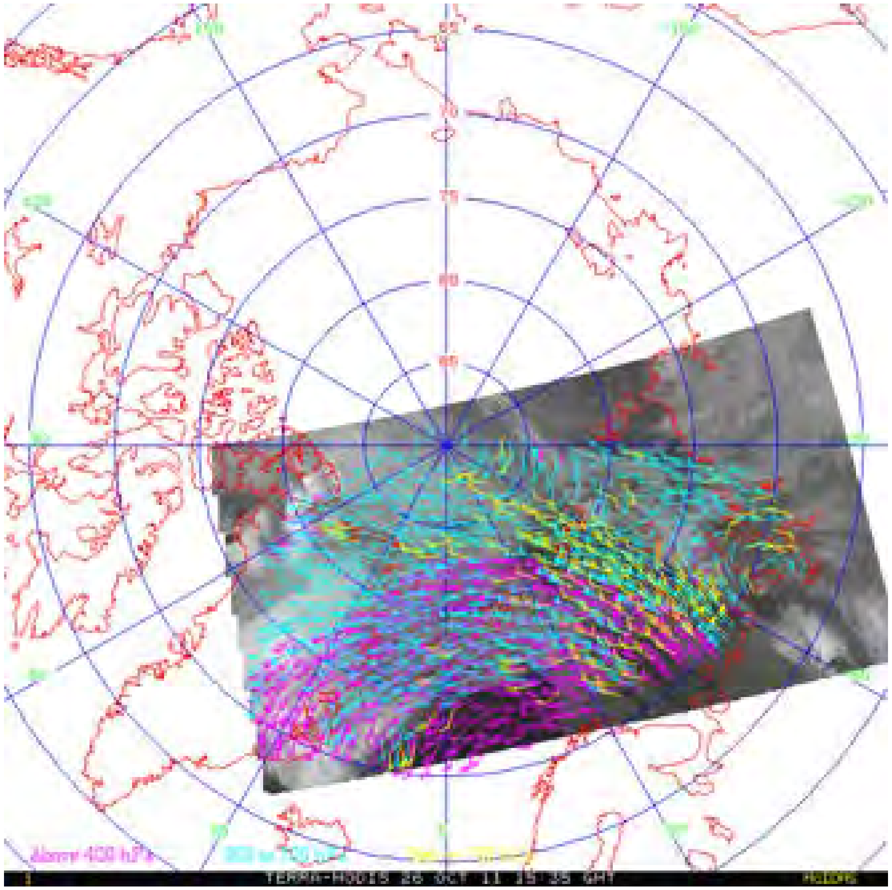

Above: MODIS winds, 26 Oct 2011

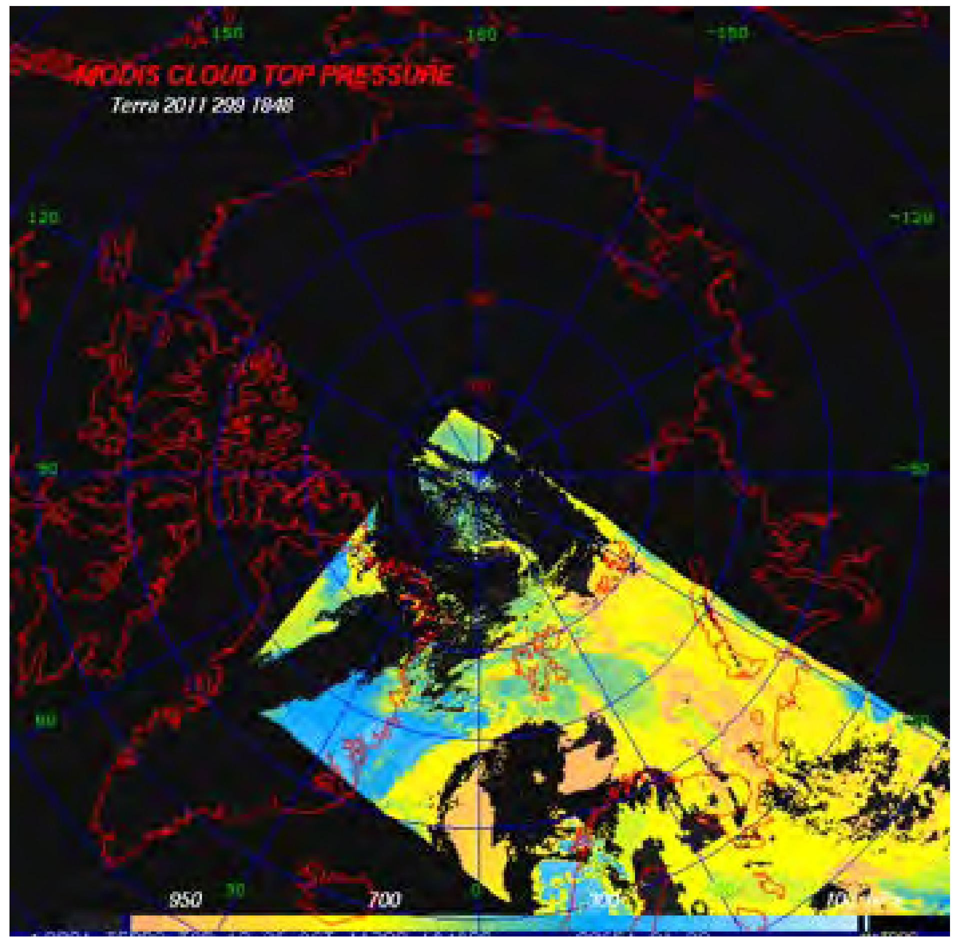

Right: MODIS cloud top pressure, 26 Oct 2011

Ice Motion

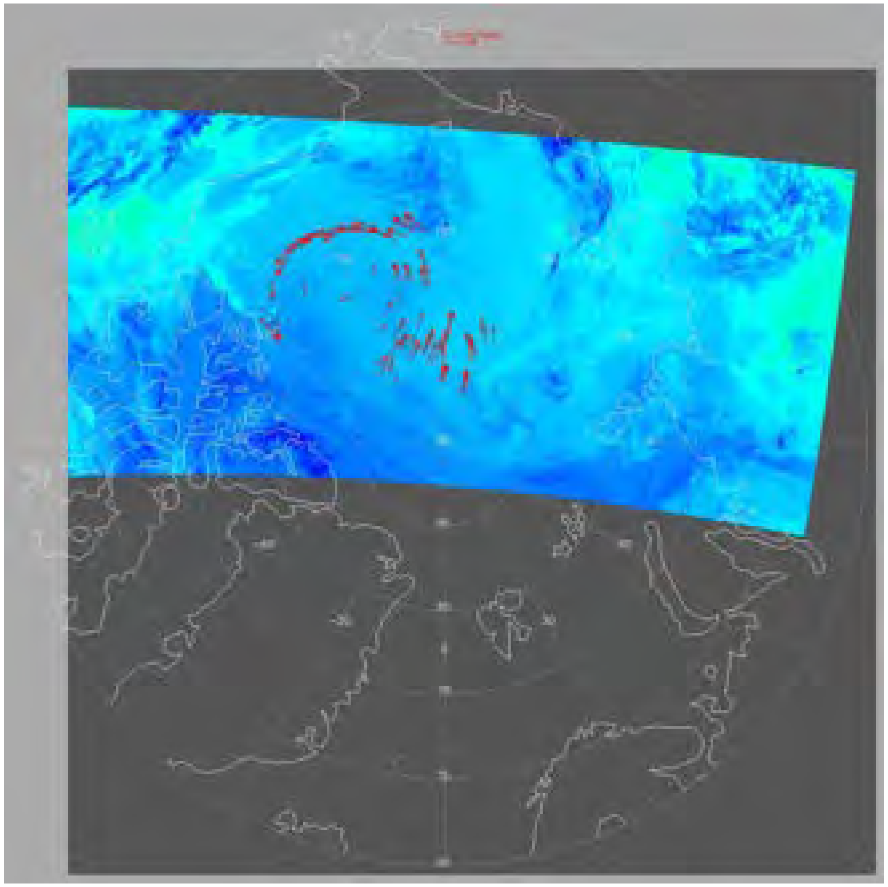

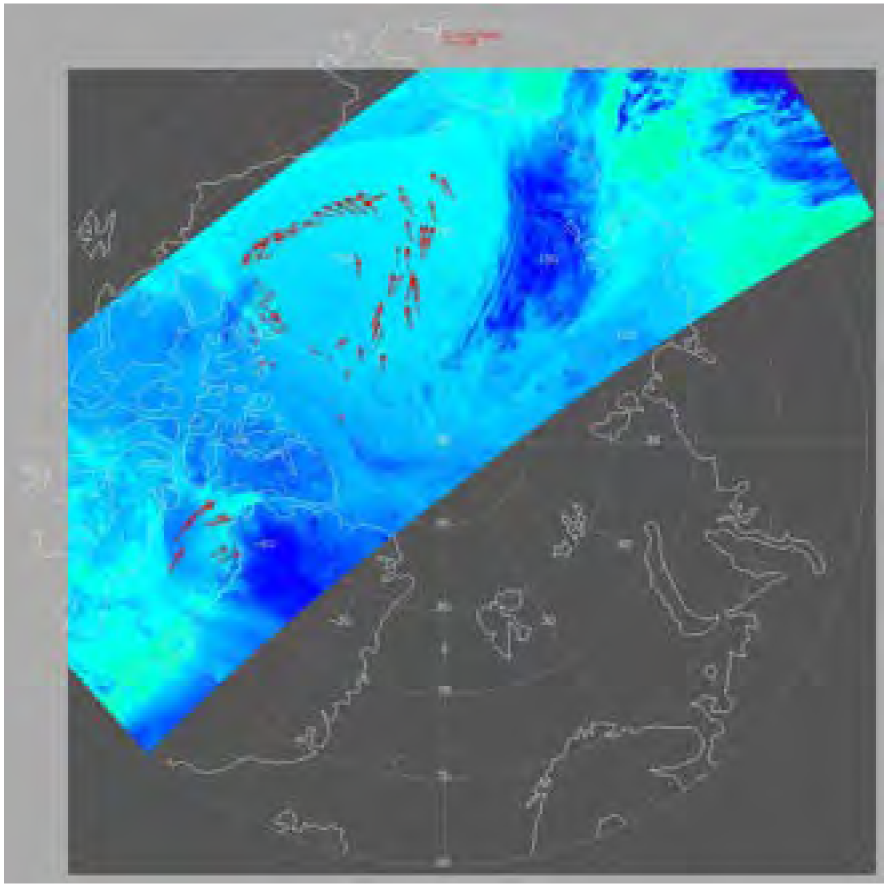

From MODIS (ideally this would be a blended microwave/vis-IR product)

(Investigator: Yinghui Liu)

Low-Level Atmospheric Temperature Inversions (MODIS)

Strength (C)

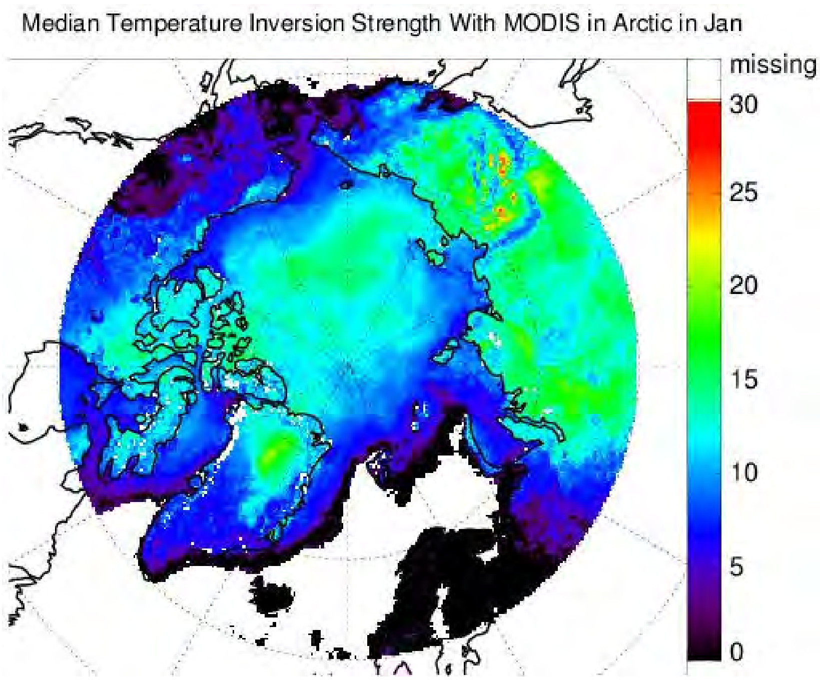

Depth (m)

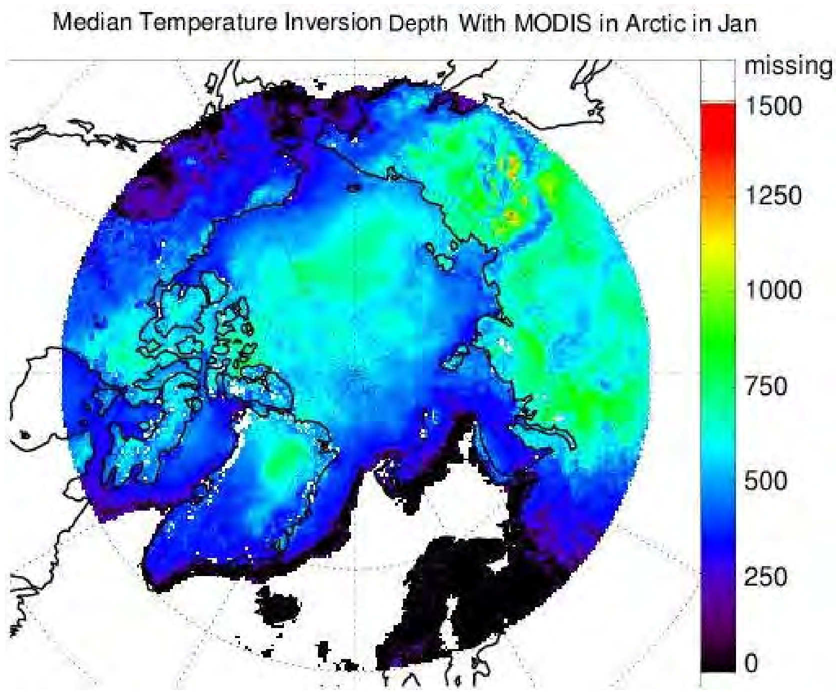

Unfortunately, this won't be available from VIIRS because it uses a low-peaking water vapor (or CO2) channel.

Transitioning from MODIS to VIIRS for remote sensing of ocean, land, and atmosphere

RT in Earth Atmosphere
Multispectral Signatures
MODIS Heritage Products
VIIRS Instrument Description
Some Anticipated VIIRS Applications
(SST, Ocean Color, Vegetation, Snow, Ice, Clouds, Moisture, Fires, Dust, Low Light Imagery)

W. Paul Menzel, University of Wisconsin- Madison

NPP is launched successfully 28 Oct 2011


VIIRS
CrIS
CERES
ATMS
OMPS

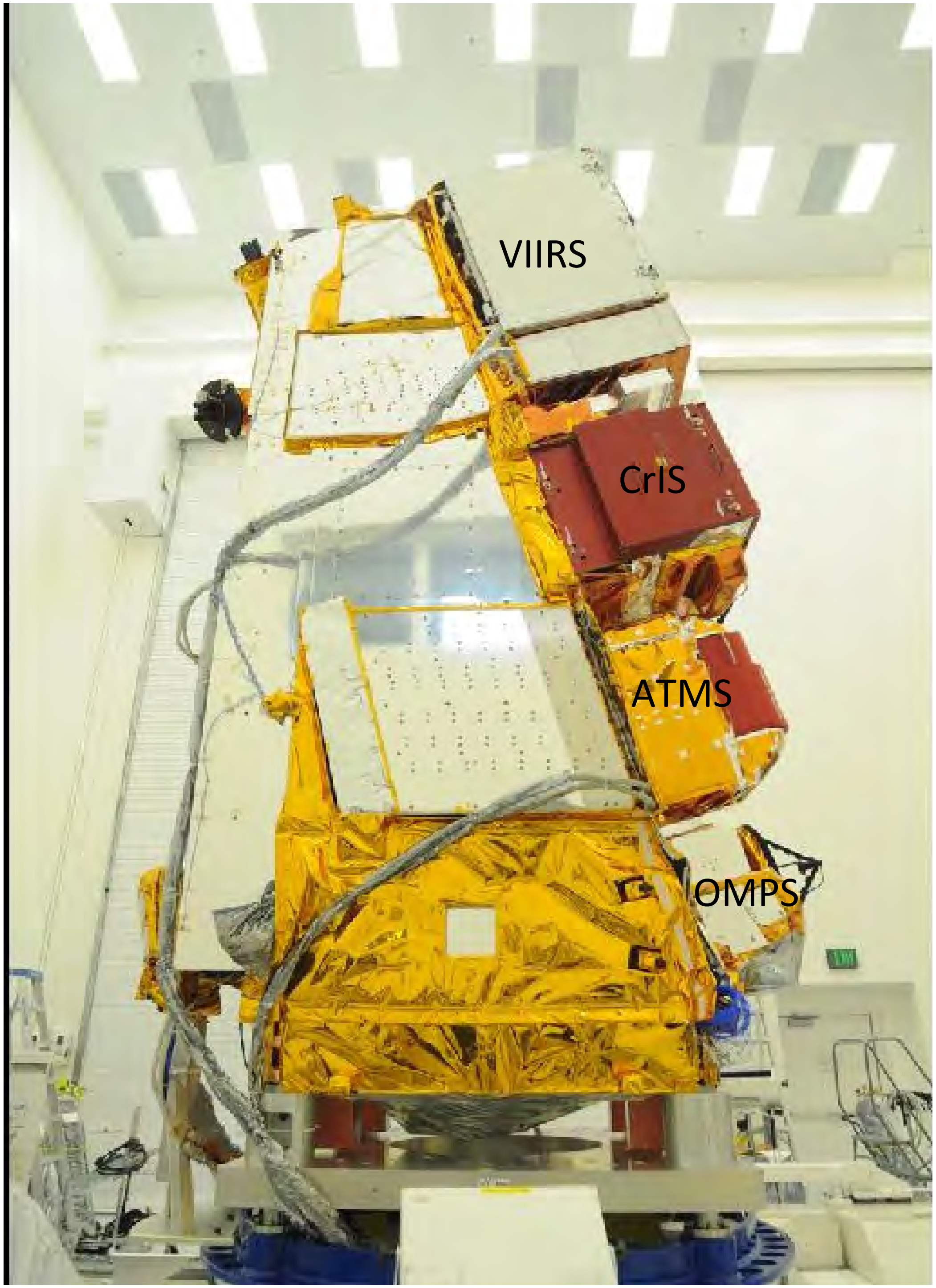
VIIRS
CrIS
ATMS
OMPS

Visible Infrared Imaging Radiometer Suite
Raytheon SAS El Segundo, Ca

Description

- **Purpose:** Global observations of land, ocean, & atmosphere parameters at high temporal resolution (~ daily)
- **Predecessor Instruments:** AVHRR, OLS, MODIS, SeaWiFS
- **Approach:** Multi-spectral scanning radiometer (22 bands between 0.4 µm and 12 µm) 12-bit quantization
- **Swath width:** 3000 km

Spatial Resolution

- 16 bands at 750m
- 5 bands at 325m
- DNB

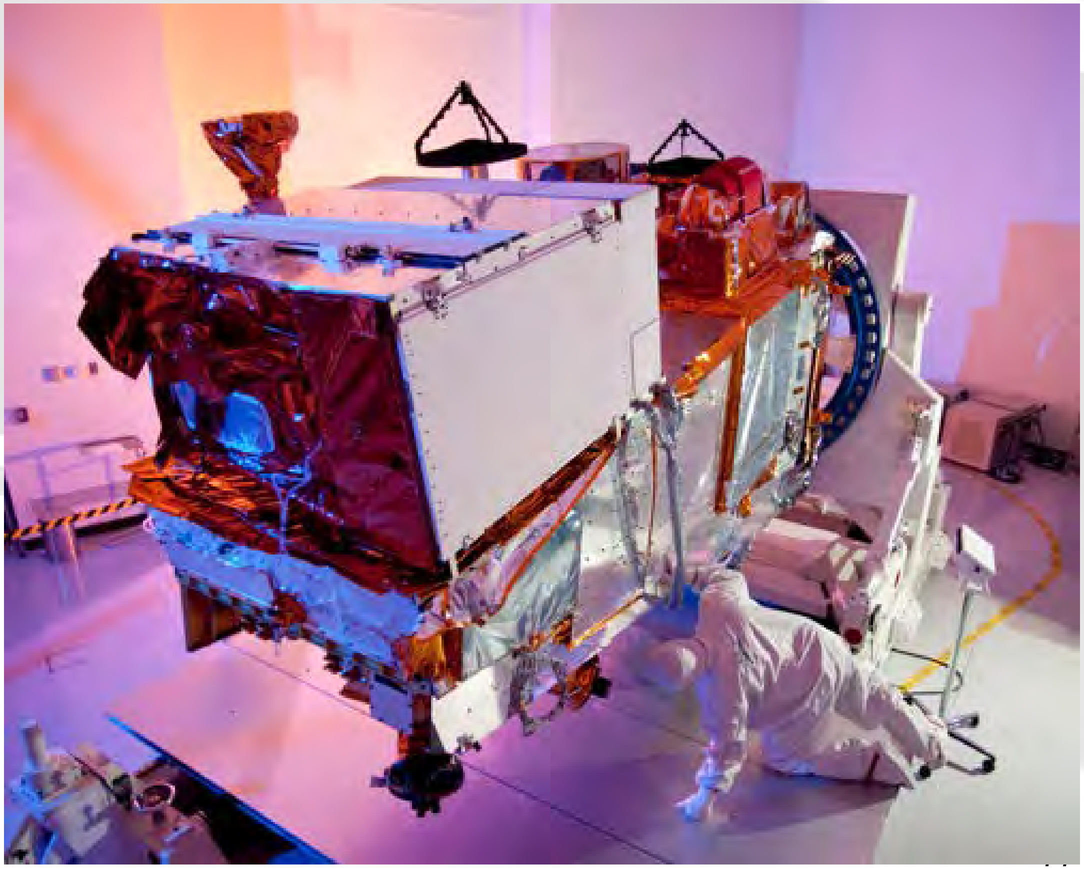

VIIRS on NPP

Single Sensor VIIRS Improves Data Quality Reduces Integration Costs

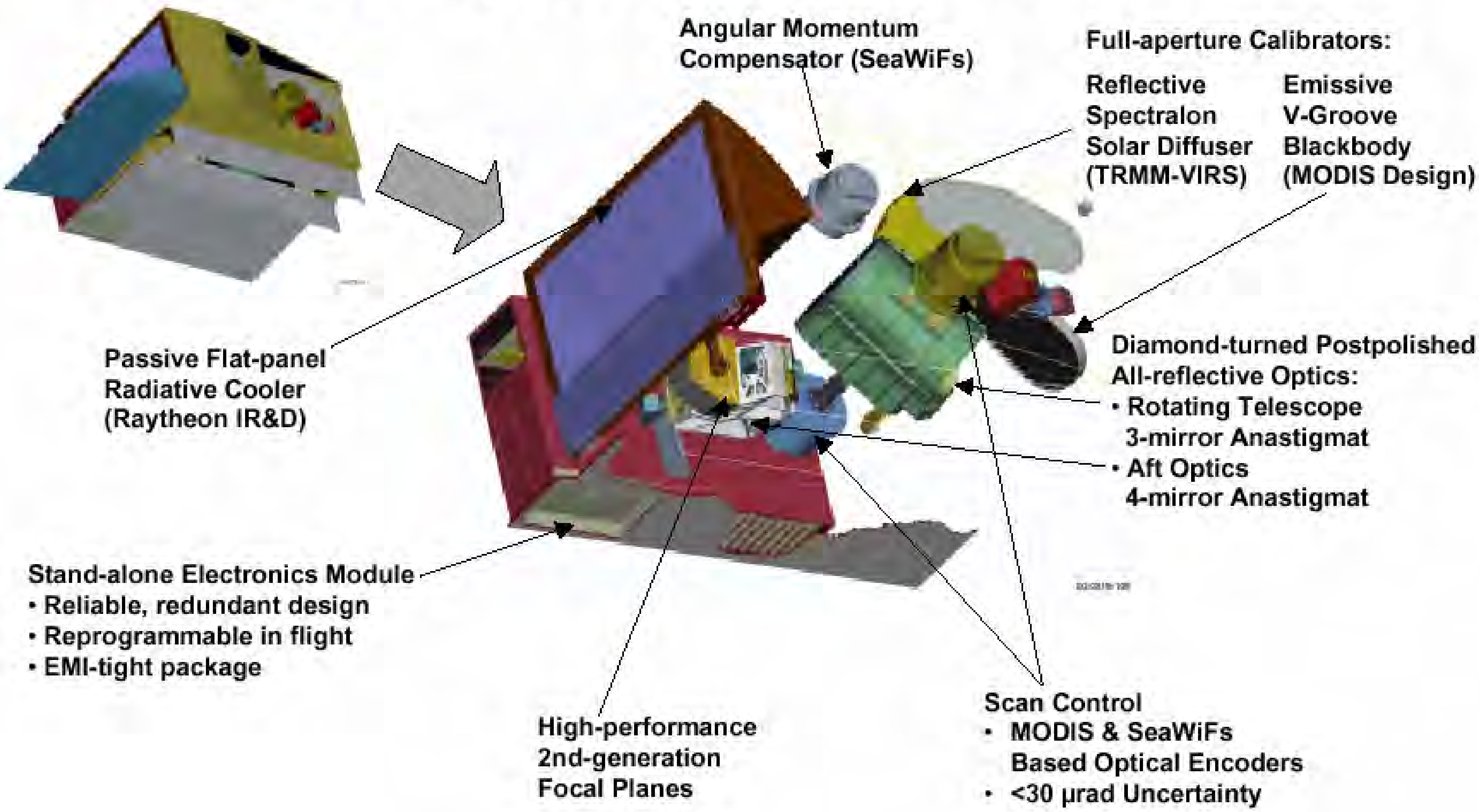

Physical Characteristics (Volume, Dimensions, Mass, Power)

VIIRS Sensor From Photons In To Bits Out

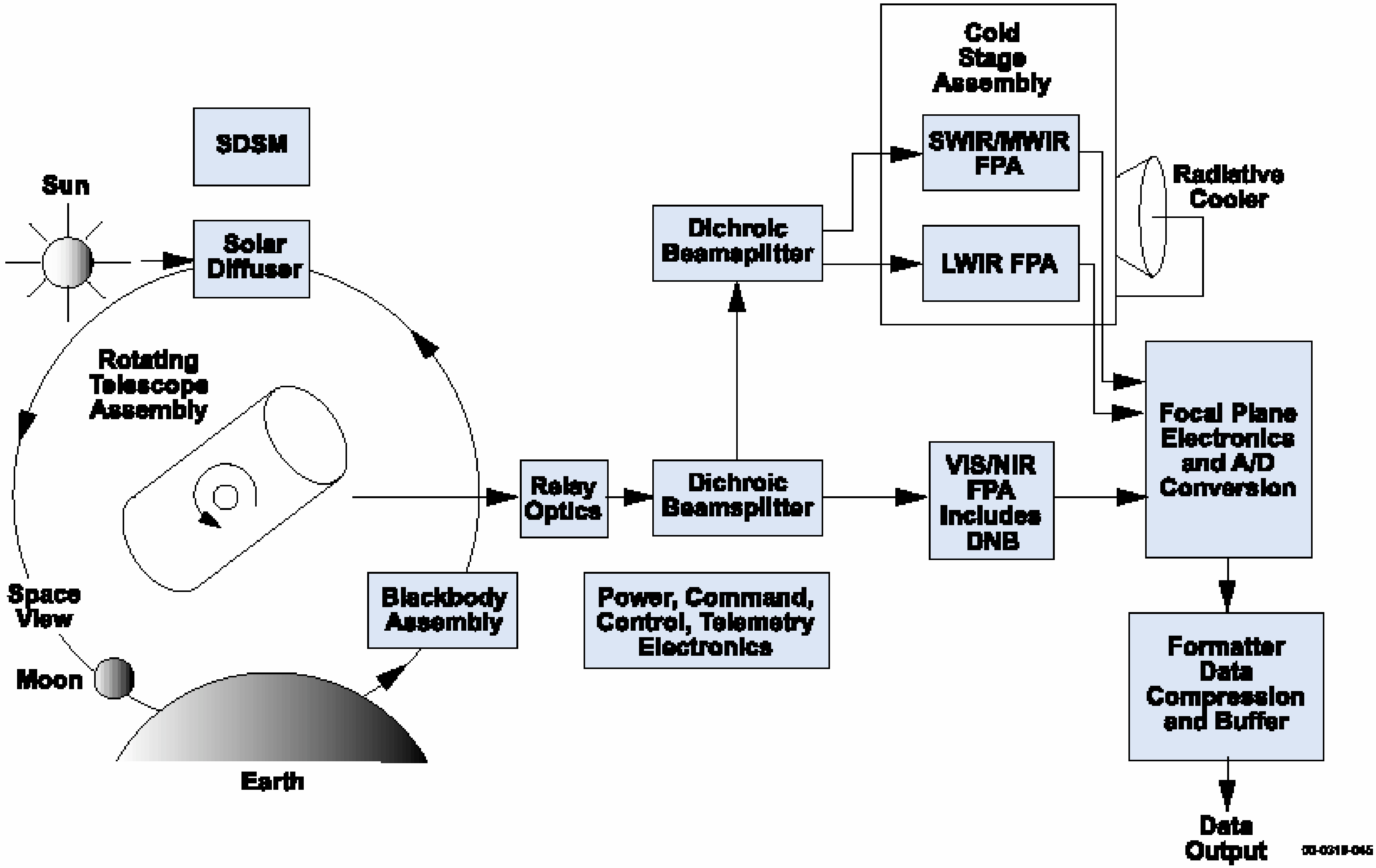

Four FPAs Cover Full Spectral Range

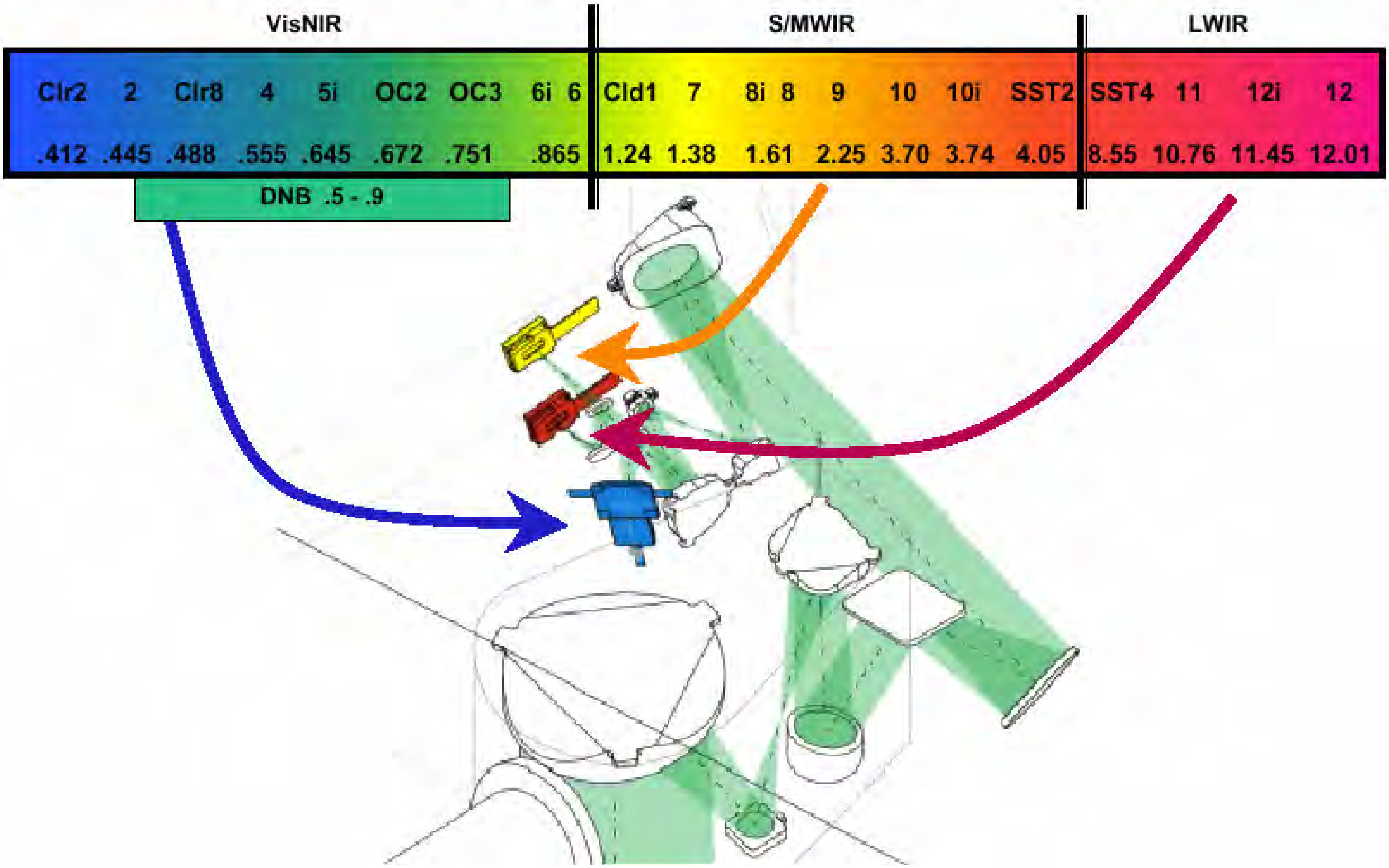

Vis/NIR Response Anomaly

(1) The smoking gun for causation of the VisNIR response anomaly has been found. Aerospace laboratory analysis of a witness sample from the same run used to coat the silver mirrors in the RTA revealed tungsten and tungsten oxides in two places, in a thin layer at the top of the coating and in smaller "trace" quantities below the silver layer. In discussions with Quantum, formerly Denton, the coating vendor, it was learned that an ion source using a tungsten filament is routinely used in a cleaning step prior to deposition of the silver as part of their normal coating process. This explains the presence of tungsten below the silver but also suggested a potential root cause for the presence of tungsten in the top layer of the coating. After reviewing their documentation of the NPP VIIRS mirror coating runs, Quantum reported that the ion source was used a second time as a final step in coating the NPP VIIRS RTA mirrors. After following the normal process it was found that reflectance did not meet specification, so Quantum used the ion source a second time to further oxidize silicon in the upper layers. This final step, which was not and is not part of Quantum's normal coating process, brought the mirrors within the reflectance specification but also introduced tungsten into the top layer of the coating. The tungsten oxides in the top layer are known to act as UV activated color centers, essentially darkening the RTA mirrors as they are exposed to UV on orbit.

To summarize, the degradation to date is about 15% in M7 and I2 (0.865 um) gain. It is within possibility that by the time we reach 0 degradation rate on these bands, we may indeed have a 30-50% total degradation, but that's a large extrapolation at this point.

SDSM Degradation

(2) Eric Johnson of Raytheon provided evidence that the root cause of the degradation of the SDSM detector response is radiation induced displacement damage within the SDSM detectors. We know from on-orbit data analysis that both MODIS and VIIRS SDSM detectors are degrading similarly with respect to spectral signature, with the greatest degradation in the longer wavelength bands. We also know that the SDSM detector response degradation is NOT UV driven, which strongly suggests that the cause of this degradation is unrelated to the response degradation in VIIRS itself. Note that the SDSM is a separate instrument used to observe the sun and VIIRS solar diffuser, and therefore has its own optics, detectors and electronics. Raytheon has data from neutron exposure testing of detectors of the type used in the SDSM, and these data show degradation with the same spectral signature observed on orbit for both MODIS and VIIRS. It is also known that both neutrons and protons cause the same type of displacement damage in detectors. The natural space environment includes high energy protons and both VIIRS and MODIS are exposed to protons, albeit at different levels due to their different orbits and different amounts of shielding inherent in the designs. Based on these facts and the sum total of the evidence presented by Eric Johnson, I believe there is a very strong case to be made for radiation induced displacement damage as root cause for the SDSM detector degradation. As to performance impacts, there is enormous SNR margin in the SDSM for both VIIRS and MODIS, so as long as VIIRS SDSM detector degradation trends continue as expected, there should be no impact on the capability to monitor solar diffuser degradation as planned throughout mission life. We will continue to trend both the SDSM detector response degradation as well as VIIRS response, needless to say, so we will become aware of any departures from the current trends that might change this assessment.

VIIRS System Provides Environmental Data Records (EDRs)

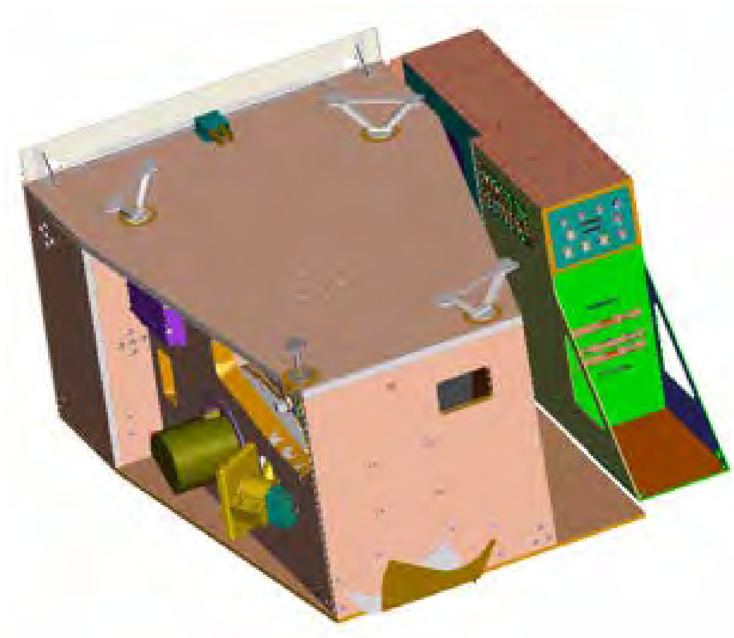

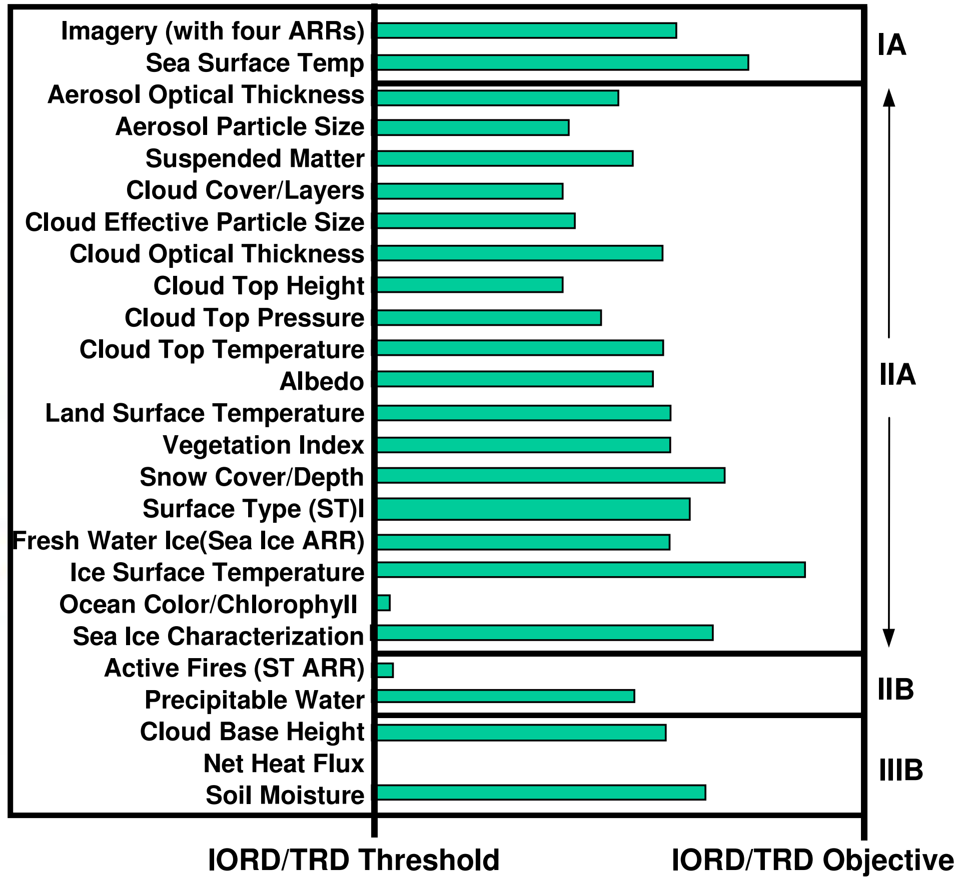

- **VIIRS System Design based on integrated Sensor and Algorithms**
- **Engineering Development Unit (EDU) approaching integration**
- **EDR Science Algorithms developed, documented, and publicly released by Raytheon Technical Services Company (RTSC) Information Technology and Scientific Services (ITSS)**

VIIRS VIS/NIR & IR Bands

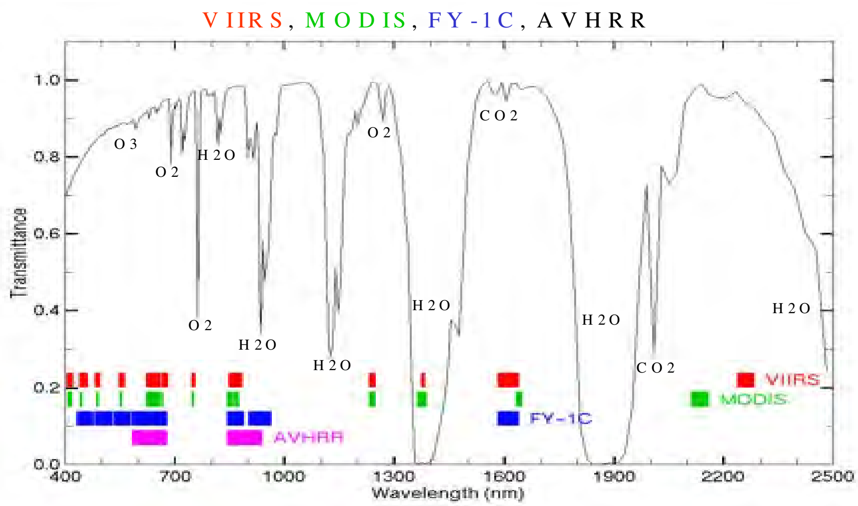

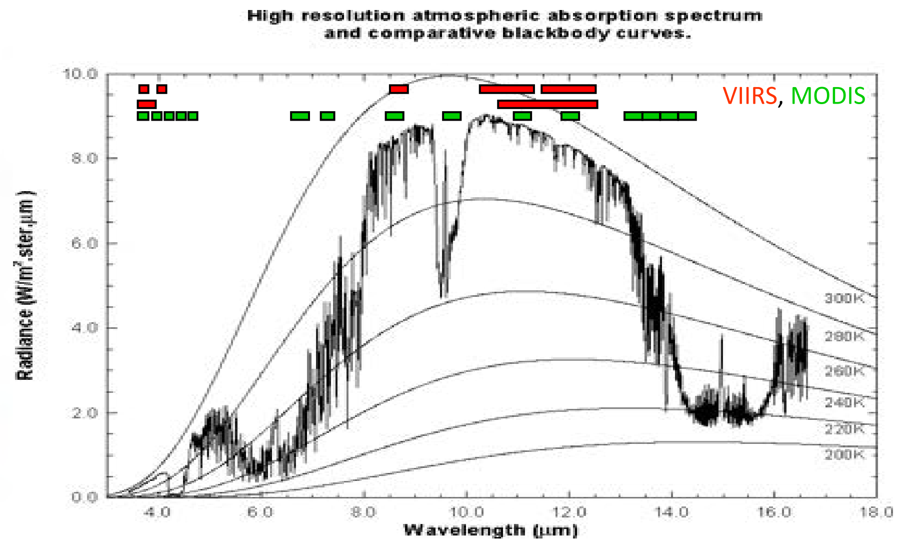

		Band No.	Wave-length (µm)	Horiz Sample Interval (km Downtrack x Crosstrack) Nadir	End of Scan	Driving EDRs	Radi-ance Range	Ltyp or Ttyp
VIS/NIR FPA	Silicon PIN Diodes	M1	0.412	0.742 x 0.259	1.60 x 1.58	Ocean Color Aerosols	Low High	44.9 155
		M2	0.445	0.742 x 0.259	1.60 x 1.58	Ocean Color Aerosols	Low High	40 146
		M3	0.488	0.742 x 0.259	1.60 x 1.58	Ocean Color Aerosols	Low High	32 123
		M4	0.555	0.742 x 0.259	1.60 x 1.58	Ocean Color Aerosols	Low High	21 90
		I1	0.640	0.371 x 0.387	0.80 x 0.789	Imagery	Single	22
		M5	0.672	0.742 x 0.259	1.60 x 1.58	Ocean Color Aerosols	Low High	10 68
		M6	0.746	0.742 x 0.776	1.60 x 1.58	Atmospheric Corr'n	Single	9.6
		I2	0.865	0.371 x 0.387	0.80 x 0.789	NDVI	Single	25
		M7	0.865	0.742 x 0.259	1.60 x 1.58	Ocean Color Aerosols	Low High	6.4 33.4
CCD		DNB	0.7	0.742 x 0.742	0.742 x 0.742	Imagery	Var.	6.70E-05
S/MWIR	PV HgCdTe (HCT)	M8	1.24	0.742 x 0.776	1.60 x 1.58	Cloud Particle Size	Single	5.4
		M9	1.378	0.742 x 0.776	1.60 x 1.58	Cirrus/Cloud Cover	Single	6
		I3	1.61	0.371 x 0.387	0.80 x 0.789	Binary Snow Map	Single	7.3
		M10	1.61	0.742 x 0.776	1.60 x 1.58	Snow Fraction	Single	7.3
		M11	2.25	0.742 x 0.776	1.60 x 1.58	Clouds	Single	0.12
		I4	3.74	0.371 x 0.387	0.80 x 0.789	Imagery Clouds	Single	270 K
		M12	3.70	0.742 x 0.776	1.60 x 1.58	SST	Single	270 K
		M13	4.05	0.742 x 0.259	1.60 x 1.58	SST Fires	Low High	300 K 380 K
LWIR	PV HCT	M14	8.55	0.742 x 0.776	1.60 x 1.58	Cloud Top Properties	Single	270 K
		M15	10.763	0.742 x 0.776	1.60 x 1.58	SST	Single	300 K
		I5	11.450	0.371 x 0.387	0.80 x 0.789	Cloud Imagery	Single	210 K
		M16	12.013	0.742 x 0.776	1.60 x 1.58	SST	Single	300 K

VIIRS' Optimized Bandset Provides Rich Data for All EDRs

nm / µm

New Band Name	DNB	M1	M2	M3	M4	I1	M5	M6	M7	I2	M8	M9	M10	I3	M11	M12	I4	M13	M14	M15	I5	M16
Old Band Name	DNB	Chlor2	2	Chlor8	4	5i	OC2	OC3	6	6i	Cloud1	7	8	8i	9	10	10i	SST2	SST4	11	12i	12
Band position	700	412	445	488	555	645	672	751	865	865	1.24	1.38	1.61	1.61	2.25	3.70	3.74	4.05	8.55	10.76	11.45	12.01
Band width	400	20	18	20	20	50	20	15	39	39	0.02	0.015	0.06	0.06	0.05	0.18	0.38	0.16	0.30	1.00	1.90	0.95
Imagery	■		■			■				■		■		■	■		■	■	■	■	■	■
Sea Surface Temp.																■		■		■		■
Soil Moisture							■		■													
Cloud Base Height																						
Cloud Cover/Layers	■					■	■		■	■		■	■	■	■	■	■	■	■	■	■	■
Cloud Particle Size							■				■		■			■				■		
Cloud Thickness							■				■		■			■				■		
Cloud Top Height							■									■				■		
Cloud Top Pressure							■									■				■		
Cloud Top Temp.							■									■				■		
Land Surface Temp.																■		■		■		■
Fire											■		■		■		■	■		■	■	
Vegetation Index				■	■	■				■												
Snow Cover(Binary)						■				■				■								
Snow Cover(Fraction)		■	■	■	■	■	■		■	■			■	■	■							
Vegetation / Type			■		■	■				■	■			■	■	■				■		■
Albedo		■	■	■	■	■				■	■			■	■							
Fresh Water Ice						■				■											■	
Ice Surface Temp.																				■		■
Littoral Transport					■		■															
Net Heat Flux		■	■	■	■		■	■	■			■	■		■							
Ocean Color / Chloro.		■	■	■	■		■	■	■													
Sea Ice age / motion		■	■	■	■	■	■		■	■			■	■	■							
Mass (turbidity)		■	■	■	■		■	■	■													
Ocean Currents																						
Aer Opt Thick (Ocean)		■	■	■	■		■		■				■		■	■						
Aer Opt Thick (Land)		■	■	■	■		■								■	■				■		■
Aer Part Size (Ocean)		■	■	■	■		■		■				■		■	■						
Aer Part Size (Land)		■	■	■	■		■								■	■				■		■
Suspended Matter		■	■	■	■		■									■		■	■	■		■
Total Prec. Water																■		■	■	■		■
Cloud mask	■					■	■		■	■		■	■	■	■	■	■	■	■	■	■	■

VIIRS Prelaunch Performance

(NPP **F1 Bands and SNR/NEDT)**

		Band No.	Driving EDR(s)	Spectral Range (um)	Horiz Sample Interval (km) (track x Scan) Nadir	End of Scan	Band Gain	Ltyp or Ttyp (Spec)	Lmax or Tmax	SNR or NEdT (K)	Measured SNR or NEdT (K)	SNR Margin (%)
				Specification								
Reflective Bands	VisNIR	M1	Ocean Color Aerosol	0.402 - 0.422	0.742 x 0.259	1.60 x 1.58	High Low	44.9 155	135 615	352 316	723 1327	105% 320%
Reflective Bands	VisNIR	M2	Ocean Color Aerosol	0.436 - 0.454	0.742 x 0.259	1.60 x 1.58	High Low	40 146	127 687	380 409	576 1076	51.5% 163%
Reflective Bands	VisNIR	M3	Ocean Color Aerosol	0.478 - 0.498	0.742 x 0.259	1.60 x 1.58	High Low	32 123	107 702	416 414	658 1055	58.2% 155%
Reflective Bands	VisNIR	M4	Ocean Color Aerosol	0.545 - 0.565	0.742 x 0.259	1.60 x 1.58	High Low	21 90	78 667	362 315	558 882	54.1% 180%
Reflective Bands	VisNIR	I1	Imagery EDR	0.600 - 0.680	0.371 x 0.387	0.80 x 0.789	Single	22	718	119	265	122.7%
Reflective Bands	VisNIR	M5	Ocean Color Aerosol	0.662 - 0.682	0.742 x 0.259	1.60 x 1.58	High Low	10 68	59 651	242 360	360 847	49% 135%
Reflective Bands	VisNIR	M6	Atmosph. Correct.	0.739 - 0.754	0.742 x 0.776	1.60 x 1.58	Single	9.6	41	199	394	98.0%
Reflective Bands	VisNIR	I2	NDVI	0.846 - 0.885	0.371 x 0.387	0.80 x 0.789	Single	25	349	150	299	99.3%
Reflective Bands	VisNIR	M7	Ocean Color Aerosol	0.846 - 0.885	0.742 x 0.259	1.60 x 1.58	High Low	6.4 33.4	29 349	215 340	545 899	154% 164%
Reflective Bands	S/MWIR	M8	Cloud Particle Size	1.230 - 1.250	0.742 x 0.776	1.60 x 1.58	Single	5.4	165	74	349	371.6%
Reflective Bands	S/MWIR	M9	Cirrius/Cloud Cover	1.371 - 1.386	0.742 x 0.776	1.60 x 1.58	Single	6	77.1	83	247	197.6%
Reflective Bands	S/MWIR	I3	Binary Snow Map	1.580 - 1.640	0.371 x 0.387	0.80 x 0.789	Single	7.3	72.5	6	165	2650.0%
Reflective Bands	S/MWIR	M10	Snow Fraction	1.580 - 1.640	0.742 x 0.776	1.60 x 1.58	Single	7.3	71.2	342	695	103.2%
Reflective Bands	S/MWIR	M11	Clouds	2.225 - 2.275	0.742 x 0.776	1.60 x 1.58	Single	0.12	31.8	10	18	80.0%
Emissive Bands	S/MWIR	I4	Imagery Clouds	3.550 - 3.930	0.371 x 0.387	0.80 x 0.789	Single	270	353	2.5	0.4	84.0%
Emissive Bands	S/MWIR	M12	SST	3.660 - 3.840	0.742 x 0.776	1.60 x 1.58	Single	270	353	0.396	0.12	69.7%
Emissive Bands	S/MWIR	M13	SST Fires	3.973 - 4.128	0.742 x 0.259	1.60 x 1.58	High Low	300 380	343 634	0.107 0.423	0.044 --	59% --
Emissive Bands	LWIR	M14	Cloud Top Properties	8.400 - 8.700	0.742 x 0.776	1.60 x 1.58	Single	270	336	0.091	0.054	40.7%
Emissive Bands	LWIR	M15	SST	10.263 - 11.263	0.742 x 0.776	1.60 x 1.58	Single	300	343	0.07	0.028	60.0%
Emissive Bands	LWIR	I5	Cloud Imagery	10.500 - 12.400	0.371 x 0.387	0.80 x 0.789	Single	210	340	1.5	0.41	72.7%
Emissive Bands	LWIR	M16	SST	11.538 - 12.488	0.742 x 0.776	1.60 x 1.58	Single	300	340	0.072	0.036	50.0%

HSI uses 3 in-scan pixels aggregation at Nadir

Courtesy of H. Oudrari

Comparable MODIS and VIIRS Channels

MODIS (1000 m)		VIIRS-M (760 m)	
8, 9	0.415, 0.443	1,2	ocean color
10, 12	0.490, 0.565	3,4	“
14-16	0.681, 0.75, 0.865	5-7	“
5**	1.24	8	cld particle size
26	1.38	9	thin cirrus
6**	1.61	10	snow
7**	2.13	11	cloud properties
20	3.75	12	sfc/cld temp
23	4.05	13	sfc temp
29	8.55	14	sfc/cld temp
31	11.0	15	sfc/cld temp
32	12.0	16	sfc/cld temp
		VIIRS-I (380 m)	
1*	0.645	1	imagery
2*	0.865	2	“
6**	1.64	3	“
20	3.75	4	“
31	11.0	5	“

* available at 250 m, ** available at 500 m resolution

SNR, NEDL, and NEDT Measured at the Radiances (and Temperatures Given in Table II(a) and (b) and the Fraction of Full-Scale Radiance Achieved and the Dynamic Range

Band	SNR Measured	SNR Required	NEDL (W/m^2-sr-μm) Measured	NEDT (K) Measured	Lsat/Lmax* Measured	Lsat/NEDL Measured
1	168.1	128.0	0.1304	-	1.11	5837
2	413.5	201.0	0.0598	-	0.97	4638
3	315.7	243.0	0.1120	-	1.19	6285
4	302.2	228.0	0.0960	-	1.13	6122
5	77.6	74.0	0.0750	-	1.19	1747
6	324.1	275.0	0.0226	-	1.07	3312
7	72.0	110.0	0.0143	-	1.14	1753
8	932.8	880.0	0.0484	-	1.28	4627
9	1324.6	838.0	0.0317	-	1.15	4845
10	1307.9	802.0	0.0247	-	1.14	4675
11	1385.0	754.0	0.0183	-	1.12	5003
12	1114.3	750.0	0.0189	-	1.12	3806
13	1162.6	910.0	0.0082	-	1.14	4466
14	1264.7	1087.0	0.0069	-	1.14	5108
15	1076.6	586.0	0.0095	-	1.12	3045
16	1000.0	516.0	0.0062	-	1.14	4654
17	339.5	167.0	0.0296	-	1.00	6232
18	89.9	57.0	0.0404	-	1.12	7088
19	510.0	250.0	0.0295	-	1.12	7184
20	882.4	470.2	0.0005	0.0275	1.06	3564
21	203.2	158.7	0.0117	0.1519	0.69(TBR)	5031
22	893.3	352.6	0.0008	0.0277	1.06	2680
23	975.3	364.1	0.0008	0.0255	1.07	2863
24	146.6	78.0	0.0012	0.1313	7.63	2236
25	440.3	95.2	0.0013	0.0540	3.11	2044
26	201.0	150.0	0.0300	-	1.09	3254
27	254.4	107.4	0.0046	0.1063	3.52	2480
28	648.8	126.7	0.0034	0.0490	2.74	3639
29	2698.6	1065.6	0.0036	0.0197	1.12	4577
30	446.2	168.5	0.0083	0.0945	2.81	2154
31	2792.4	1362.3	0.0034	0.0244	1.06	9050
32	1839.5	1475.2	0.0049	0.0402	0.99	5127
33	451.1	247.0	0.0100	0.1367	1.82	1192
34	299.1	233.5	0.0126	0.1955	2.27	908
35	220.1	220.6	0.0141	0.2492	2.47	774
36	106.9	135.1	0.0195	0.4418	4.09	621

TBR - To Be Reviewed

* Sub-km bands averaged over even/odd samples to 1-km effective size

From Barnes et al 1998 IEEE Geo and Rem Sens Vol 36 No 4

VIIRS	meas SNR (1:1 agg)	MODIS	meas SNR	wavelength (um)
M1	723	8	933	0.415
M2	576	9	1325	0.443
M3	658	10	1308	0.490
M4	558	12	1114	0.565
M5	360	14	1265	0.681
M6	394	15	1077	0.750
M7	545	16	1000	0.865
M8	349	5	78	1.24
M9	247	26	201	1.38
M10	695	6	324	1.61
M11	18	7	72	2.13
M12	0.12 C	20	0.03 C	3.75
M13	0.04 C	23	0.03 C	4.05
M14	0.04 C	29	0.02 C	8.55
M15	0.03 C	31	0.02 C	11.0
M16	0.04 C	32	0.04 C	12.0
I1	265 (370 m)	1	168 (250 m)	0.64
I2	299 (370 m)	2	413 (250 m)	0.86
I3	165 (370 m)	6	324 (500 m)	1.61
I4	0.4 C (370 m)	20	0.03 C (1 km)	3.75
I5	0.4 C (370 m)	31	0.02 C (1 km)	11.5

Spectral Bias Adjustment Factor

$$\overline{\rho}_{\lambda(A)} = \frac{\int \rho_\lambda RSR_\lambda d\lambda}{\int RSR_\lambda d\lambda}$$

$$SBAF = \frac{\overline{\rho}_{\lambda(A)}}{\overline{\rho}_{\lambda(B)}} = \frac{\left(\int \rho_\lambda RSR_{\lambda(A)} d\lambda\right) / \left(\int RSR_{\lambda(A)} d\lambda\right)}{\left(\int \rho_\lambda RSR_{\lambda(B)} d\lambda\right) / \left(\int RSR_{\lambda(B)} d\lambda\right)}$$

$$\overline{\rho}^{*}{}_{\lambda(A)} = \overline{\rho}_{\lambda(A)} / SBAF$$

Where

RSR_λ = Relative Spectral Response of the sensor [unitless]

ρ_λ = Hyperspectral TOA reflectance profile [unitless]

$\overline{\rho}_{\lambda(A)}$ = Simulated TOA reflectance for sensor A [unitless]

$\overline{\rho}_{\lambda(B)}$ = Simulated TOA reflectance for sensor B [unitless]

$\overline{\rho}^{*}{}_{\lambda(A)}$ = Compensated TOA reflectance for sensor A using the SBAF to match sensor B TO/
[unitless]

		DNB	M1	M2	M3	M4	I1	M5	M6	M7	I2	M8	M9	M10	I3	M11	M12	I4	M13	M14	M15	I5	M16
	Wavelength (um)	0.7	0.412	0.445	0.488	0.555	0.64	0.672	0.746	0.865	0.865	1.24	1.378	1.61	1.61	2.25	3.7	3.74	4.05	8.55	10.76	11.45	12.01
1	Imagery	x	x		x	x	x	x	x	x	x	x	x	x	x	x	x	x	x	x	x	x	x
2	Sea Surface Temp																x				x		x
3	Soil Moisture		Uses VCM, VIIRS LST and several CMIS products, but no SDRs																				
4	Cloud Base Height							x				x		x			x		x	x	x		x
5	Cloud cover/Layers							x				x		x			x		x	x	x		x
6	Cloud Optical Part Size							x				x		x			x			x	x		x
7	Cloud Thickness							x				x		x			x			x	x		x
8	Cloud Top Height							x				x		x			x		x	x	x		x
9	Cloud Top Pressure							x				x		x			x		x	x	x		x
10	Cloud Top Temp							x				x		x			x		x	x	x		x
11	Land Surface Temp.																x		x		x		x
12	Active Fires							x		x						x			x		x		x
13	Vegetation Index				x		x				x												
14	Snow Cover (Binary)						x				x				x						x	x	x
15	Snow Cover (Fraction)		x		x	x				x		x		x		x							
16	Surface Type		x	x	x	x	x	x		x	x	x		x		x	x		x	x	x		x
17	Surface Albedo		x	x	x	x		x		x		x		x		x							
18	Ice Surface Temp.																				x		x
19	Net Heat Flux		Uses VCM and other VIIRS EDRs, but no SDRs																				
20	Surface Temperature (IP)																				x	x	x
21	Ocean Color / Chloro		x	x	x	x		x	x	x													
22	Sea Ice Age						x				x										x	x	x
23	Aer Opt Thick (Ocean)					x		x	x	x		x	x	x		x	x				x		
24	Aer Opt Thick (Land)		x	x	x	x		x					x			x	x				x		
25	Aer Part Size (Ocean)	Uses AOT, but no SDRs																					
26	Aer Part Size (Land)	Uses AOT, but no SDRs																					
27	Suspended Matter																			x	x		x
28	Total Prec Water																x		x	x	x		x
29	Cloud Mask (IP)		x				x	x		x	x		x	x		x	x	x	x	x	x	x	x
30	Ice Location/Conc. (IP)		Imagery Application is not re				x				x										x	x	x
31	Sfc Reflectance (IP)		x	x	x	x	x	x		x	x	x		x	x	x							

Ocean
Land
Aerosol
Clouds
Ice and Snow

Dual Gain Bands: M1-M5, M7, M13

VIS	NIR	SWIR	MWIR	LWIR

x Denotes bands that are **Not** primary inputs into algorithm. Used as internal check for algorithm.

Better than 1.3 km Horizontal Sample Interval (HSI) Well Past 1700km

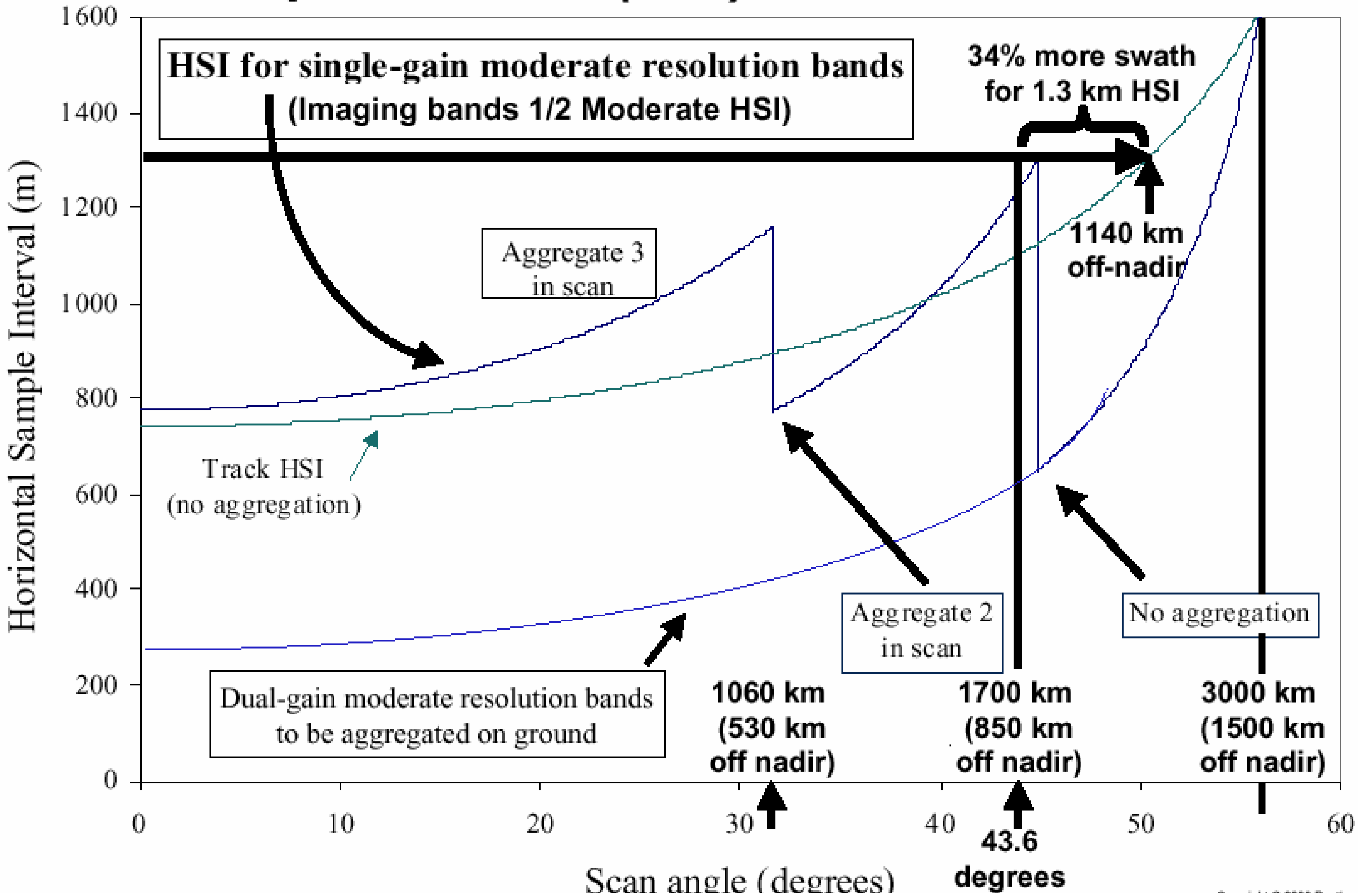

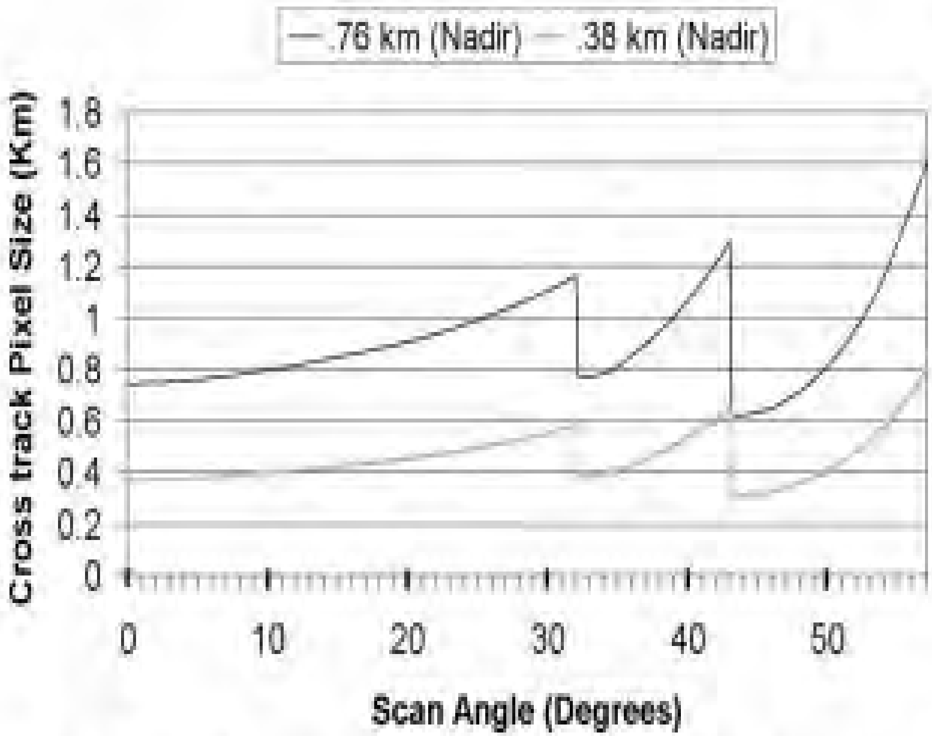

FIG. 2. VIIRS cross-track variation in pixel size as a function of scan angle away from nadir. Both resolutions will be used in the construction of true color.

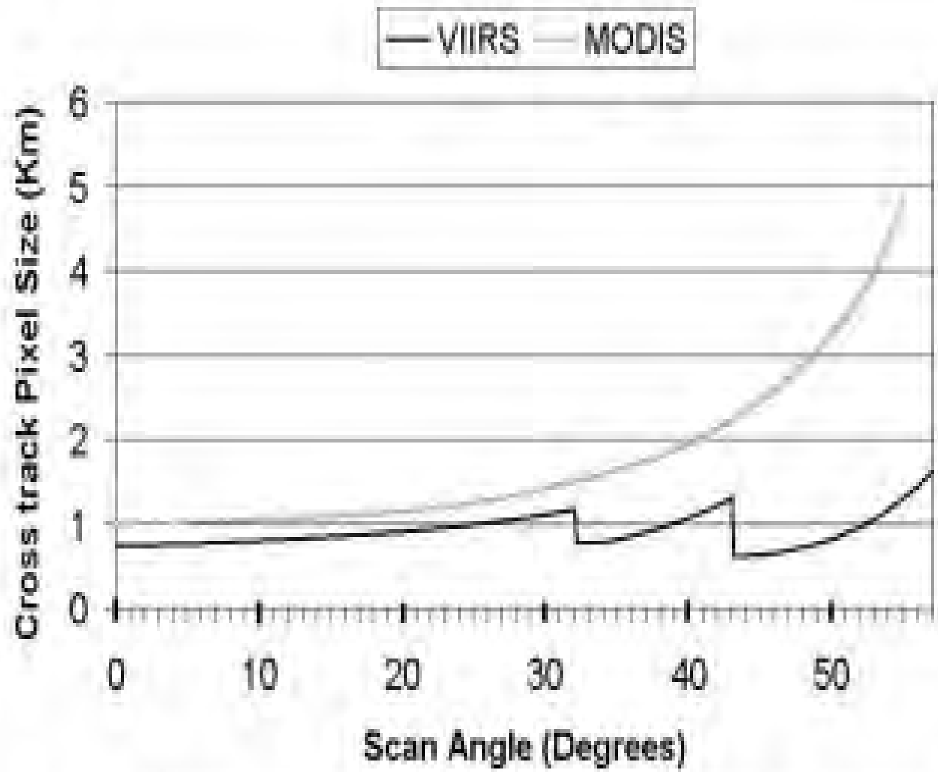

FIG. 4. Comparison of 1-km (nadir) resolution used for 29 of 36 MODIS channels with 0.76-km (nadir) resolution for VIIRS at moderate resolution. Of the 22 VIIRS channels, 17 use the resolution shown here. Five use a higher resolution of 0.38 km (nadir).

Finer Sampling, Spatial Resolution, & Better Sensitivity

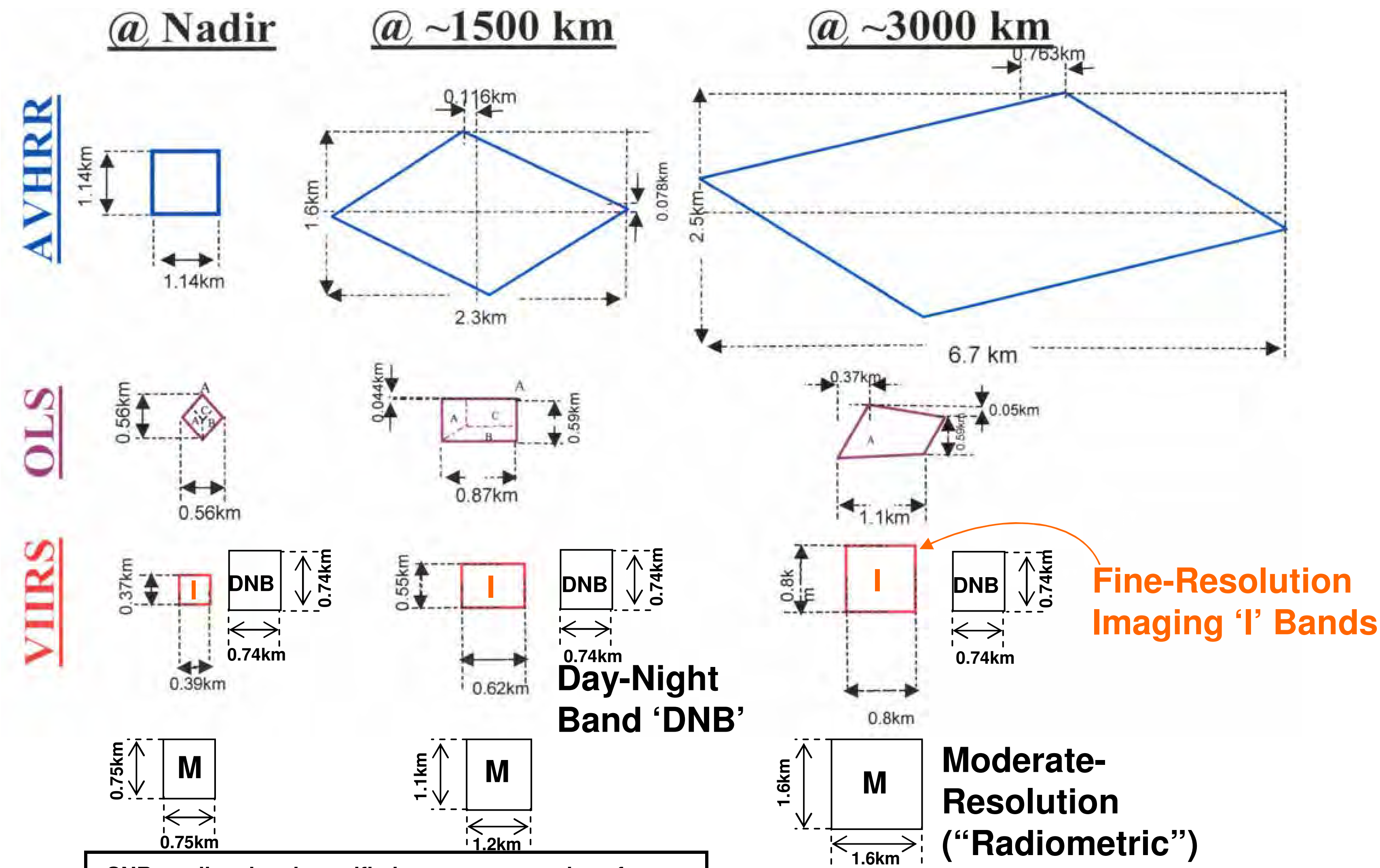

SNR predicted and specified at worst-case edge of scan:
~60% better nadir SNR *and* finer spatial resolution

VIIRS has a very large cross track and near constant spatial resolution

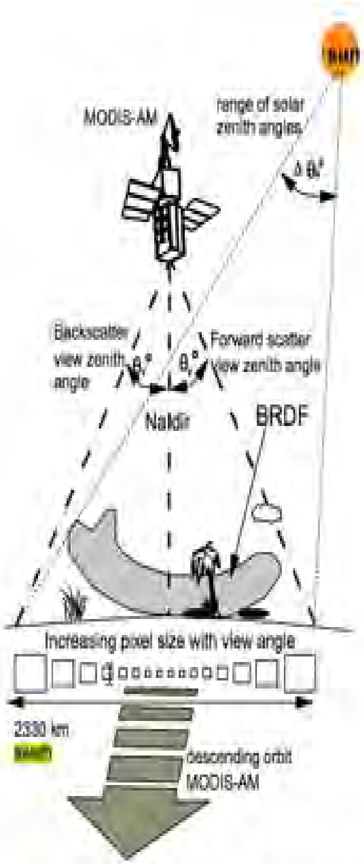

Figure 3.2.3: Illustration of MODIS data acquisition on the EOS-AM platform (not to scale). The bidirectional reflectance distribution function (BRDF) changes with view and sun geometry. Notice the shadow caused by clouds and canopy. MODIS pixel dimensions, cross-track and along-track, change with scan angles: 0° - 250 x 250 m; 15° - 270 x 260 m; 30° - 350 x 285 m; 45° - 610 x 380 m

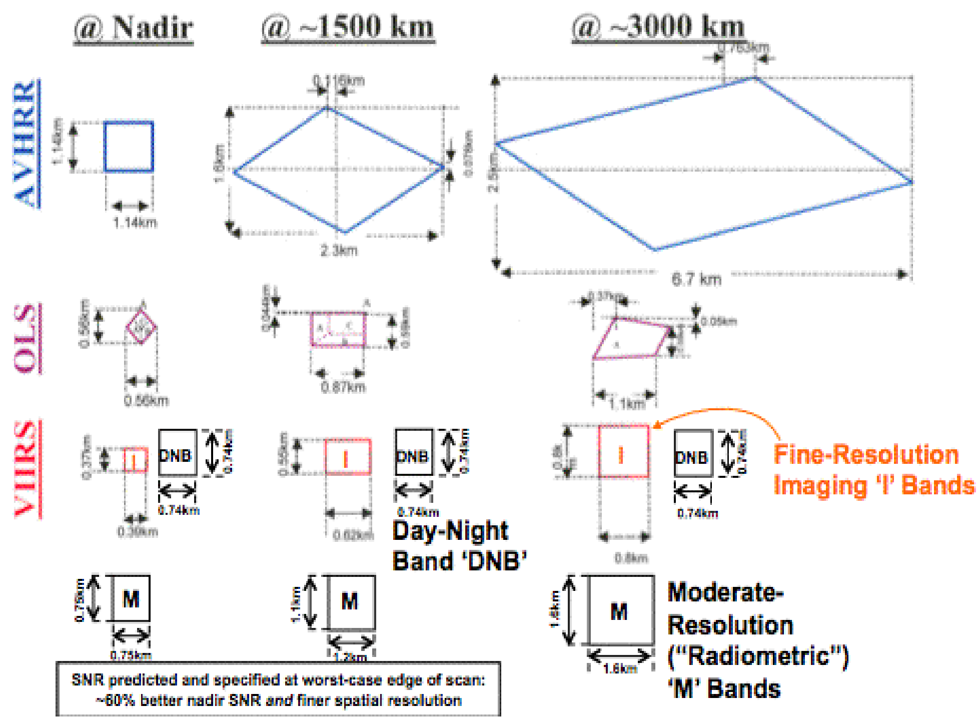

SNR@L_{typ} by Aggregation Zone

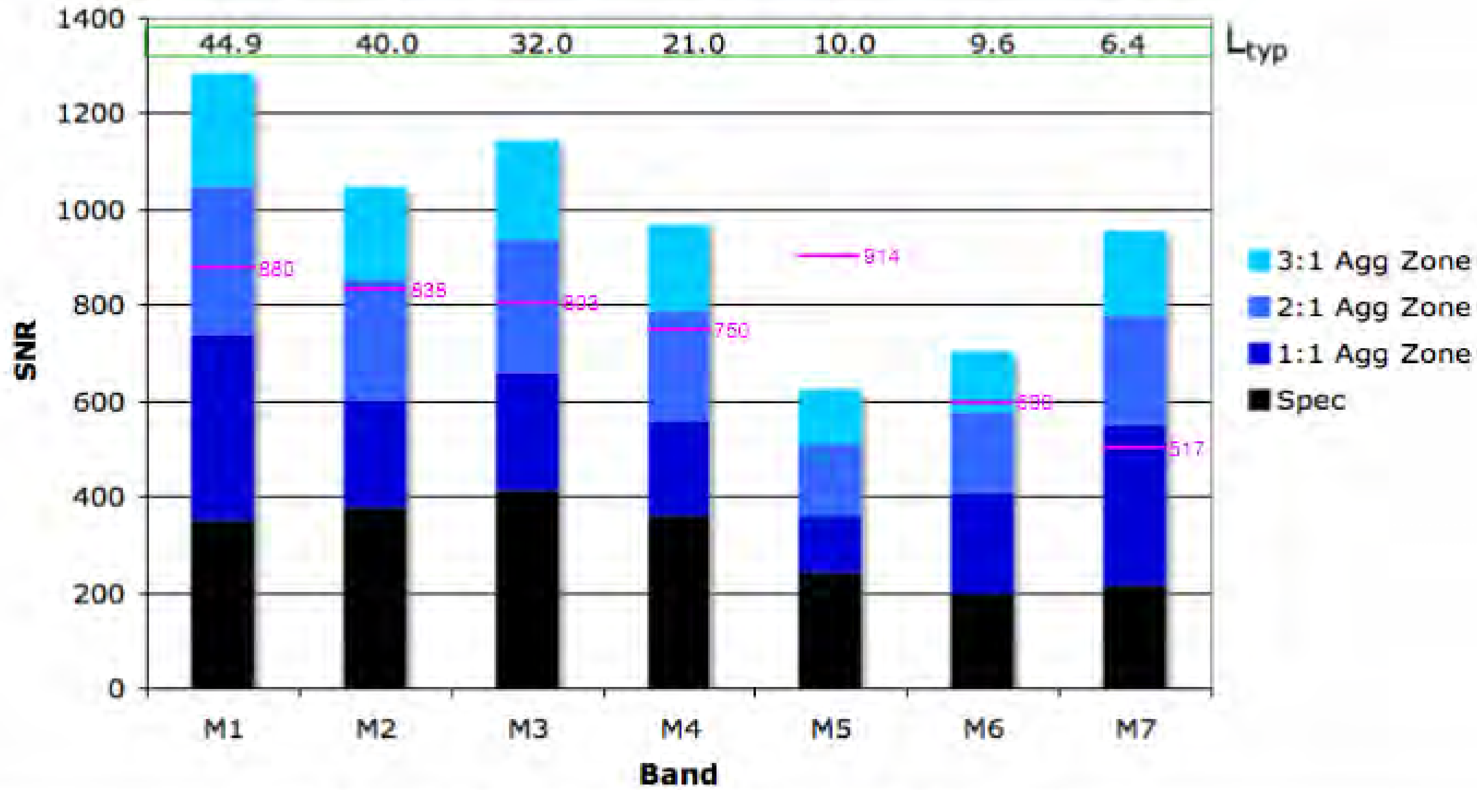

Scan Aggregation Zones

Dual-gain Bands - samples aggregated on ground.
Singe-gain Bands - samples aggregated on-board (only M6 for ocean bands).

source: MDFCB, 4 Nov 2004

NPP VIIRS True Color Examples

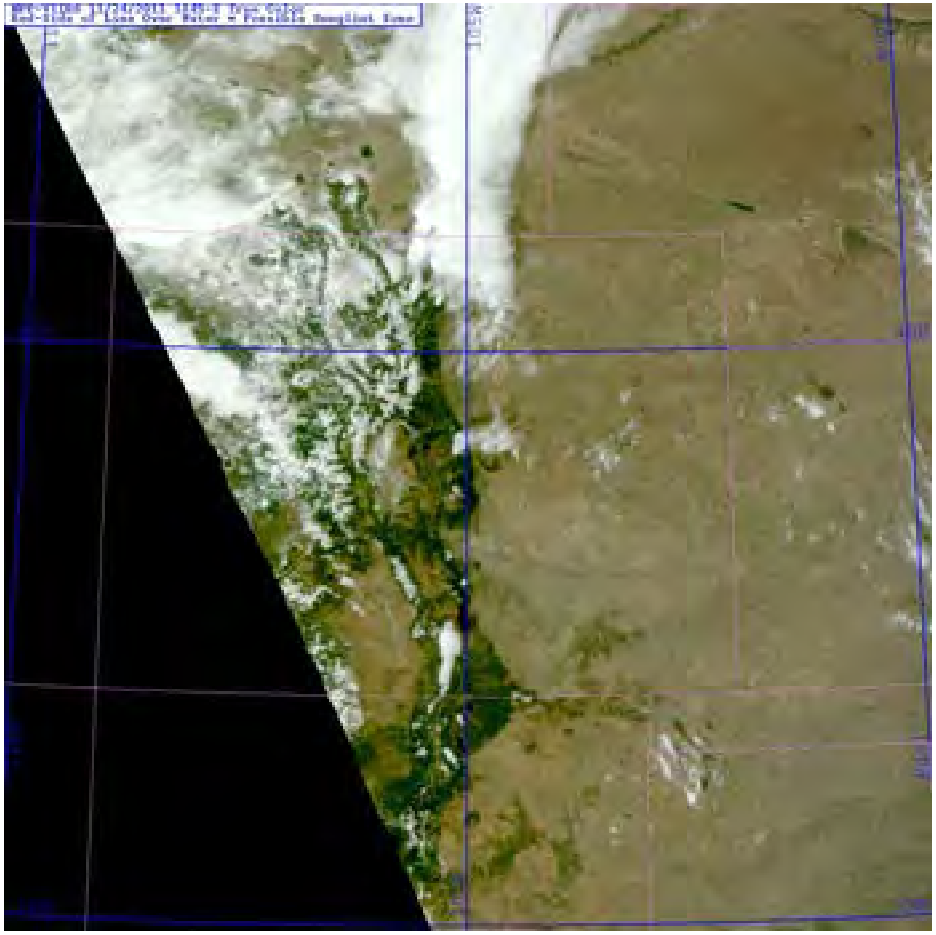

11.24.2011 2028 UTC, Near Nadir

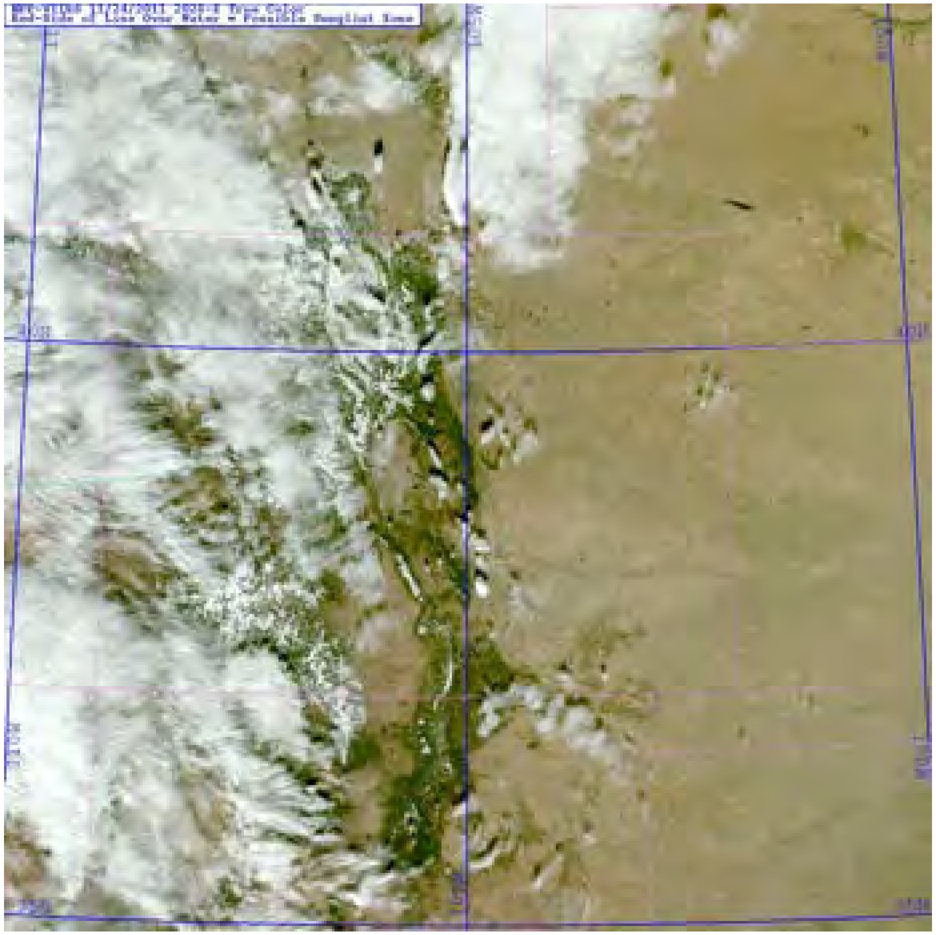

→ VIIRS maintains similar spatial resolution quality at edge of 3000 km swath

NPP VIIRS True Color Examples

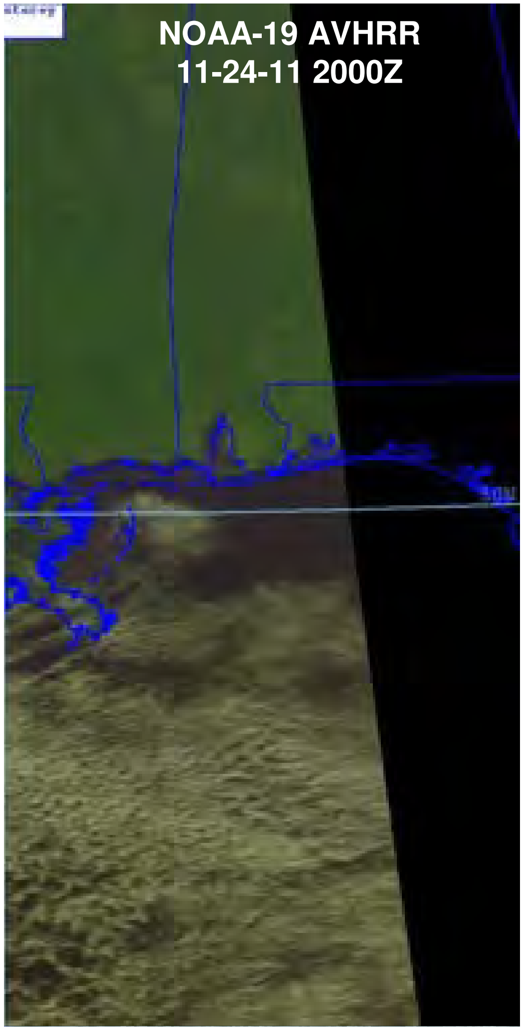

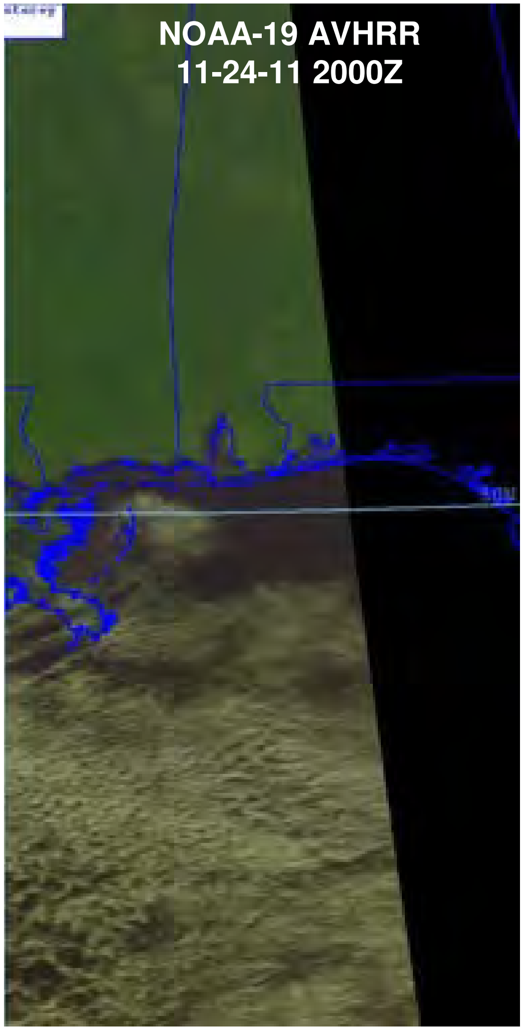

Quality of Subsectors

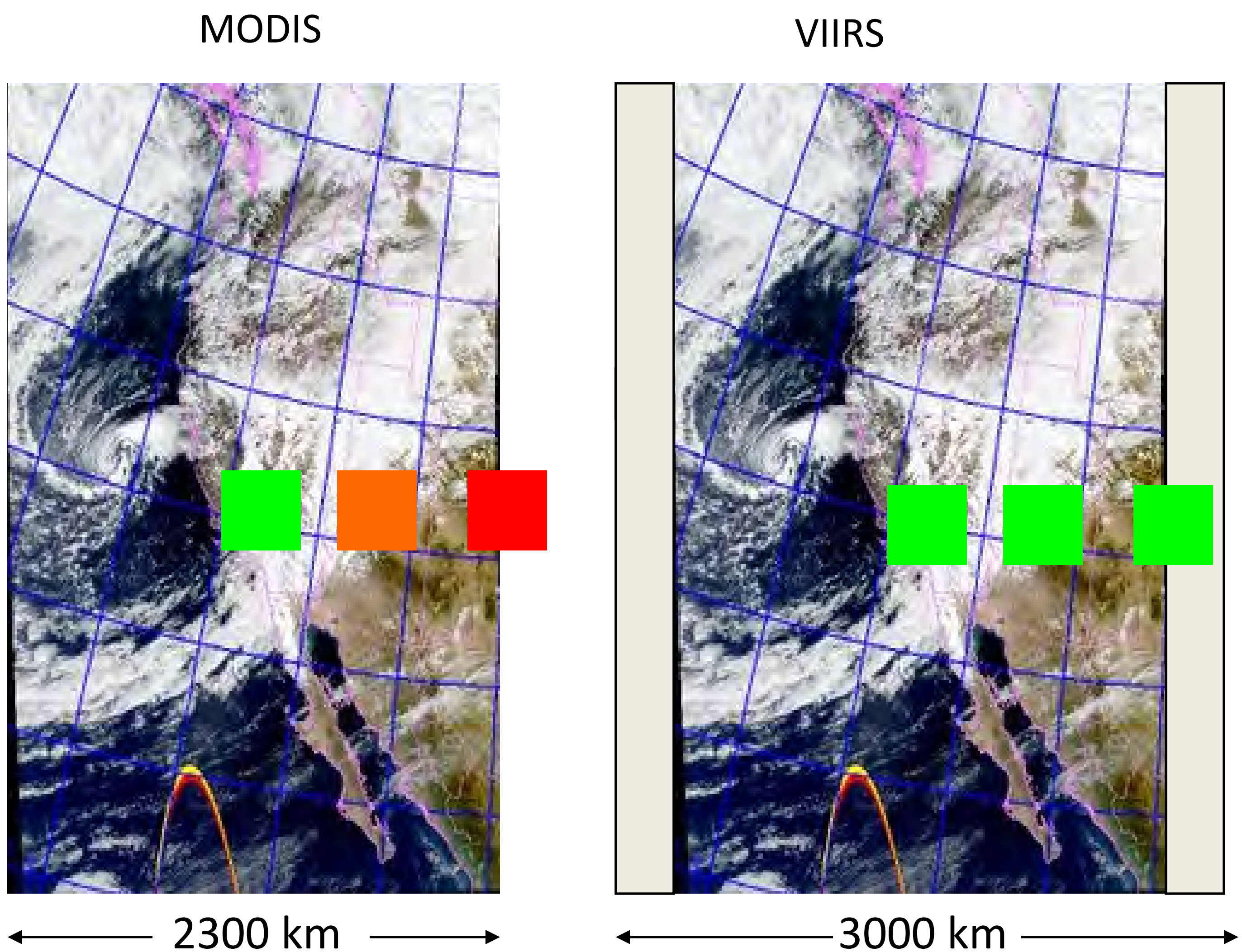

First Global VIIRS Image

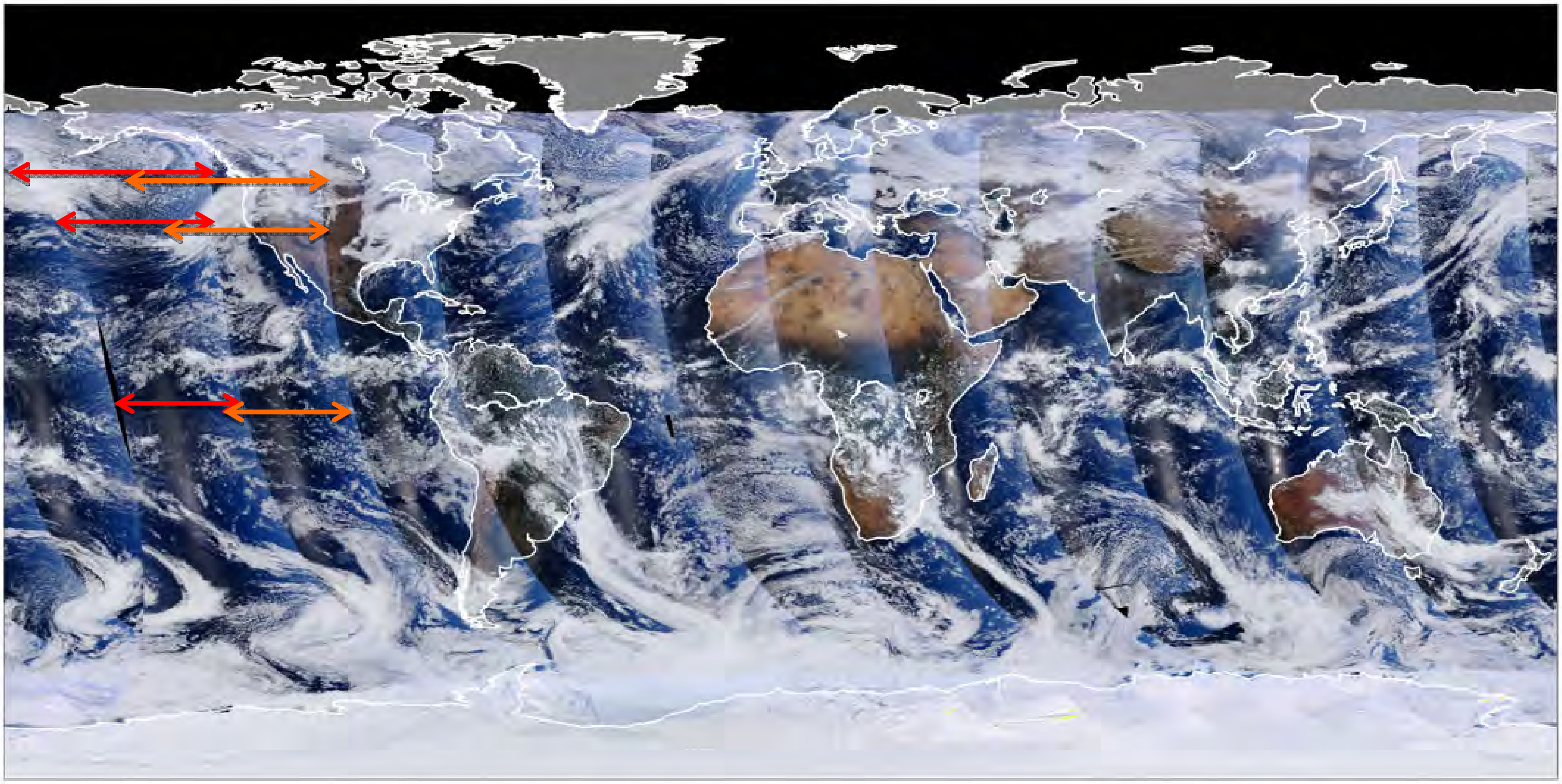

VIIRS RGB (True Color), 20111122

R : M05 (0.672 μm); G : M04 (0.555 μm); B : M02 (0.445 μm)

Creation date: 2011-11-26 07:19:26 Z

Transitioning from MODIS to VIIRS for remote sensing of ocean, land, and atmosphere

RT in Earth Atmosphere
Multispectral Signatures
MODIS Heritage Products
VIIRS Instrument Description
Some Anticipated VIIRS Applications
(SST, Ocean Color, Vegetation, Snow, Ice, Clouds, Moisture, Fires, Dust, Low Light Imagery)

W. Paul Menzel, University of Wisconsin- Madison

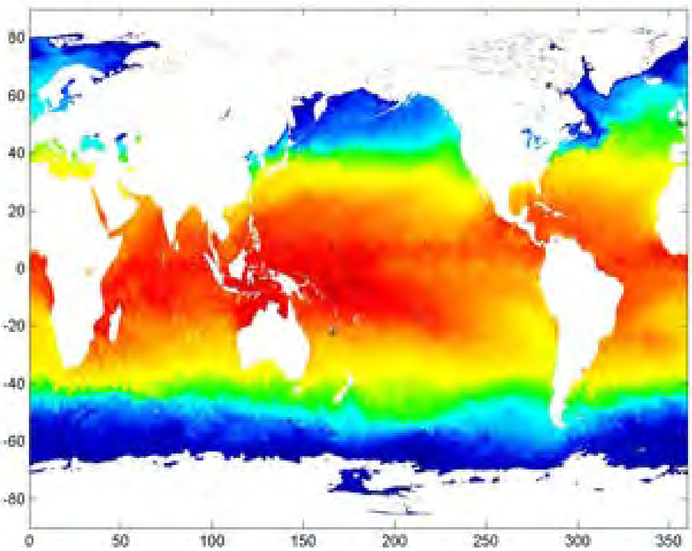

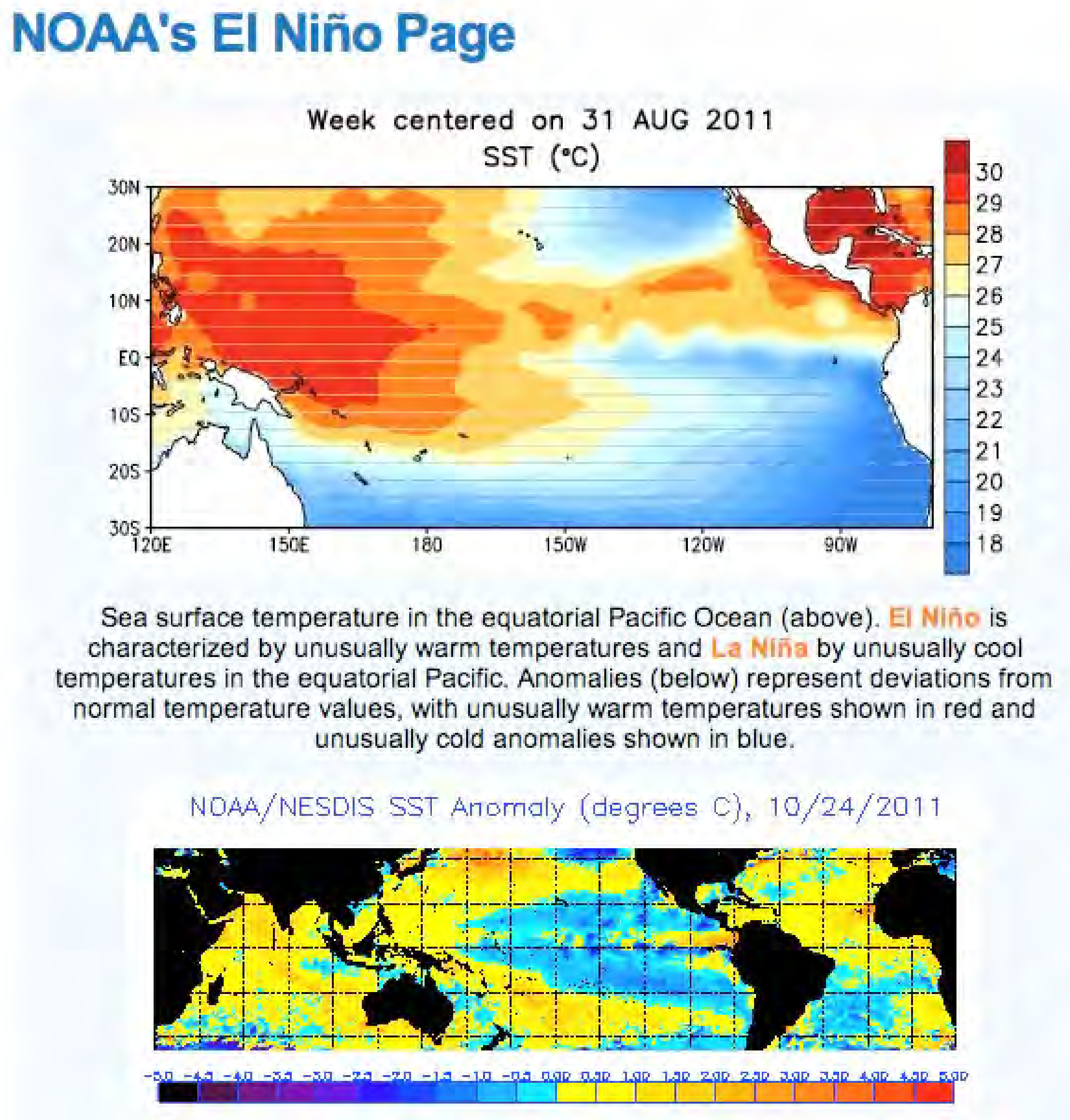

VIIRS will provide improved SST

Monitoring Biosphere

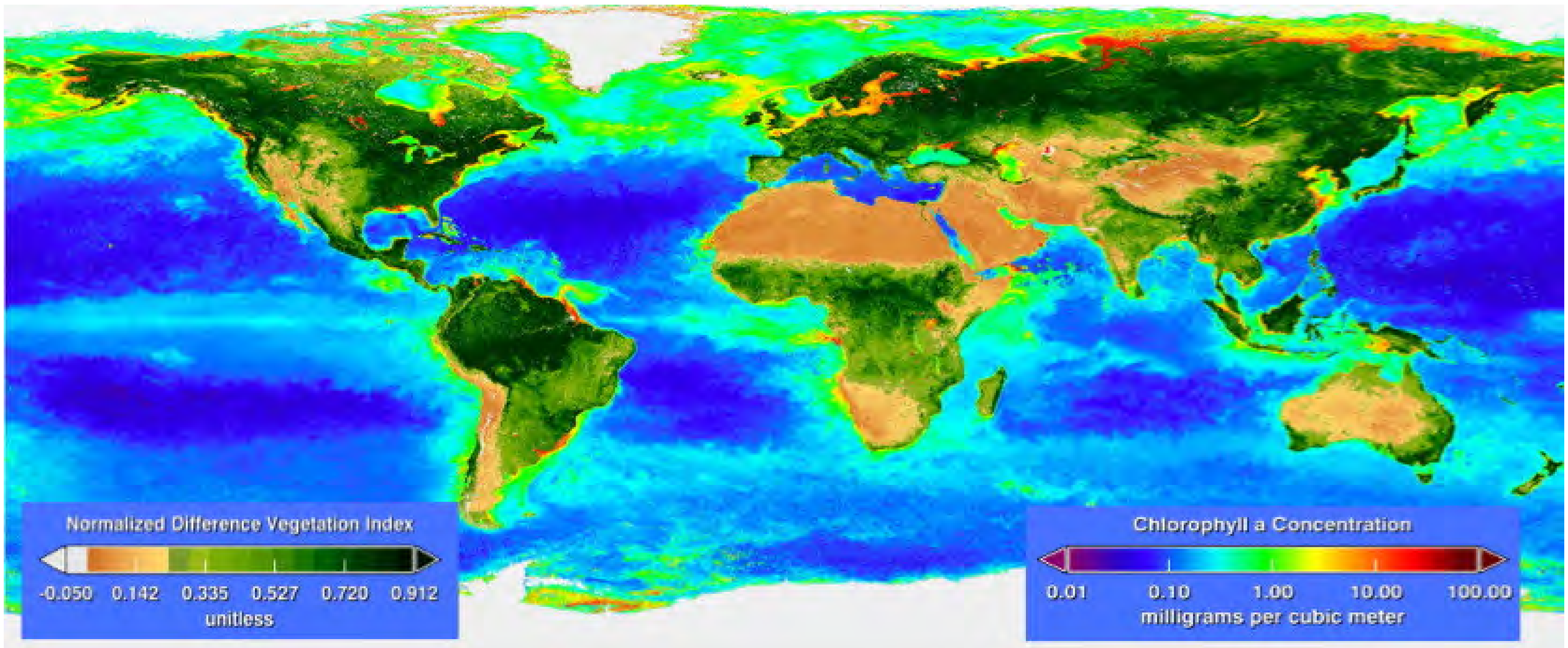

Cloud/Snow Discrimination

- Complex snow/cloud scenes during winter in Southwest Asia
- Difficult to distinguish clouds from snow in single visible and window-infrared channels
- The ability to determine the presence of cloud over a snow field is useful to targeting, surveillance, navigation, etc.

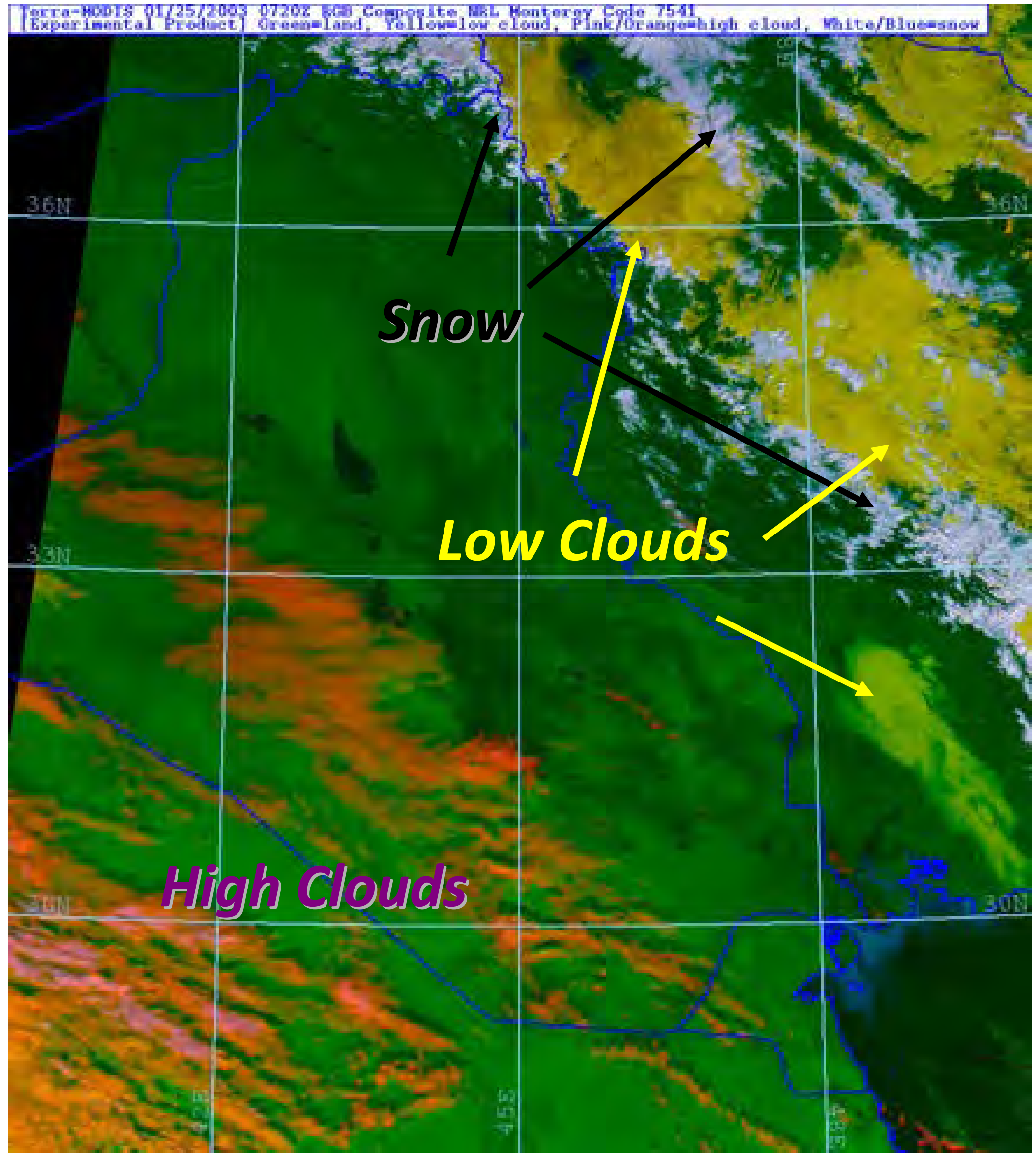

TC Funso- VIIRS

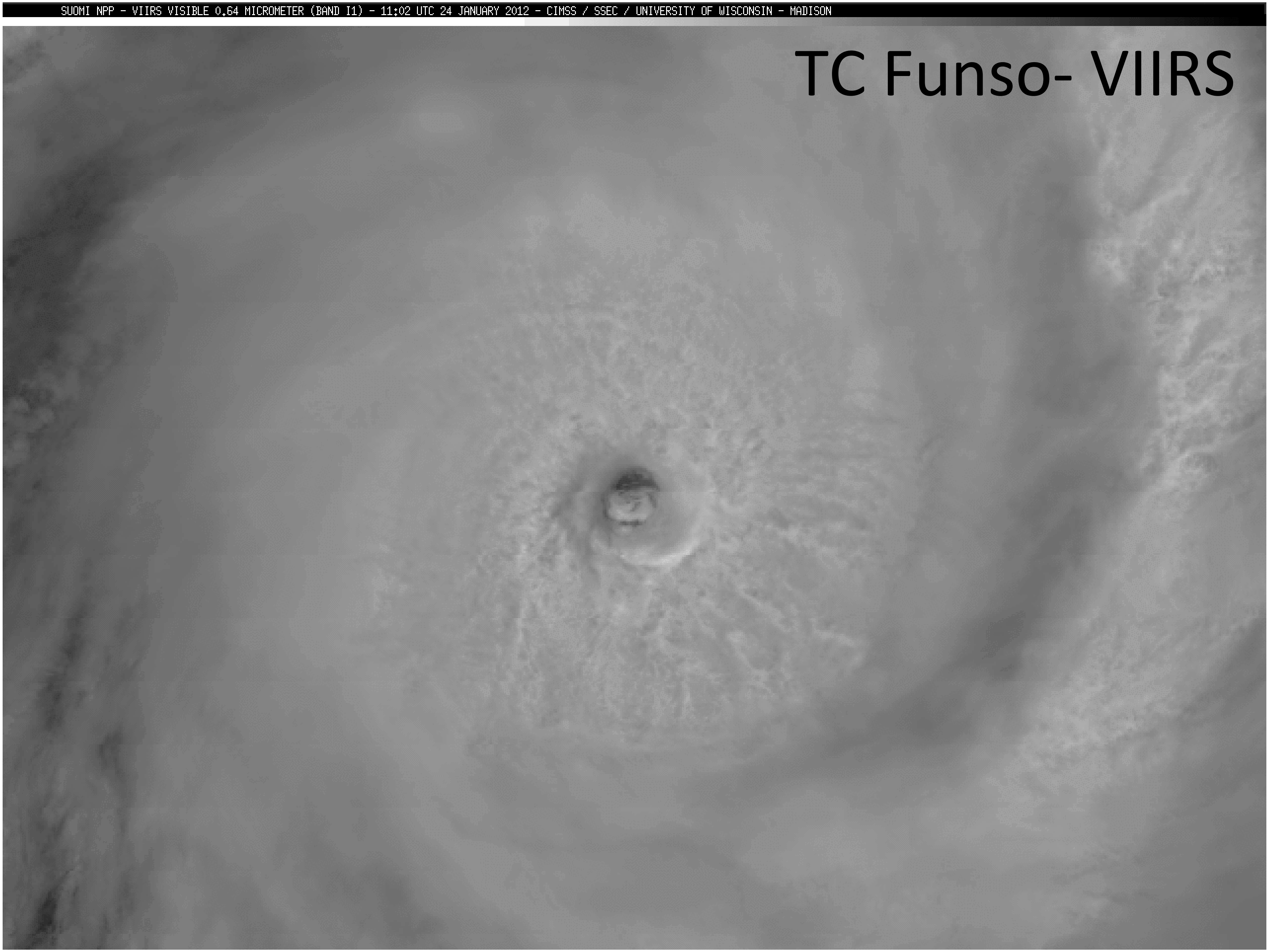

VIIRS Snow Cover EDR

- ***EDR description:*** Snow Cover/Depth is defined to be the horizontal and vertical extent of snow cover. In addition, a binary product will give a snow/no-snow flag. While the original EDR definition included snow depth, the current specification is for snow cover only.
- ***Current Retrieval Strategy:***
  - Algorithm Heritage: MODIS MOD10 L2 “SnowMap” algorithm (NASA) based on the Normalized Difference Snow Index (NDSI).
  - A threshold-based decision-tree algorithm is employed to separate snow free and snow covered pixels. An external cloud mask is used to exclude cloudy pixels from the classification process.
  - A snow cover binary map produced at the VIIRS imagery resolution. Snow cover fraction is calculated by 2X2 aggregation of the binary snow cover map is produced at VIIRS moderate resolution.
- ***Product Status and Expected Updates****:* The Binary Snow Map product should meet its target requirement of 90% probability of correct classification.

RGB Image

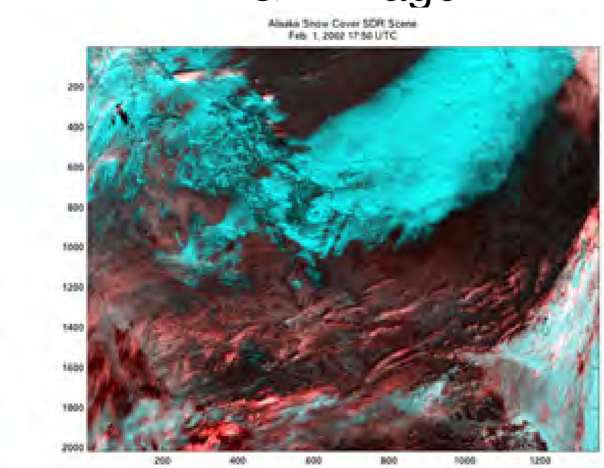

VIIRS Snow Map

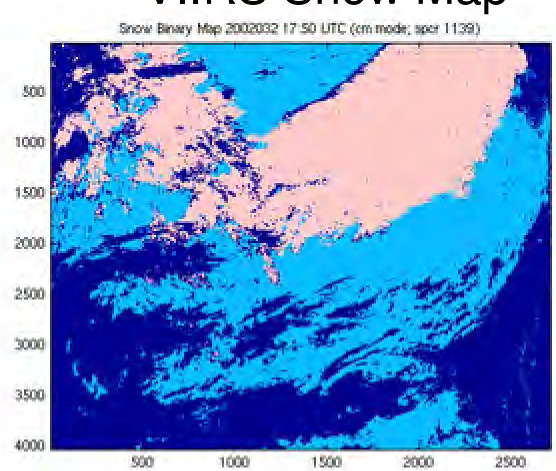

MOD10 Snow Map

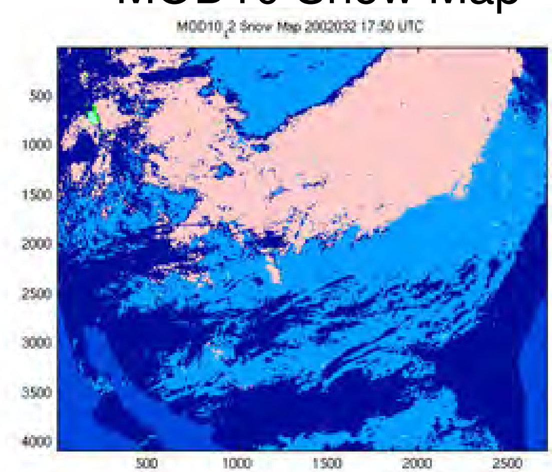

VIIRS Ice Characterization EDR

- ***EDR description:*** An ice age classification for the categories: Ice -free, New/Young Ice (less than 30 cm thickness), and All Other ice. Freshwater ice is not included.
- ***Current Retrieval Strategy:***
  - An energy budget approach is used to estimate sea ice ice thickness.
  - Daytime and nighttime algorithms use different approaches.
  - While the algorithm generates age categories, it actually uses temperature, reflectance and estimated thickness as proxies for age (i.e., age is not calculated directly).
  - Ice concentration is a intermediate product (IP) in the ice characterization EDR.
- ***Product Status and Expected Updates****:* The uncertainty of the product is highest for nighttime retrievals. An alternative model is being investigated.

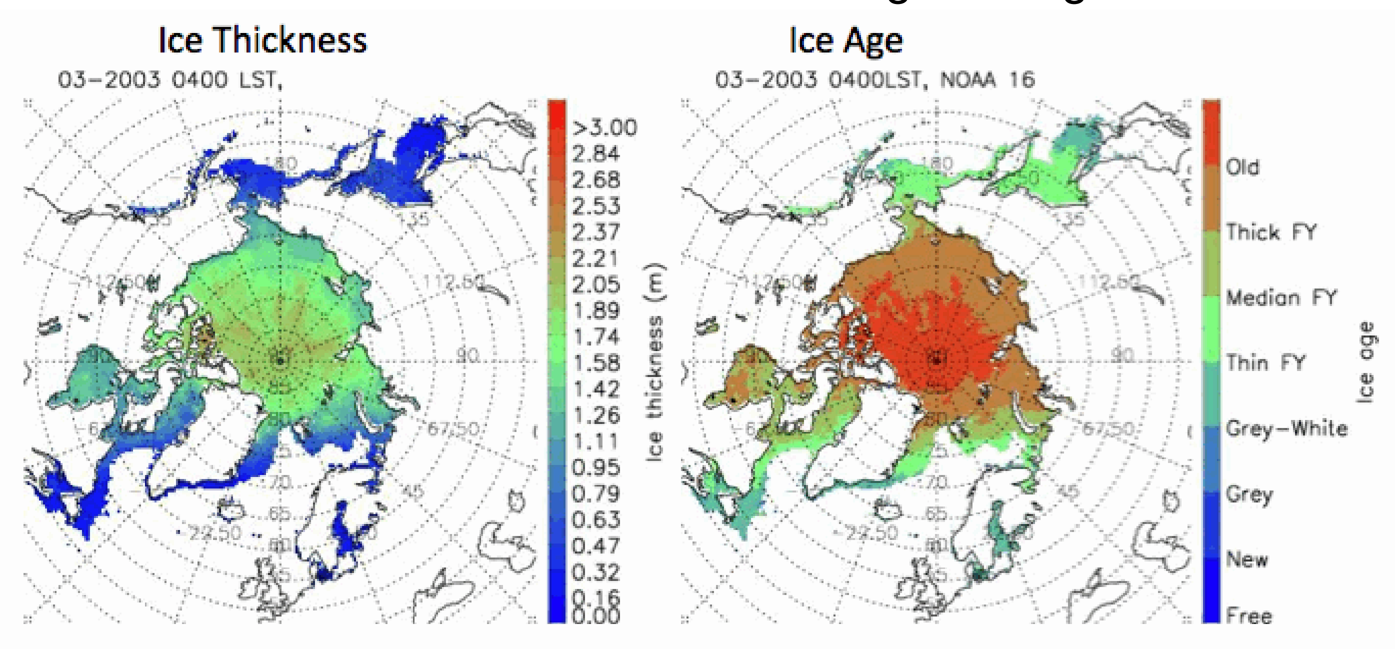

Examples of ice thickness (left) and ice age (right) over the Arctic.

VIIRS Ice Surface Temperature EDR

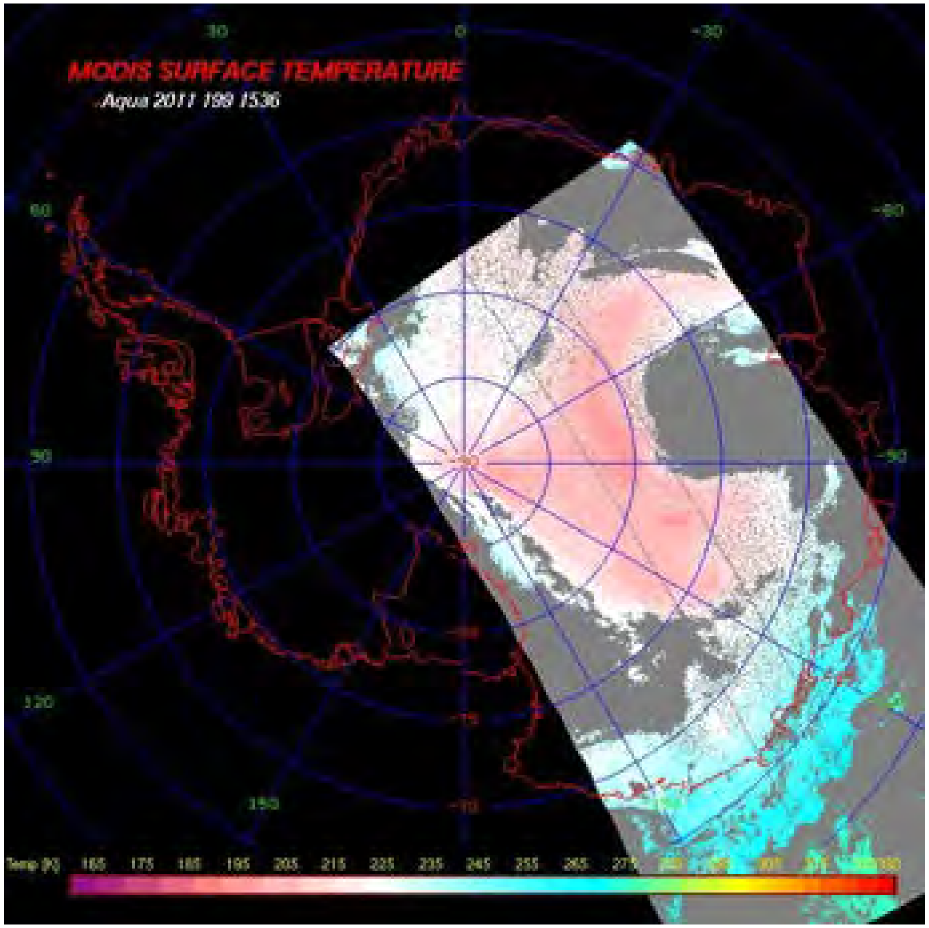

The surface temperature over part of the Antarctic ice sheet and surrounding sea ice derived from MODIS data with a VIIRS-like algorithm.

- ***Description:*** The surface (skin, or radiating) temperature over snow and ice.
- ***Retrieval Strategy:***
  - The algorithm incorporates an empirical correction for water vapor absorption.
  - It is a split-window approach similar to that used for sea surface temperature (SST).
- ***Current Challenges****:* Based on the performance of its heritage AVHRR and MODIS algorithms, the IST EDR should meet its accuracy specification for the two-channel method, although additional tuning would be beneficial.

Aircraft Contrails

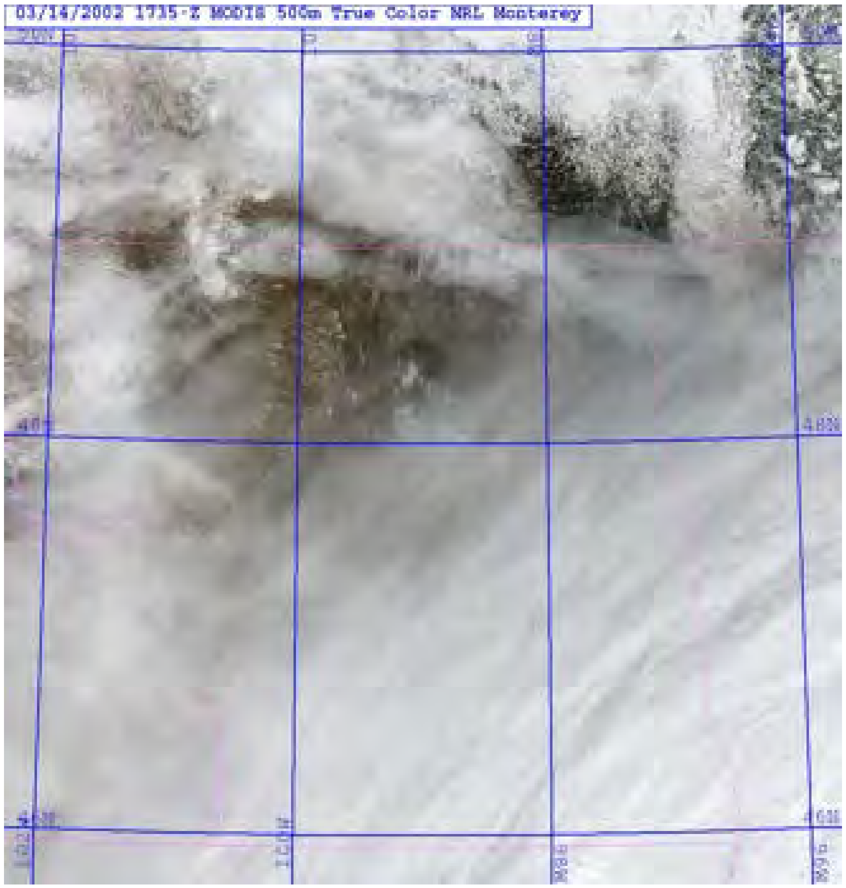

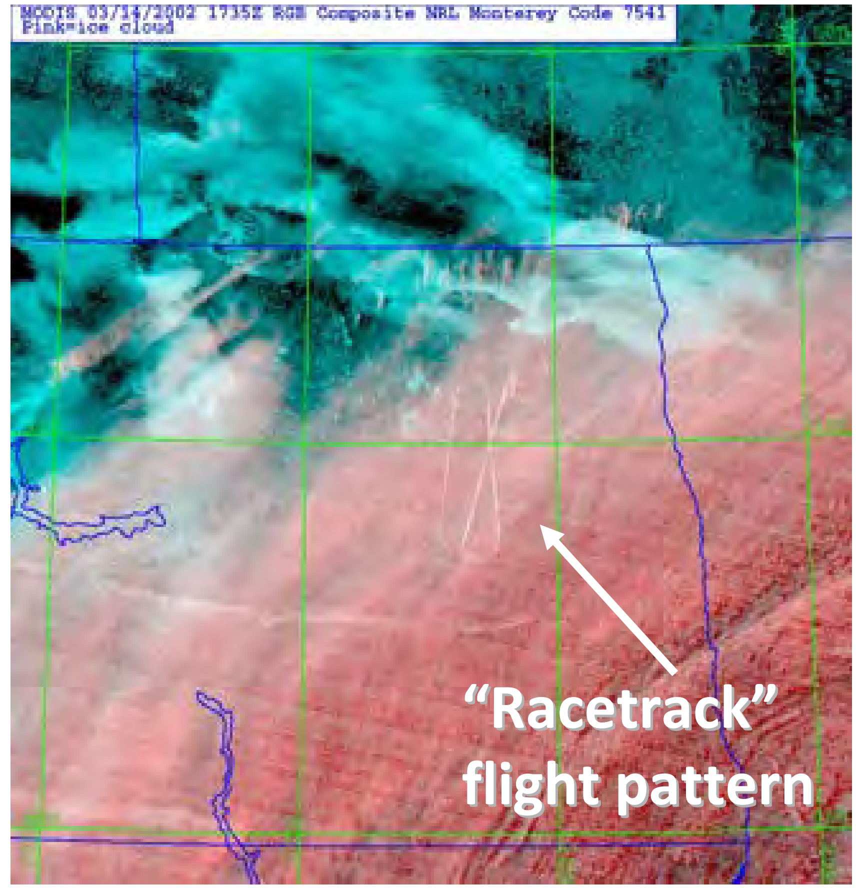

Fog - MODIS

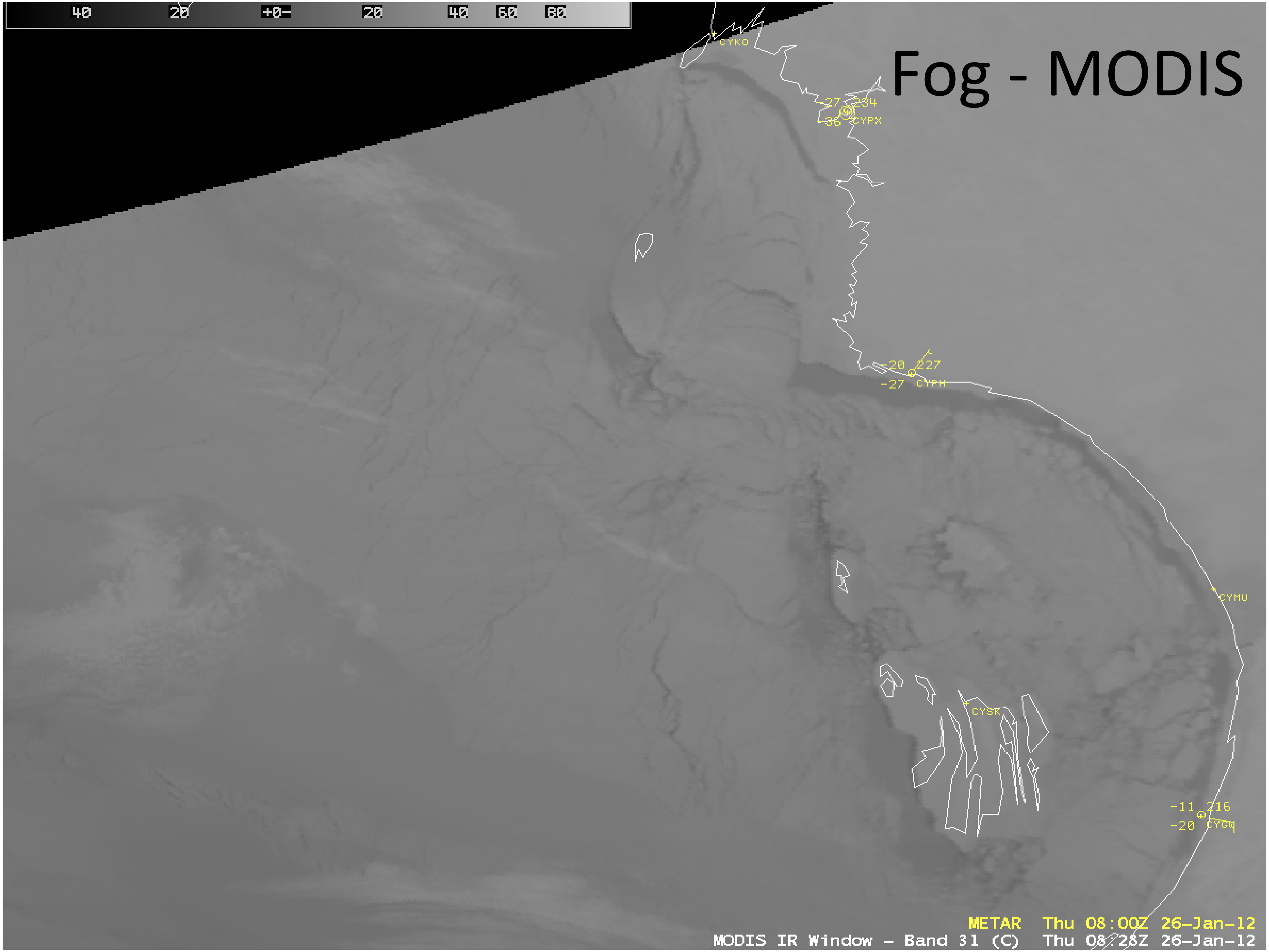

40
20
+0-
20
40
60
80
CYKO
CYPX
CYPH
CYMU
CYSK
CYGQ
METAR Thu 08:00Z 26-Jan-12
MODIS IR Window - Band 31 (C) Thu 08:28Z 26-Jan-12

Fog - VIIRS

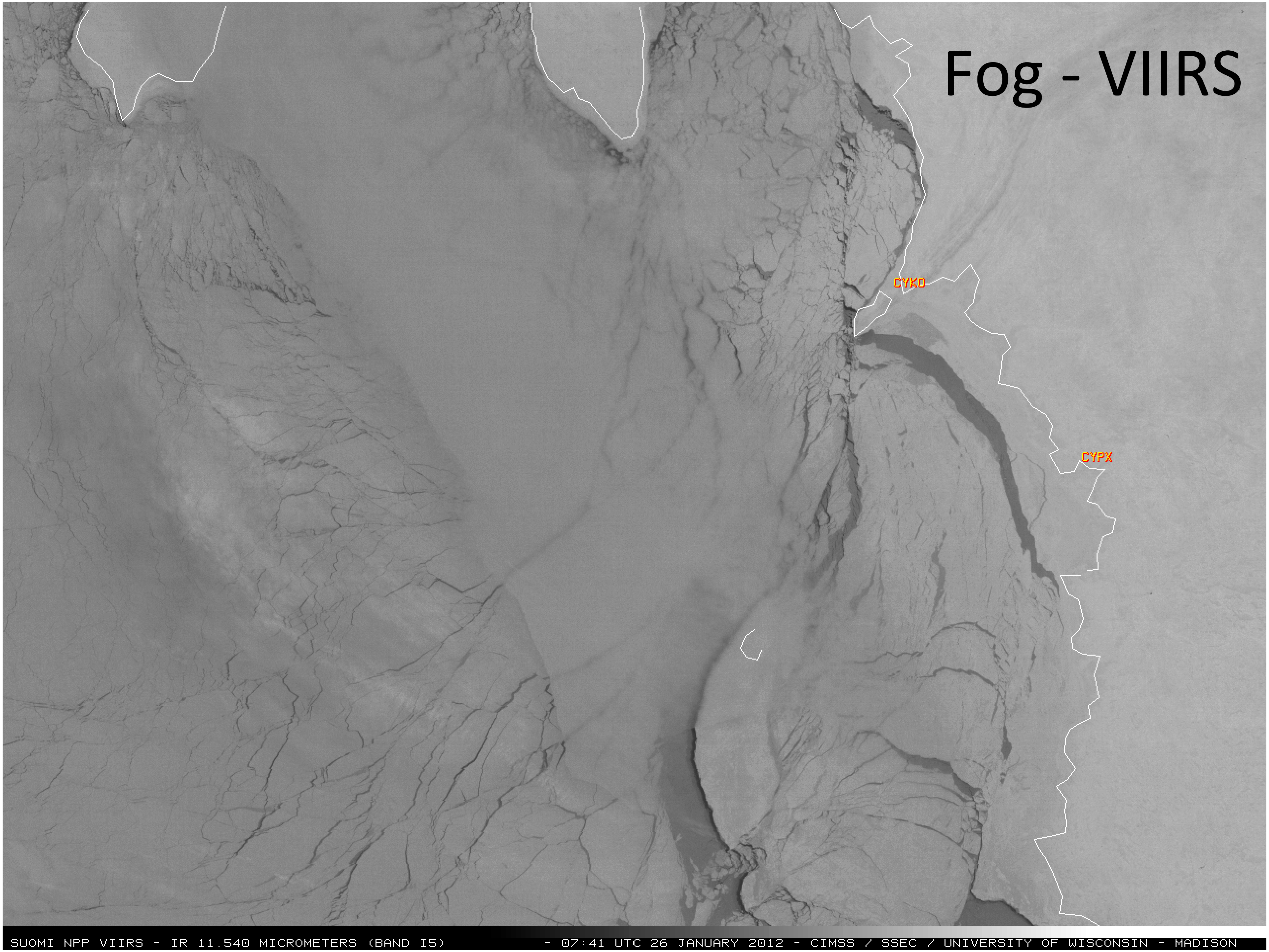
CYKO
CYPX
SUOMI NPP VIIRS - IR 11.540 MICROMETERS (BAND I5)
- 07:41 UTC 26 JANUARY 2012 - CIMSS / SSEC / UNIVERSITY OF WISCONSIN - MADISON

Fire Detection

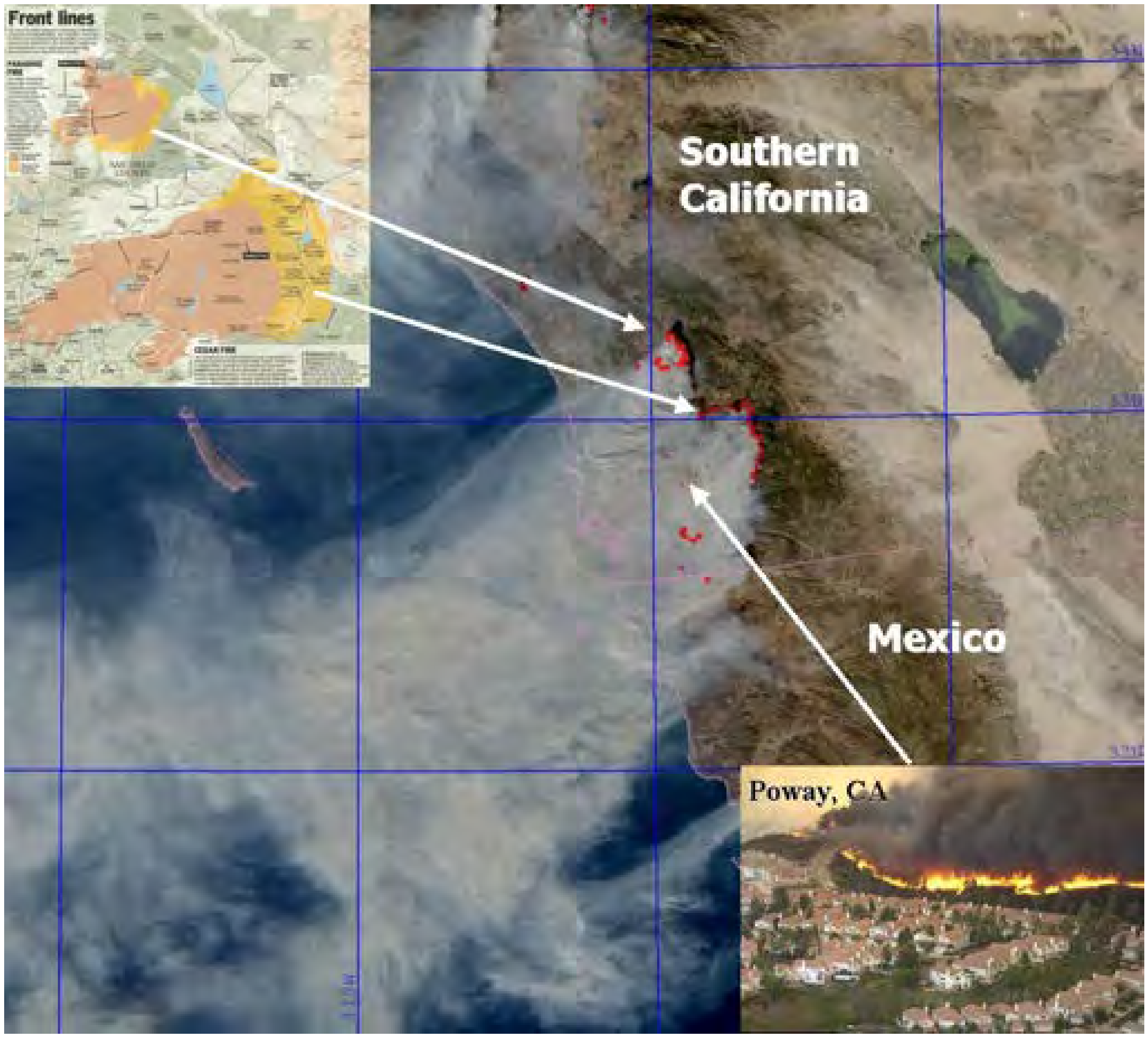

Fire - AVHRR

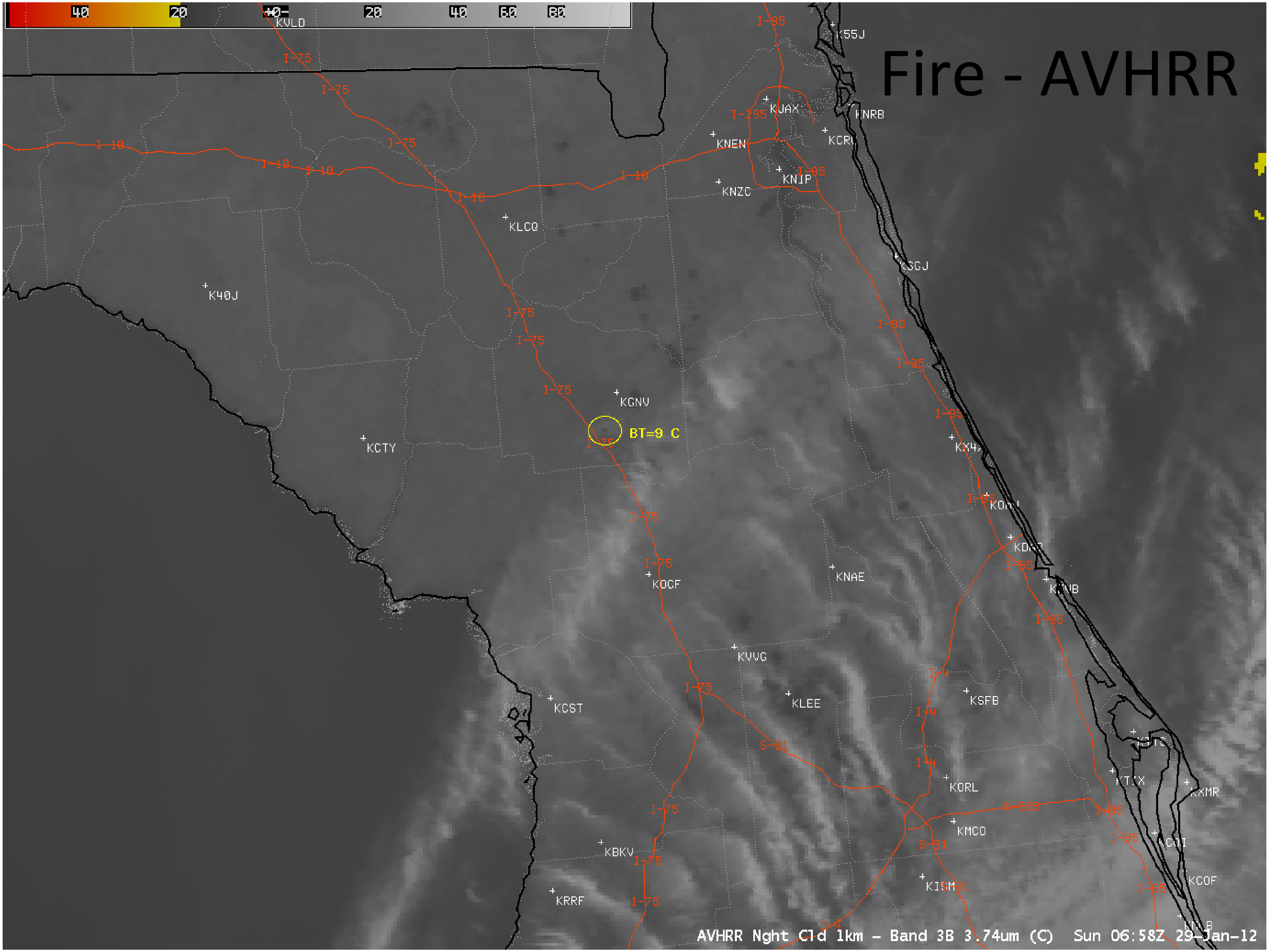

40
20
-0-
20
40
60
80
BT=9 C
KGNV
KLCQ
KJAX
KOCF
KCTY
AVHRR Nght Cld 1km - Band 3B 3.74um (C) Sun 06:58Z 29-Jan-12

Fire - VIIRS

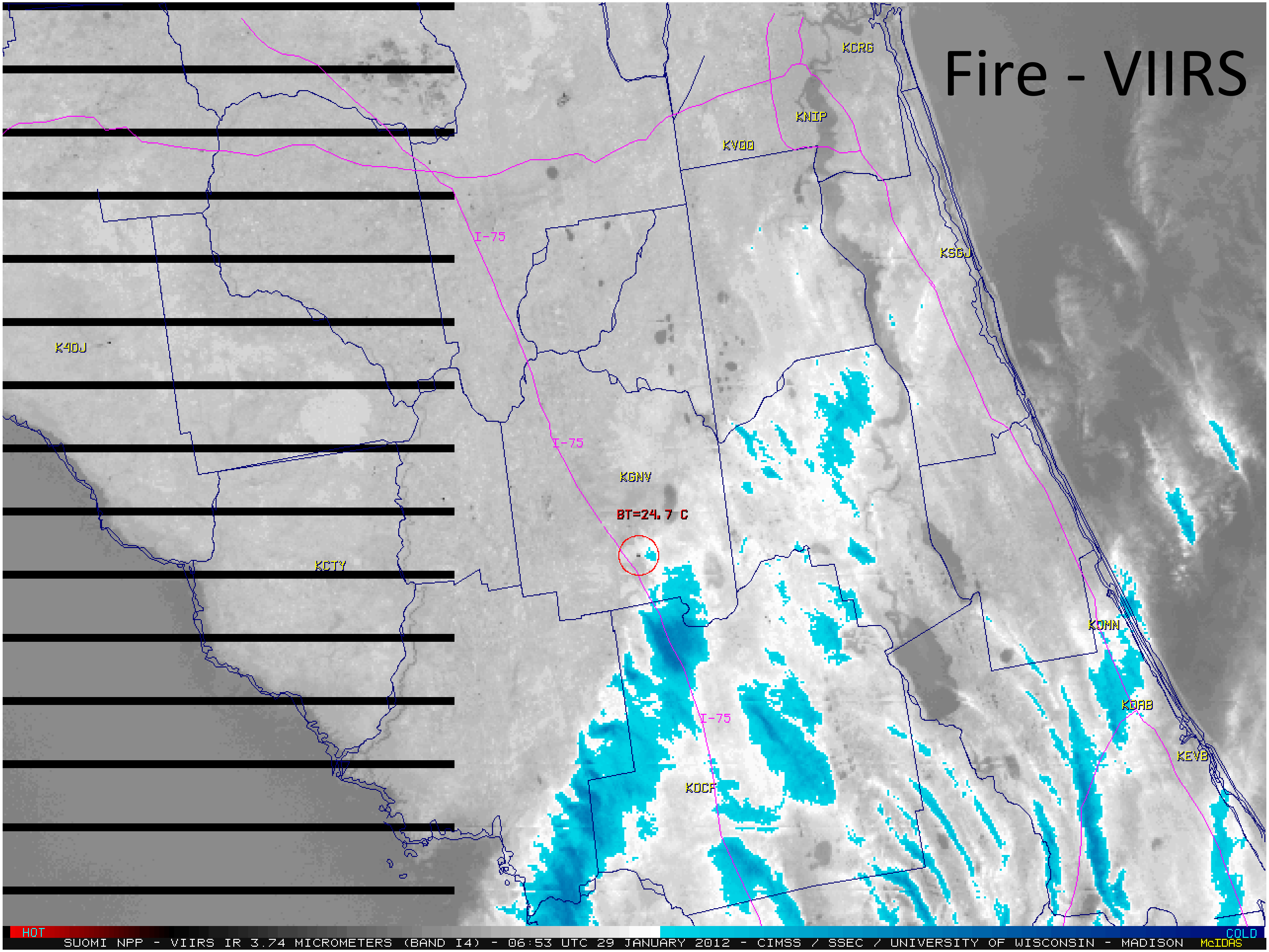
KCRG
KNIP
KVQQ
KSGJ
K4OJ
I-75
I-75
KGNV
BT=24.7 C
KCTY
KOMN
KDAB
I-75
KEVB
KOCF
HOT
COLD
SUOMI NPP - VIIRS IR 3.74 MICROMETERS (BAND I4) - 06:53 UTC 29 JANUARY 2012 - CIMSS / SSEC / UNIVERSITY OF WISCONSIN - MADISON
McIDAS

Dust Storms

True Color

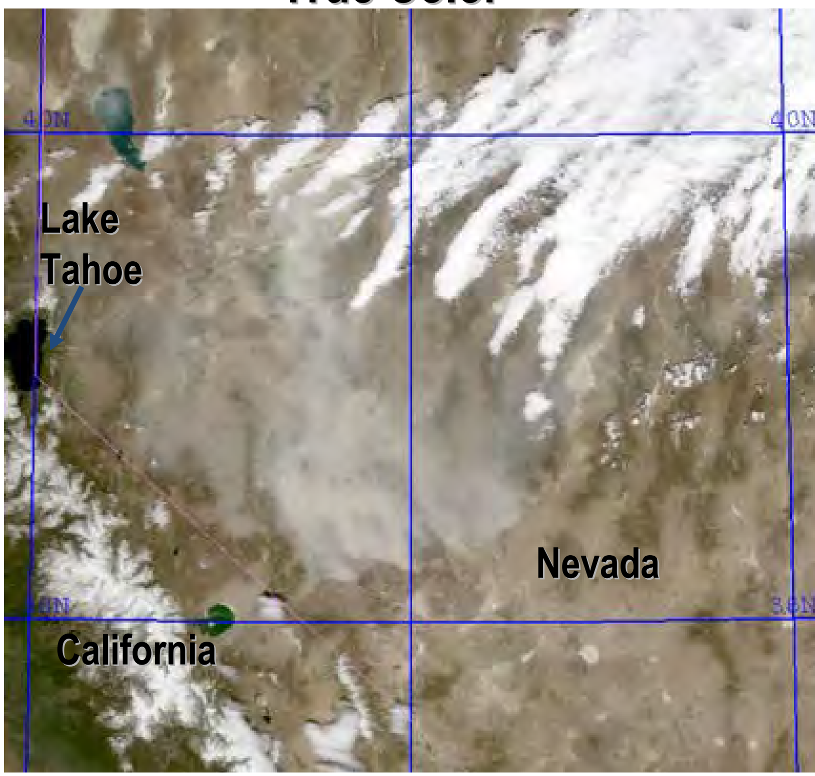

Dust Enhancement

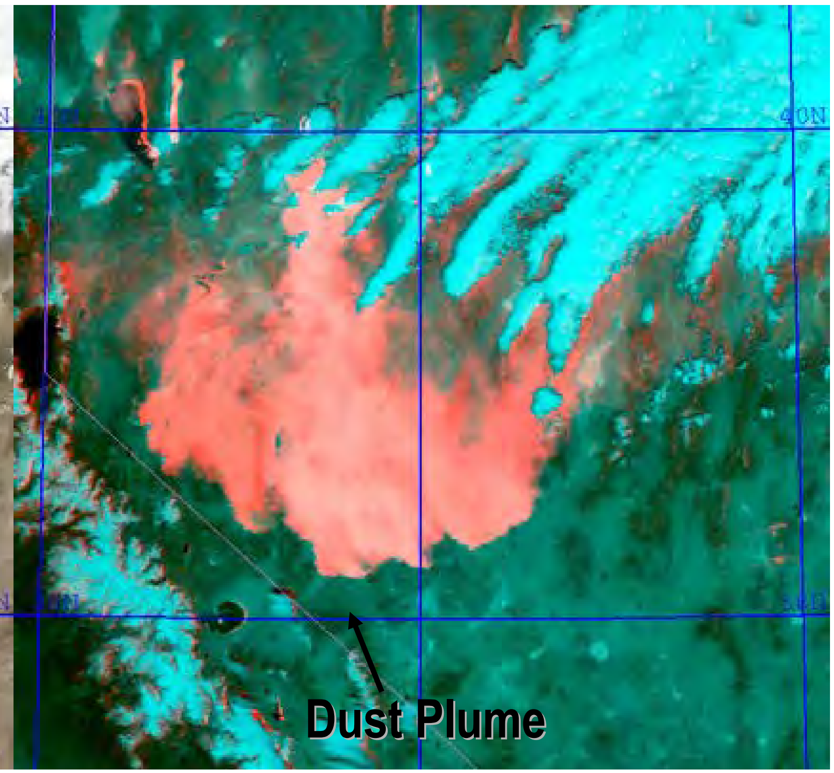

DayNight Band (DNB)

- Purpose: Replicate OLS capability but with updated technology and improvements
- 0.5 -- 0.9 µm broadband visible
- Detectors are aggregated to produce near-constant resolution
- More detectors aggregated near nadir for high SNR; fewer aggregated near edge for lower SNR

DNB “Constant Contrast”

Three Gains	Relative Gain
High	119,000
Medium	477
Low	1

- Improves SNR at low radiances
- All pixels are imaged with all three gains
- Onboard processing selects the most sensitive gain setting without saturation for transmission to the ground
- Goal is “constant contrast” imagery

VIIRS Improvement for DNB

DMSP OLS	NPOESS VIIRS
1. 64 Gray shades	64 X = 4096 Gray shades
2. 2.2 km Field of View	0.75 km Field of View
3. Limited Pixel Expansion	No Pixel Expansion
4. Numerous Image Artifacts	Artifacts Eliminated

Full Moon

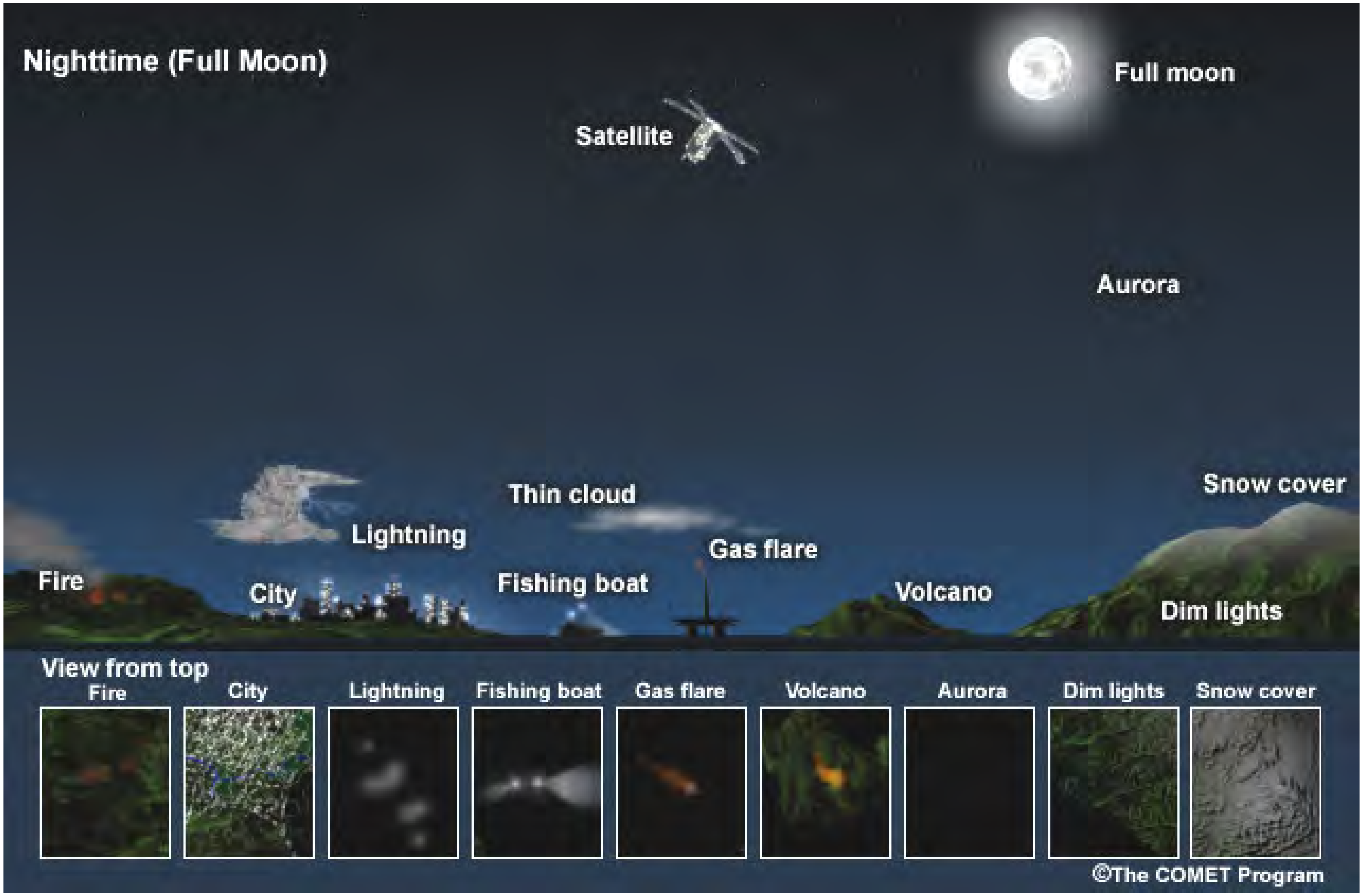

Nighttime (Full Moon)
Full moon
Satellite
Aurora
Snow cover
Thin cloud
Lightning
Gas flare
Fire
City
Fishing boat
Volcano
Dim lights
View from top
Fire
City
Lightning
Fishing boat
Gas flare
Volcano
Aurora
Dim lights
Snow cover
©The COMET Program

Clouds Illuminated by the Moon

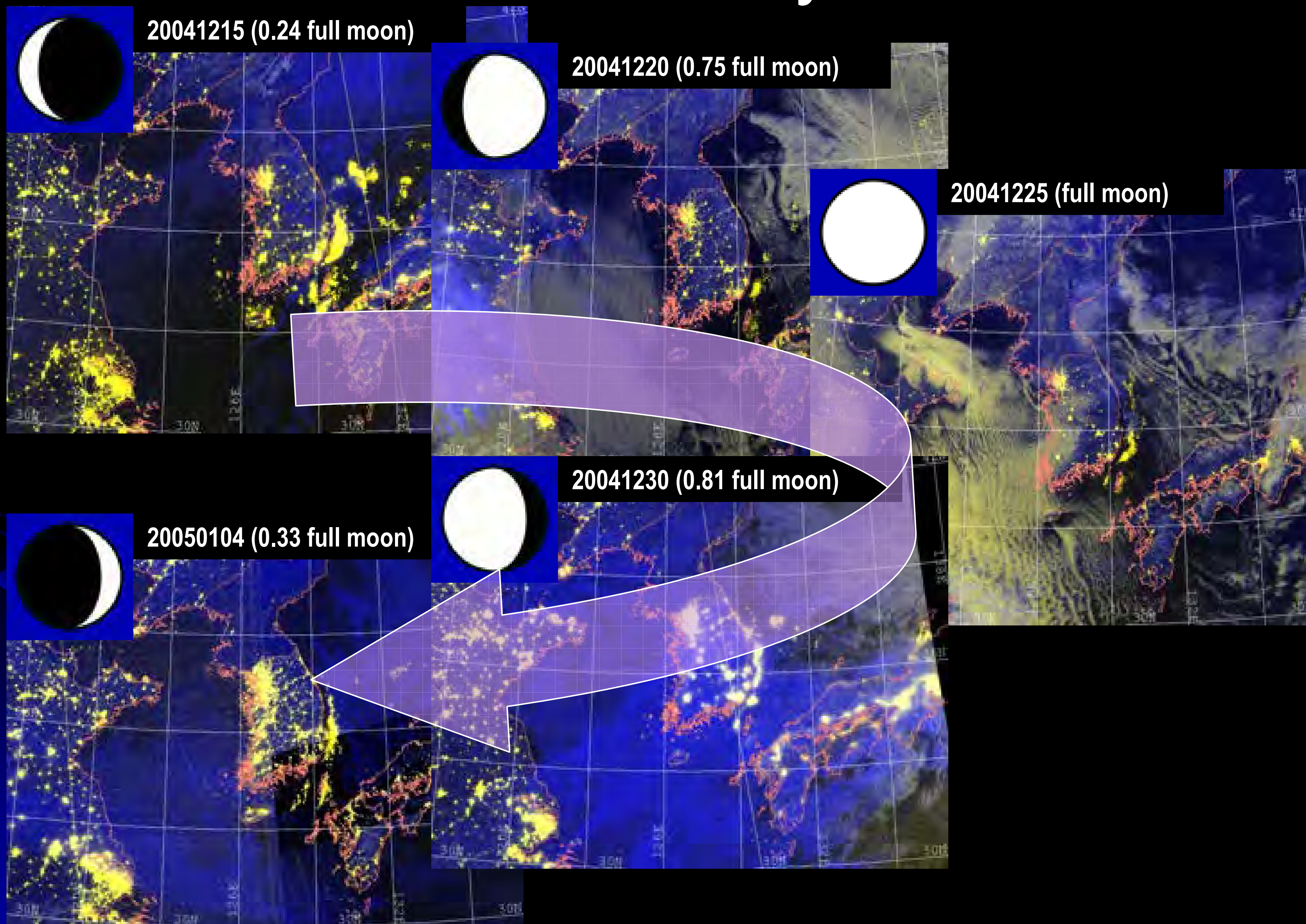

Lights over Korea

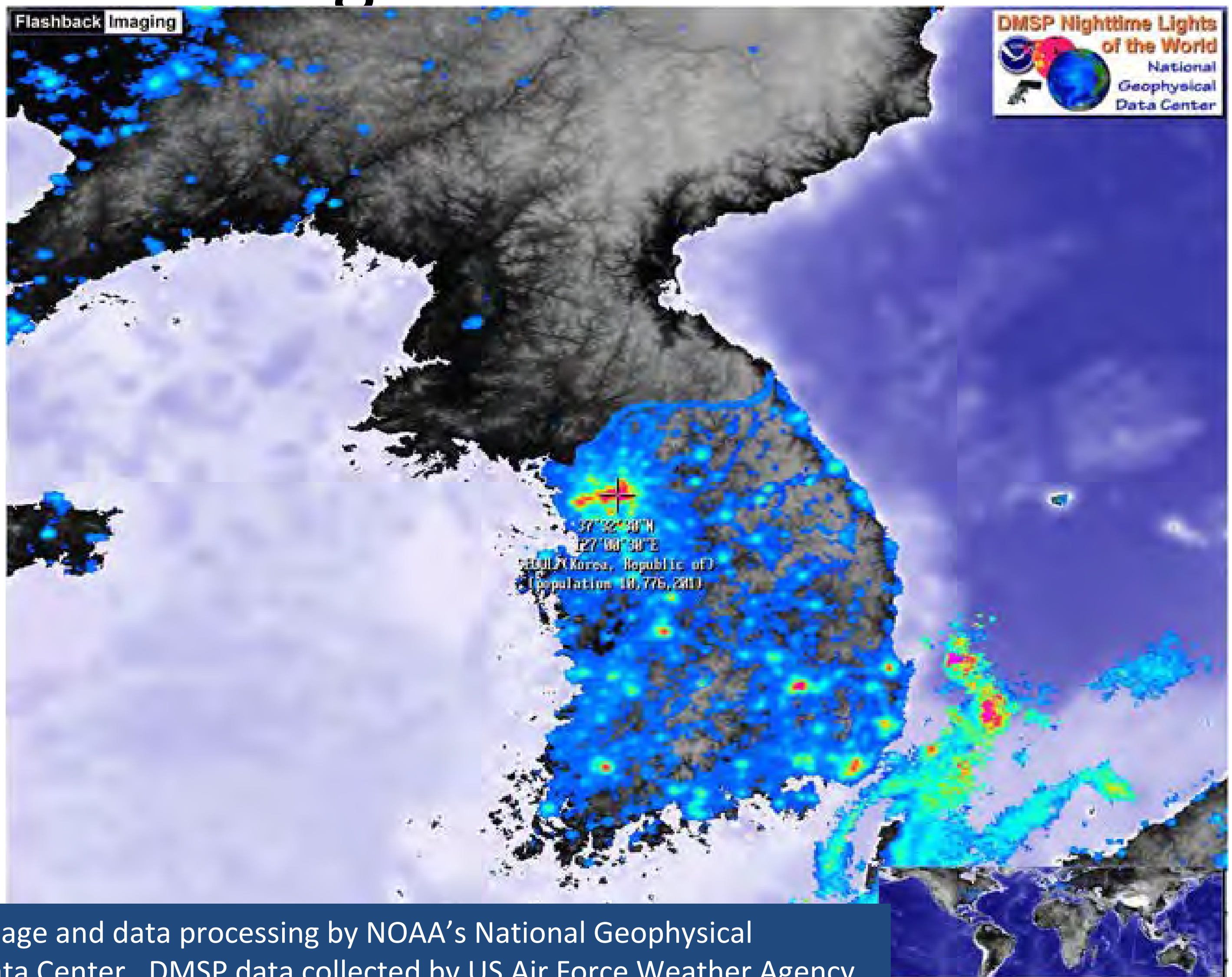

Image and data processing by NOAA's National Geophysical Data Center. DMSP data collected by US Air Force Weather Agency

NPP VIIRS DNB Example

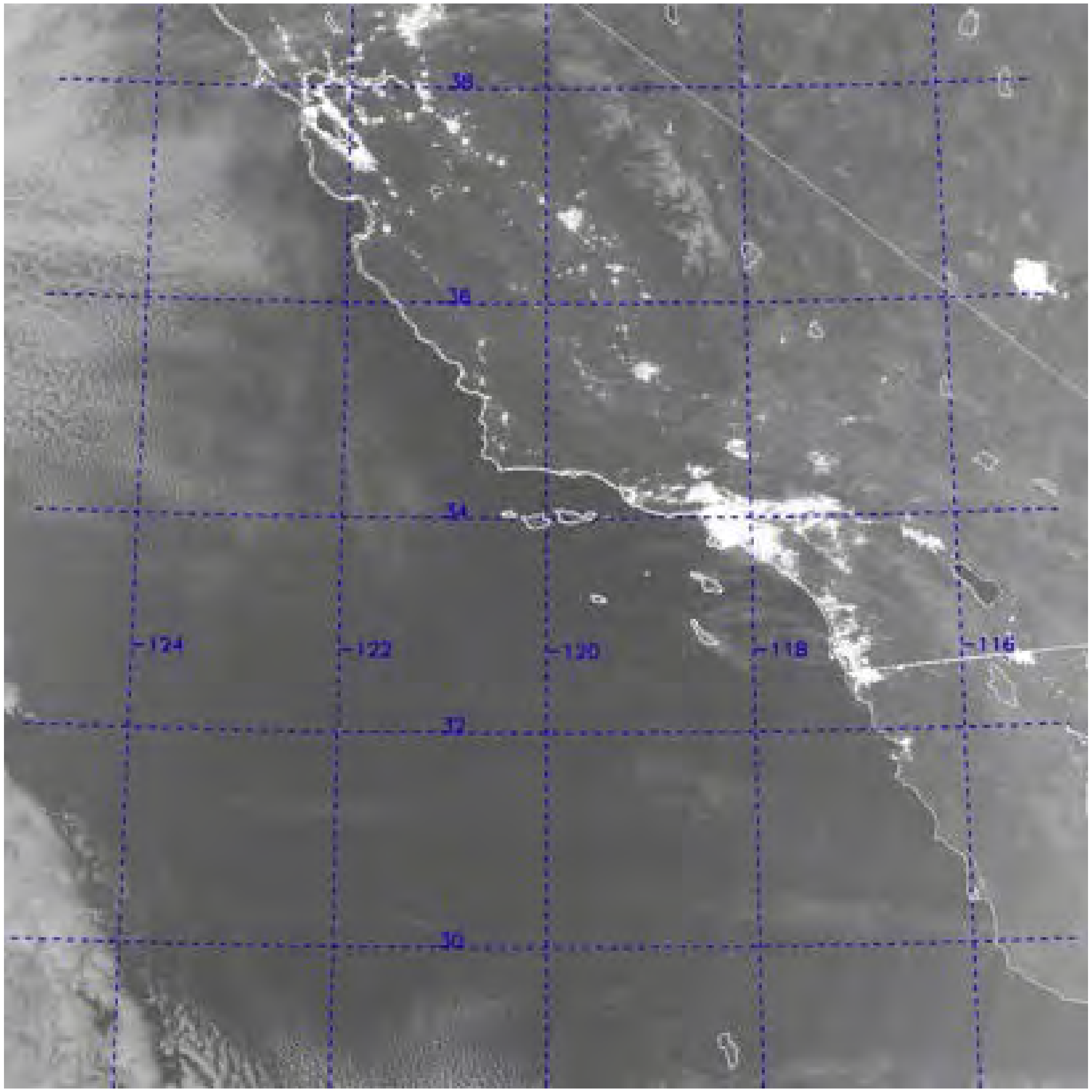

Low Clouds & Fog Over Cold Terrain

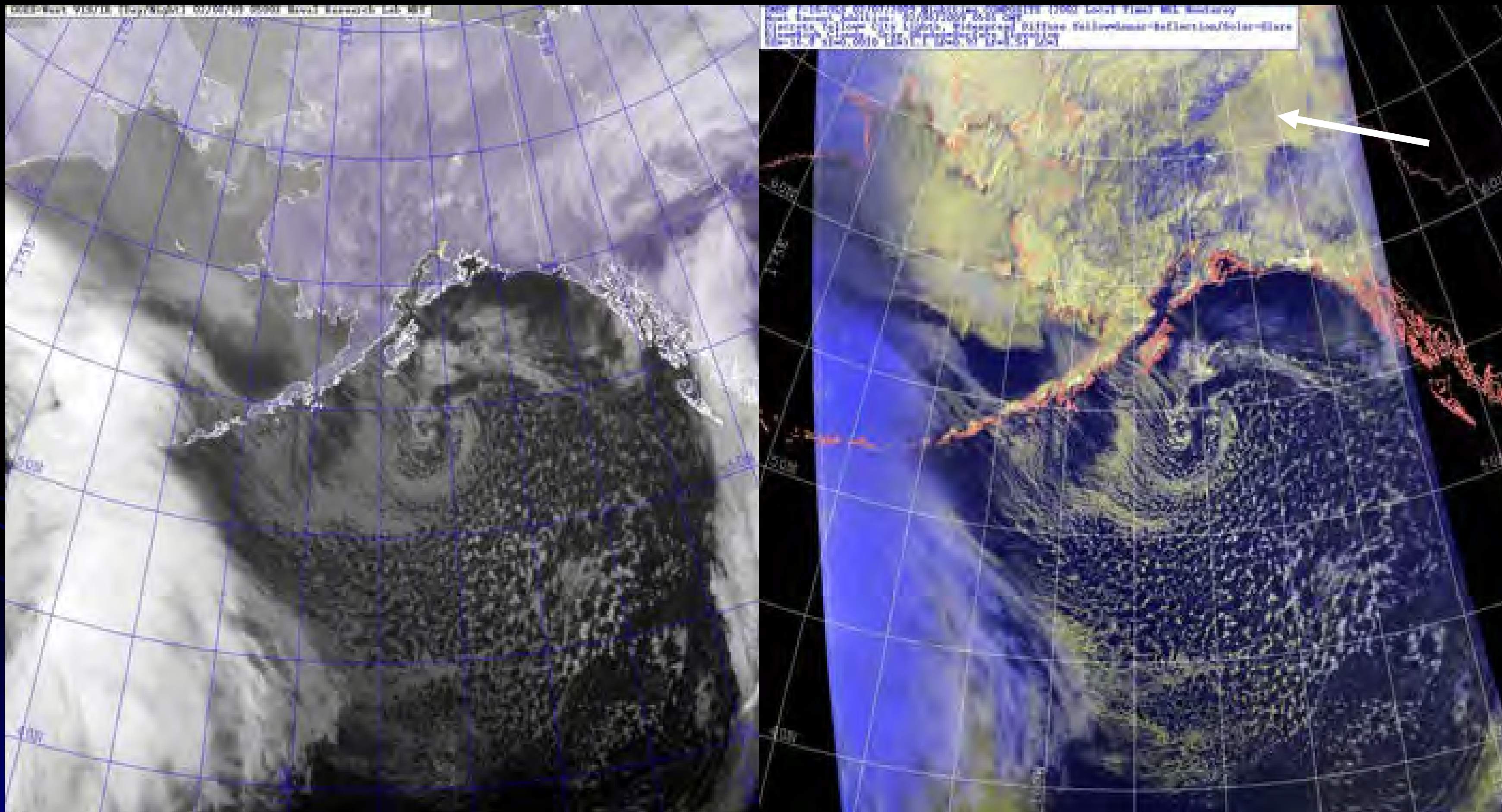

→ Detection enabled where conventional IR techniques often fail due to extremely cold surfaces…

Ship Tracks

GOES VIS loop Courtesy CIMSS

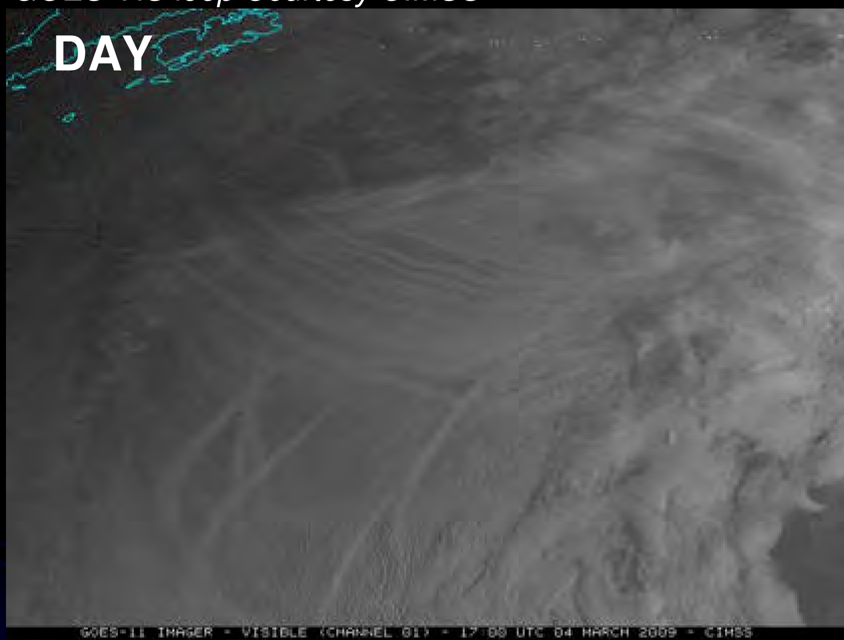

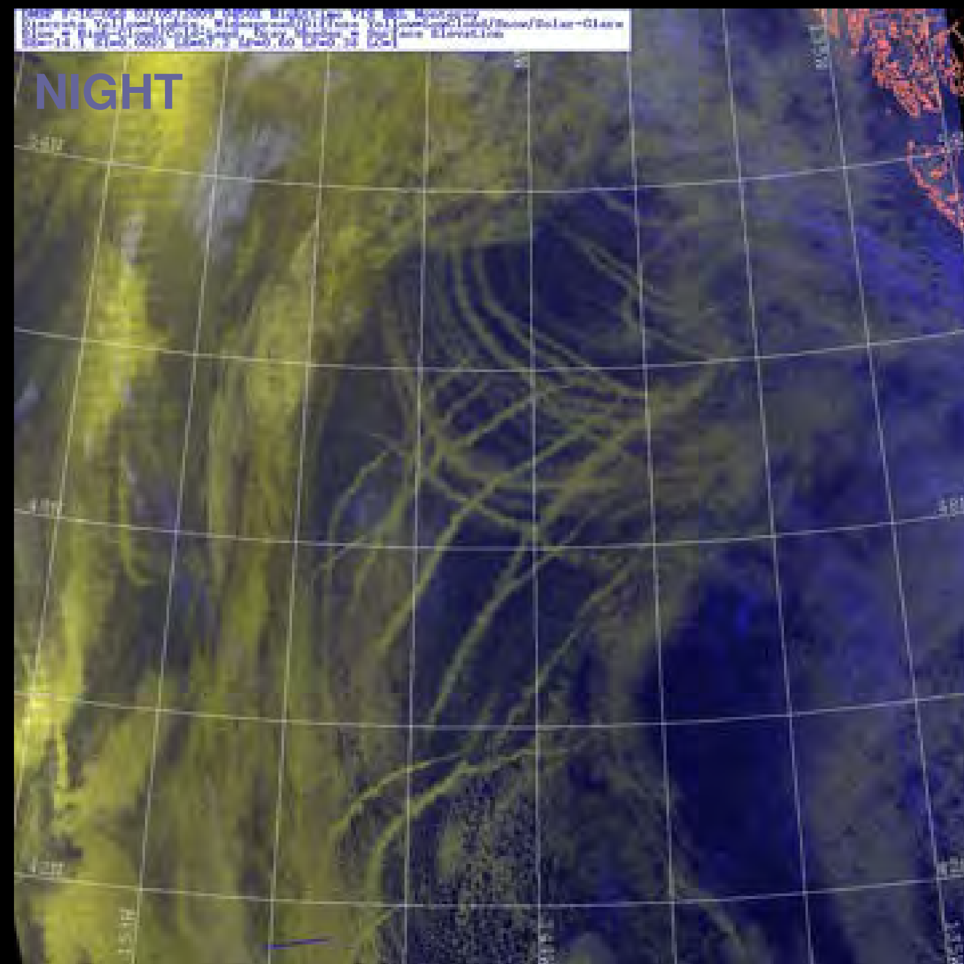

- → Day/Night Band's sensitivity to reflected moonlight will improve the detection of ship tracks and other low-cloud features at night…

Tropical Cyclone LLC Center

- Exposed low-level circulation occurs when storms enter a high vertical shear environment
- Decoupling of the upper and lower level cloud fields
- Displacements between upper and lower level centers can exceed 100 km in some cases

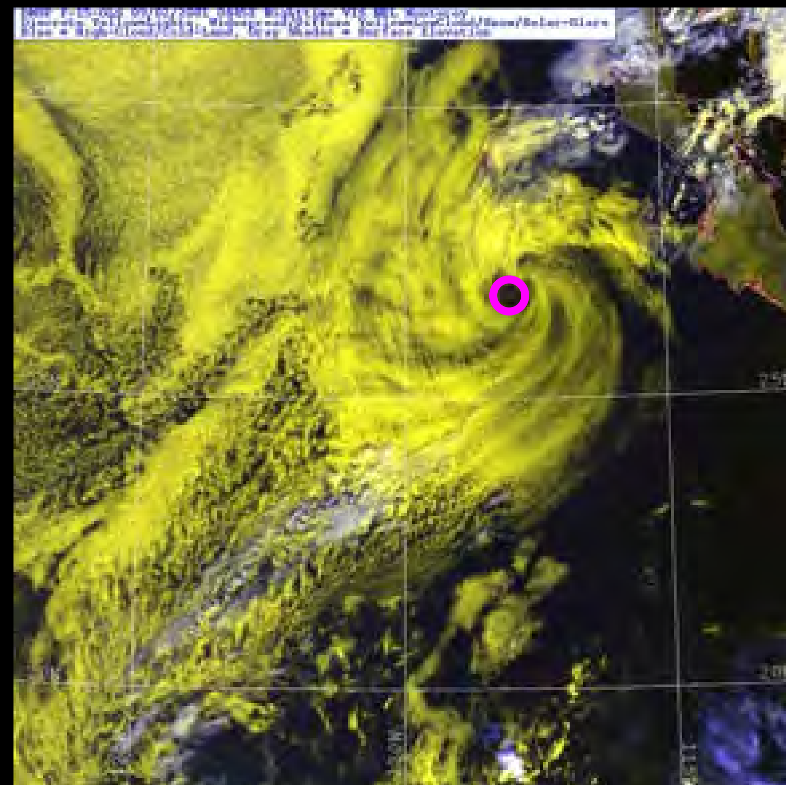

Helps avoid the “Sunrise Surprise”

Cloud Overlap Detection

Limited information on cloud layering is available from multi-spectral VIS/IR measurements: thin cirrus atop thick lower-level clouds

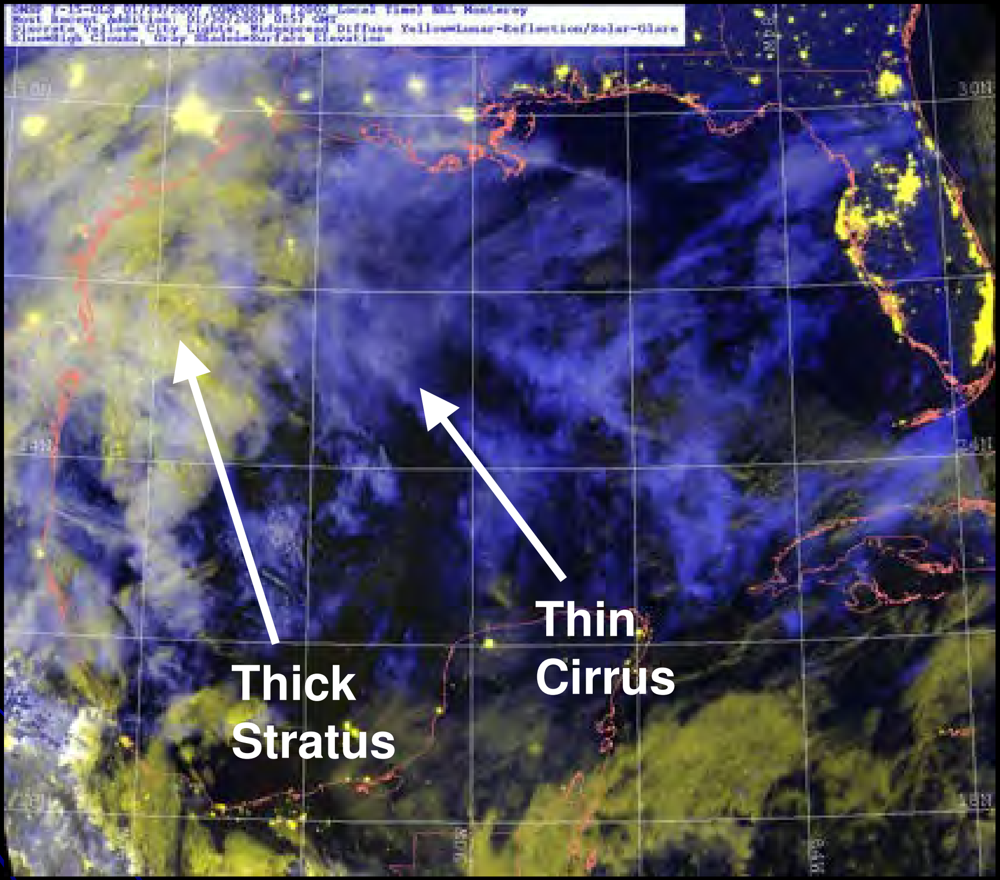

→ **The VIIRS DNB will offer the *only* capability for detecting such two-layer cloud structures at night.**

Snow Cover Detection

Multi-spectral techniques that include a nighttime visible band can separate cloud from snow cover and sea-ice.

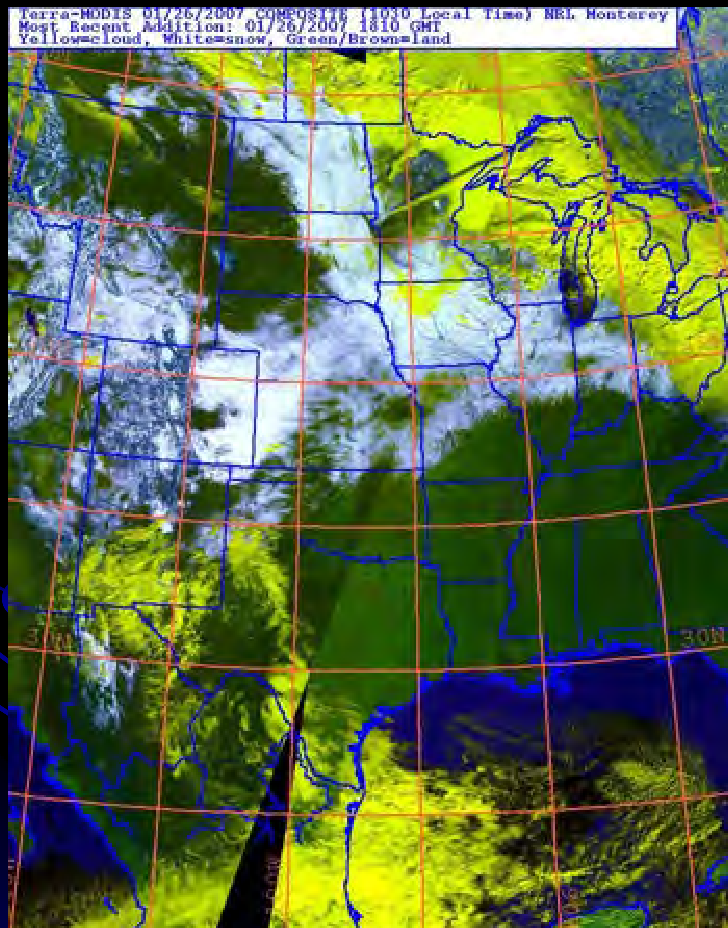

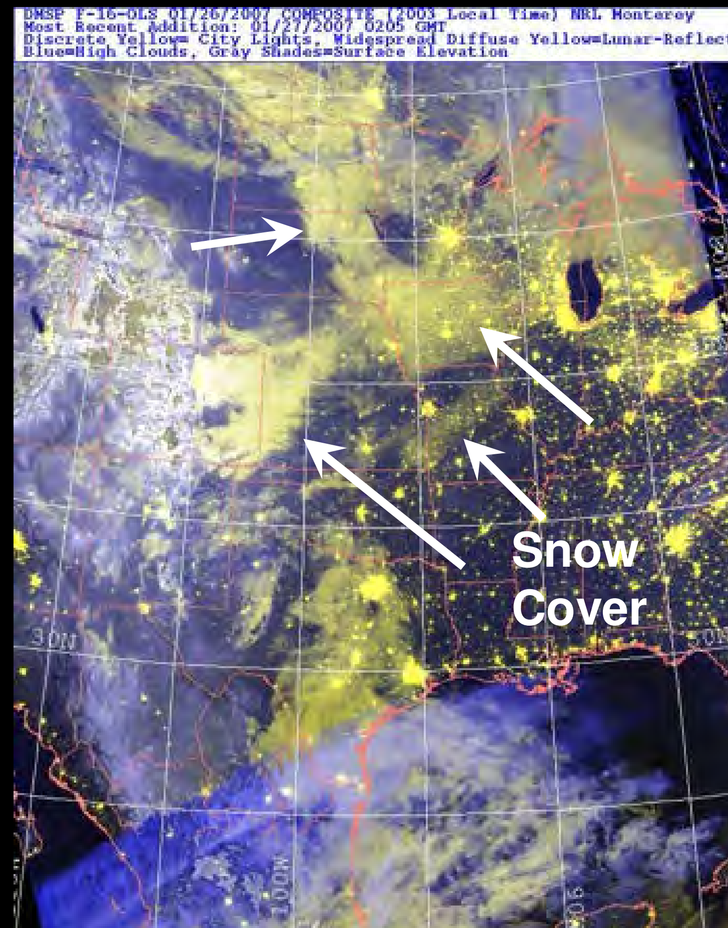

→ We can simulate the capability of VIIRS via space/time matching of OLS and sensors possessing NIR channels…

NexSat: Web Design

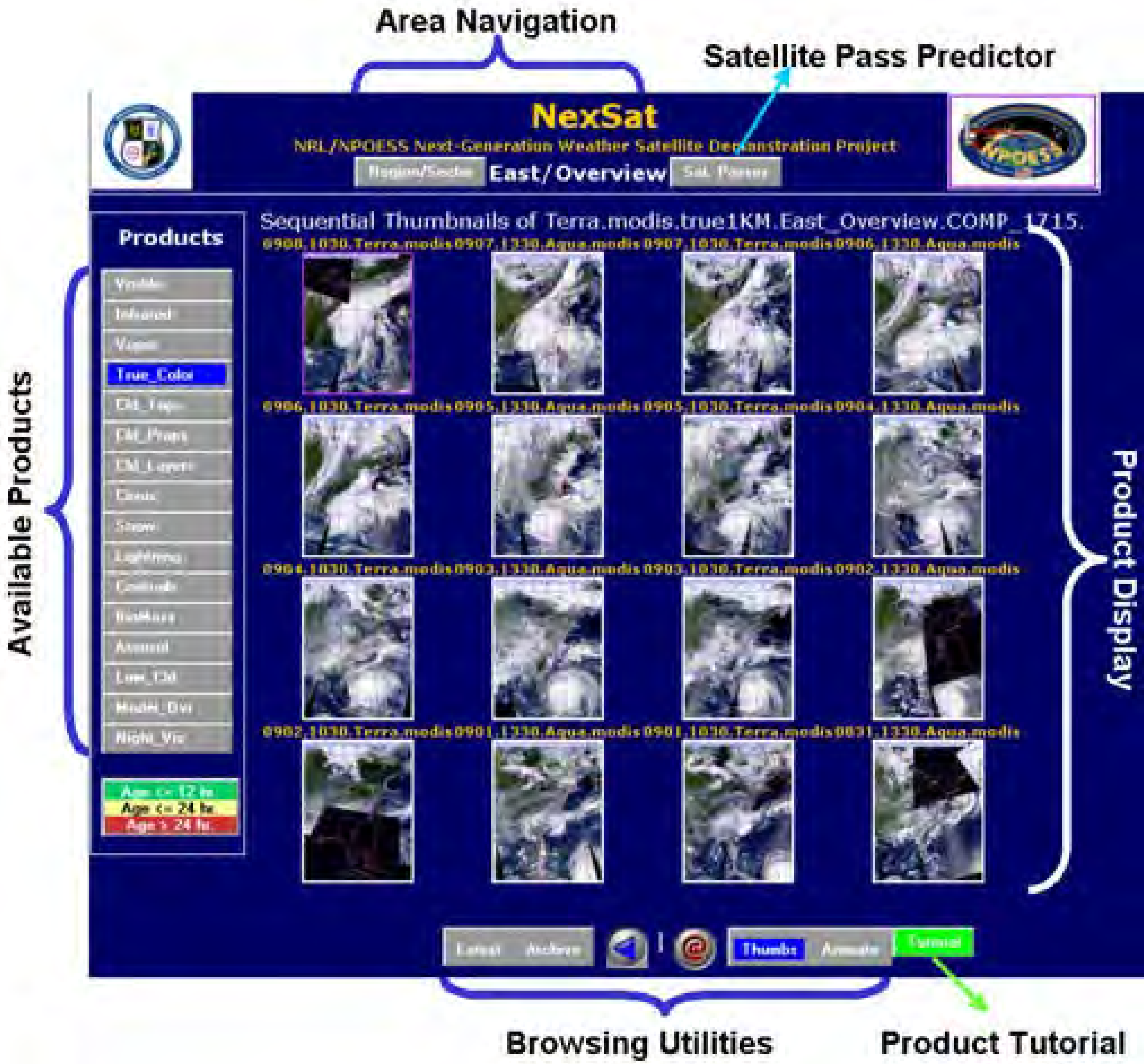

http://www.nrlmry.navy.mil/nexsat-bin/nexsat.cgi

Near-Realtime Polar Products from NexSat

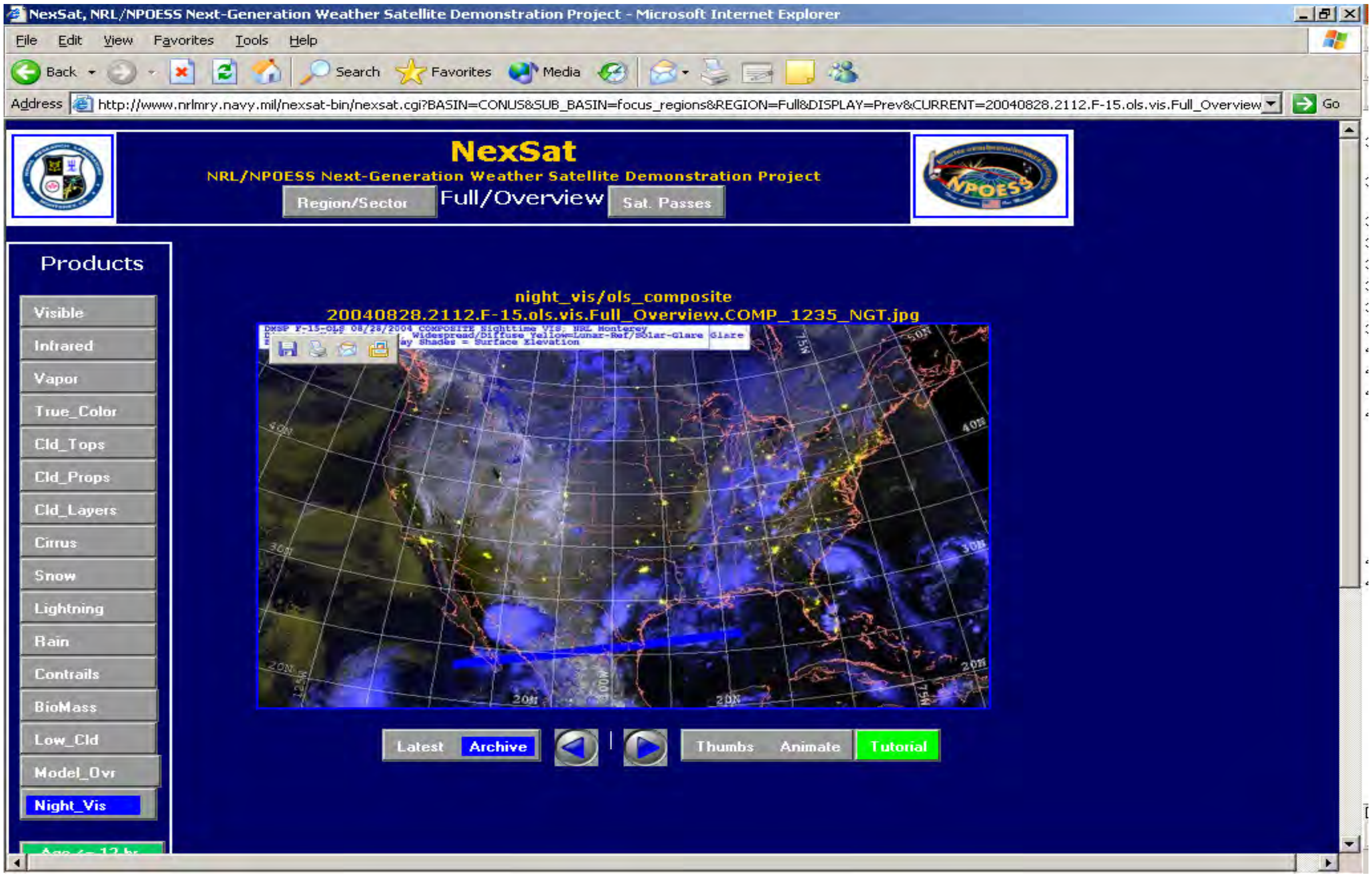

http://www.nrlmry.navy.mil/nexsat_pages/nexsat_home.html

25 October 2011

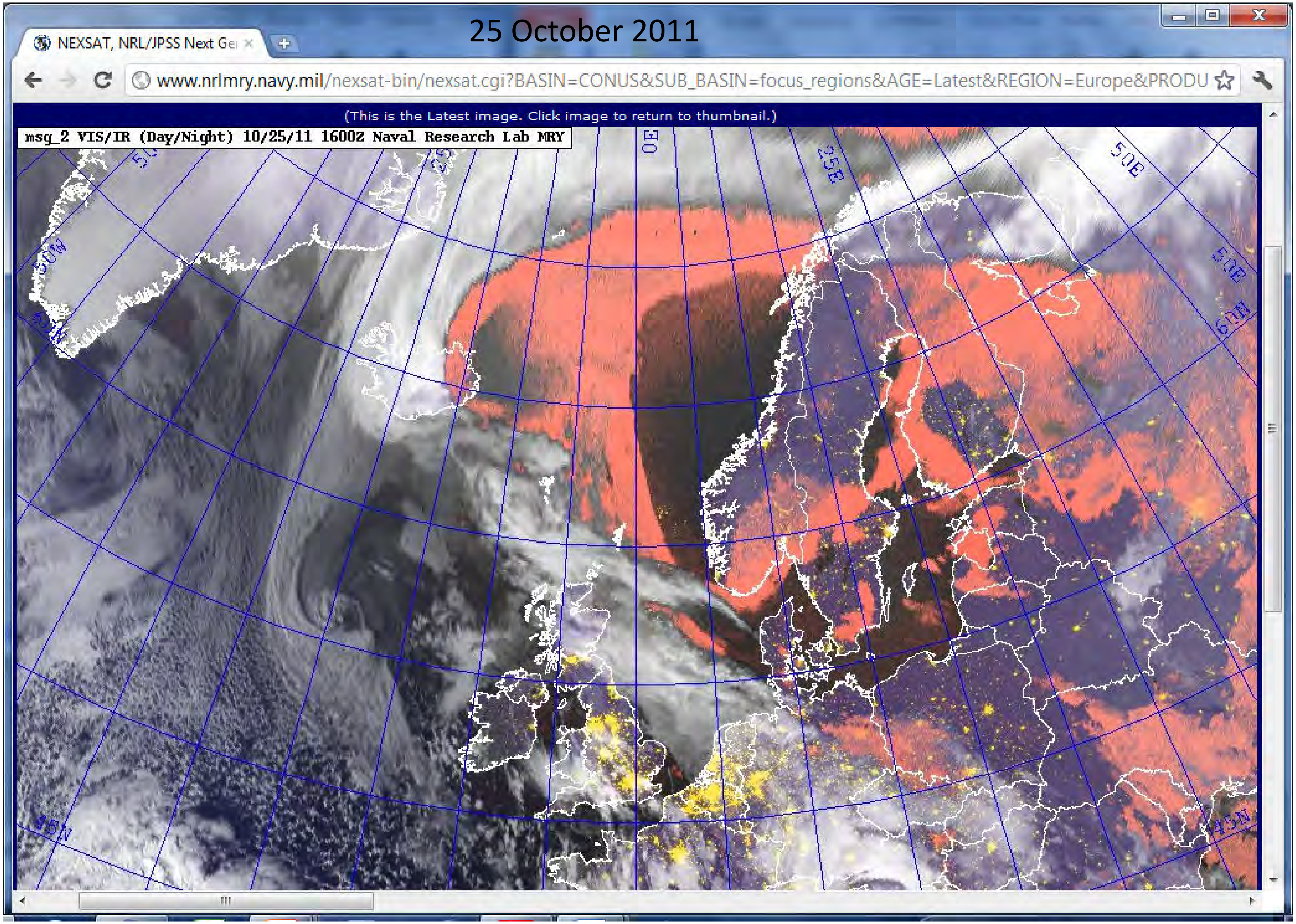

Conclusions

- VIIRS adds advanced capability not available from MODIS
- JPSS will be a forecaster's system
- Constant-Contrast/Constant-Resolution Data will produce vivid, information-rich images for DNB
- Preservation of footprint size will facilitate more usable images
- VIIRS fine channels replicate the capability of AVHRR
- Many products will complement EDRs

NPP is launched successfully 28 Oct 2011

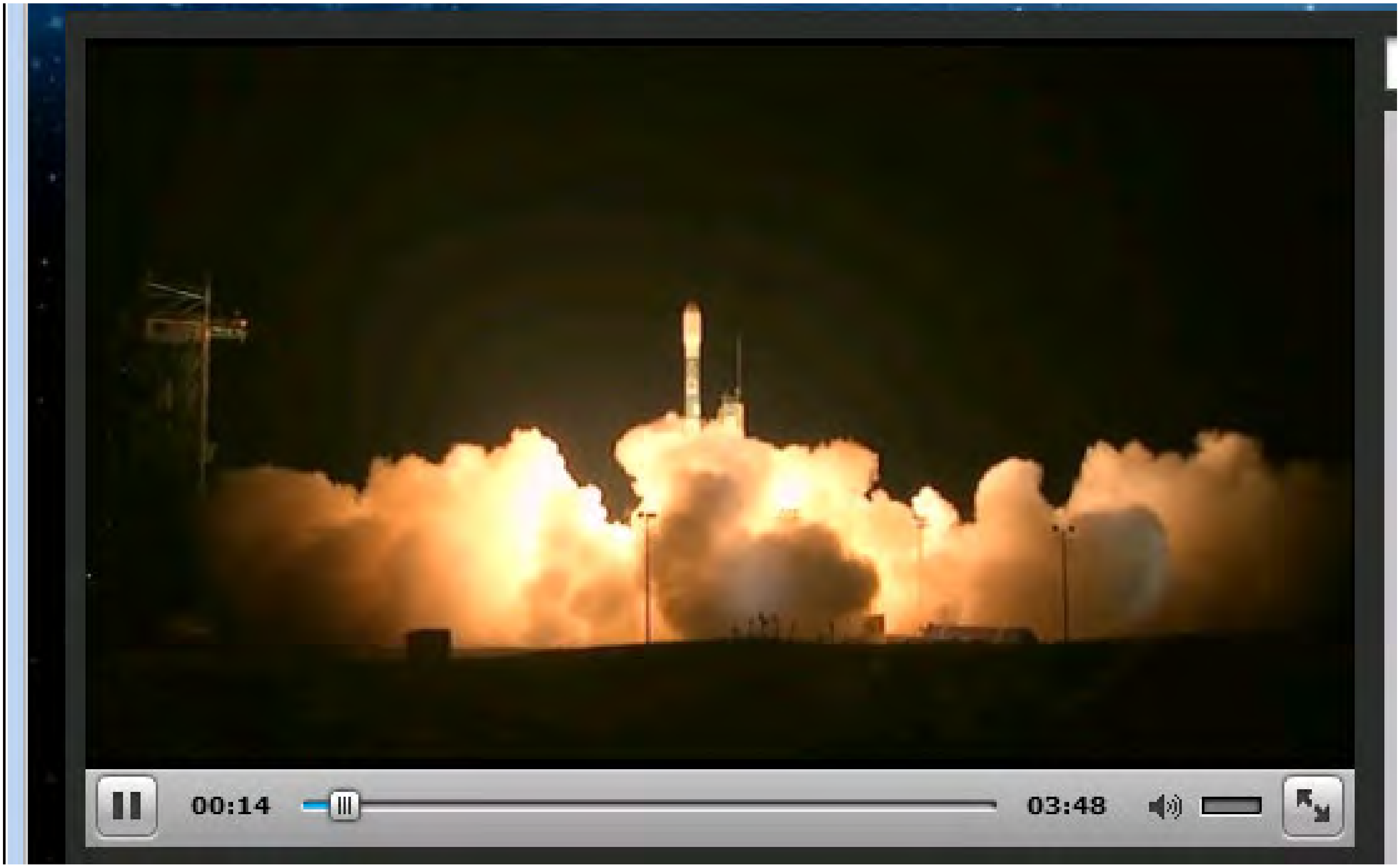

ATMS

Advanced Technology Microwave Sounder Northrop Grumman Electronic Systems

Description

- Purpose: In conjunction with CrIS, global observations of temperature and moisture profiles at high temporal resolution (~ daily).
- Predecessor Instruments: AMSU A1 / A2, MHS
- Approach: Scanning passive microwave radiometer
- 22 channels (23GHz - 183GHz)
- Swath width: 2600 km
- Co-registration: with CrIS

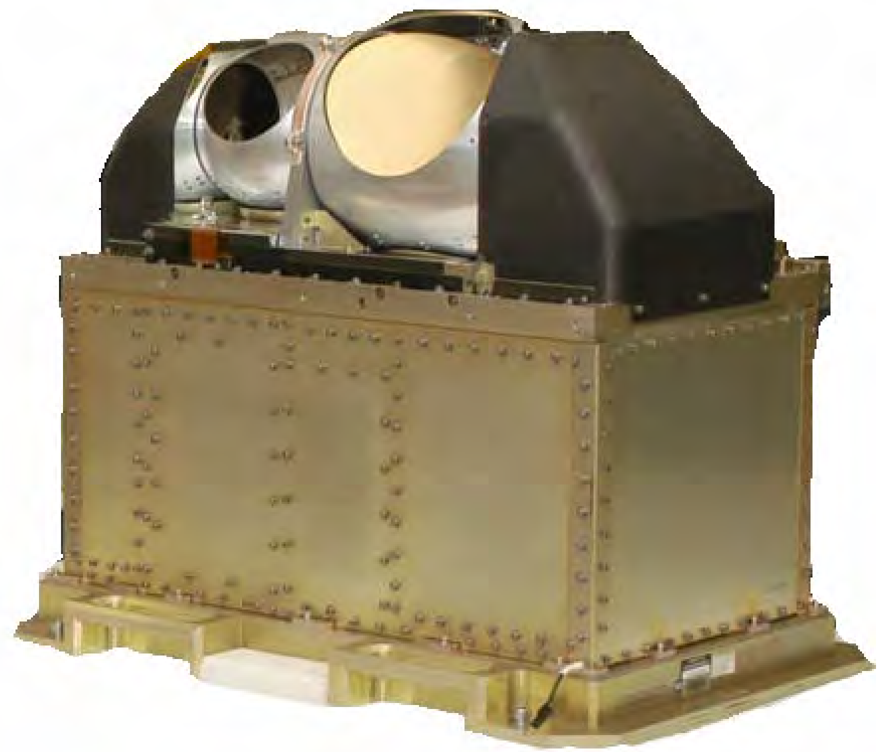

ATMS Design Challenge

AMSU-A1

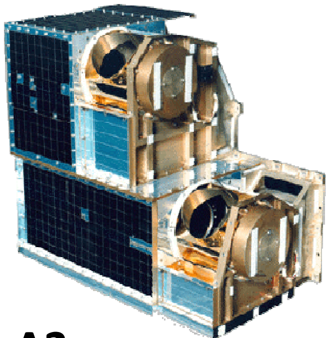

- 73x30x61 cm
- 67 W
- 54 kg
- 3-yr life

AMSU-A2

- 75x70x64 cm
- 24 W
- 50 kg
- 3-yr life

MHS

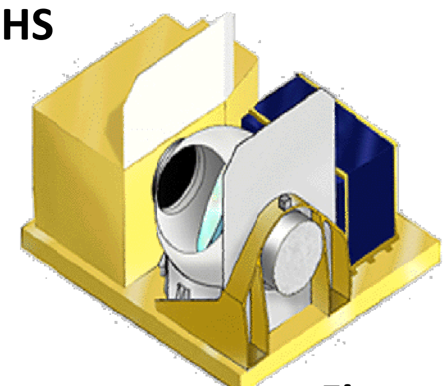

- 75x56x69 cm
- 61 W
- 50 kg
- 4-yr life

Figure courtesy NGES, Azusa, CA

Reduce the volume by 3x

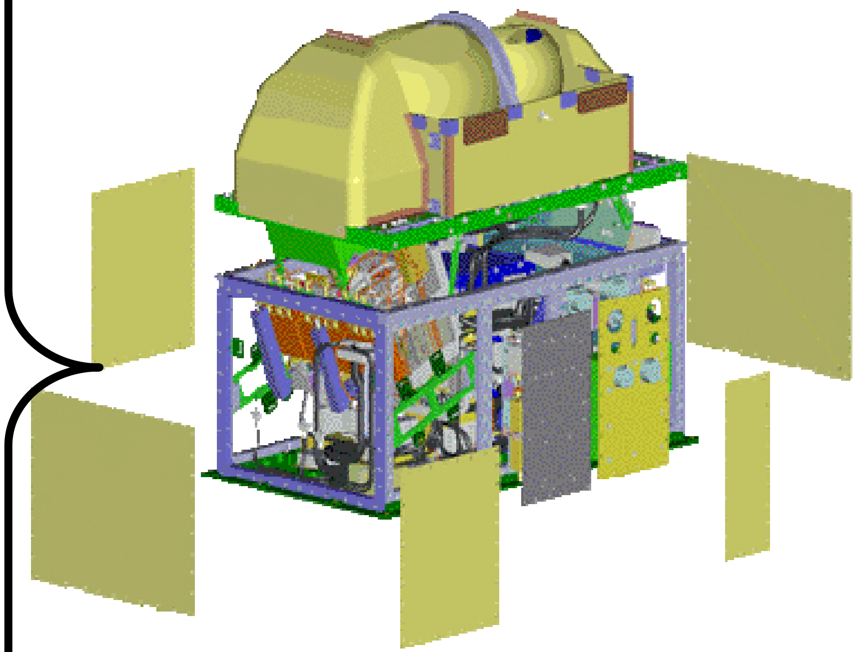

– 70x40x60 cm
– 110 W
– 85 kg
– 8 year life

First global ATMS image showing the channel 18-microwave antenna temperature at 183.3 GHz on November 8, 2011

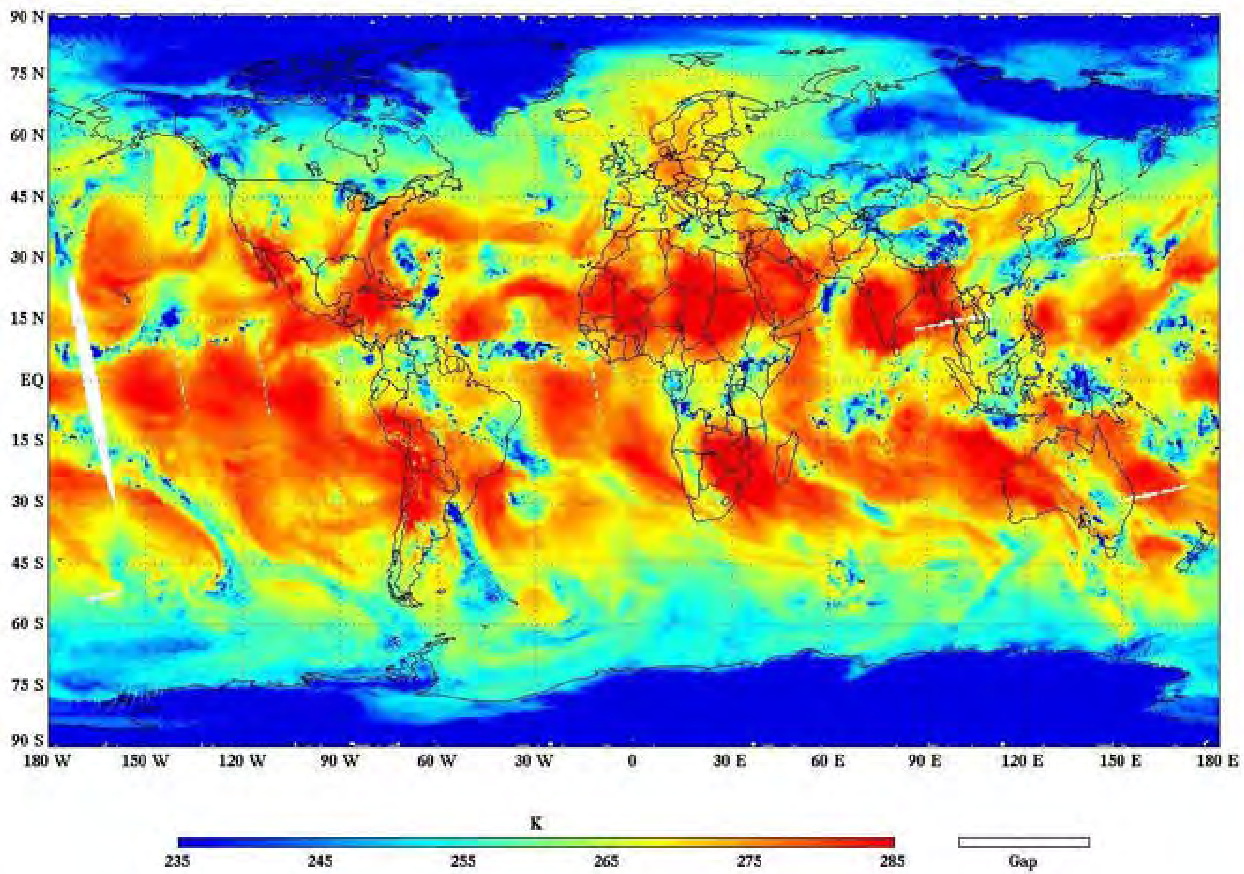

The ATMS data were processed at the NOAA Satellite Operations Facility (NSOF) in Suitland, MD and the image was generated by STAR

Quality of the image is superb, no indication of instrument artifacts, and by design no orbital gaps

This channel measures atmospheric water vapor; note that Tropical Storm Sean is visible in the data, as the blue patch due to heavy precipitation, in the Atlantic off the coast of the Southeastern United States. ATMS provides critical water vapor information for weather forecasting and storm intensity assessments

ATMS Preliminary Assessment
Total Precipitable Water

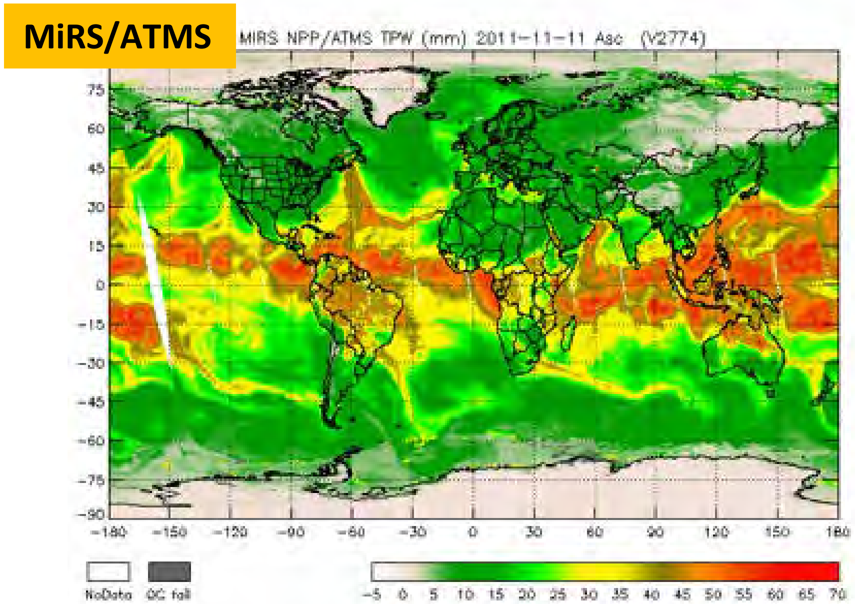

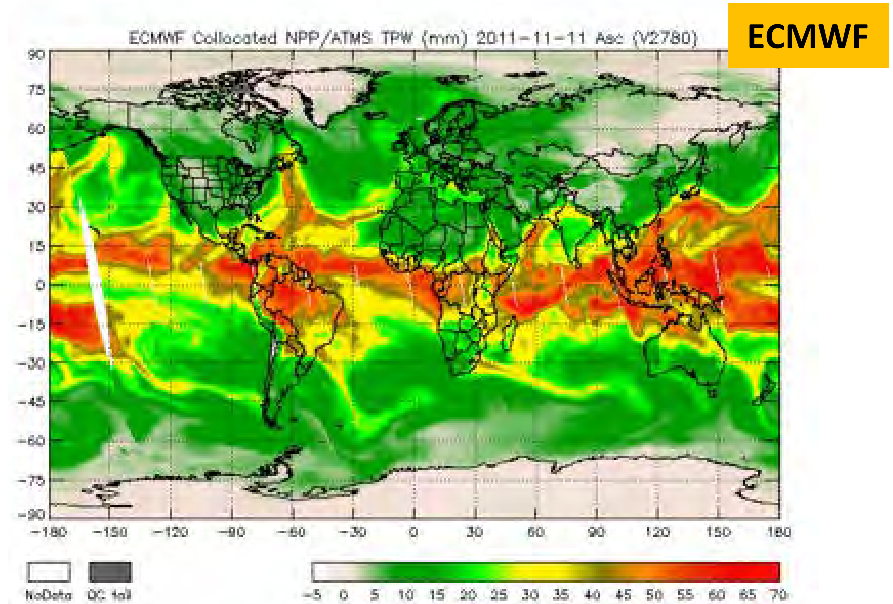

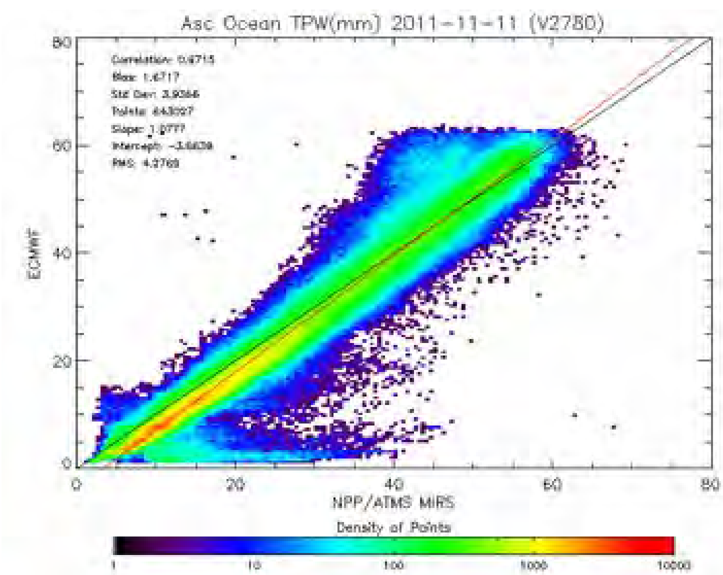

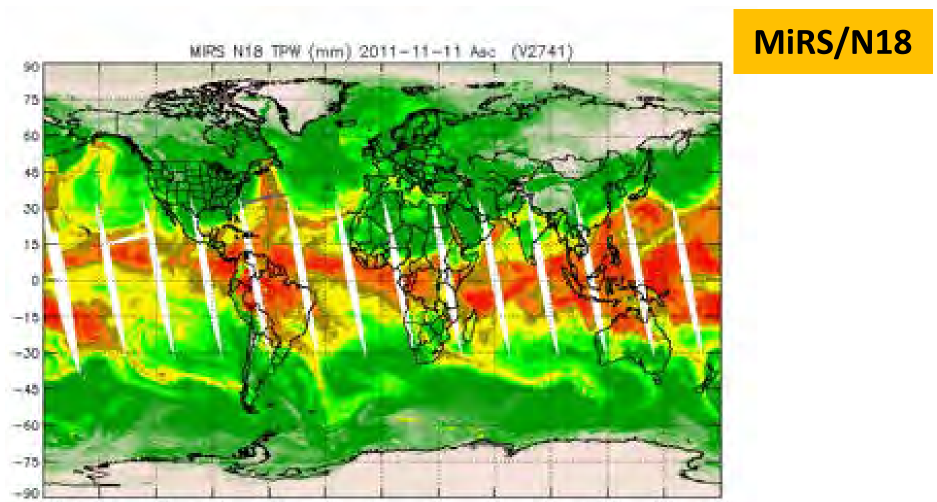

ATMS Preliminary Assessment
(Rainfall Rate)

MiRS/ATMS

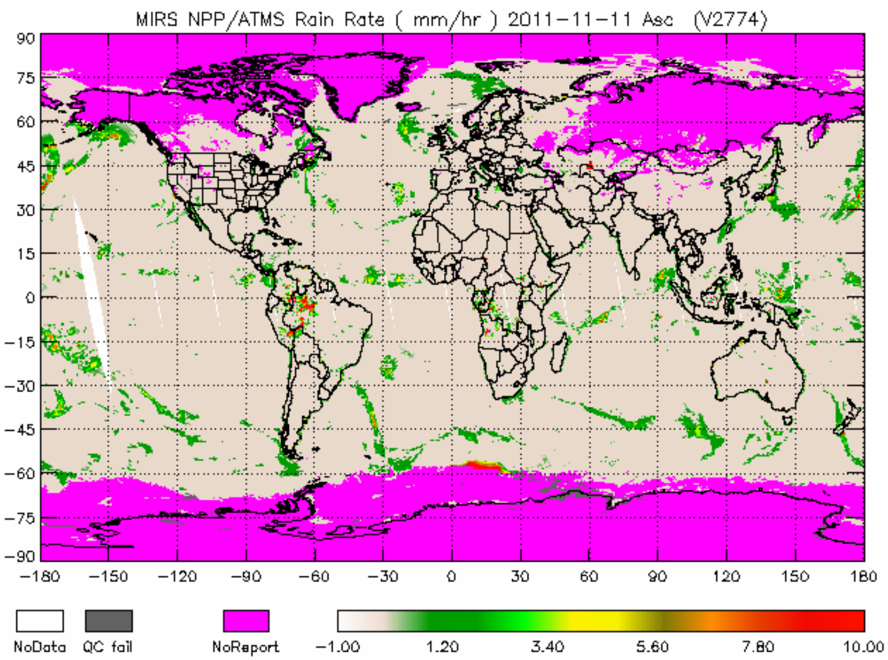

MiRS/N19 AMSU-MHS

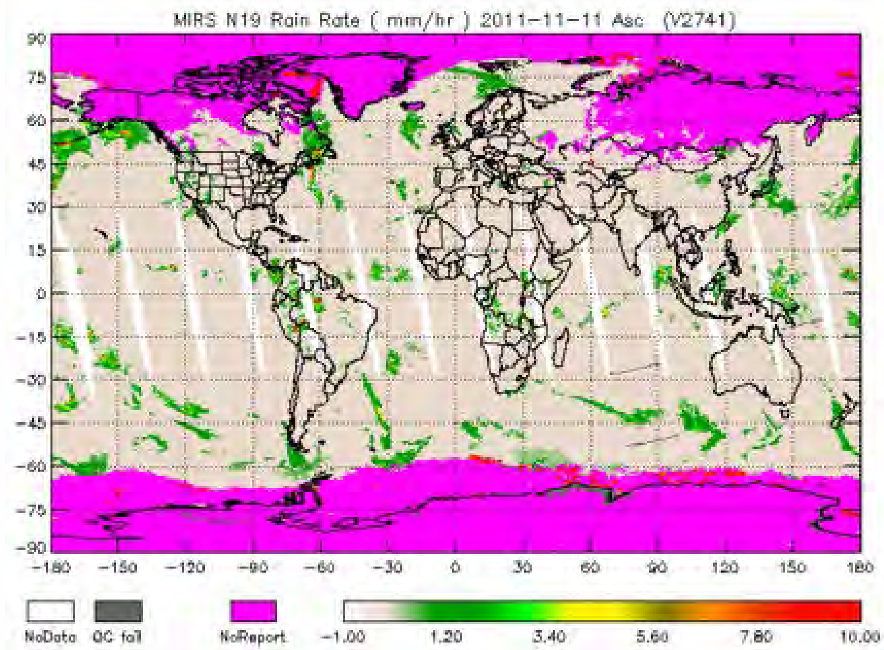

MiRS ATMS Rainfall rate (left) and MiRS N19 Rainfall rate (right) screened out over snow cover and sea-ice.

ATMS Preliminary Assessment

(Temperature Soundings Using ECMWF as a reference)

MiRS ATMS 500 mb T

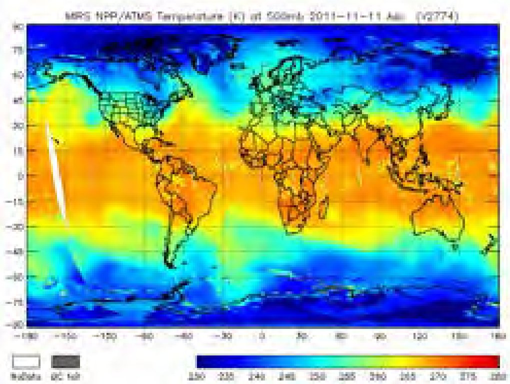

ECMWF 500 mb T

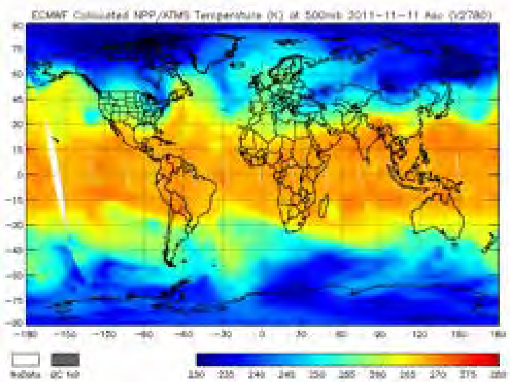

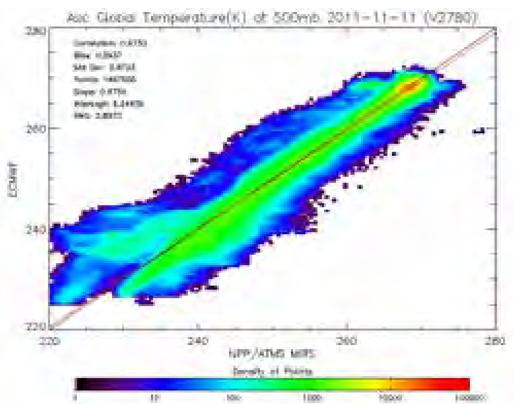

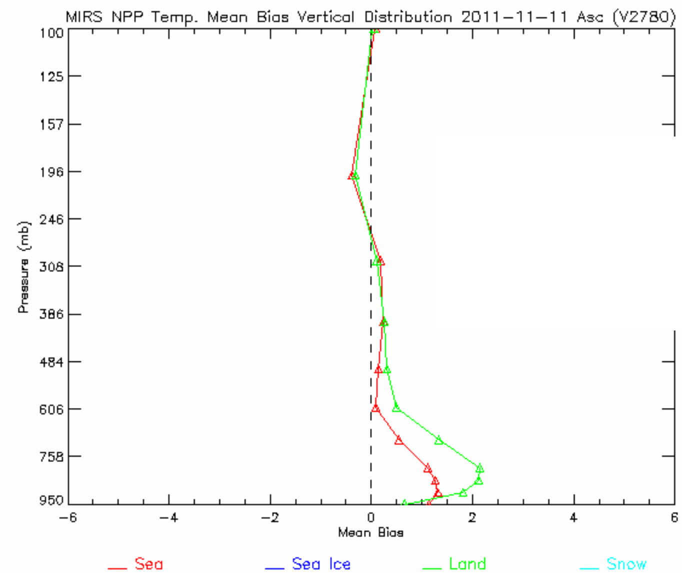

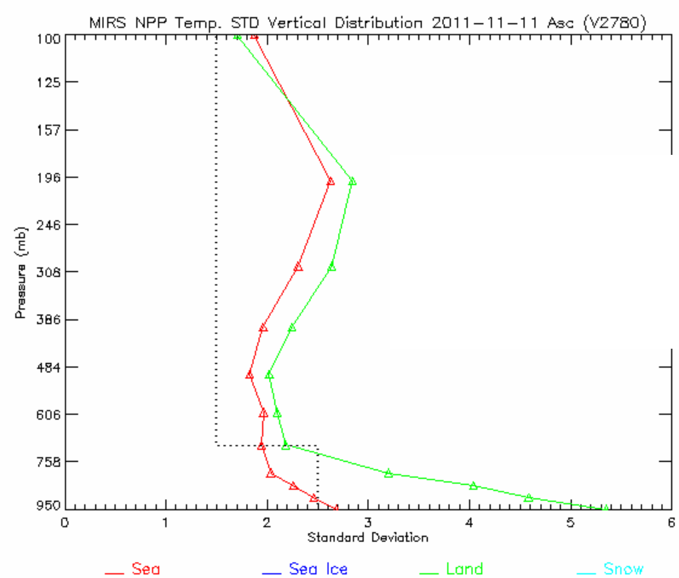

CrIS

Cross-Track Infrared Sounder (CrIS)

NPOESS Preparatory Satellite – Launch: October 2011

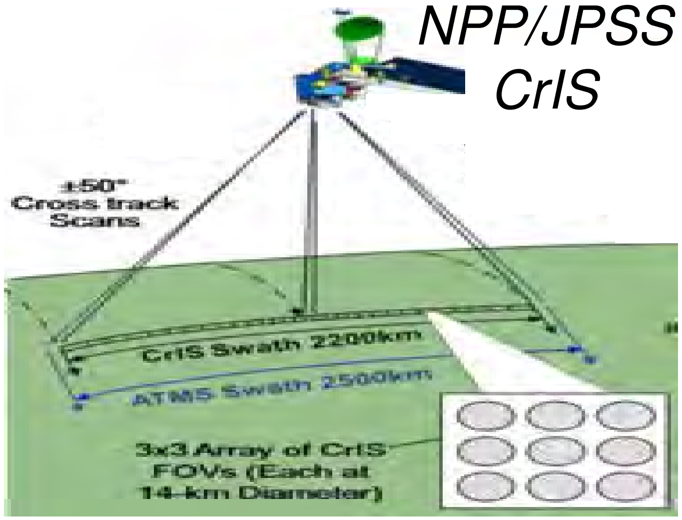

- **Michelson Interferometer: 0.625,1.25, 2.5cm^{-1} (resolving power of 1000)**
- **Spectral range: 660-2600 cm^{-1}**
- **3 x 3 HdCdTe focal plane passively cooled (4-stages) to 85K**
- **Focal plane 27 detectors, 1305 spectral channels**
- **310 K Blackbody and space view provides radiometric calibration**
- **NEDT ranges from 0.05 K to 0. 5 K**

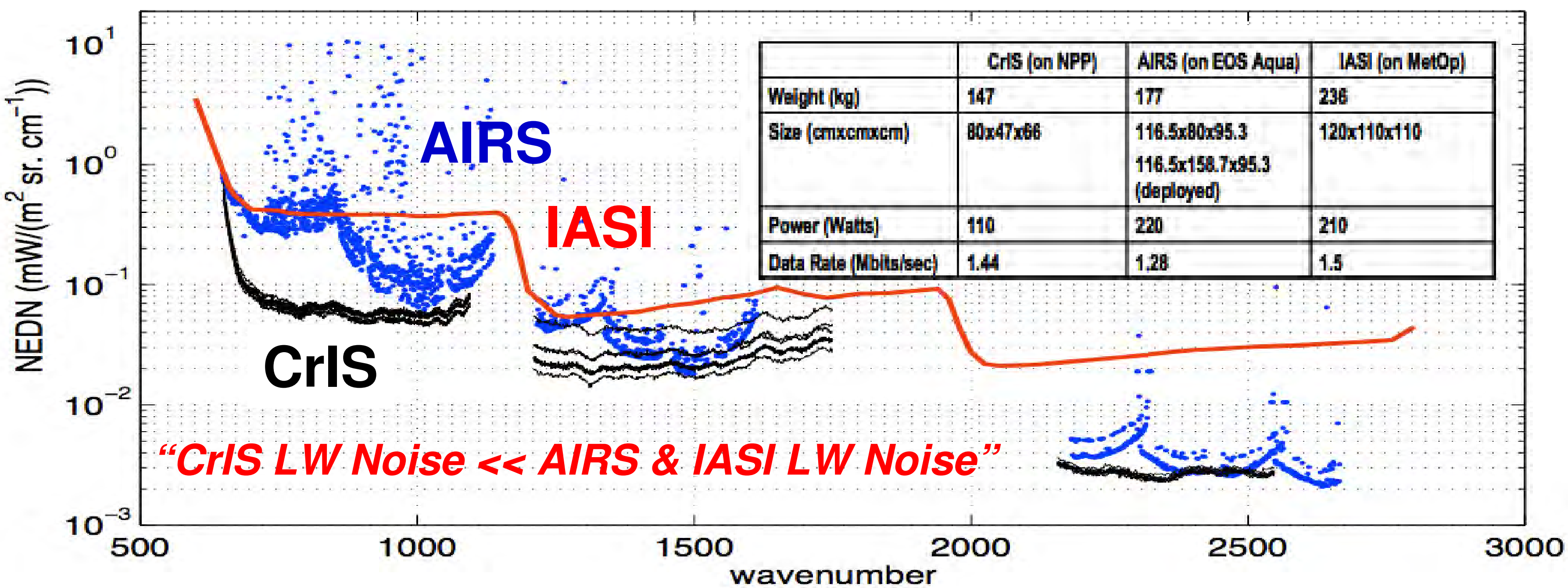

	CrIS (on NPP)	AIRS (on EOS Aqua)	IASI (on MetOp)
Weight (kg)	147	177	236
Size (cmxcmxcm)	80x47x66	116.5x80x95.3 116.5x158.7x95.3 (deployed)	120x110x110
Power (Watts)	110	220	210
Data Rate (Mbits/sec)	1.44	1.28	1.5

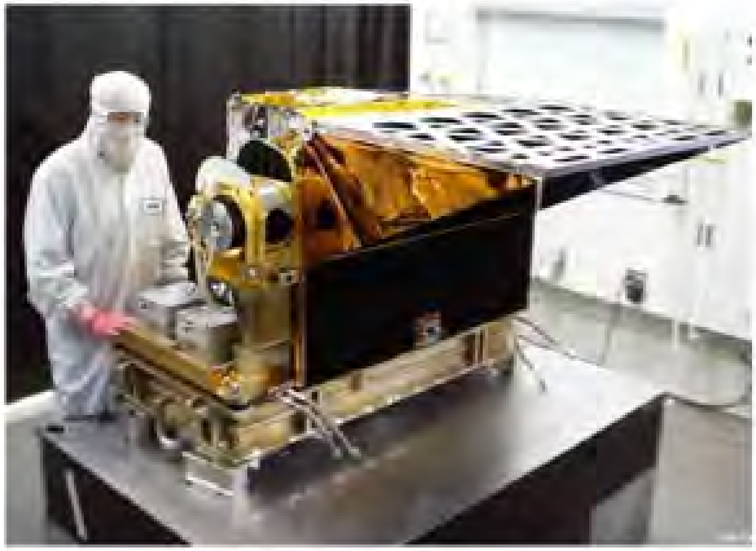

AIRS
Atmospheric InfraRed Sounder
Grating spectrometer
166 kg, 256 W
13.5 km FOV at nadir, contiguous
Launched on Aqua in 2002

IASI
Infrared Atmospheric Sounding Interferometer
Michelson interferometer
236 kg, 210 W
2x2 12 km FOVs at nadir, non-contiguous
Launched on Metop-A in 2006

CrIS
Cross-track Infrared Sounder
Michelson interferometer
146 kg, 110 W
3x3 14 km FOVs at nadir, contiguous
To be launched on NPP

Spectral Coverage and Example Observations of AIRS, IASI, and CrIS

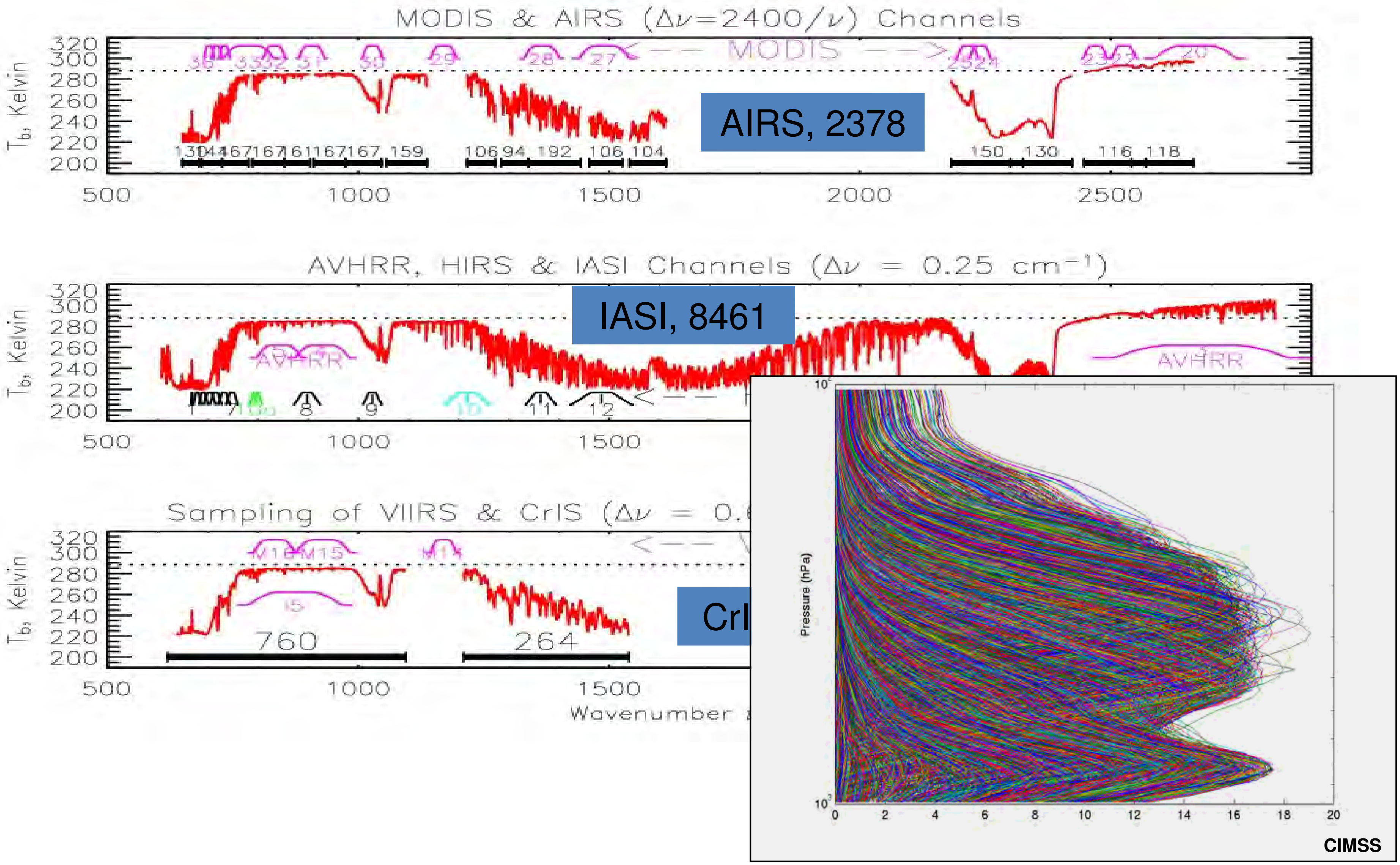

900 cm-1 map 20 Jan 2012

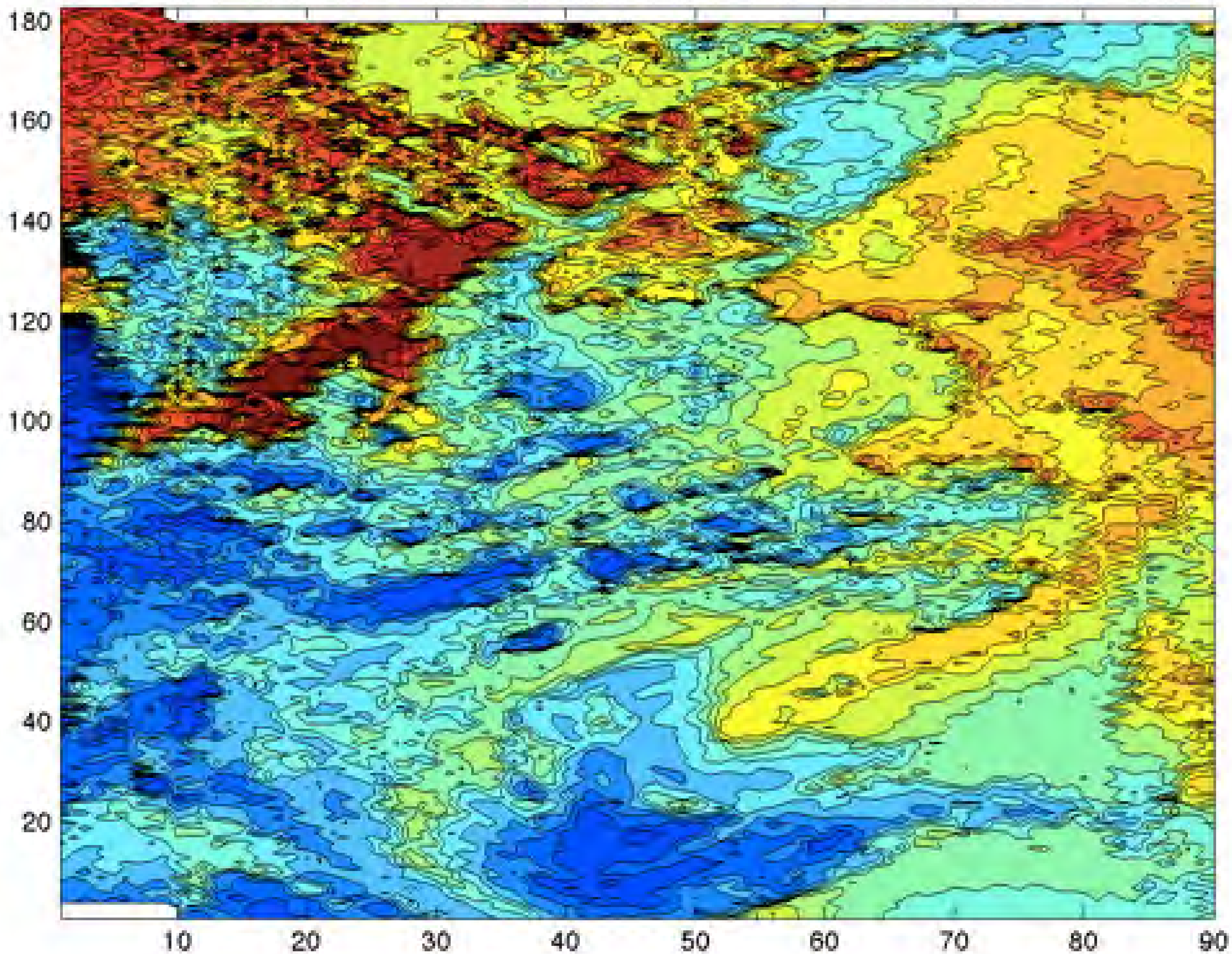

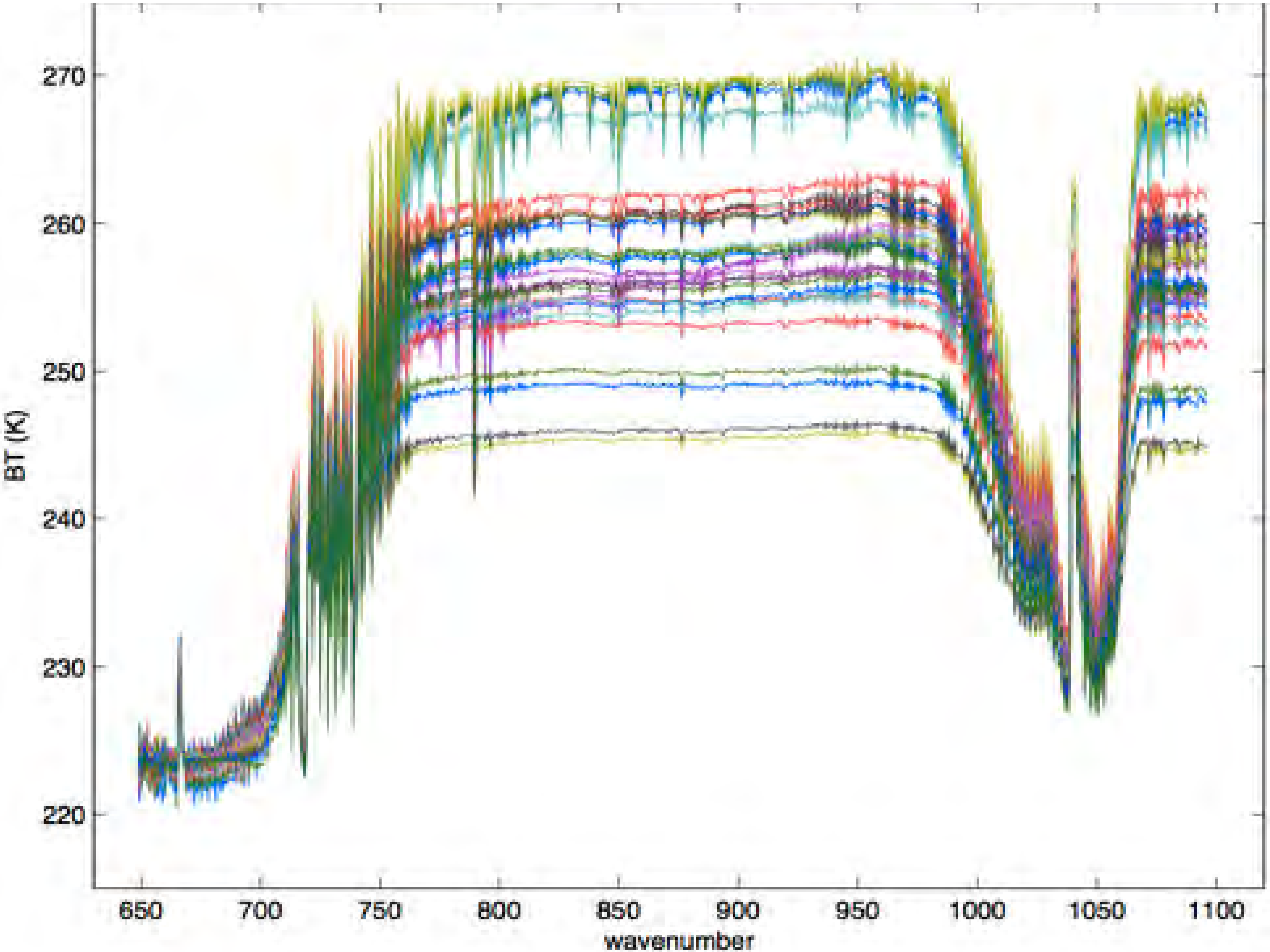
270
260
250
240
230
220
BT (K)
650
700
750
800
850
900
950
1000
1050
1100
wavenumber

20 Jan 2012

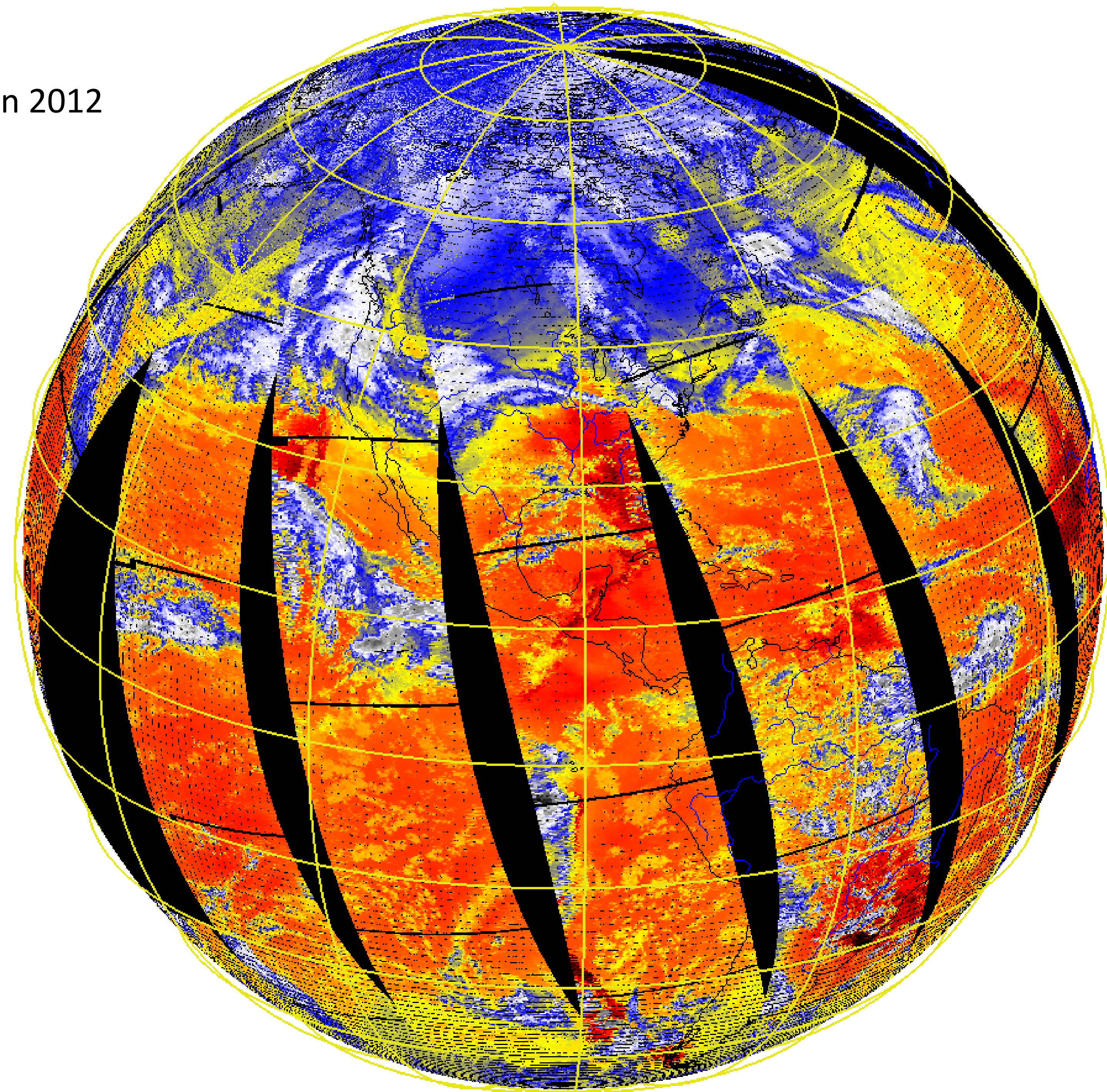

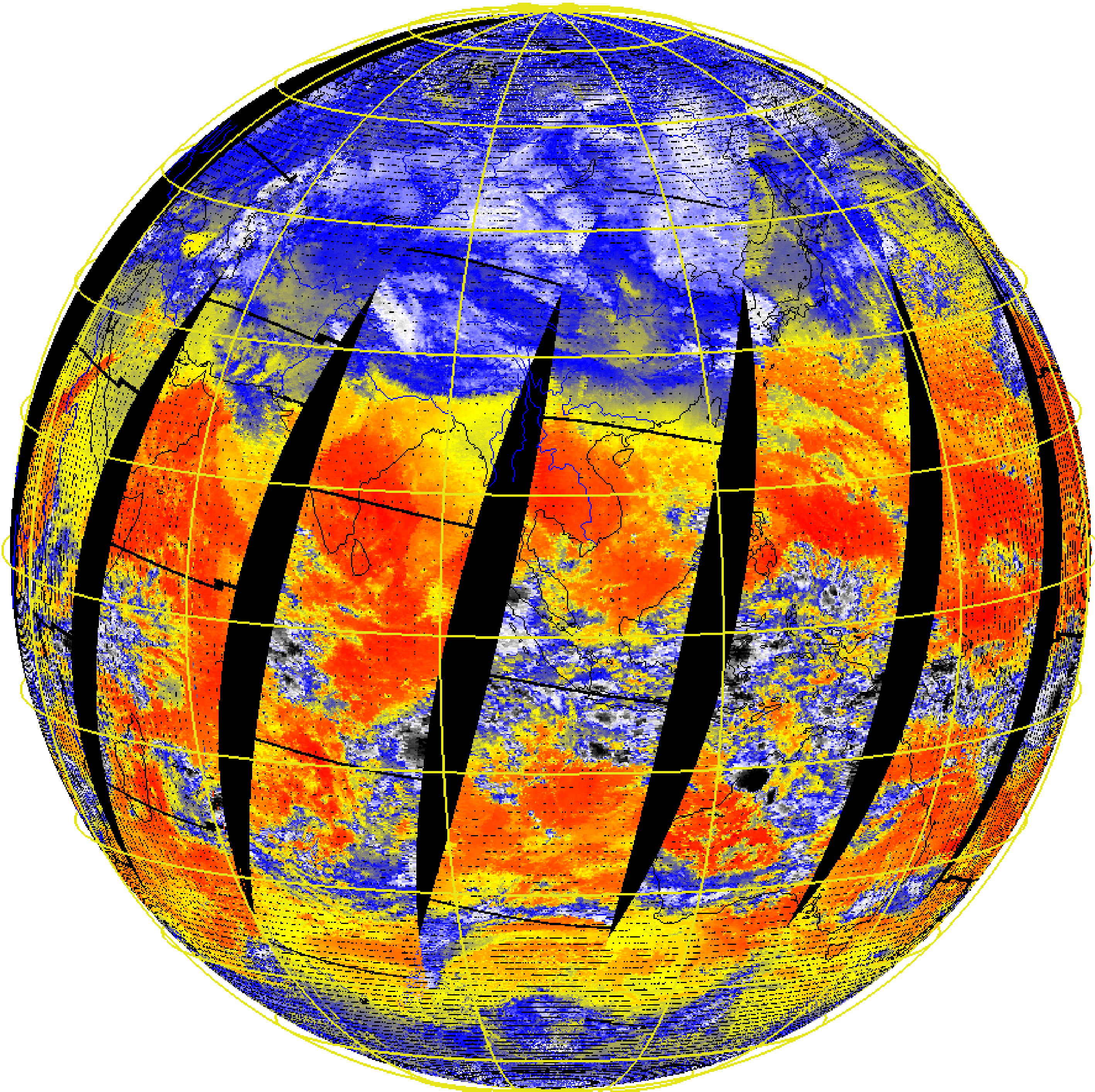

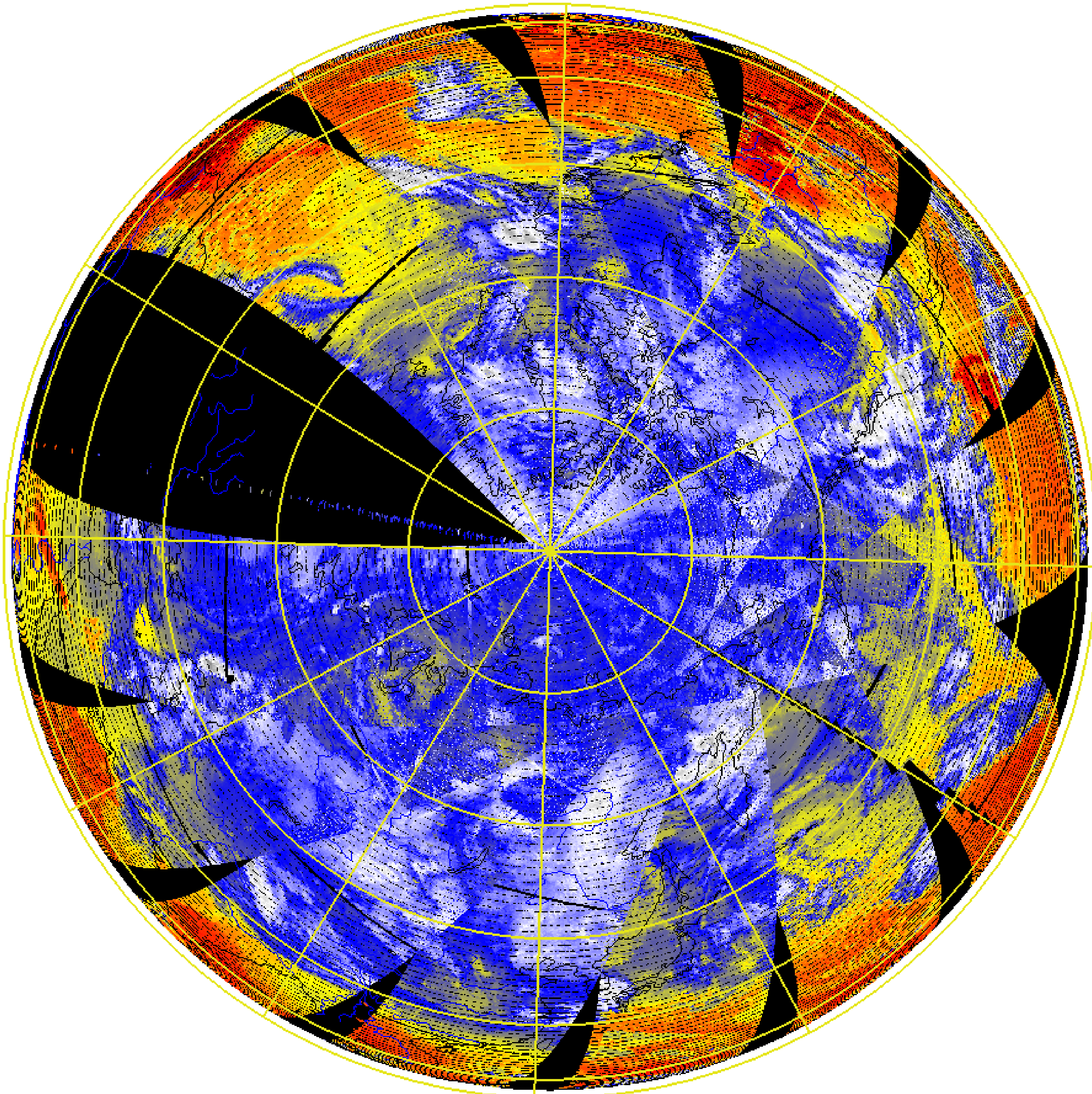

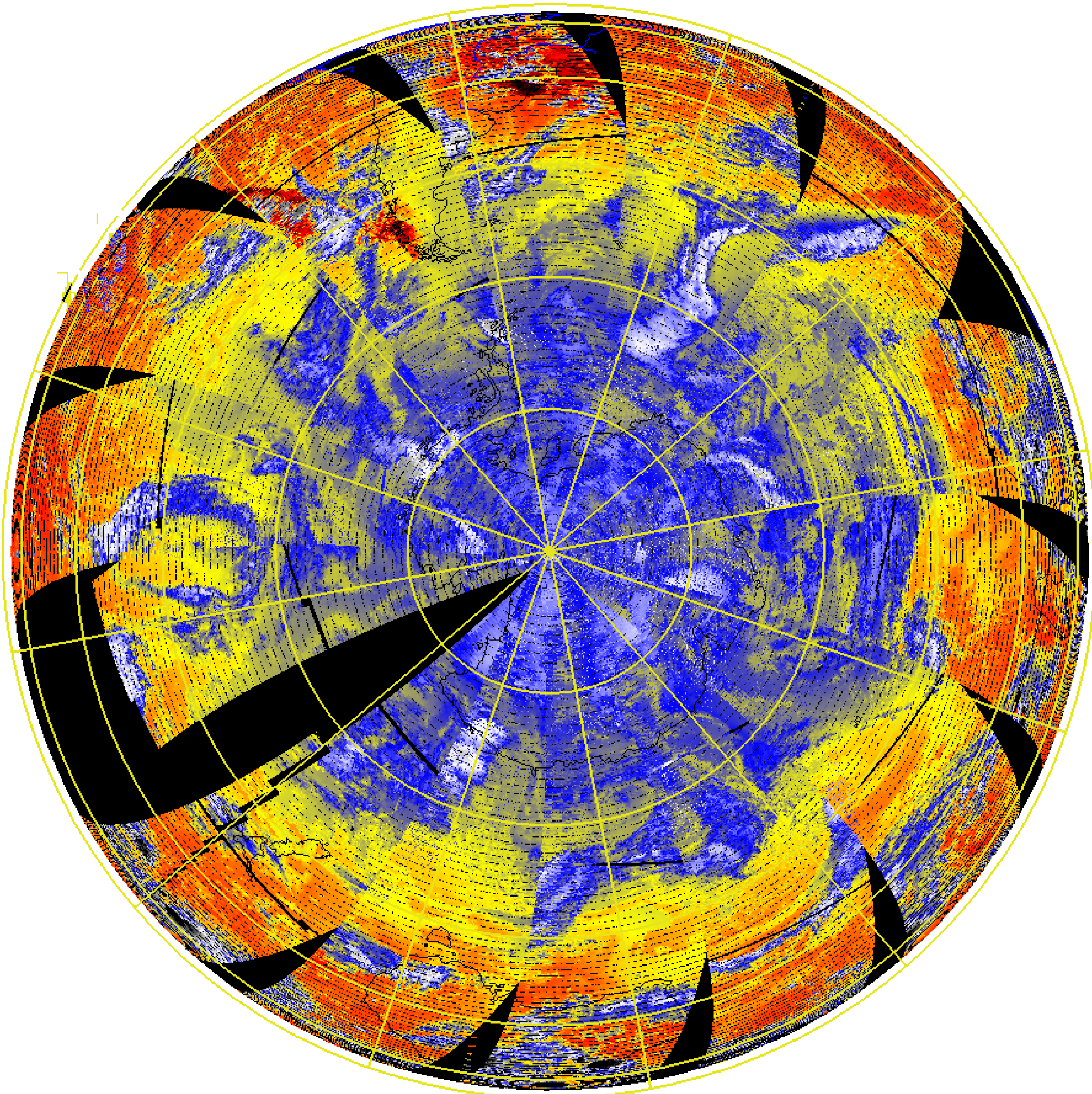

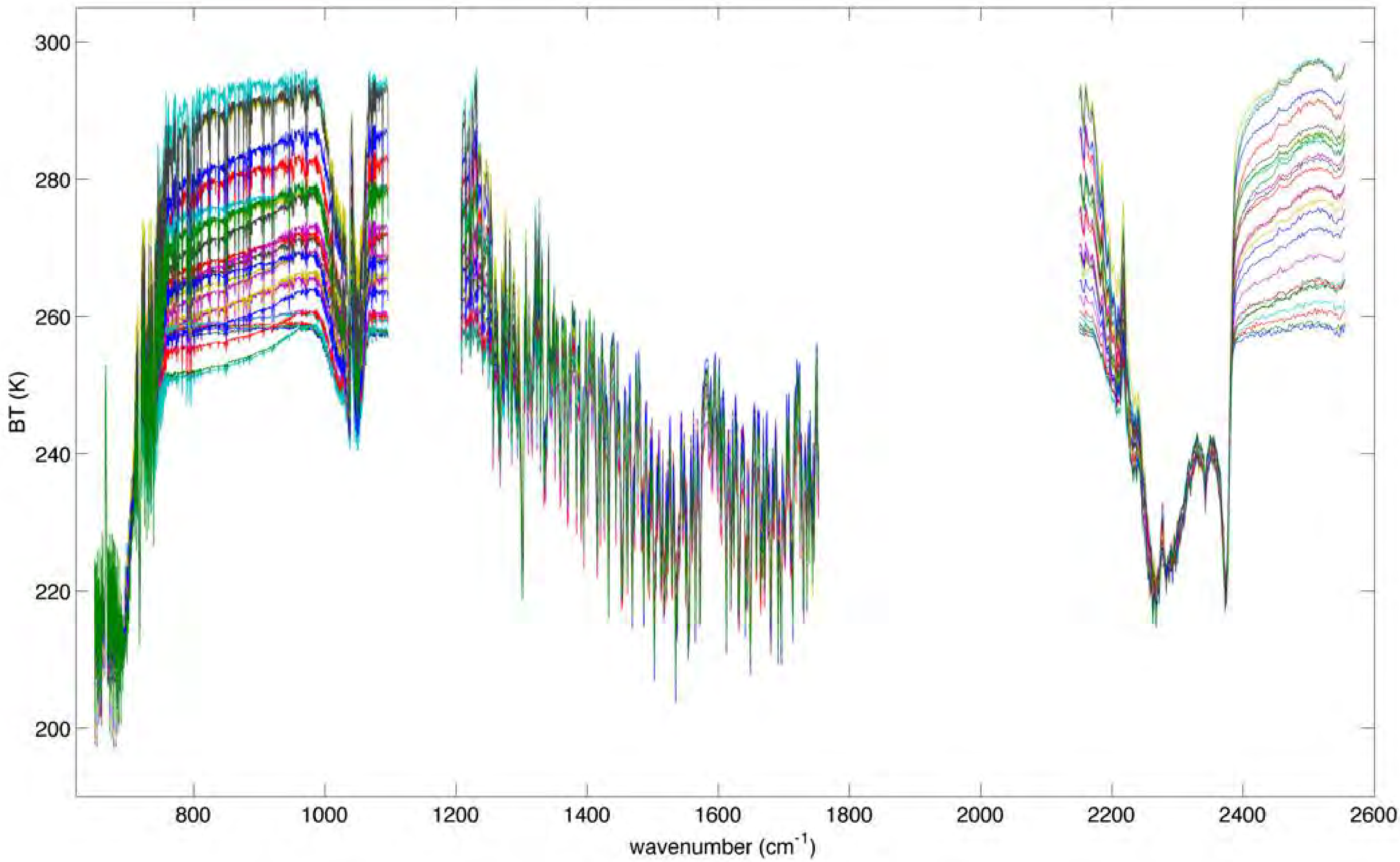

BT (K)
300
280
260
240
220
200
800
1000
1200
1400
1600
1800
2000
2200
2400
2600
wavenumber (cm-1)

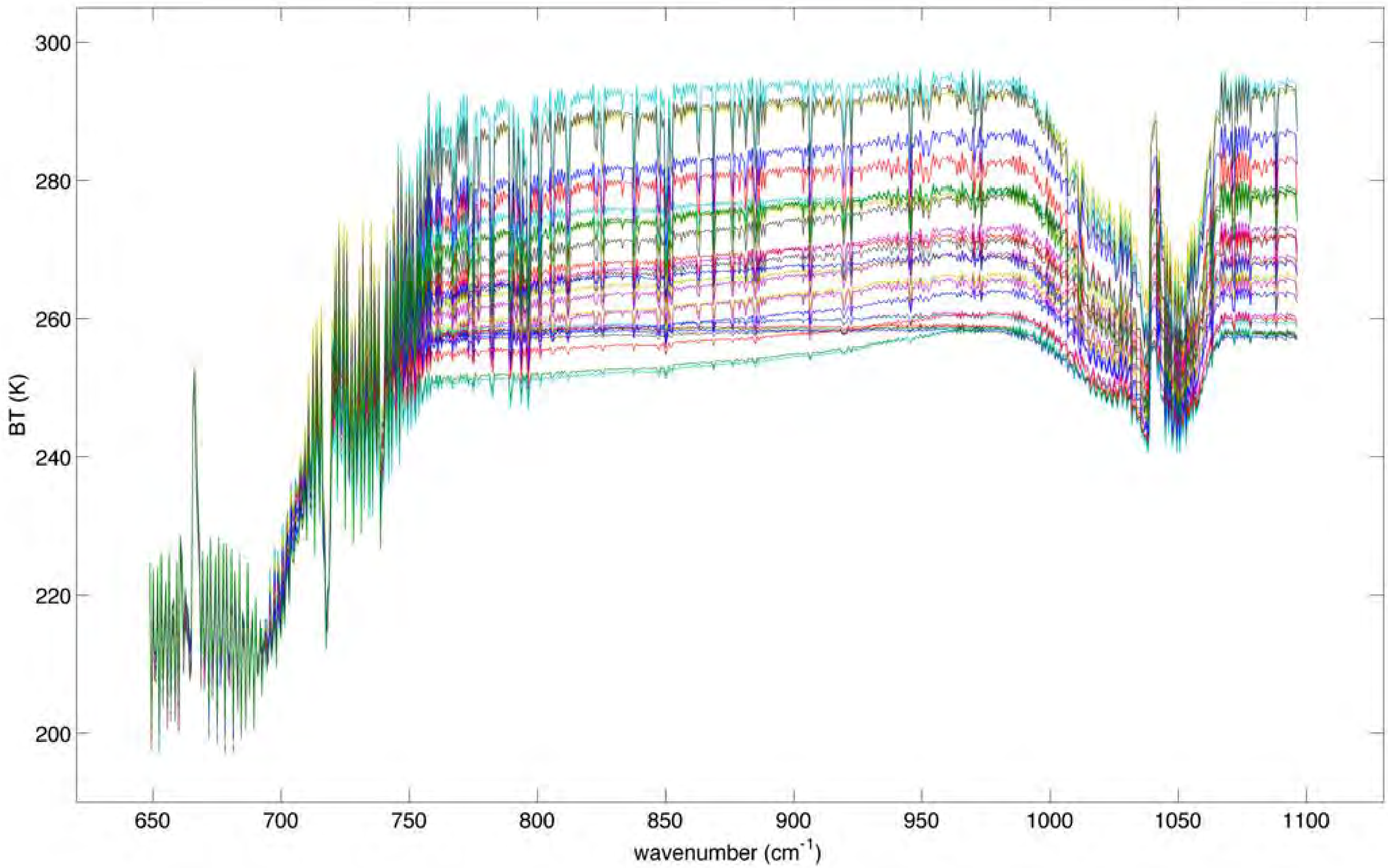

300
280
260
240
220
200
BT (K)
650
700
750
800
850
900
950
1000
1050
1100
wavenumber (cm^{-1})

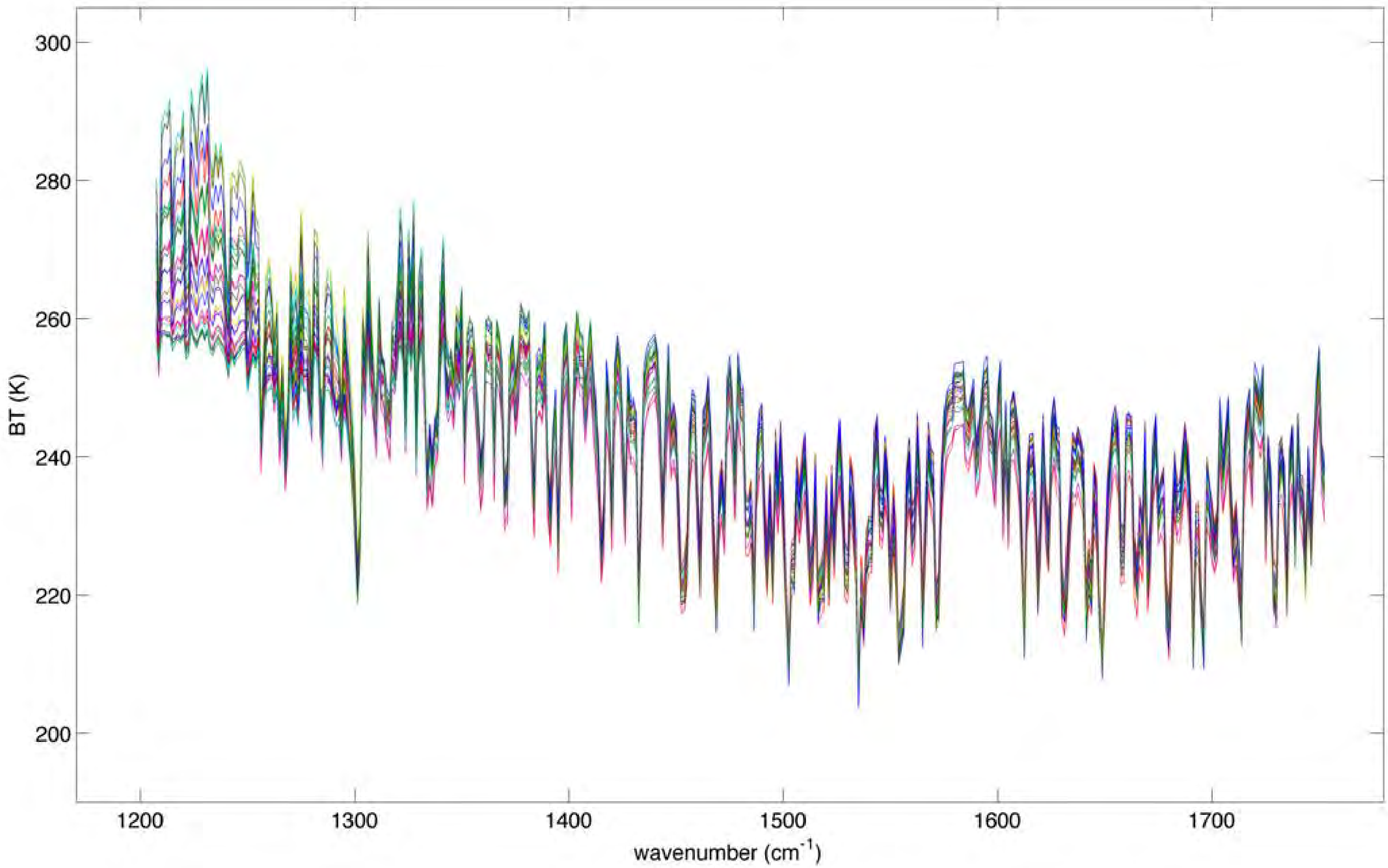

300
280
260
240
220
200
BT (K)
1200
1300
1400
1500
1600
1700
wavenumber (cm-1)

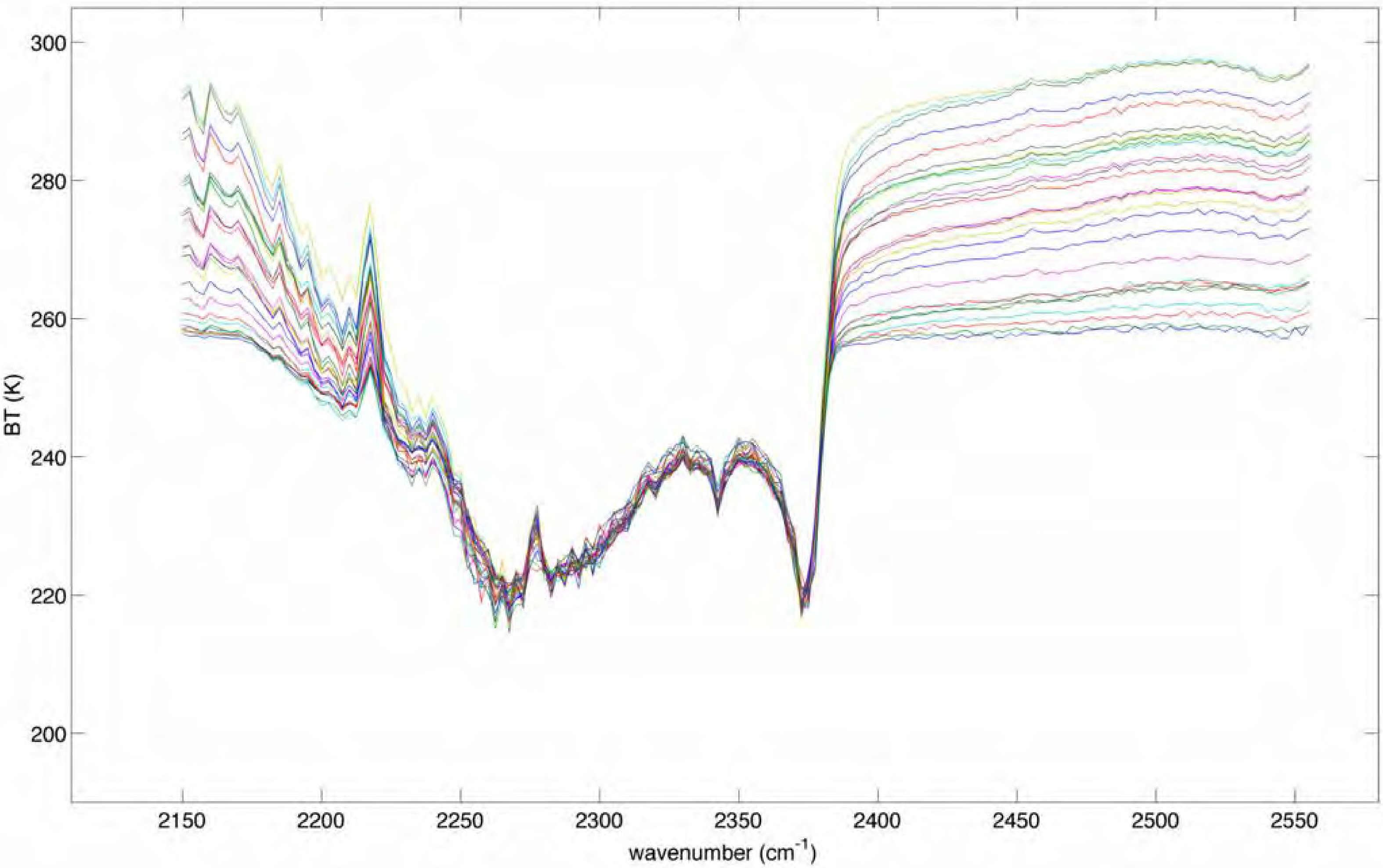
300
280
260
240
220
200
BT (K)
2150
2200
2250
2300
2350
2400
2450
2500
2550
wavenumber (cm^{-1})